AD676547

AN APPROACH TO RAY OPTICS
IN ANISOTROPIC MEDIA

by

H. L. Bertoni   and   A. Hessel

Polytechnic Institute of Brooklyn
Department of Electrophysics
Long Island Graduate Center
Farmingdale, New York 11735

DDC
RECEIVED
OCT 29 1968

POLYTECHNIC INSTITUTE OF BROOKLYN

ARPA Order No. 529

AN APPROACH TO RAY OPTICS
IN ANISOTROPIC MEDIA

by

H L Bertoni   and   A. Hessel

Polytechnic Institute of Brooklyn
Department of Electrophysics
Long Island Graduate Center
Farmingdale, New York 11735

ACKNOWLEDGEMENT

ABSTRACT

A description of the far fields radiated by an electromagnetic point source in the presence of bounded, lossless, anisotropic media is formulated in terms of ray optics. The ray-optical description is a generalization of classical geometrical optics and has previously been used to describe the fields radiated in isotropic media and those radiated by line sources in anisotropic media. In formulating the ray-optical description, the fields radiated by a point source in the presence of a planar interface between two homogeneous, lossless media of arbitrary anisotropy are first represented in terms of a double Fourier integral. This rigorous integral representation is then evaluated asymptotically to find the first-order stationary point, branch curve and surface wave pole contributions.

Using the equality of group velocity and velocity of energy transport for plane waves in anisotropic media, the stationary point contributions are interpreted in terms of direct and scattered (transmitted and reflected) rays and the associated fields are cast into ray-optical form. Locally, the direct and scattered ray fields are those of plane waves carrying energy in the ray direction and are scattered at the interface according to Snell's law. The ray-optical forms of these ray fields exhibit their dependence on properties local to the ray path, thus permitting the extension of the ray-optical results to problems not amenable to rigorous analysis. Such an extension is considered for the case of scattering at a gently curved interface between two homogeneous anisotropic media. The branch curve contributions are interpreted in terms of lateral rays whose fields also are locally those of plane waves carrying energy in the ray direction.

In order to interpret the surface wave pole contributions in ray-optical terms, it is shown that the group velocity of a modal surface wave in a plane-stratified, lossless, anisotropic medium is equal to the velocity of energy transport of the surface wave as a whole. Using this relation, the surface wave pole contributions are interpreted in terms of surface wave rays whose fields are locally those of modal surface waves carrying energy in the ray direction. Two examples of the effect of anisotropy on surface wave propagation are considered.

iii

TABLE OF CONTENTS

vi

LIST OF FIGURES AND TABLES

INTRODUCTION

In recent years considerable attention has been given to the prob-
lem of evaluating the fields radiated by localized, time-harmonic, electro-
magnetic sources in the presence of bounded anisotropic media. Interest
in this topic has been stimulated by the growing importance of communica-
tion links, such as earth-satellite links, involving propagation through the
earth's ionosphere. Previous studies in this area have been limited to in-
finite media[1, 2] and, when boundaries are present, to the fields radiated
by an infinite line source[3, 4, 5, 6] or to radiation from a point source when
the configuration possesses rotational symmetry about the optic axis of the
medium.[7, 8]

The purpose of the analysis given here is to describe the far fields
radiated by a point source in the presence of lossless, bounded anisotropic
media when no simplifying symmetries are present. In carrying out this
study, a description of the point source fields was sought in terms of ra-
optics. The ray-optical description is a generalization of classical geo-
metrical optics and has been applied successfully to diffraction problems
in isotropic media[9, 10, 11] and to line source problems in anisotropic
media.[4, 5, 6, 12]

The procedure employed in this study to develop a ray-optical de-
scription of the point source radiation is to first solve a problem that is
amenable to rigorous analysis and that embodies the features found in a
larger class of problems that are of interest. The formal solution to this
canonical problem is then approximated asymptotically for observation
points far from the source and the various contributions to the approxima-
tion are then interpreted in ray-optical terms. In the ray-optical inter-
pretation, one looks for ray paths that can be viewed as trajectories of
energy flow. The fields associated with the rays are then cast into a form
displaying their dependence on properties local to the ray path. Having
obtained a ray interpretation dependent on properties local to the ray path
in the canonical problem, the effect of varying the local properties can be

determined. Thus, problems not amenable to rigorous analysis can be solved by considering the propagation of individual rays, whose behavior is determined from the canonical problem.

The canonical problem considered here consists of a time-harmonic, electromagnetic point source radiating in the presence of a planar interface between two homogeneous, lossless, anisotropic, dielectric half-spaces. No restriction is placed on the anisotropic media filling the half-spaces, except that it be lossless, e. g. , the optic axes of the media may be oriented arbitrarily with respect to each other and with respect to the interface. A rigorous double Fourier integral representation for the fields radiated by the point source is derived in Chapter I in terms of the plane wave or modal fields of the individual media. The stationary point, branch curve and real pole contributions to the asymptotic evaluation of the double Fourier integral representation and their ray-optical interpretations are given in subsequent chapters.

The method used in performing the first-order asymptotic evaluation of the double Fourier integrals is to first apply the steepest descent technique to the integration over one of the transform variables. The result of the first integration, which contains saddle point, branch point and surface wave pole contributions, is then integrated over the remaining transform variable, to first order, by the method of stationary phase. The advantage of this method for performing the asymptotic evaluation lies in the fact that it yields the first-order branch curve and real pole contributions, as well as the stationary point contributions. Furthermore, the first-order contributions are sufficient for the description of the direct, reflected and transmitted ray fields and the lateral ray and surface wave ray fields. While more sophisticated techniques exist that give all orders of the stationary point contributions, they do not give the branch curve and real pole contributions.

In Chapter II, the stationary point contributions to the double Fourier integrals are found to first order for observation points in the far field and interpreted in terms of direct, reflected and transmitted rays. The local behavior of these rays suggests a method whereby the rays reflected from

and transmitted through a curved interface can be found from ray-optical calculations. This method is discussed in Chapter II. The branch curve contributions to the double Fourier integrals are also found to first order in Chapter II and interpreted in terms of lateral rays. The ray-optical formalism given here is consistent with Keller's diffraction theory for isotropic media.[9]

In order to interpret the real pole contributions to the double Fourier integrals, it was found necessary to derive the relation between group velocity and the velocity of energy transport for propagating modal surface waves in plane-stratified, anisotropic, lossless media. Chapter III is devoted to a proof of the equality of group velocity and the velocity of energy transport for modal surface waves in an arbitrarily plane-stratified lossless medium. The group velocity of a surface wave is the gradient, in the transverse wave number plane, of the solution of the surface wave dispersion relation for the angular frequency as a function of transverse wave numbers. Since the group velocity vector is independent of the coordinate of stratification, it cannot always be parallel to the real part of the local Poynting vector of the surface wave, which can vary with this coordinate. However, the group velocity vector is shown to be equal to the real part of the total Poynting vector, which is the integral over the coordinate of stratification of the local Poynting vector, divided by the corresponding integral of the local energy density, i.e., the surface wave energy velocity. It is also demonstrated in Chapter III that the energy flow and stored energy in a plane-stratified, lossless configuration that can be represented by an anti-Hermitian dyadic surface impedance are simply expressed in terms of the derivatives of the impedance with respect to the transverse wave numbers and frequency. The significance of the impedance relations for surface waves is also discussed.

As an illustration of the surface wave group velocity-energy velocity relation derived in Chapter III, this relation is verified in Chapter IV by direct calculation for a specific configuration. The configuration studied consists of a uniaxially anisotropic plasma slab in free space. The plasma anisotropy is assumed to be produced by an infinite static magnetic field

parallel to the slab. This configuration exemplifies the marked direction-
al dependence of surface waves that is possible in anisotropic media.

The first-order asymptotic evaluation of the surface wave pole con-
tributions to the far fields excited by the point source is given in Chapter V.
Using the relation between surface wave group velocity and energy velocity
derived in Chapter III, the pole contributions are interpreted in terms of
surface wave rays, which are the two-dimensional trajectories of energy
flow. In order to illustrate the effects of anisotropy on the radiation due
to a point source in the presence of a planar interface, the results of
Chapter II and the first section of Chapter V are used to compute the fields
radiated in a gyrotropic plasma above a perfectly conducting plane. The
static magnetic field is taken parallel to the interface and the R. F. fields
are excited by an electric field impressed in a slot cut in the conductor.
For one set of plasma parameters, the direct ray and surface wave radia-
tion patterns are calculated and clearly exhibit the effects of the anisotropy.

Chapter I

FORMAL SOLUTION FOR THE FIELDS RADIATED BY A POINT SOURCE IN THE PRESENCE OF A PLANAR INTERFACE

A. INTRODUCTION

In this chapter, the form of the double Fourier integral representation will be established for the fields radiated by a time-harmonic electromagnetic point source in the presence of a planar interface between two arbitrary homogeneous, lossless, anisotropic, dispersive dielectric half-spaces. The techniques of modal analysis will be used in developing the Fourier integral representation for the fields. Using a notation similar to that of reference (13), an orthogonality statement will be developed for the transverse modal fields of each medium that will prove helpful in deriving the excitation, transmission and reflection coefficients appearing in the Fourier integral representation.

Without loss of generality, the interface between the two homogeneous half-spaces is taken to be the $z = 0$ plane of a rectangular coordinate system and the point source is assumed to be located at $(0, 0, z')$ with $z' < 0$ --- see Fig. 1. The effect of the medium filling the half-space $z < 0$ on the propagation of time-harmonic electromagnetic waves is assumed to be described by the relative dielectric tensor $\underset{\sim}{\epsilon}_1$ while the effect of the medium filling the half-space $z > 0$ is assumed to be described by the relative dielectric $\underset{\sim}{\epsilon}_2$. For convenience, both media are assumed to have permabilities equal to that of free space. However, an analysis of the more general case of media having tensor permability would yield the same basic results obtained in this chapter. The relative dielectric tensors $\underset{\sim}{\epsilon}_1$ and $\underset{\sim}{\epsilon}_2$ must be Hermitian since the media are assumed to be lossless,[14,15] but are otherwise arbitrary, e.g., the optic axes may be oriented arbitrarily with respect to each other and with respect to the interface.

B. THE FIELD TRANSFORMS

The fields radiated by a localized source in the presence of a planar interface between two media are the solutions of the inhomogeneous Maxwell equations satisfying the radiation condition at infinity and the continuity conditions at the interface. For sources having harmonic time dependence $e^{j\omega t}$, Maxwell's equations in an anisotropic dielectric are

$$\left. \begin{aligned} \nabla \times \underline{E}\,(\underline{r}) &= -j\omega\mu_0\,\underline{H}(\underline{r}) - \underline{M}(\underline{r}) \\[2mm] \nabla \times \underline{H}\,(\underline{r}) &= j\omega\epsilon_0\,\underset{\sim}{\epsilon}\cdot\underline{E}(\underline{r}) + \underline{J}(\underline{r}) \end{aligned} \right\} \tag{1}$$

where the factor $e^{j\omega t}$ has been omitted. In (1), ϵ_0 and μ_0 are the free space dielectric constant and permeability and $\underset{\sim}{\epsilon} = \underset{\sim}{\epsilon}_1$ for $z < 0$ while for $z > 0$, $\underset{\sim}{\epsilon} = \underset{\sim}{\epsilon}_2$. Also, $\underline{M}$ and $\underline{J}$ are the magnetic and electric source current densities, respectively. Since x and y can vary over the infinite interval, the electric and magnetic fields may be represented by a double Fourier transform as

$$\left. \begin{aligned} \underline{E}(\underline{r}) \\ \underline{H}(\underline{r}) \end{aligned} \right\} = \int\!\!\int_{-\infty}^{\infty} \left\{ \begin{aligned} \underline{\mathscr{E}}(\underline{k}_t, z) \\ \underline{\mathscr{H}}(\underline{k}_t, z) \end{aligned} \right\} e^{-jk_0(\xi x + \eta y)}\, d\xi\, d\eta \tag{2}$$

where $k_0 = \omega\sqrt{\epsilon_0\mu_0}$, $\underline{r} = \underline{x}_0 x + \underline{y}_0 y + \underline{z}_0 z$ and $\underline{k}_t = \underline{x}_0\xi + \underline{y}_0\eta$, $\underline{x}_0$, $\underline{y}_0$ and $\underline{z}_0$ being unit vectors along x, y and z, respectively. Using the orthogonality and completeness of the exponentials on the infinite interval, it is found that the field transforms satisfy

$$\left. \begin{aligned} (-jk_0\underline{k}_t + \underline{z}_0\frac{d}{dz}) \times \underline{\mathscr{E}} &= -j\omega\mu_0\,\underline{\mathscr{H}} - \underline{\mathfrak{m}} \\[2mm] (-jk_0\underline{k}_t + \underline{z}_0\frac{d}{dz}) \times \underline{\mathscr{H}} &= j\omega\epsilon_0\,\underset{\sim}{\epsilon}\cdot\underline{\mathscr{E}} + \underline{\mathfrak{J}} \end{aligned} \right\} \tag{3}$$

where

$$\left. \begin{aligned} \underline{\mathfrak{J}}(\underline{k}_t, z) \\ \underline{\mathfrak{m}}(\underline{k}_t, z) \end{aligned} \right\} = \left(\frac{k_0}{2\pi}\right)^2 \int\!\!\int_{-\infty}^{\infty} \left\{ \begin{aligned} \underline{J}(\underline{r}) \\ \underline{M}(\underline{r}) \end{aligned} \right\} e^{jk_0(\xi x + \eta y)}\, dx\, dy . \tag{4}$$

In order to solve the equations in (3), they are first decomposed into their transverse and longitudinal parts by writing $\underset{\sim}{\epsilon}$ in dyadic form

$$\underset{\sim}{\epsilon} = \underset{\sim}{\epsilon}_t + \epsilon_{zz} \underline{z}_o \underline{z}_o + \underline{z}_o \underline{\epsilon}_{zt} + \underline{\epsilon}_{tz} \underline{z}_o \tag{5}$$

where

$$
\left.
\begin{aligned}
\underset{\sim}{\epsilon}_t &= \epsilon_{xx} \underline{x}_o \underline{x}_o + \epsilon_{xy} \underline{x}_o \underline{y}_o + \epsilon_{yx} \underline{y}_o \underline{x}_o + \epsilon_{yy} \underline{y}_o \underline{y}_o \\[2ex]
\epsilon_{zt} &= \epsilon_{zx} \underline{x}_o + \epsilon_{zy} \underline{y}_o \\[2ex]
\underline{\epsilon}_{tz} &= \epsilon_{xz} \underline{x}_o + \epsilon_{yz} \underline{y}_o
\end{aligned}
\right\} \tag{6}
$$

With the help of (6), the longitudinal part of (3) can be written as

$$
\left.
\begin{aligned}
-jk_o \underline{k}_t \times \underline{\mathscr{E}}_t &= -j\omega \mu_o \underline{z}_o \mathscr{H}_z - \underline{z}_o \mathscr{M}_z \\[2ex]
-jk_o \underline{k}_t \times \underline{\mathscr{H}}_t &= j\omega \epsilon_o \underline{z}_o (\underline{\epsilon}_{zt} \cdot \underline{\mathscr{E}}_t + \epsilon_{zz} \mathscr{E}_z) + \underline{z}_o \mathscr{J}_z
\end{aligned}
\right\} \tag{7}
$$

and the transverse part of (3) can be written as

$$
\left.
\begin{aligned}
\frac{d}{dz} \underline{z}_o \times \underline{\mathscr{E}}_t - jk_o \underline{k}_t \times \underline{z}_o \mathscr{E}_z &= -j\omega \mu_o \underline{\mathscr{H}}_t - \underline{\mathscr{M}}_t \\[2ex]
\frac{d}{dz} \underline{z}_o \times \underline{\mathscr{H}}_t - jk_o \underline{k}_t \times \underline{z}_o \mathscr{H}_z &= j\omega \epsilon_o (\underset{\sim}{\epsilon}_t \cdot \underline{\mathscr{E}}_t + \underline{\epsilon}_{tz} \mathscr{E}_z) + \underline{\mathscr{J}}_t
\end{aligned}
\right\} \tag{8}
$$

Equations (7) and (8) may be put into a compact form using a notation similar to that of reference (13). This notation is based on the use of matrices whose elements are operators -- in this case, two-dimensional dyadics and vectors and scalars -- and will prove convenient in developing an orthogonality statement for the modal fields. The orthogonality statement will in turn simplify the calculation of excitation, transmission and reflection coefficients and discussion of their properties. The matrices necessary for this notation are

$$\Gamma_z = \begin{bmatrix} 0 & -\underline{z}_o \times \underset{\sim}{1}_t \\ \underline{z}_o \times \underset{\sim}{1}_t & 0 \end{bmatrix} \quad , \qquad (9)$$

where $\underset{\sim}{1}_t = \underline{x}_o\,\underline{x}_o + \underline{y}_o\,\underline{y}_o$ is the transverse unit dyadic,

$$W_t = \begin{bmatrix} \omega\,\epsilon_o\,\underset{\sim}{\epsilon}_t & 0 \\ 0 & \omega\mu_o\,\underset{\sim}{1}_t \end{bmatrix} \quad , \qquad (10)$$

$$W_{tz} = \begin{bmatrix} \omega\,\epsilon_o\,\underline{\epsilon}_{tz} & -k_o\,\underline{z}_o \times \underline{k}_t \\ k_o\,\underline{z}_o \times \underline{k}_t & 0 \end{bmatrix} \quad , \qquad (11)$$

$$W_{zt} = \begin{bmatrix} \dfrac{1}{\epsilon_{zz}}\,\underline{\epsilon}_{zt} & \dfrac{k_o}{\omega\,\epsilon_o\,\epsilon_{zz}}\,\underline{z}_o \times \underline{k}_t \\ -\dfrac{k_o}{\omega\mu_o}\,\underline{z}_o \times \underline{k}_t & 0 \end{bmatrix} \quad , \qquad (12)$$

$$W_z = \begin{bmatrix} \dfrac{1}{\omega\,\epsilon_o\,\epsilon_{zz}} & 0 \\ 0 & \dfrac{1}{\omega\mu_o} \end{bmatrix} \quad , \qquad (13)$$

$$\Phi_t = \begin{bmatrix} \mathscr{J}_t \\ \underline{m}_t \end{bmatrix}, \qquad \Phi_z = \begin{bmatrix} \mathscr{J}_z \\ m_z \end{bmatrix} \qquad (14)$$

and

$$\Psi_t = \begin{bmatrix} \underline{\mathscr{E}}_t \\ \underline{\mu}_t \end{bmatrix} \quad , \qquad \Psi_z = \begin{bmatrix} \mathscr{E}_z \\ \mu_z \end{bmatrix} \qquad . \qquad (15)$$

With the above definitions, (7) and (8) can be rewritten as

$$\frac{d}{dz} \Gamma_z \cdot \Psi_t = -jW_t \cdot \Psi_t - jW_{tz} \Psi_z - \hat{\Phi}_t \tag{16}$$

and

$$\Psi_z = -W_{zt} \cdot \Psi_t + jW_z \hat{\Phi}_z \quad . \tag{17}$$

As indicated in (16), the dyadic elements of Γ_z and W_t are to be dotted into the appropriate vector elements of Ψ_t while the vector elements of W_{tz} are to be multiplied by the scalar elements of Ψ_z. In (17), the vector elements of W_{zt} are to be dotted with the appropriate elements of Ψ_t and the product $W_z \hat{\Phi}_z$ is formed by ordinary matrix multiplication. Substituting Ψ_z from (17) into (16) it is found that Ψ_t satisfies the vector differential equation

$$\frac{d}{dz} \Gamma_z \cdot \Psi_t + jW \cdot \Psi_t = -\hat{\Phi}_t \tag{18}$$

where

$$W = W_t - W_{tz} W_{zt} \tag{19}$$

and the equivalent transverse source transform $\hat{\Phi}_t$ is given by

$$\hat{\Phi}_t = \Phi_t - W_{tz} W_z \hat{\Phi}_z \quad . \tag{20}$$

The elements of the product matrix $W_{tz} W_{zt}$ in (19) are dyadics, i.e.,

$$W_{tz} W_{zt} = \begin{bmatrix} \dfrac{\omega \epsilon_o}{\epsilon_{zz}} \underline{\epsilon}_{tz} \underline{\epsilon}_{zt} + \omega \epsilon_o (\underline{z}_o \times \underline{k}_t)(\underline{z}_o \times \underline{k}_t) & \dfrac{k_o}{\epsilon_{zz}} \underline{\epsilon}_{tz} (\underline{z}_o \times \underline{k}_t) \\[4ex] \dfrac{k_o}{\epsilon_{zz}} (\underline{z}_o \times \underline{k}_t) \underline{\epsilon}_{zt} & \dfrac{\omega \mu_o}{\epsilon_{zz}} (\underline{z}_o \times \underline{k}_t)(\underline{z}_o \times \underline{k}_t) \end{bmatrix} \quad . \tag{21}$$

Observe that W is a function of z in that $\underline{\epsilon} = \underline{\epsilon}_1$ for $z < 0$ while for $z > 0$, $\underline{\epsilon} = \underline{\epsilon}_2$.

C.   THE MODAL FIELDS

When the equivalent transverse source transform $\hat{\mathfrak{F}}_t$ has z dependence $\delta(z-z')$, the solution of (18) satisfying the continuity condition at $z=0$ ($\underline{\mathscr{E}}_t$ and $\underline{\mathscr{H}}_t$, and hence Ψ_t, are continuous across the interface) and the radiation condition at $|z| = \infty$ is the one-dimensional Green's function of the transform problem. The radiation condition requires that the Green's function be bounded as $|z| \to \infty$ and that the z component of the Poynting vector, which is given by $\text{Re}(\underline{\mathscr{E}}_t \times \underline{\mathscr{H}}_t^*)$, be such that energy is carried away from the source for $|z| \to \infty$. The radiation condition must be imposed in order to uniquely determine the one-dimensional Green's function. Furthermore, it ensures that the actual fields satisfy the radiation condition in that the total power passing through any constant z plane, which is given by $\text{Re}\iint \underline{E}_t \times \underline{H}_t^* \, dx \, dy = \text{Re}(\frac{k_0}{2\pi})^2 \iint \underline{\mathscr{E}}_t \times \underline{\mathscr{H}}_t^* \, d\xi \, d\eta$, will be away from the source for $|z| \to \infty$ --- see Arbel[7] for further discussion.

The Green's function can be constructed from the homogeneous solutions of (18) for each medium considered separately, i. e., from the solutions of

$$\frac{d}{dz}\Gamma_z \cdot \Psi_t + jW \cdot \Psi_t = 0 \tag{22}$$

where W is made independent of z by using the dielectric tensor appropriate to the medium under study for all z. Equation (22) represents four coupled, first-order, ordinary linear differential equations with constant coefficients whose unknowns are the four transform components $\mathscr{E}_x$, $\mathscr{E}_y$, $\mathscr{H}_x$ and $\mathscr{H}_y$. Such a system of equations has solutions whose z dependence is of the form $e^{-jk_0 \varkappa z}$. Substituting this z dependence into (22) gives

$$\left[\varkappa \Gamma_z - \frac{1}{k_0} W\right] \cdot \Psi_t = 0 \tag{23}$$

which is an eigenvalue problem equivalent to the simultaneous diagonalization of two 4x4 matrices.

For (23) to have non-trivial solutions, the determinant of the matrix representation of the operation $\left[\varkappa \Gamma_z - \frac{1}{k_o} W\right]$ must be zero. This condition determines the eigenvalues or propagation constants $\varkappa_n$ for each medium, which when substituted into (23) allow the determination of the corresponding eigen or mode vectors $\Psi_t(\varkappa_n)$. Since the matrix representation of the operator $\left[\varkappa \Gamma_z - \frac{1}{k_o} W\right]$ is fourth order, the eigenvalues $\varkappa_n$ are the roots of a quartic so that, in general, four eigenvalues and eigenvectors satisfy (23). The coefficients of the quartic depend on ξ and η so that the vanishing of the determinant yields the plane wave dispersion relation

$$D_p(\xi, \eta, \varkappa) = 0 \qquad . \qquad (24)$$

For lossless media $\underset{\sim}{\epsilon}$ is Hermitian and hence W is Hermitian for real ξ and η, as can readily be verified. Thus, since Γ_z is real and symmetric, for lossless media and real ξ and η, the coefficients of the quartic will be real, indicating that the $\varkappa_n$'s are real or occur in complex conjugate pairs.

When the four eigenvalues of (23) are distinct, the four eigenvectors of (23) are linearly independent, and hence complete, in the four-dimensional space formed by the union of the two-dimensional $\underline{\mathscr{E}}_t$ and $\underline{\mathscr{H}}_t$ spaces. This follows from the fact that Γ_z is non-singular so that (23) is equivalent to the eigenvalue problem $\frac{1}{k_o} \Gamma_z^{-1} \cdot W \cdot \Psi_t = \varkappa \Psi_t$, which is known to have linearly independent eigenvectors when the eigenvalues are distinct.[16]

In order to find excitation, transmission and reflection coefficients, it is first necessary to establish the orthogonality properties of the eigenvectors. To this end, let $\varkappa_n$ and $\varkappa_m$ be any two eigenvalues of (23) and let Ψ_t^+ be the 2x1 matrix, with vector elements, that is the transpose conjugate of the 1x2 matrix Ψ_t. Consider now the quantity

$$\Psi_t^+(\varkappa_m) \cdot (\varkappa_n \Gamma_z - \frac{1}{k_o} W) \cdot \Psi_t(\varkappa_n) - \left[(\varkappa_m \Gamma_z - \frac{1}{k_o} W) \cdot \Psi_t(\varkappa_m)\right]^+ \cdot \Psi_t(\varkappa_n) ,$$

$$(25)$$

which is zero since $\varkappa_m$ and $\varkappa_n$ are eigenvalues of (23). Since Γ_z is real and symmetric and W is Hermitian, one can write, for example,

$$\left[W \cdot \Psi_t(\varkappa_m) \right]^+ \cdot \Psi_t(\varkappa_n) = \Psi_t^+(\varkappa_m) \cdot W \cdot \Psi_t(\varkappa_n) \tag{26}$$

so that (25) reduces to

$$(\varkappa_n - \varkappa_m^*) \left[\Psi_t^+(\varkappa_m) \cdot \Gamma_z \cdot \Psi_t(\varkappa_n) \right] = 0 \quad . \tag{27}$$

If the eigenvalues of (23) are distinct (27) implies that

$$\Psi_t^+(\varkappa_m) \cdot \Gamma_z \cdot \Psi_t(\varkappa_n) = M_n \delta_{\varkappa_n, \varkappa_m^*} \tag{28}$$

where

$$\delta_{\varkappa_n, \varkappa_m^*} = \begin{cases} 0 & \varkappa_n \neq \varkappa_m^* \\ \\ 1 & \varkappa_n = \varkappa_m^* \end{cases} \tag{29}$$

and M_n is the normalizing constant

$$M_n = \Psi_t^+(\varkappa_n^*) \cdot \Gamma_z \Psi_t(\varkappa_n) \quad . \tag{30}$$

Thus, for distinct eigenvalues, the eigenvectors of (23) are orthogonal with respect to the weight operator Γ_z in the sense indicated in (28).

If all the eigenvalues of (23) are distinct, then none of the M_n's are zero. To verify this statement, observe that the diagonal 4x4 matrix $\left[M_n \right]$ whose diagonal elements are the M_n's is given by

$$\left[M_n \right] = \left[\Psi_t^*(\varkappa_n^*) \right] \left[\Gamma_n \right] \left[(\Psi_t(\varkappa_n)) \right] \quad . \tag{31}$$

In (31), the 4x4 matrix $\left[\Psi_t^*(\varkappa_n^*) \right]$ has for its rows the conjugate of the eigenvectors of (23) corresponding to the eigenvalues $\varkappa_n^*$ while the 4x4 matrix $\left[(\Psi_t(\varkappa_n)) \right]$ has the eigenvectors for its columns. Also, $\left[\Gamma_z \right]$ is the 4x4 matrix representation of Γ_z. If the eigenvalues of (23) are all distinct, the eigenvectors are linearly independent,[16] and hence $\det \left[\Psi_t^*(\varkappa_n^*) \right]$ and $\det \left[(\Psi_t(\varkappa_n)) \right]$ are non-zero. Furthermore, since $\det \left[\Gamma_z \right]$ is not zero, $\det \left[M_n \right] \neq 0$, so that none of the M_n's are zero.

When the medium under consideration is anisotropic, the eigen-

values of (23), considered as function of the transverse wave numbers ξ and η, will be distinct except on certain branch curves in the real (ξ, η) plane. On these curves, two or more eigenvalues will be equal, i.e., two or more solutions of the dispersion relation (24) will have branch-type singularities, and the corresponding M_n's will be zero. The effect of these singularities on the radiated fields will be considered in Chapter II.

If the medium under consideration is isotropic, i.e., the relative dielectric tensor is $\underset{\sim}{\epsilon} = \epsilon \underset{\sim}{1}$ where $\underset{\sim}{1}$ is the unit tensor, the dispersion relation (24) reduces to

$$D_p(\xi, \eta, \varkappa) = k_o^4 (\epsilon - \xi^2 - \eta^2 - \varkappa^2)^2 = 0 \tag{32}$$

and hence there are at most two distinct eigenvalues of (23) given by $\pm \sqrt{\epsilon - \xi^2 - \eta^2}$. While the eigenvalues are degenerate in this case, if $\epsilon - \xi^2 - \eta^2 \neq 0$, four linearly independent eigenvectors of (23) can be constructed satisfying an orthogonality condition similar to (28). The E and H modes commonly used in the solution or radiation problems are one possible selection. By direct substitution it is easily shown that the E and H modes satisfy (28) with $\delta_{\varkappa_n, \varkappa_m^*}$ defined

$$\delta_{\varkappa_n, \varkappa_m^*} = \left\{ \begin{array}{l} 0, \quad \varkappa_n \neq \varkappa_m^* \quad \text{or one mode is E and the} \\ \qquad\qquad\qquad \text{other H} \\ 1, \quad \varkappa_n = \varkappa_m^* \quad \text{and both are E or H modes} \end{array} \right\} . \tag{33}$$

Throughout this discussion, the case of isotropic media is included if it is assumed that the eigenvectors have been selected so as to satisfy an orthogonality condition similar to that described above. Finally, if $\epsilon - \xi^2 - \eta^2 = 0$, all four eigenvalues are zero and the eigenvectors are no longer linearly independent.

Physically, the orthogonality statement (28) can be interpreted as a power orthogonality condition for the z component of the modal power. By direct expansion, (28) can be rewritten as $\underline{z}_o \cdot (\underline{\mathscr{E}}_{tn} \times \underline{\mathscr{H}}_{tm}^* + \underline{\mathscr{E}}_{tm}^* \times \underline{\mathscr{H}}_{tn}) = M_n \delta_{\varkappa_n, \varkappa_m^*}$, where $\underline{\mathscr{E}}_{tn}$ and $\underline{\mathscr{H}}_{tn}$ are the electric and magnetic field components of the eigen or mode vector $\Psi_t(\varkappa_n)$ and $\underline{\mathscr{E}}_{tm}$ and $\underline{\mathscr{H}}_{tm}$ are those of

$\Psi_t(\varkappa_m)$. Thus it is seen that the modal fields for each mode having real propagation constant $\varkappa_n$ carry energy in the z direction independently of all other modes. For such modes $M_n = 2\,\mathrm{Re}\,(\underline{z}_o \cdot \underline{\mathcal{E}}_{tn} \times \underline{\mathcal{H}}_{tn}^*)$ is twice the z component of the real modal power. In the case when $\varkappa_n$ is complex or imaginary, it is seen that the corresponding modal fields cannot by themselves carry energy in the z direction. However, if both the modal fields having complex or imaginary wave number $\varkappa_n$ and the modal fields having wave number $\varkappa_n^*$ are present, the combined fields can carry energy in the z direction.

D. EVALUATION OF THE ONE-DIMENSIONAL GREEN'S FUNCTION

Assuming the eigenvalues and eigen or mode vectors for both the ϵ_1 and ϵ_2 media to be known, the one-dimensional Green's function, which is the solution (18) satisfying the radiation condition and the continuity condition at $z = 0$, can be constructed. Corresponding to a point source located at $(0, 0, z')$, the electric and magnetic current densities $\underline{J}$ and $\underline{M}$ are of the form

$$\left.\begin{array}{c} \underline{J}(r) \\ \underline{M}(r) \end{array}\right\} = \left\{\begin{array}{c} \underline{J}_o \\ \underline{M}_o \end{array}\right\} \delta(x)\,\delta(y)\,\delta(z - z') \tag{34}$$

where $\underline{J}_o$ and $\underline{M}_o$ are the vector source strengths. From (4), (12), (13), (14) and (20), the form of $\underline{J}$ and $\underline{M}$ given in (34) is seen to imply that the equivalent transverse source transform $\hat{\Psi}_t(\underline{k}_t, z)$ can be written as

$$\hat{\Psi}_t(\underline{k}_t, z) = \hat{\Psi}_o(\underline{k}_t)\,\delta(z - z') \tag{35}$$

where

$$\hat{\Psi}_o(\underline{k}_t) = \left(\frac{k_o}{2\pi}\right)^2 \left\{\begin{bmatrix} \underline{J}_{ot} \\ \underline{M}_{ot} \end{bmatrix} - W_{tz}\,W_z \begin{bmatrix} J_{oz} \\ M_{oz} \end{bmatrix}\right\}. \tag{36}$$

Since the source term in (18) is localized to $z = z'$, for $z \neq z'$ the one-dimensional Green's function will be a superposition of appropriate modes.

For a lossless medium and any real ξ and η, if the dispersion relation (24) has complex solutions, they occur as conjugate pairs. Thus (24) has zero, two or four real solutions for any particular real ξ and η. At this point it is necessary to assume that half of the real solutions of (24) for either medium correspond to modes carrying energy in the positive z direction and the remaining real solutions correspond to modes carrying energy in the negative z direction.[*] With this assumption, of the four modes

---

[*] In Chapter II, where the asymptotic evaluation of the Fourier integral representation is carried out, it will also be assumed that the four solutions $\varkappa_n$ of the dispersion relation (24), which are functions of ξ and η, can be defined such that for each n, $\varkappa_n(\xi, \eta)$ is a continuous function of ξ and η that corresponds either to an upgoing mode for all ξ and η or to a downgoing mode for all ξ and η.

in each medium, two modes carry energy or decay in the positive z direction -- upgoing modes -- and two modes carry energy or decay in the negative z direction -- downgoing modes. If this were not the case, some problems with impedance boundary conditions would not have solutions that satisfied the radiation condition. In the ε_1 medium, the upgoing modes are labeled with $n = \vec{1}, \vec{2}$ and the downgoing modes with $n = \overleftarrow{1}, \overleftarrow{2}$. In the ε_2 medium, the $n = \vec{3}, \vec{4}$ modes are upgoing and the $n = \overleftarrow{3}, \overleftarrow{4}$ modes are downgoing. This labeling scheme is indicated in Fig. 1 where the arrows indicate the direction of energy flow or decay.
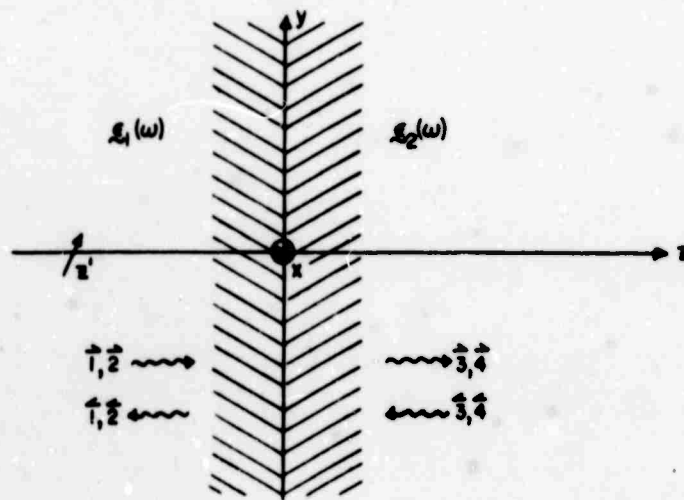
Fig. 1-1   Interface between two homogeneous, anisotropic media

In view of the foregoing assumption on the energy flow of the modes, for $z' < 0$, i.e., for the source below the $z = 0$ plane, the radiation condition implies that in the region $z > 0$, the Green's function will be a superposition to the $n = \vec{3}, \vec{4}$ modes of the ε_2 medium, while in the region $z < z'$, it will be a superposition of the $n = \overleftarrow{1}, \overleftarrow{2}$ modes of the ε_1 medium. For $z' < z < 0$, the Green's function will be a superposition of all four modes of the ε_1 medium. Thus, the one-dimensional Green's function $\Psi_t(z)$ can be written as

$$
\Psi_t(z) = \begin{cases} \displaystyle\sum_{\vec{3},\,\vec{4}} b_m \Psi_t(\varkappa_m)\, e^{-jk_o\varkappa_m z} & (z > 0) \\[2em] \displaystyle\sum_{\vec{1},\,\vec{2}} a_n \Psi_t(\varkappa_n)\, e^{-jk_o\varkappa_n z} + \sum_{\overleftarrow{1},\,\overleftarrow{2}} c_m \Psi_t(\varkappa_m)\, e^{-jk_o\varkappa_m z} & (z' < z < 0) \\[2em] \displaystyle\sum_{\overleftarrow{1},\,\overleftarrow{2}} a_n \Psi_t(\varkappa_n)\, e^{-jk_o\varkappa_n z} \quad \sum_{\overleftarrow{1},\,\overleftarrow{2}} c_m \Psi_t(\varkappa_m)\, e^{-jk_o\varkappa_m z} & (z < z') \end{cases}
$$

$$(37)$$

where the amplitudes a_n, b_m and c_m are to be found from the continuity conditions at $z = 0$ and the jump conditions at the source. In (37) $\Psi_t(z)$ for $z < z'$ has been written for convenience in terms of two sums, the first of which can be interpreted as a direct field contribution and the second as reflected contribution, as will be seen presently.

When the source term in (18) is of the form given in (35), $\Psi_t(z)$ can have no stronger discontinuity that a step at $z = z'$. Thus integrating (18) from $z' - \Delta$ to $z' + \Lambda$, where Δ is a small positive quantity, gives

$$
\Gamma_z \cdot \left[\Psi_t(z' + \Lambda) - \Psi_t(z' - \Lambda) \right] = -\hat{\Phi}_o \ . \tag{38}
$$

Substituting for $\Psi_t(z' + \Lambda)$ and $\Psi_t(z' - \Delta)$ the forms given in (37) and taking the limit as $\Delta \to 0$, (38) becomes

$$
\Gamma_z \cdot \left[\sum_{\vec{1},\,\vec{2}} a_n \Psi_t(\varkappa_n)\, e^{-jk_o\varkappa_n z'} - \sum_{\overleftarrow{1},\,\overleftarrow{2}} a_n \Psi_t(\varkappa_n)\, e^{-jk_o\varkappa_n z'} \right] = -\hat{\Phi}_o \ . \tag{39}
$$

Dotting both sides of (39) by $\Psi_t^+(\varkappa_n^*)$ and using the orthogonality relation (28), the amplitudes are found to be

$$
a_n = -e_n \left[\Psi_t^+(\varkappa_n^*) \cdot \hat{\Phi}_o \right] e^{jk_o\varkappa_n z'} \Big/ M_n \tag{40}
$$

where

$$e_n = \begin{cases} 1; & n = \vec{1}, \ \vec{2} \\ -1; & n = \overleftarrow{1}, \ \overleftarrow{2} \end{cases} .$$

(41)

The coefficients b_m and c_m can be found in terms of the a_n's from the continuity of $\Psi_t(z)$ at $z = 0$, i.e., the continuity of the transverse fields across the interface. Since $\Psi_t(z)$ is continuous at $z = 0$, it is seen from (37) that

$$\sum_{\vec{3}, \vec{4}} b_m \Psi_t(\varkappa_m) = \sum_{\vec{1}, \vec{2}} a_n \Psi_t(\varkappa_n) + \sum_{\overleftarrow{1}, \overleftarrow{2}} c_m \Psi_t(\varkappa_m),$$

(42)

which is equivalent to four equations in four unknowns. In order to solve (42) for the b_m's, dot both sides of (42) with $\Psi_t^+(\varkappa_{\overleftarrow{1}}^*) \cdot \Gamma_z$ and then with $\Psi_t^+(\varkappa_{\overleftarrow{2}}^*) \cdot \Gamma_z$ to obtain the set of equations

$$a_{\overleftarrow{1}} M_{\overleftarrow{1}} = M_{\overleftarrow{1}\,\vec{3}} \ b_{\vec{3}} + M_{\overleftarrow{1}\,\vec{4}} \ b_{\vec{4}} \ \Bigg\}$$

(43)

$$a_{\overleftarrow{2}} M_{\overleftarrow{2}} = M_{\overleftarrow{2}\,\vec{3}} \ b_{\vec{3}} + M_{\overleftarrow{2}\,\vec{4}} \ b_{\vec{4}}$$

where

$$M_{nm} = \Psi_t^+(\varkappa_n^*) \cdot \Gamma_z \cdot \Psi_t(\varkappa_m) .$$

(44)

In (44), $\varkappa_n^*$ is an eigenvalue of the $\underset{\sim}{\epsilon}_1$ medium while $\varkappa_m$ is an eigenvalue of the $\underset{\sim}{\epsilon}_2$ medium. The solution of (43) for the b_m's is

$$b_m = \sum_{n=\vec{1}, \vec{2}} \Gamma_{mn} a_n , \quad m = \vec{3}, \vec{4}$$

(45)

where

$$\Gamma_{\vec{3}\,\overleftarrow{1}} = M_{\overleftarrow{1}} M_{\overleftarrow{2}\,\vec{4}} / d ; \quad \Gamma_{\vec{3}\,\overleftarrow{2}} = -M_{\overleftarrow{2}} M_{\overleftarrow{1}\,\vec{4}} / d ; \ \Bigg\}$$

(46)

$$\Gamma_{\vec{4}\,\overleftarrow{1}} = -M_{\overleftarrow{1}} M_{\overleftarrow{2}\,\vec{3}} / d; \quad \Gamma_{\vec{4}\,\overleftarrow{2}} = M_{\overleftarrow{2}} M_{\overleftarrow{1}\,\vec{3}} / d$$

with

$$d = M_{\vec{1}\,\vec{3}}\; M_{\vec{2}\,\vec{4}} - M_{\vec{1}\,\vec{4}}\; M_{\vec{2}\,\vec{3}} \quad . \tag{47}$$

In order to solve (42) for the c_m's, dot both sides of (42) with $\Psi_t^{+}(\varkappa_{\overleftarrow{1}}^{*}) \cdot \Gamma_z$ and then with $\Psi_t^{+}(\varkappa_{\overleftarrow{2}}^{*}) \cdot \Gamma_z$ to obtain the equations

$$\left.
\begin{aligned}
C_{\overleftarrow{1}}\; M_{\overleftarrow{1}} &= M_{\overleftarrow{1}\,\vec{3}}\; b_{\vec{3}} + M_{\overleftarrow{1}\,\vec{4}}\; b_{\vec{4}} \\[2mm]
C_{\overleftarrow{2}}\; M_{\overleftarrow{2}} &= M_{\overleftarrow{2}\,\vec{3}}\; b_{\vec{3}} + M_{\overleftarrow{2}\,\vec{4}}\; b_{\vec{4}}
\end{aligned}
\right\} \tag{48}$$

where M_{nm} is as defined in (44). Using (45) for the b_m's, c_1 and c_2 can be written as

$$c_m = \sum_{n=\vec{1},\,\vec{2}} \Gamma_{mn}\, a_n , \quad m = \overleftarrow{1},\, \overleftarrow{2} \tag{49}$$

where

$$\left.
\begin{aligned}
\Gamma_{\overleftarrow{1}\,\vec{1}} &= (M_{\overleftarrow{1}\,\vec{3}}\; M_{\vec{2}\,\vec{4}} - M_{\overleftarrow{1}\,\vec{4}}\; M_{\vec{2}\,\vec{3}})M_{\vec{1}} / M_{\overleftarrow{1}}\, d \\[3mm]
\Gamma_{\overleftarrow{1}\,\vec{2}} &= (M_{\overleftarrow{1}\,\vec{4}}\; M_{\vec{1}\,\vec{3}} - M_{\overleftarrow{1}\,\vec{3}}\; M_{\vec{1}\,\vec{4}})\, M_{\vec{2}} / M_{\overleftarrow{1}}\, d \\[3mm]
\Gamma_{\overleftarrow{2}\,\vec{1}} &= (M_{\overleftarrow{2}\,\vec{3}}\; M_{\vec{2}\,\vec{4}} - M_{\overleftarrow{2}\,\vec{4}}\; M_{\vec{2}\,\vec{3}})\, M_{\vec{1}} / M_{\overleftarrow{2}}\, d \\[3mm]
\Gamma_{\overleftarrow{2}\,\vec{2}} &= (M_{\overleftarrow{2}\,\vec{4}}\; M_{\vec{1}\,\vec{3}} - M_{\overleftarrow{2}\,\vec{3}}\; M_{\vec{1}\,\vec{4}})\, M_{\vec{2}} / M_{\overleftarrow{2}}\, d
\end{aligned}
\right\} \quad . \tag{50}$$

All of the coefficients in the one-dimensional Green's function (37) have thus been determined in terms of the propagation constants $\varkappa_n$ and the mode vectors $\Psi_t(\varkappa_n)$ of the two media and the equivalent transverse source transform $\hat{\Phi}_o$. The terms in (37) whose amplitudes are the a_n's may be interpreted as representing modes excited directly by the source. Those terms in (37) whose amplitudes are the b_m's and c_m's can be interpreted in

terms of modes excited at the interface by the incident $n = \vec{1}, \vec{2}$ modes. The interpretation of the terms in (37) whose amplitudes are the a_n's follows from the fact that expression (40) for a_n depends only on the propagation constants and mode vectors of the medium in which the source is located, i.e., it is not influenced by the presence of the interface. In addition, the corresponding modes are such that they carry energy or decay away from the source. The interpretation of the terms in (37) having the b_m's and c_m's as amplitudes is based on (45) and (49), which state that b_m and c_m depend linearly on the incident mode amplitudes $a_{\vec{1}}$ and $a_{\vec{2}}$ and on the coefficients Γ_{mn} that describe the plane wave scattering (reflection and transmission) properties of the planar interface. Moreover, in this case the corresponding modes are such that they carry energy or decay away from the interface.

The z component $\Psi_z(z)$ of the field transforms can be found from (17), which for $z \neq z'$ gives

$$\Psi_z(z) = - W_{zt} \cdot \Psi_t(z) \quad . \tag{51}$$

Since W_{zt} can be taken inside the summation signs of (37), $\Psi_z(z)$ will be given by (37) with $\Psi_t(\varkappa_n)$ replaced by

$$\Psi_z(\varkappa_n) = - W_{zt} \cdot \Psi_t(\varkappa_n) \quad , \tag{52}$$

which represents the z components of the modal fields. Finally, defining

$$\left. \begin{aligned} \Psi(z) &\equiv \Psi_t(z) + \underline{z}_o \Psi_z(z) \\[2ex] \Psi(\varkappa_n) &\equiv \Psi_t(\varkappa_n) + \underline{z}_o \Psi_z(\varkappa_n) \end{aligned} \right\} \tag{53}$$

it is seen that the complete Fourier transform $\Psi(z)$ of the fields radiated by the point source is given by (37) with $\Psi_t(\varkappa_n)$ replaced by $\Psi(\varkappa_n)$. Note that the electric and magnetic field vectors $\underline{\mathcal{E}}_n$ and $\underline{\mathcal{H}}_n$ in $\Psi(\varkappa_n)$ are those of the plane wave propagating as $\exp[-jk_o(\xi x + \eta y + \varkappa_n z)]$ in the appropriate medium.

For convenience in later chapters, let

$$A_n = - e_n \left[\Psi^+(\varkappa_n^*) \cdot \hat{\Phi}_o \right] / M_n \tag{54}$$

so that a_n in (40) becomes $a_n = A_n e^{jk_o \varkappa_n z'}$ (in Appendix A, a useful form for A_n is derived for the case of real $\varkappa_n$). Substituting $\Psi(z)$ as given in (37) with $\Psi_t(\varkappa_n)$ replaced by $\Psi(\varkappa_n)$, into (2) and using (40), (45), (49) and (54), the actual fields radiated by the point source can be written as

$$\left.\begin{matrix} \underline{E}(\underline{r}) \\ \underline{H}(\underline{r}) \end{matrix}\right\} = \sum_{m=\vec{3},\vec{4}} \sum_{n=\vec{1},\vec{2}} \iint_{-\infty}^{\infty} \left\{\begin{matrix} \underline{\mathcal{E}}_m \\ \underline{\mathcal{H}}_m \end{matrix}\right\} \Gamma_{mn} A_n e^{-jk_o\left[\xi x + \eta y + \varkappa_m z - \varkappa_n z'\right]} d\xi \, d\eta \tag{55}$$

in the region $z > 0$, while in the region $z' < z < 0$,

$$\left.\begin{matrix} \underline{E}(\underline{r}) \\ \underline{H}(\underline{r}) \end{matrix}\right\} = \sum_{n=\vec{1},\vec{2}} \int_{-\infty}^{\infty}\!\!\int \left\{\begin{matrix} \underline{\mathcal{E}}_n \\ \underline{\mathcal{H}}_n \end{matrix}\right\} A_n e^{-jk_o\left[\xi x + \eta y + \varkappa_n(z - z')\right]} d\xi \, d\eta$$

$$+ \sum_{m=\vec{1},\vec{2}} \sum_{n=\vec{1},\vec{2}} \iint_{-\infty}^{\infty} \left\{\begin{matrix} \underline{\mathcal{E}}_m \\ \underline{\mathcal{H}}_m \end{matrix}\right\} \Gamma_{mn} A_n e^{-jk_o\left[\xi x + \eta y + \varkappa_m z - \varkappa_n z'\right]} d\xi \, d\eta \tag{56}$$

where $\underline{\mathcal{E}}_n$ and $\underline{\mathcal{H}}_n$ are the electric and magnetic field polarization vectors in $\Psi(\varkappa_n)$, i.e., they are the vector amplitudes of the plane wave fields propagating as $e^{-jk_o(\xi x + \eta y + \varkappa_n z)}$. In the region $z < z'$

$$\left.\begin{matrix} \underline{E}(\underline{r}) \\ \underline{H}(\underline{r}) \end{matrix}\right\} = \sum_{n=\vec{1},\vec{2}} \iint_{-\infty}^{\infty} \left\{\begin{matrix} \underline{\mathcal{E}}_n \\ \underline{\mathcal{H}}_n \end{matrix}\right\} A_n e^{-jk_o\left[\xi x + \eta y + \varkappa_n(z - z')\right]} d\xi \, d\eta$$

$$+ \sum_{m=\vec{1},\vec{2}} \sum_{n=\vec{1},\vec{2}} \iint_{-\infty}^{\infty} \left\{\begin{matrix} \underline{\mathcal{E}}_m \\ \underline{\mathcal{H}}_m \end{matrix}\right\} \Gamma_{mn} A_n e^{-jk_o\left[\xi x + \eta y + \varkappa_m z - \varkappa_n z'\right]} d\xi \, d\eta \; . \tag{57}$$

In writing (55), (56) and (57) the order of integration and summation has been interchanged to facilitate the asymptotic evaluation of the fields. Also, while the integrations are indicated as being over the real (ξ, η) plane in (55), (56) and (57), the actual surfaces of integration must be suitable deformed into complex (ξ, η) space about the singularities of the various integrands, as will be discussed presently.

The first sums in (56) and (57) represent the primary or direct fields radiated by the source into the ε_1 medium while the double sums in (55), (56) and (57) represent the secondary or scattered fields generated by the direct field incident on the interface. The asymptotic evaluation and ray-optical interpretation of the various integral contributions in (55), (56) and (57) are considered in subsequent chapters.

Chapter II

EVALUATION AND INTERPRETATION OF THE DIRECT, SCATTERED
AND LATERAL RAY CONTRIBUTIONS TO THE FAR FIELDS

A. INTRODUCTION

In Chapter I a rigorous Fourier integral representation was found
for the fields radiated by a time-harmonic point source in the presence of
a planar interface between two homogeneous, lossless, anisotropic media.
The asymptotic evaluation of this integral representation for observation
points in the far-field region is considered in this chapter. The results of
the asymptotic evaluation are cast into a coordinate invariant, ray-optical
form containing such physically significant quantities as ray directions, ray
lengths, ray phases, divergence coefficients and plane wave scattering
coefficients. This ray-optical form exhibits explicitly the local nature of
wave propagation. It is precisely this local behavior that permits a gen-
eralization of the ray-optical theory to gently curved geometries, which may
not be amenable to a rigorous treatment. The ray-optical formalism deve-
loped here for anisotropic media is consistent with Keller's theory of
diffraction in isotropic media. [9]

The asymptotic evaluation of the double Fourier integral representa-
tion is carried out by first integrating over one of the transform variables
using the steepest descent technique (see Appendix B). The result of the
steepest descent evaluation is then integrated over the second transform
variable by the method of stationary phase (see Section B and the first part
of Section E). In Section C, the stationary point contributions to the asymp-
totic evaluation are interpreted in terms of direct, reflected and transmitted
rays. Some properties of the scattered ray fields that are associated with
caustics are considered in Appendix C. The lateral ray interpretation of
the branch curve contributions is given in Section E and Appendix E.

An extension of the ray-optical results obtained for the planar inter-
face problem is postulated whereby the fields reflected from and transmitted
through an arbitrary gently curved interface between two arbitrary homo-

geneous, anisotropic, lossless media can be found. The details of this extension are presented in Section D and are found to require a suitable modification of the ray divergence coefficient, which is carried out in Appendix D.

The ray interpretation of the surface wave contribution to the far fields is not considered in this chapter since it requires a knowledge of the relation between the group velocity of surface waves and their energy flow. This relation is derived in Chapter III and the ray interpretation of the surface wave contribution is given in Chapter V.

B.   ASYMPTOTIC EVALUATION OF THE GENERIC INTEGRALS

As discussed in Chapter I, the fields radiated by the point source in Fig. I-1 contain a component $\underline{E}_d$ radiated directly by the source into the $\underset{\sim}{\epsilon}_1$ medium and a scattered component $\underline{E}_\Gamma$ generated by the direct field incident on the interface.[*]   From (I-56) and (I-57), the direct component $\underline{E}_d$ is seen to be

$$\underline{E}_d = \sum_n \underline{I}_n \, , \quad n = \begin{cases} \vec{1}, \, \vec{2} & \text{for } z' \lessgtr z < 0 \\ \overleftarrow{1}, \, \overleftarrow{2} & \text{for } z < z' \end{cases} \tag{1}$$

where

$$\underline{I}_n = \int\!\!\!\int\limits_{-\infty}^{\infty} A_n(\xi, \eta) \, \underline{\pmb{\delta}}_n(\xi, \eta) e^{-jk_o\left[\xi x + \eta y + \varkappa_n(z - z')\right]} \, d\xi \, d\eta \, , \tag{2}$$

$\underline{\pmb{\delta}}_n(\xi, \eta)$ being the polarization vector of the nth plane wave and $A_n(\xi, \eta)$ its excitation coefficient.   The scattered component $\underline{E}_r$ is seen from (I-55), (I-56) and (I-57) to be

$$\underline{E}_\Gamma = \sum_n \sum_m \underline{I}_{mn}, \quad n = \vec{1}, \, \vec{2} \; ; \; m = \begin{cases} \vec{3}, \, \vec{4} & \text{for } z > 0 \\ \overleftarrow{1}, \, \overleftarrow{2} & \text{for } z < 0 \end{cases} \tag{3}$$

where

$$\underline{I}_{mn} = \int\!\!\!\int\limits_{-\infty}^{\infty} \underline{\pmb{\delta}}_m(\xi, \eta) \, \Gamma_{mn}(\xi, \eta) A_n(\xi, \eta) e^{-jk_o\left[\xi x + \eta y + \varkappa_m z - \varkappa_n z'\right]} \, d\xi \, d\eta \tag{4}$$

and the scattering coefficients $\Gamma_{mn}(\xi, \eta)$ are found from the continuity conditions at the interface.   Recall from Chapter I that the $n = \vec{1}, \, \vec{2}$ plane waves of the $\underset{\sim}{\epsilon}_1$ medium are upgoing (they carry energy or decay in the positive z direction) while the $n = \overleftarrow{1}, \, \overleftarrow{2}$ plane waves are downgoing (they carry energy or decay in the negative z direction).   In the $\underset{\sim}{\epsilon}_2$ medium the $n = \vec{3}, \vec{4}$ plane

---

[*] For simplicity, only the expressions for the electric field are given here. The expressions for the magnetic field differ from those for the electric field only in that the plane-wave magnetic field polarization vector $\underline{\pmb{\mu}}_n$ replaces $\underline{\pmb{\delta}}_n$.

waves are upgoing and the $n = \overleftarrow{3}, \overleftarrow{4}$ plane waves are downgoing, as is depicted in Fig. I-1.

The integrals defined in both (2) and (4) are of the generic form

$$I = \int\int_{-\infty}^{\infty} \underline{F}(\xi, \eta) \, e^{-jk_o P(\xi, \eta)} \, d\xi \, d\eta \tag{5}$$

and will be evaluated for large values of k_o. The asymptotic evaluation of (5) is predicated on the existence of a large parameter in the exponent, which we have taken to be k_o for convenience. However, a more detailed investigation of the exponents appearing in (2) and (4) will show that the distance from the source to the observation point can also be factored out of $P(\xi, \eta)$, thus permitting the removal of the restriction on k_o, substituting instead the requirement that the observation point be many free-space wave lengths from the source. This comment applies throughout.

1. Comments on the Method of Integration

The method employed in performing the asymptotic evaluation of the integrals appearing in (5) is to first apply the steepest descent technique to the η integration with ξ an arbitrary real parameter. This result, which includes the saddle point, brach point and pole contributions, is then integrated over ξ to first order by the method of stationary phase. This method of evaluating the double Fourier integrals has been chosen since it yields both the branch curve contributions (lateral rays) and the real pole contributions (surface wave rays) in addition to the first-order, real stationary point contributions (direct and scattered rays).

The stationary points are those values of ξ and η at which the first derivatives of the phase with respect to ξ and η are zero and it is from the neighborhood of the stationary points that the principal contributions to (2) and (4) arise. The complete asymptotic series representing the stationary point contributions for the double integrals has been found by several authors -- see Chako[17,18,19], Nagel[20] and Jones and Kline[21], who survey previous work. The terms in the asymptotic series go as integral powers of $1/k_o$, i.e., the first term goes as $1/k_o$, the second as $1/k_o^2$, etc. At those

stationary points for which the phase function is real, the evaluation of
the double integrals used in this paper gives the first term of the asymptotic
series. This term results from the saddle point contribution to the inte-
gration and is the only term of importance in formulating the ray-optical
representation for the stationary point contribution to the far fields of
the source.

However rigorously other methods are able to describe the stationary
point contributions to the double integrals of (2) and (4), they do not as yet
seem to have been developed sufficiently to give the branch curve contribu-
tions or the pole contributions.[*] The branch curves are the loci of points
in the (ξ, η) plane at which two or more of the four solutions of (I-24) for
$\varkappa_n$ of the $\underset{\sim}{\epsilon}_1$ medium are equal, or at which two or more solutions of (I-24)
for $\varkappa_n$ of the $\underset{\sim}{\epsilon}_2$ medium are equal. Branch curve contributions, which
occur only in the scattered field integrals (4), arise from the branch point
contributions to the steepest descent integration over η and will be shown in
Section E to be $0(1/k_o^2)$. Although the second term in the asymptotic series
for the stationary point contribution, which is also $0(1/k_o^2)$, will be neglected,
the branch curve contribution is retained since in shadow regions, where all
orders of the stationary point contributions are exponentially small, the
branch curve contribution, when present, is of algebraic order and thus will
give the dominant contribution to the far fields. The method used here to
evaluate the branch curve contributions was previously employed in a
different context by Rosenbaum[5] for double integrals of a somewhat simpler
generic form.

For completeness, a brief discussion of the steepest descent integra-
tion over η, which has been discussed by several authors, is given in
Appendix B.

2. Evaluation of the Stationary Point Contribution

The first-order saddle point contribution to the η integration of (5)

----

[*] The poles give rise to residues in the η integral, which are then integrated
over ξ by the method of stationary phase. This contribution can be inter-
preted in terms of surface wave rays using the energy transport properties
of surface waves in plane-stratified, anisotropic, lossless media, which are
derived in Chapter III.

is given by (B-3) of Appendix B, which is valid when the saddle points are isolated from one another and from the branch points of $\underline{F}(\xi,\eta)$ and $P(\xi,\eta)$. Since $P_2(\xi,\eta) \equiv \partial P(\xi,\eta)/\partial \eta$ is a function of ξ and η, solving the saddle point condition $P_2(\xi,\eta) = 0$ or η_s gives the possibly multivalued function

$$\eta_s = \eta_s(\xi) \quad . \tag{6}$$

If $\eta_s(\xi)$ is indeed a multivalued function with branch points at which $P(\xi,\eta_s)$ is real, then two or more saddle points will coalesce as ξ approaches the branch point of $\eta_s(\xi)$ and $P_{22}(\xi,\eta_s)$ will approach zero. Near the branch point of $\eta_s(\xi)$, (B-3) is invalid so that the branch point of $\eta_s(\xi)$ would seem to be a singular point for the stationary point result. This is, however, not generally the case, since this singularity is usually introduced only by the choice of the (x, y) coordinates and its location depends on the choice of the coordinates. Accordingly, it will be seen that the stationary point result for the point source is not necessarily singular at points for which $P_{22} = 0$.

While the saddle points may be isolated from the branch points of $\underline{F}(\xi,\eta)$ and $P(\xi,\eta)$ for most values of ξ, as ξ varies a saddle point and branch point may approach each other and coalesce at some value of ξ. However, as long as the stationary phase points in the ξ integration are not near the values of ξ at which a saddle point and a branch point coalesce in the complex η plane, the stationary phase evaluation will be valid since the principal contribution to the integral of the terms of (B-3) over ξ comes from neighborhoods of the stationary phase points. The actual singularities of the stationary point contributions to the point source fields will be discussed later.

The stationary phase points for the integration of each term of (B-3) over ξ are those values of ξ for which $P(\xi,\eta_s)$ is real and

$$\frac{d}{d\xi} P(\xi,\eta_s) = P_1(\xi,\eta_s) + P_2(\xi,\eta_s)\frac{d}{d\xi}\eta_s(\xi) = 0 \tag{7}$$

(the subscripts 1 and 2 refer to partial differentiation with respect to ξ and η).*

----
* Note that $\operatorname{sgn} P_{22}(\xi,\eta_s)$ in (B-3) is constant except for a jump of ± 2 occurring at the branch points of $\eta_s(\xi)$, where $P_{22}(\xi,\eta_s) = 0$.

But $P_2(\xi, \eta_s) = 0$ is the saddle point condition in the η integration so that, in view of the sum in (B-3), a contribution to the double integral comes from each stationary point (ξ_s, η_s), defined by the condition

$$P_1(\xi, \eta) = P_2(\xi, \eta) = 0 \tag{8}$$

for which $P(\xi_s, \eta_s)$ is real. Note that the above analysis does not apply when the solution of (8) for ξ_s is such that $\dfrac{d\eta_s}{d\xi} = -\dfrac{P_{12}(\xi, \eta_s)}{P_{22}(\xi, \eta_s)} \to \infty$ (see after (10)) since this would imply that in the η integration two saddle points are close together or that a branch point of $P(\xi, \eta)$ is near the saddle point. Performing the stationary phase integration[22] of the terms in (B-3) over ξ and summing over all stationary points gives the stationary point contribution $\underline{I}_s$ to the integral in (5) as

$$\underline{I}_s \sim \frac{2\pi}{k_o} \sum_{\text{S.P.}} \left\{ \frac{\underline{F}(\xi, \eta) e^{-jk_o P(\xi, \eta)}}{\sqrt{|P_{22}|\,|d^2 P/d\xi^2|}} \, e^{-j\frac{\pi}{4}\left(\operatorname{sgn} P_{22} + \operatorname{sgn} \frac{d^2 P}{d\xi^2}\right)} \right\}_{(\xi_s, \eta_s)} \tag{9}$$

where (ξ_s, η_s) is the stationary point and $d^2 P/d\xi^2$ is the total second derivative of $P[\xi, \eta_s(\xi)]$. Using (7) and (8), the total second derivative of $P(\xi, \eta_s)$ is seen to be

$$\frac{d^2 P}{d\xi^2} = P_{11} + 2 P_{12} \frac{d\eta_s}{d\xi} + P_{22} \left(\frac{d\eta_s}{d\xi}\right)^2 . \tag{10}$$

Furthermore, since $P_2[\xi, \eta_s(\xi)] \equiv 0$ for all ξ, $d\eta_s/d\xi = -P_{12}/P_{22}$ at $\eta = \eta_s(\xi)$ so that (10) can be written

$$\frac{d^2 P}{d\xi^2} = \frac{1}{P_{22}} (P_{11} P_{22} - P_{12}^2) . \tag{11}$$

Substituting (11) into the denominator of (9) gives

$$\underline{I}_s \sim \frac{2\pi}{k_o} \sum_{S.P.} \left\{ \frac{F(\xi, \eta) e^{-jk_o P(\xi, \eta)}}{\sqrt{|P_{11} P_{22} - P_{12}^2|}} e^{-j\frac{\pi}{4} \delta} \right\}_{(\xi_s, \eta_s)}$$ (12)

where δ is defined by

$$\delta \equiv \text{sgn } P_{22} + \text{sgn } \frac{d^2 P}{d\xi^2} = \text{sgn } P_{22} + \text{sgn} \left(\frac{P_{11} P_{22} - P_{12}^2}{P_{22}} \right). \quad (13)$$

In Appendix C it is shown that δ can be written as

$$\delta = \text{sgn } P_{uu} + \text{sgn } P_{vv} \qquad (14)$$

where P_{uu} and P_{uv} are the second partial derivatives of P in the (u, v) coordinate system, which is rotated from the (ξ, η) coordinate system and for which the mixed second partial $P_{uv} = 0$. This expression for δ will prove useful later on.

The stationary point result given in (12) is valid whenever $P_{11} P_{22} - P_{12}^2 \neq 0$ and, as previously mentioned, is the first term in the complete asymptotic series for the contribution from isolated stationary points. Observe that if $P_{22} = 0$, in which case (B-3) is not valid, the quantity $P_{11} P_{22} - P_{12}^2$ need not be zero. The Hessian $P_{11} P_{22} - P_{12}^2$ will be zero when the observation point lies on a caustic surface or on a shadow boundary of the point source. For such observation points a different asymtotic expansion than that leading to (12) is required for the evaluation of (5).

C. RAY INTERPRETATION FOR THE STATIONARY POINT CONTRIBUTIONS

The ray interpretations of the stationary point contributions to the integrals defined in (2) and those defined in (4) will be considered separately. The ultimate goal will be to obtain a coordinate-independent representation for the stationary point contributions in terms of physically significant ray-optical quantities.

Many aspects of the ray interpretation of the stationary point contributions, as well as the branch curve contributions, will be explained in terms of the plane wave dispersion surfaces of the ϵ_1 and ϵ_2 media. For this reason a brief discussion is given below of several important properties of the dispersion surfaces that are pertinent to the present discussion. The plane wave dispersion surface of either medium is the locus of points in real (ξ, η, κ) space that satisfy (I-24). The shape and orientation of the dispersion surface for each medium is determined by the parameters and optic axes of the medium and does not depend on the choice of the (x, y, z) coordinate system. The most important property of these surfaces for the ray interpretation of the far fields in lossless media is that the real part of the complex Poynting vector of a plane wave having wave vector $\underline{k} = \underline{x}_o \xi + \underline{y}_o \eta + \underline{z}_o \kappa$ is parallel to the unit normal $\underline{\nu}$ to the dispersion surface at the point (ξ, η, κ) on the surface. [15, 23] In all that follows, the unit normal $\underline{\nu}$ will be assumed to have the same sense as the real **part** of the complex Poynting vector of the corresponding plane wave.

The nth branch of the dispersion surface will be defined as the set of points $[\xi, \eta, \kappa_n(\xi, \eta)]$ where $\kappa_n(\xi, \eta)$ is a continuous, single-valued solution of (I-24) and ξ and η are such that $\kappa_n(\xi, \eta)$ is real. A branch of the dispersion surface may be of infinite extent, i.e., $\kappa_n(\xi, \eta)$ real for all ξ and η. However, if $\kappa_n(\xi, \eta)$ is not real for all real ξ and η, the nth branch of the dispersion surface will have a boundary curve or rim. The projection of this rim into the (ξ, η) plane is a poartion of the branch curve since $\kappa_n(\xi, \eta)$ changes from real to complex as the projected curve is crossed,

which can happen only if two or more real solutions of the quartic (I-24) are equal on the projected curve. Furthermore, if the dispersion surfaces are smooth, i.e., the unit normal to the surface is a continuous function of position on the surface, the normal to the surface at points on the rim will be parallel to the (ξ, η) plane.* It is assumed that the $\underset{\sim}{\varepsilon}_1$ and $\underset{\sim}{\varepsilon}_2$ media are such that the dispersion surfaces are smooth. Uniaxial crystals and gyrotropic, cold, electron plasmas, except at plasma or hybrid resonances,[24] are examples of such media.

1. Direct Rays

For the integrals defined in (2), $P(\xi, \eta) = \xi x + \eta y + \varkappa_n(z - z')$ and the stationary point condition (8) becomes

$$x + (z - z') \frac{\partial \varkappa_n}{\partial \xi} = y + (z - z') \frac{\partial \varkappa_n}{\partial \eta} = 0 : n = \begin{cases} \vec{1}, \vec{2} & \text{for } z - z' > 0 \\ \overleftarrow{1}, \overleftarrow{2} & \text{for } z - z' < 0 \end{cases} .$$

(15)

In order to interpret (15) in ray-optical terms observe that the unit normal $\underline{\nu}_n$ to the nth branch of the dispersion surface may be expressed as

$$\underline{\nu}_n = \pm (\underline{x}_o \frac{\partial \varkappa_n}{\partial \xi} + \underline{y}_o \frac{\partial \varkappa_n}{\partial \eta} - \underline{z}_o) \Big/ \sqrt{\left(\frac{\partial \varkappa_n}{\partial \xi}\right)^2 + \left(\frac{\partial \varkappa_n}{\partial \eta}\right)^2 + 1} \quad (16)$$

where the minus sign is to be used for $n = \vec{1}, \vec{2}$, since $\underline{\nu}_n$ has been assumed to be in the direction of energy flow of the corresponding plane wave and for these values of n, the plane waves carry power in the positive z direction. For similar reasons, the plus sign must be used for $n = \overleftarrow{1}, \overleftarrow{2}$. In subsequent sections where the normal to the dispersion surface of the $\underset{\sim}{\varepsilon}_2$ medium will be needed, (16) can be used with the minus sign for $n = \vec{3}, \vec{4}$ and the plus sign for $n = \overleftarrow{3}, \overleftarrow{4}$.

Defining $\underline{L} = \underline{x}_o x + \underline{y}_o y + \underline{z}_o (z - z')$, which is the displacement of the observation point from the source, it is seen that (15) is equivalent to the

---

* By direct expansion of (I-30) for $\varkappa_n$ real it can be shown that $M_n = 2\text{Re}(\underline{z}_o \cdot \underline{\mathcal{E}}_n \times \underline{\mathcal{H}}_n^*)$ so that $M_n = 0$ on the rim of the nth branch of the dispersion surface, i.e., when the eigenvalues of (I-23) are degenerate.

statement that $\underline{L} \times \underline{\nu}_n = 0$ and $\underline{L} \cdot \underline{\nu}_n > 0$, i.e., that $\underline{\nu}_n$ be in the direction of $\underline{L}$. In view of the sum in (12), the stationary point condition (15) for the direct field integrals defined in (2) implies that a contribution to $\underline{I}_n$ comes from every point on the nth branch of the dispersion surface at which $\underline{\nu}_n$ is parallel to and has the same sense as $\underline{L}$. Hence, taking into account the sum indicated in (1), a stationary point contribution to the direct fields at a point in the $\underline{\varepsilon}_1$ medium arises from every point on the entire dispersion surface of the $\underline{\varepsilon}_1$ medium at which $\underline{\nu}$ is in the same direction as the displacement vector $\underline{L}$. In other words, while the source radiates a continuum of rays corresponding to all points on the dispersion surface of the $\underline{\varepsilon}_1$ medium, only those rays in the direction $\underline{L}$ contribute to the fields at the observation point.

For the direct field integrals (2), $\underline{F}(\xi, \eta)$ evaluated at the stationary point is the vector amplitude $A_n \, \underline{b}_n$ of the plane wave carrying energy in the direction of $\underline{L}$. Since the wave vector of this plane wave is $\underline{k}_n = \underline{x}_o \xi + \underline{y}_o \eta + \underline{z}_o \varkappa_n$, for the integrals defined in (2), $P(\xi_s, \eta_s) = LN_n$ where $L = |\underline{L}|$ and

$$N_n = \underline{\nu}_n \cdot \underline{k}_n \tag{17}$$

is the ray-refractive index of the nth branch of the dispersion surface.

The quantity $P_{11} P_{22} - P_{12}^2$ in (14) can be put into ray-optical terms if it is recognized that the Gaussian curvature G_n of the nth branch of the dispersion surface can be written[25]

$$G_n = \left[\frac{\partial^2 \varkappa_n}{\partial \xi^2} \frac{\partial^2 \varkappa_n}{\partial \eta^2} - \left(\frac{\partial^2 \varkappa_n}{\partial \xi \, \partial \eta} \right)^2 \right] \cos^4 \theta_n \tag{18}$$

where θ_n is the angle between $\underline{\nu}_n$ and $\underline{z}_o$. Because of the form of $P(\xi, \eta)$ in the integrals given in (2), using (18) it is seen that

$$P_{11} P_{22} - P_{12}^2 = L^2 G_n / \cos^2 \theta_n \quad . \tag{19}$$

Finally, in Appendix C it is shown that δ defined in (13) can be written in terms of the principal curvatures K_{n1} and K_{n2} of the nth branch of the

dispersion surface as

$$\delta = \text{sgn } K_{n1} + \text{sgn } K_{n2} \quad . \tag{20}$$

Equation (20) was derived assuming the principal curvatures to be positive if the associated centers of curvature lie on the same side of the dispersion surface as $\underline{\nu}_n$ and negative otherwise.

Using (19) and (20) in (12) as well as the form for $P(\xi_s, \eta_s)$ and $\underline{F}(\xi_s, \eta_s)$ described above, the stationary point contributions to the direct fields (1) are given by

$$\underline{E}_d \sim \frac{2\pi}{k_o} \sum_n \sum_{\text{S.P.}} \left\{ \frac{A_n \underline{b}_n |\cos \theta_n|}{L \sqrt{|G_n|}} e^{-jk_o L N_n} e^{-j\frac{\pi}{4}(\text{sgn} K_{n1} + \text{sgn} K_{n2})} \right\}_{(\xi_s, \eta_s)}$$

$$\tag{21}$$

which is the total far-field ray contribution to the direct fields (no branch point or pole contributions occur in the η integration in (2), as is discussed in Appendix B). In (21), $n = \vec{1}, \vec{2}$ for $z' < z < 0$ while for $z < z'$, $n = \overleftarrow{1}, \overleftarrow{2}$. As previously explained, the double sum in (21) is equivalent to summing over the contributions from every point on the total dispersion surface of the $\underline{\epsilon}_1$ medium at which $\underline{\nu}$ is in the same direction as $\underline{L}$.

The term $|\cos \theta_n|$ in (21) does not describe a fundamental property of the ray fields since from (A-7) it is seen that

$$A_n |\cos \theta_n| = - (\frac{k_o}{2\pi})^2 (\underline{b}_n^* \cdot \underline{J}_o + \underline{\mu}_n^* \cdot \underline{M}_o) / 2 | \text{Re}(\underline{b}_n \times \underline{\mu}_n^*)| \quad , \tag{22}$$

which is independent of the choice of the (x, y, z) coordinate system. That $A_n |\cos \theta_n|$, and hence (21), are independent of the choice of the (x, y, z) coordinate system reflects the fact that expressions (1) and (2) for the direct field are the same as those representing the fields radiated by a point source in an infinite $\underline{\epsilon}_1$ medium, which can be evaluated in any (x, y, z) system. [2] Moreover, while the derivation leading to (21) is not valid for $\cos \theta_n \approx 0$ (the stationary points are near branch curves), the ray fields of (21) are still valid since for another choice of the z axis, the stationary points would not be near the corresponding branch curves. The asymptotic expression for

$\underline{E}_d$ given in (21) is not valid for observation points near a shadow boundary, in which case $G_n \approx 0$ at a stationary point.

Examining the ray fields in (21), they are seen to be determined by the following factors: a) the polarization vector $\underline{b}_n$ of the plane wave carrying energy in the direction of $\underline{L}$; b) the invariant excitation coefficient $\frac{2\pi}{k_o} A_n |\cos \theta_n|$ of this plane wave, which together with $\exp\left[-j\frac{\pi}{4} (\text{sgn } K_{n1} + \text{sgn } K_{n2})\right]$ gives the ray field excitation; c) the phase change $\exp(-jk_o LN_n)$ of the plane wave along the ray; d) the angular ray divergence coefficient $L\sqrt{|G_n|}$. The quantity $1/L^2 |G_n|$ is the relative ray flux density at a distance L along the ray.

2. Reflected and Transmitted Rays

Starting with the formal asymptotic stationary point result given in (12), this result will be interpreted for the scattered (reflected and transmitted) fields. As a first step, the ray interpretation of the stationary point condition will be considered. Subsequently, the significance of the various quantities appearing in (12) and their ray-optical interpretation will be considered.

In the integrals defined in (4), the phase function is $P(\xi, \eta) = \xi x + \eta y + \varkappa_m z - \varkappa_n z'$ so that the stationary point condition (8) is

$$x + \frac{\partial \varkappa_m}{\partial \xi} - z' \frac{\partial \varkappa_n}{\partial \xi} = y + z \frac{\partial \varkappa_m}{\partial \eta} = 0 : n = \vec{1}, \vec{2} ; \quad m = \begin{Bmatrix} \vec{3}, \vec{4} & \text{for } z > 0 \\ \vec{1}, \vec{2} & \text{for } z < 0 \end{Bmatrix}.$$

(23)

with the assumption that $\underline{\nu}$ has the same sense as energy flow, (23) can be interpreted as requiring ξ_s and η_s to be such that a ray leaves the source along the direction $\underline{\nu}_n(\xi_s, \eta_s)$ and upon incidence on the interface at $(x', y', 0)$ is reflected or transmitted from this point along the direction $\underline{\nu}_m(\xi_s, \eta_s)$ to the observation point (x, y, z) -- see Fig. 1. Defining $\underline{L}_n = \underline{x}_o x + \underline{y}_o y - \underline{z}_o z'$ and $\underline{L}_m = \underline{x}_o (x - x') + \underline{y}_o(y - y') + \underline{z}_o z$ and using (16),

it is easily shown that (23) is equivalent to the conditions $\underline{\nu}_n \times \underline{L}_n = \underline{\nu}_m \times \underline{L}_m = 0$ for the same ξ_s and η_s with $\underline{\nu}_n \cdot \underline{L}_n$ and $\underline{\nu}_m \cdot \underline{L}_m$ positive. Thus (23) implies that for lossless media, the ray path, whose segments are $\underline{L}_n$ and $\underline{L}_m$, is the trajectory of energy flow of locally plane waves that are scattered at the interface according to Snell's law.

For the integrals under discussion, $\underline{F}(\xi_s, \eta_s) = \underline{b}_m \Gamma_{mn} A_n$ is the vector amplitude of the scattered plane wave carrying energy in the direction of $\underline{L}_m$. Also, since $P(\xi, \eta)$ can be written in the form $P(\xi, \eta) = \xi x' + \eta y' - \varkappa_n z' + \xi(x - x') + \eta(y - y') + \varkappa_m z$, it is seen that $P(\xi_s, \eta_s) = L_n N_n + L_m N_m$ where $L_n = |\underline{L}_n|$, $L_m = |\underline{L}_m|$ and N_n and N_m are the ray-refractive indices defined in (17) of the nth and m^{th} branches of the dispersion surfaces evaluated at the stationary point.

A ray-optical form for the Hessian $P_{11} P_{22} - P_{12}^2$ can be found with the help of the relation $z = L_m \cos \theta_m$, where $\cos \theta_m = \underline{\nu}_m \cdot \underline{z}_0$, and expression (18) for the Gaussian curvature G_m of the mth branch of the dispersion surface. Using these and for $G_m \neq 0$,

$$P_{11} P_{22} - P_{12}^2 = \frac{G_m}{\cos \theta_m} \left\{ L_m^2 - L_m z' \frac{\cos^3 \theta_m}{G_m} \left[\frac{\partial^2 \varkappa_m}{\partial \xi^2} \frac{\partial^2 \varkappa_n}{\partial \eta^2} + \frac{\partial^2 \varkappa_m}{\partial \eta^2} \frac{\partial^2 \varkappa_n}{\partial \xi^2} \right. \right.$$

$$\left. - 2 \frac{\partial^2 \varkappa_m}{\partial \xi \partial \eta} \frac{\partial^2 \varkappa_n}{\partial \xi \partial \eta} \right] + z'^2 \frac{\cos^2 \theta_m}{G_m} \left[\frac{\partial^2 \varkappa_n}{\partial \xi^2} \frac{\partial^2 \varkappa_n}{\partial \eta^2} - \left(\frac{\partial^2 \varkappa_n}{\partial \xi \partial \eta} \right)^2 \right] \right\} . \tag{24}$$

The coefficients of z'^2 and $L_m z'$ in (24) can easily be put into invariant form; however, such an expression for the coefficient of $L_m z'$ is complicated. The expression inside the brackets of (24) is quadratic in L_m and thus if the roots of the quadratic are designated by L_{m1} and L_{m2}, (24) can be written as

$$P_{11} P_{22} - P_{12}^2 = \frac{G_m}{\cos^2 \theta_m} (L_m - L_{m1})(L_m - L_{m2}) . \tag{25}$$

The roots L_{m1} and L_{m2} are invariant under a rotation of the (ξ, η) coordinate system since the Hessian $P_{11} P_{22} - P_{12}^2$ is, thus permitting the ray-optical interpretation of (24), which will be given presently.
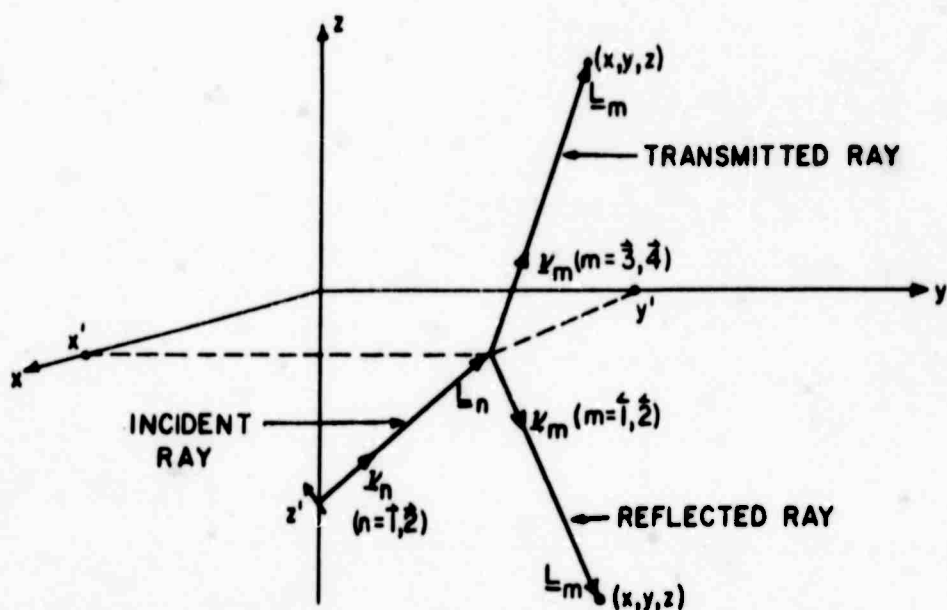
(a) Ray structure for the scattered fields
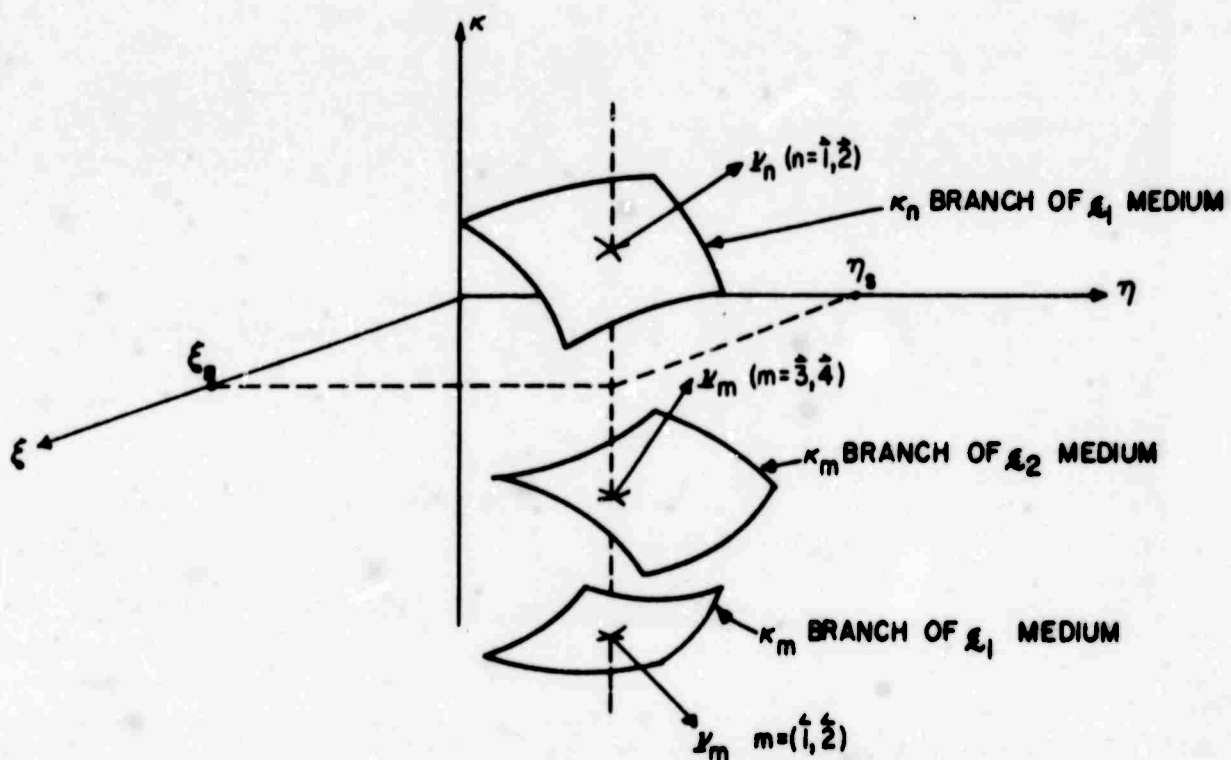
(b) Determination of scattered ray directions from the dispersion surfaces

Using the form for $\underline{F}(\xi_s, \eta_s)$ and $P(\xi_s, \eta_s)$ discussed above and writing δ of (14) as δ_{mn}, it is seen with the help of (25) and (12) that the stationary point contribution to $\underline{E}_\Gamma$ of (3) can be written as

$$(\underline{E}_\Gamma)_{S.P.} \sim \frac{2\pi}{k_o} \sum_{m,n} \sum_{S.P.} \left\{ \frac{\underline{b}_m \Gamma_{mn} A_n |\cos\theta_m| e^{-j\frac{\pi}{4}\delta_{mn}}}{\sqrt{|G_m|} \sqrt{|L_m - L_{m1}|} |L_m - L_{m2}|} e^{-jk_o(L_n N_n + L_m N_m)} \right\}_{(\xi_s, \eta_s)}$$

$$(26)$$

where $n = \vec{1}, \vec{2}$ and for observation points in the ε_2 medium $m = \vec{3}, \vec{4}$ while for observation points in the ε_1 medium $m = \overleftarrow{1}, \overleftarrow{2}$. The first sum in (26) is taken over all possible stationary points for particular values of m and n, and together with the second sum indicates that contributions come from all possible scattered rays reaching the observation point.

The characteristic features of the scattered ray fields are contained contained in the denominator of (26) and δ_{mn}, which will be considered together with their ray-optical interpretation in relation to the caustics of the scattered ray fields. Along the reflected ($m = \overleftarrow{1}, \overleftarrow{2}$) or transmitted ($m = \vec{3}, \vec{4}$) portion of a ray, L_m is positive and measures the distance along the ray from the interface. Thus, for each term L_{m1} and L_{m2} in (26) that is positive real, there will be an observation point along the ray at which $P_{11}P_{22} - P_{12}^2$, and hence the denominator of (26), are zero, indicating that the scattered portion of the ray is tangent to the caustic at this observation point.[*] Similarly, to each term L_{m1} and L_{m2} that is negative real, there will be a point on the mathematical extension of the scattered portion of the ray to negative values of L_m at which the extension is tangent to a virtual caustic. Hence for L_{m1} and L_{m2} real, $(L_m - L_{m1})$ and $(L_m - L_{m2})$ represent distances along the scattered ray to the observation point from the ray tangencies to real or virtual caustics. However, L_{m1} and L_{m2} may be a complex conjugate pair, in which case the particular scattered ray will never be tangent to a caustic, virtual or real. A discussion of the possibility of predicting whether L_{m1} and L_{m2} are complex, positive real or negative real from a simple inspection of

[*] The vanishing of G_m for a particular ray indicates that the entire scattered portion of the ray lies in a caustic or shadow boundary or that the denominator of (26) is linear in L_m, i.e., one of the roots of (24) is at infinity.

the dispersion surfaces is given in Appendix C.

Consider now the phase term δ_{mn} in (26), which is defined in (14). Although (14) does not display the ray-optical character of δ_{mn}, a ray-optical expression for it does exist; however, the ray-optical expression is not always simple and useful. In order to verify this statement, first consider the behavior of δ_{mn} as deduced from (14). Since P_{uu} and P_{vv} are equal to the eigenvalues of the symmetric matrix whose elements are $\partial^2/\partial\xi^2(\varkappa_m z - \varkappa_n z')$, $\partial^2/\partial\eta^2(\varkappa_m z - \varkappa_n z')$ and $\partial^2/\partial\xi\,\partial\eta\,(\varkappa_m z - \varkappa_n z')$, they will be continuous functions of $L_m = z/\cos\theta_m$ along a scattered ray. As such, P_{uu} and P_{vv} can change sign along a scattered ray only by going through zero, in which case $P_{11}P_{22} - P_{12}^2 = P_{uu}P_{vv} = 0$ and the ray is tangent to a caustic Consequently, δ_{mn}, which from (14) can only take on the values 0 or ± 2, will be constant along the ray except for jumps across the ray tangencies to a caustic of value ± 2 if the tangency is simple, i.e., $L_{m1} \neq L_{m2}$. As $L_m \to \infty$, the term $\varkappa_n z'$ in P can be neglected as compared to $\varkappa_m z$ in calculating the signs of P_{uu} and P_{vv}. Hence as $L_m \to \infty$ the value of δ_{mn} becomes equal to that for a point source located at the origin in an infinite medium having $\varkappa_m$ as a branch of its dispersion surface, and from (21) is seen to be

$$\delta_{mn} = \text{sgn } K_{m1} + \text{sgn } K_{m2} \tag{27}$$

where K_{m1} and K_{m2} are the principal curvatures of the mth branch of the dispersion surface. Since δ_{mn} changes only at the ray tangencies to a caustic, δ_{mn} is as given in (27) for all $L_m > \max.(L_{m1}, L_{m2})$.

As a result of the behavior of δ_{mn} described above, one is led to conjecture for L_{m1} and L_{m2} real that δ_{mn} can be written as $\text{sgn } K_{m1}(L_m - L_{m1}) + \text{sgn } K_{m2}(L_m - L_{m2})$ since this quantity is constant along a ray except at the ray tangencies to a caustic, across which it jumps by ± 2, and since it reduces to (27) for $L_m > \max.(L_{m1}, L_{m2})$. The foregoing expression can readily be identified as δ_{mn} when K_{m1} and K_{m2} are of the same sign --- see the first four cases in Table C-1 of Appendix C. However, in order to use the above expression when K_{m1} and K_{m2} are of opposite sign, it is essential to have a rule for assigning the proper curvature to L_{m1} and L_{m2}. Incorrect assignment

will yield a change in δ_{mn} across the ray tangencies that if of opposite sign to the correct value. In order correctly assign the principal curvatures in this case, one should first find the change of δ_{mn} across the ray tangencies from (14) or from (C-20) of Appendix C. Although the description of the change in δ_{mn} given in (C-20) is a purely ray-optical one, (C-20) is not very convenient to use since it requires a knowledge of the normal to the caustic surface at the ray tangency in question. For this reason, when K_{m1} and K_{m2} are of opposite sign, δ_{mn} is most easily found directly from (14) or, when applicable, from the fifth case in Table C-1.

The description of δ_{mn} given in the first five cases of Table C 1 is derived from (27) and the facts that $\delta_{mn} = 0, \pm 2$; the change in δ_{mn} is ± 2 for $L_{m1} \neq L_{m2}$; at $L_m = 0$, i.e., on the interface, and hence everywhere between the interface and the first ray tangency to a caustic,

$$\delta_{mn} = \operatorname{sgn} K_{n1} + \operatorname{sgn} K_{n2}. \tag{28}$$

Relation (28) holds since at $z = L_m \cos \theta_m = 0$, $P(\xi, \eta)$ is identical with the phase function for the direct fields at $z = 0$. In the last case of Table C-1, δ_{mn} cannot be simply specified when L_{m1} and L_{m2} are positive real since it will depend on the magnitude of the curvatures and the orientation of the mth and n^{th} branches of the dispersion surfaces. When L_{m1} and L_{m2} are complex or negative real in the last case of Table C-1, $\delta_{mn} = 0$ everywhere along the scattered ray. If $L_{m1} = L_{m2}$, the point of tangency of the ray to the caustic is also a focus and δ_{mn} changes by 0 or ± 4. In effect, the phase factor $e^{-j\frac{\pi}{4} \delta_{mn}}$ gives the connection formula for the fields along the ray as the point of tangency is crossed.

Aside from observation points on or near a caustic or shadow boundary, (26) is not valid when a stationary point is near a brach curve of either κ_m or κ_n ($\underline{L}_m$ or $\underline{L}_n$ is approximately parallel to the interface when this happens). Since the interface, in general, couples the plane waves corresponding to all branches of the dispersion surfaces of both media, Γ_{mn} will depend on all the

$\varkappa$'s. Thus it is possible for a stationary point to be near a branch curve of the dispersion surfaces that appears in Γ_{mn} but is not a branch curve of $\varkappa_m$ or $\varkappa_n$. In this case, which corresponds to the onset of lateral rays, the stationary point result in (26) is a first approximation to the $1/k_o$ term in the correct asymptotic expansion. (26)

D. RAY-OPTICAL SOLUTION FOR THE FIELDS SCATTERED FROM A CURVED INTERFACE

In the preceding section it was shown that for lossless media the stationary point contributions to the fields can be interpreted as the fields associated with rays of energy proceeding from the source to the interface and thence to the observation point. Locally the ray fields are plane waves since the stationary point condition implies quadratic phase change (no linear change) between neighboring rays when the observation point moves in a plane perpendicular to the wave vector of the ray. The ray scattering at the planar interface obeys Snell's law, and the scattering coefficients are those found from a plane wave analysis.

In this section the ray-optical method for finding the scattered fields will be generalized to the case of a gently curved, but otherwise arbitrary, interface. This extension is suggested by the fact that only the local, plane wave properties of the fields incident on a planar boundary determine the scattered rays so that only the local properties of the curved interface would be expected to govern ray scattering at the curved interface. The ray-optical method is essentially one of ray tracing with the scattering at the interface being determined by the locally plane wave properties of the ray fields. This method permits one to calculate the scattered far fields for problems not amenable to a rigorous treatment. Conceptually, at least, this method is easily extended to take into account multiple scattering of the rays.

A point source is assumed to be located in a homogeneous, lossless medium, described by the dielectric tensor $\underset{\sim}{\varepsilon}_1$, that adjoins a second homogeneous, lossless medium, described by $\underset{\sim}{\varepsilon}_2$, at some gently curved surface --- see Fig. 2-a. Based on the analysis for the planar interface problem, it is assumed that the source radiates direct ray fields into the $\underset{\sim}{\varepsilon}_1$ medium as if this medium were unbounded. Consider now one such ray originating from the source and corresponding to a point on the dispersion surface of the $\underset{\sim}{\varepsilon}_1$ medium defined by the wave vector $\underline{k}_n$. If this ray is incident on the interface, its field $\underline{E}_n$ at the interface will be one of the terms in (21) with $\underline{L} = \underline{L}_n$, as shown in Fig. 2-a.

If the principal radii of curvature of the interface are large compared to wave length, it is reasonable to expect that the ray scattering occurs in a similar manner to the scattering at a planar interface when this planar interface is taken to be the tangent plane to the curved interface at the point of incidence. The scattered rays are shown in Fig. 2-a. Their directions are inferred from the dispersion surfaces of the two media and Snell's law, $\underline{k}_n - \underline{n}_o(\underline{k}_n \cdot \underline{n}_o) = \underline{k}_m - \underline{n}_o(\underline{k}_m \cdot \underline{n}_o)$, where $\underline{n}_o$ is the normal to the interface at the point of incidence and $\underline{k}_m$ is the wave vector of a scattered ray. Geometrically, the scattered ray direction can be determined by finding the intersection in $\underline{k}$ space of a line through the tip of $\underline{k}_n$, and parallel to $\underline{n}_o$, with the mth branch of the dispersion surface, as is illustrated in Fig. 2-b for the $m = \vec{4}$ scattered ray of Fig. 2-a. The radius vector to the point of intersection is $\underline{k}_m$ and the normal $\underline{\nu}_m$ at this point is in the direction taken by the scattered ray. Knowing $\underline{k}_m$ and $\underline{\nu}_m$, the ray-refractive index $N_m = \underline{k}_m \cdot \underline{\nu}_m$ and the corresponding plane wave polarization vector $\underline{b}_m$ of the scattered ay field can be found. The ray scattering coefficient Γ_{mn} is taken to be that of a planar interface when the tangent plane is regarded as the interface between the $\underline{\epsilon}_1$ and $\underline{\epsilon}_2$ media.

With the above results, one can write the fields along the mth scattered ray as the product of the following factors: a) the amplitude of the incident ray at the interface, which is the coefficient of $\underline{b}_n$ in (2 1); b) the scattering coefficient Γ_{mn}; c) the phase factor $e^{-jk_oN_mL_m}$ along the scattered portion of the ray; d) the reciprocal of the ray flux tube divergence coefficient D_{mn}, which will be discussed presently; e) the additional phase change that occurs when the ray is tangent to a caustic surface, which will be combined with the incident ray phase factor $\operatorname{sgn}K_{n1} + \operatorname{sgn}K_{n2}$ and the combination written as δ_{mn}. Consequently, the scattered ray field $\underline{E}_m$ due to a point source in the presence of a gently curved interface is

$$\underline{E}_m(L_m) \sim \frac{2\pi}{k_o} \frac{\underline{b}_m \Gamma_{mn} A_n |\cos\theta_n|}{L_n\sqrt{|G_n|}\ D_{mn}}\ e^{-jk_o(L_nN_n + L_mN_m)}\ e^{-j\frac{\pi}{4}\delta_{mn}} \ .$$

$$(29)$$
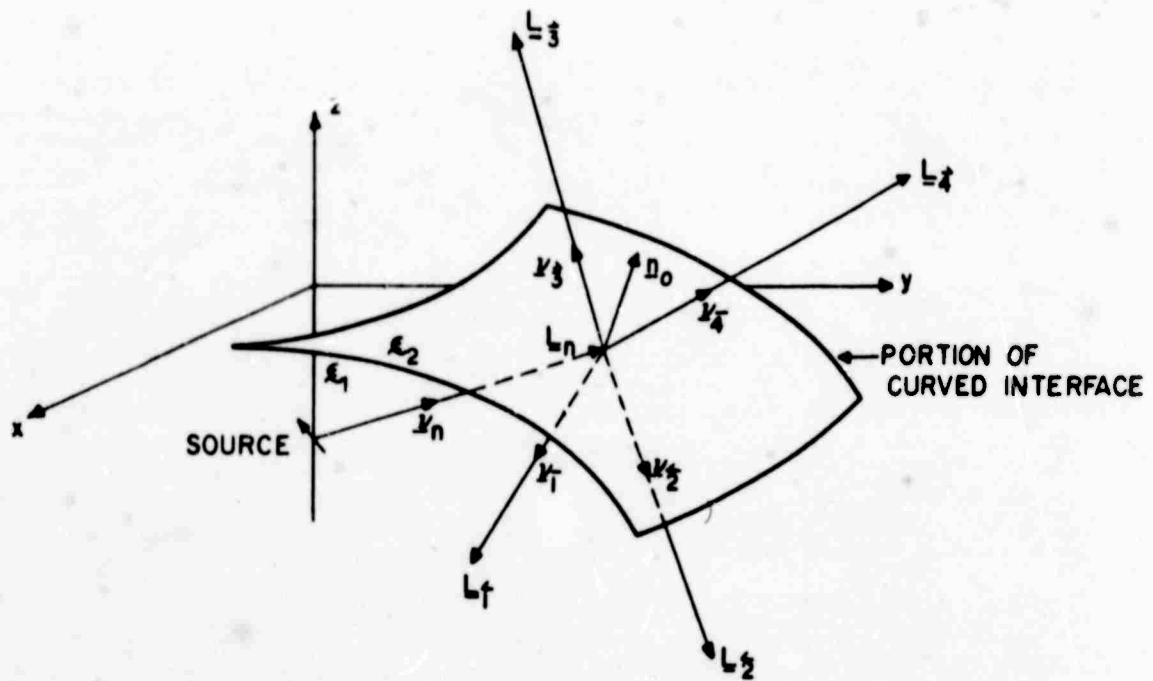
(a) Ray scattering at a curved interface
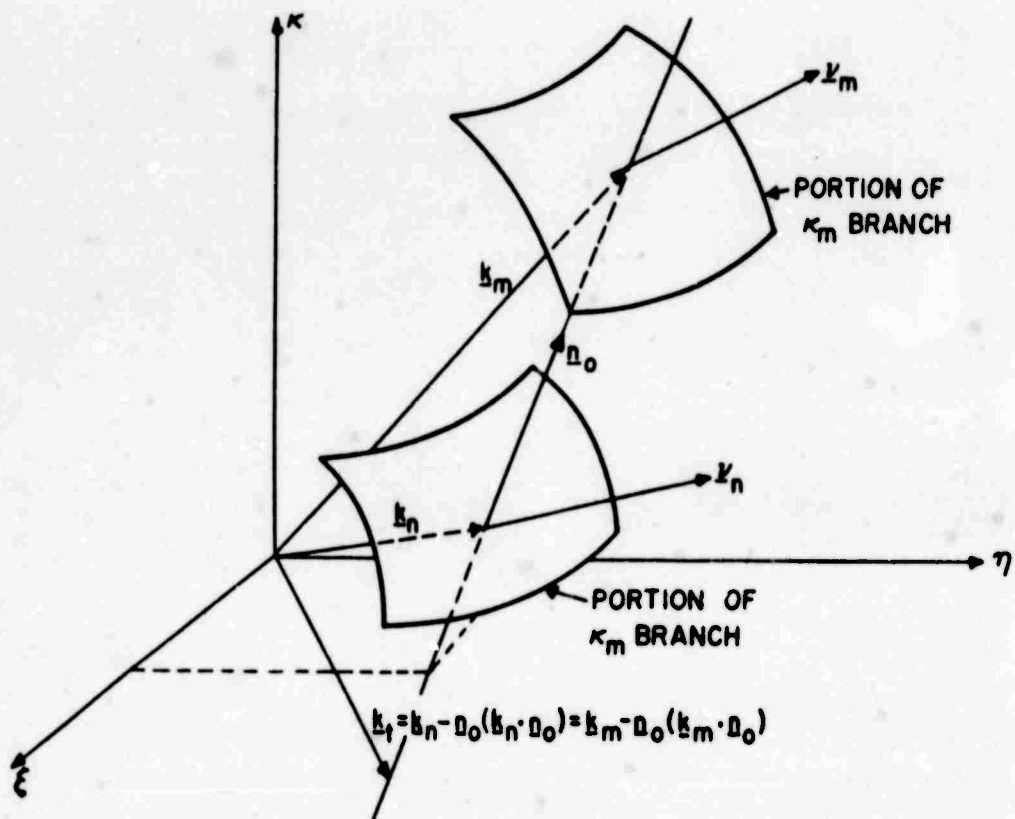
(b) Construction for finding the direction of the scattered
     $(m = \vec{4})$ ray

Fig. II-2

Calculation of the divergence factor D_{mn} is based on the principal of power conservation in the scattered portion of a tube of rays, i.e., equality of the power passing any cross-section of the scattered portion of the ray tube. If $da(L_m)$ is the area of the normal cross-section of the scattered portion of a narrow tube of rays at a distance L_m along the scattered ray tube, the power passing through this cross-section is $da(L_m) \, Re \left\{ \underline{\nu}_m \cdot \left[\underline{E}_m(L_m) \times \underline{H}_m^*(L_m) \right] \right\}$. Here $\underline{E}_m(L_m)$ is given by (29) and $\underline{H}_m(L_m)$ is also given by (29) with $\underline{\delta}_m$ replaced by the properly defined magnetic field polarization vector $\underline{\mu}_m$. At $L_m = 0$ the divergence coefficient D_{mn} must be unity if, as has been assumed, the amplitude of the scattered field at the interface is to differ from that of the incident field only by the scattering coefficient Γ_{mn}. Using this fact and requiring the power passing through any cross-section of the scattered portion or the ray tube to be equal to the power passing through the cross-section at $L_m = 0$, one finds that

$$D_{mn}(L_m) = \sqrt{ da(L_m)/da(o) } \qquad . \qquad (30)$$

The area ratio in (30) is determined by the shape of the mth and n^{th} branches of the dispersion surfaces in the vicinity of the points $\underline{k}_m$ and $\underline{k}_n$ and from the curvature of the interface. An expression for the area ratio is derived in Appendix D.

In order to calculate the total field due to several ray contributions, it is essential to know the phase term δ_{mn} in (29) along the individual rays. At the interface $\delta_{mn} = \delta_n$ and it remains constant along the scattered portion of the ray except across the points of tangency of the ray to a caustic, where it changes by ± 2 if the tangency is simple. Note that D_{mn}, as discussed in Appendix D, is quadratic in L_m. Hence, at most two such points of tangency exist for each ray. In order to evaluate this change in δ_{mn} it is assumed that the structure of a scattered ray pencil can be determined solely from the phase distribution over a cross-section of the pencil and the κ_m branch of the dispersion surface. This assumption is consistent with the local nature of the ray-optical fields and can be used to obtain a Fourier

representation that asymptotically gives the fields of the scattered ray pencil, including the change in δ_{mn} across a caustic. The cross-section is taken to be the intersection of the pencil and a constant z plane lying between the interface, at the points of incidence of the rays in the pencil, and the points of tangency of the rays in the pencil to a caustic. This selection of the cross-section is depicted in side view in Fig. 3 for a transmitted ray pencil. The (x, y, z) coordinate system in Fig. 3 is taken such that x and y lie in the plane used in forming the cross-section.

Performing a double Fourier transformation on the ray fields at the cross-section by assuming the ray fields outside this cross-section to be zero results in a transform of the form $\underline{b}_m A_m e^{-jk_o \Phi (\xi, \eta)}$. Here $\underline{b}_m$ and A_m are slowly varying compared to $k_o \Phi (\xi, \eta)$. Using this transform, the ray fields of the pencil at $z \neq 0$ can be found from the first-order asymptotic evaluation of the inverse double Fourier transform

$$\underline{E}_m = \int\int_{-\infty}^{\infty} \underline{b}_m A_m e^{-jk_o \left[\xi x + \eta y + \varkappa_m z + \Phi (\xi, \eta) \right]} d\xi \, d\eta \ . \qquad (31)$$

The justification of expression (31) for $\underline{E}_m$ is found in the fact that the asymptotic evaluation of the double integrals will yield the ray fields of the pencil with the original phase distribution in the $z = 0$ cross-section.

From the representation of the ray fields given in (31), the change in δ_{mn} across the ray tangency to a caustic can be calculated without an actual knowledge of $\Phi (\xi, \eta)$ if the caustic itself is known. In order to see this, recognize that the phase term in (31) is of the same form as that found for the scattered ray integrals (4) in the planar interface problem with $-\varkappa_n z'$ replaced by $\Phi (\xi, \eta)$. With this observation we can use the results derived at the end of Appendix C to find the change $\Delta \delta_{mn}$ in δ_{mn} across a ray tangency to a caustic, i.e.,

$$\Delta \delta_{mn} = 2 \ \text{sgn} \ C_m \qquad (32)$$

where C_m is the curvature at the point $\underline{k}_m$ on the dispersion surface of the curve formed by the intersection of the $\varkappa_m$ branch of the dispersion surface
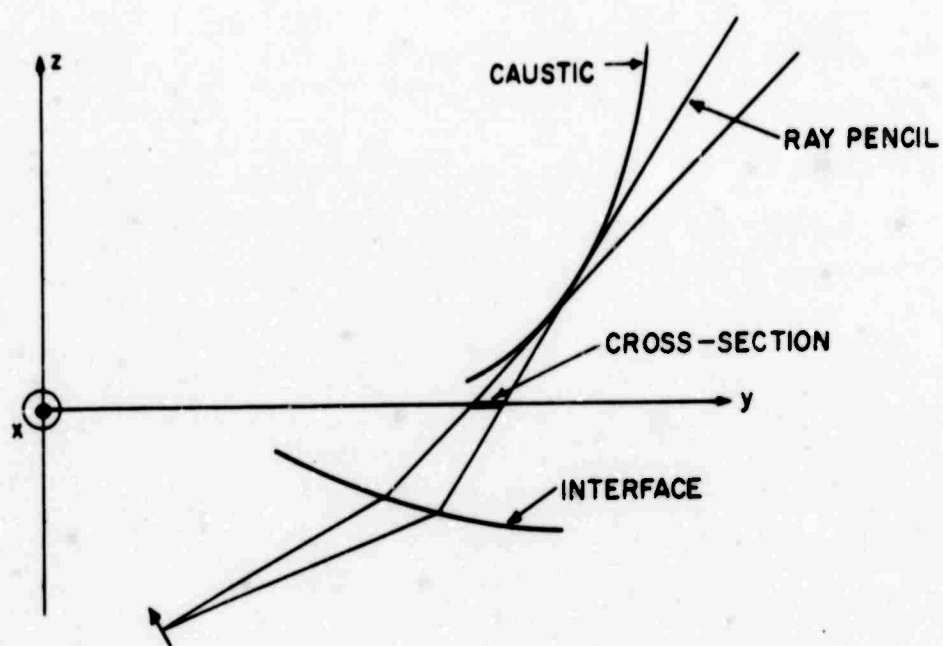
Fig. II-3   Side view of cross-section used in formulating the
Fourier representation of the fields of a scattered
ray pencil

with the plane parallel to $\underline{\nu}_m$ and to the normal to the caustic. The term $\Phi(\xi, \eta)$ influences (32 only through the normal to the caustic. The normal may be found from the ray equations $\underline{\nu}_n \times \underline{L}_n = \underline{\nu}_m \times \underline{L}_m = 0$ and the caustic condition $D_{mn} = 0$. Thus, knowing that $\delta_{mn} = \delta_n$ at the interface and that δ_{mn} is constant along the ray except for the change given in (32) at the ray tangency to a caustic, δ_{mn} can be found everywhere along the scattered ray.

With the foregoing results, the functional form of all the terms in (29), and hence the scattered ray fields $\underline{E}_m$ due to a point source in the presence of a gently curved interface, can be found directly from ray-optical considerations. Note that the method described in this section gives the locus cf observation points at which a particular scattered ray contributed to the fields. While the inverse problem of determining the rays that contribute at a given observation point for the case of a curved interface would be based on the same ray tracing concepts, in general it poses a much more difficult analytical problem. This is especially true if multiply scattered rays are present.

E. BRANCH CURVE CONTRIBUTIONS TO THE FAR FIELDS

In this section the branch curve contributions to the far fields will be evaluated and interpreted in terms of lateral rays. The branch curve contributions first appear as the branch point contributions to the steepest descent integration over η as found in Appendix B. Recall from the discussion given in Appendix B that a branch point contribution to the η integration may occur in the scattered field Fourier integrals (4) but not in the direct field integrals (2). Such contributions arise only from those branch points of the $\varkappa_\ell$'s appearing in $\underline{F}(\xi, \eta)$ that are not at the same time branch points of $\varkappa_m$ and $\varkappa_n$ appearing in $P(\xi, \eta)$. Furthermore, branch point contributions to the total fields come from only those branch points of $\varkappa_\ell$ at which $\varkappa_\ell$ is real --- see Appendix B. Finally, in Appendix B only the branch points of $\varkappa_\ell$ lying on the real η axis and at which $\varkappa_m$ and $\varkappa_n$ are real were considered since the contributions from branch points not satisfying these conditions are exponentially small.

1. Stationary Phase Evaluation

In the isolated saddle point contribution (B-3) to the η integration, $\underline{F}\left[\xi, \eta_s(\xi)\right]$ will have branch point singularities at the branch points of $\varkappa_\ell\left[\xi, \eta_s(\xi)\right]$. However, these branch points do not give rise to lateral rays and hence, only the branch point contributions to the η integration give rise to lateral rays. This conclusion follows from the fact that for ξ near a branch point of $\varkappa_\ell\left[\xi, \eta_s(\xi)\right]$, in the η integration a branch point of $\underline{F}(\xi, \eta)$, considered as a function of η, lies near a saddle point. When a more accurate steepest descent integration over η is carried out for this case, it is found that the branch point in ξ occurring in the isolated saddle point result is no longer present. [26]

A more detailed discussion of the nature of $\underline{F}(\xi, \eta)$ near the branch curves than given in Appendix B is necessary in order to cast the branch curve contribution into ray-optical terms. To this end consider the vicinity of a branch curve of some $\varkappa_\ell$ that appears in $\underline{F}(\xi, \eta)$ but that is not a branch of $P(\xi, \eta)$. In the vicinity of the branch curve of $\varkappa_\ell$ but away from cusps

or crossings of the branch curve, $\varkappa_\ell \approx g_\ell^o(\xi,\eta) \pm \sqrt{g_\ell(\xi,\eta)}$ where g_ℓ^o and g_ℓ are real and regular and g_ℓ is zero on the branch curve -- the zero is simple along any trajectory crossing the branch curve. For convenience, the plus sign before the root is taken if $\varkappa_\ell$ corresponds to an upgoing wave, and the minus sign is taken otherwise. The argument of $\sqrt{g_\ell(\xi,\eta)}$ is assumed to be defined in such a way that the above sign convention holds. The branch curve condition $g_\ell(\xi,\eta) = 0$ can be solved for η as a possibly multivalued function

$$\eta = \eta_b(\xi) \quad . \tag{33}$$

In the vicinity of the branch curve and excluding cusps or crossings of the branch curve, $g_\ell(\xi,\eta)$ can be approximated as[*]

$$g_\ell(\xi,\eta) \approx \left[\eta - \eta_b(\xi)\right]\left[\frac{\partial}{\partial\eta} g_\ell(\xi,\eta)\right]_{\eta=\eta_b(\xi)} \quad , \quad \left[\frac{\partial}{\partial\eta} g_\ell(\xi,\eta)\right]_{\eta=\eta_b(\xi)} \neq 0 \quad . \tag{34}$$

Since $\underline{F}(\xi,\eta)$ is explicitly a function of $\varkappa_\ell$, in the vicinity of the branch curve of $\varkappa_\ell$ one can write $\underline{F}(\xi,\eta) = \underline{F}(\xi,\eta, \sqrt{g_\ell})$. Using this form for $\underline{F}(\xi,\eta)$ and with the help of (34), $\underline{F}(\xi,\eta)$ for constant ξ can be approximated to first order about $\eta = \eta_b(\xi)$ as

$$\underline{F}(\xi,\eta) \approx \hat{\underline{F}} + \frac{\partial \hat{\underline{F}}}{\partial\eta}(\eta-\eta_b) + \frac{\partial \hat{\underline{F}}}{\partial\sqrt{g_\ell}}\sqrt{\frac{\partial g_\ell}{\partial\eta}}\sqrt{\eta-\eta_b} \tag{35}$$

where $\hat{\underline{F}}$, $\partial\hat{\underline{F}}/\partial\eta$, $\partial\hat{\underline{F}}/\sqrt{g_\ell}$ and $\partial g_\ell/\partial\eta$ are all evaluated at $\eta=\eta_b(\xi)$. Comparing the expansion in (35) with that given in (B-4) it is seen that the

----

[*] The condition $\left[\frac{\partial}{\partial\eta} g_\ell(\xi,\eta)\right]_{\eta=\eta_b} \approx 0$ corresponds to two branch points being close together in the η integration for this value of ξ. For critical points at these values of ξ and η, the derivation of the branch curve contribution is no longer valid but the ray-optical representation for the contribution is, since this singularity is introduced only by the choice of the (x, y) coordinates.

quantity $\partial \underline{\overline{F}} / \partial \sqrt{\eta - \eta_b}$ appearing in the branch point contribution (B-7) can

be replaced by $\dfrac{\partial \hat{\underline{F}}}{\partial \sqrt{g_\ell}} \sqrt{\dfrac{\partial g_\ell}{\partial \eta}}$. Recall that in Appendix B, $\sqrt{\eta - \eta_b}$ was taken

to be positive for $\eta - \eta_b$ positive real, thus requiring from (34) that

$\arg \sqrt{\partial g_\ell (\xi, \eta_b)/\partial \eta} = \arg \sqrt{g_\ell(\xi, \eta_b + \Delta)}$ where $\Delta > 0$ is small.

The integral of (B-7) over ξ can now be evaluated by the method of stationary phase,[22] thus obtaining the branch curve contribution $\underline{I}_{B.C.}$ to the integrals in (4). The stationary phase points in the ξ integration of the terms in (45) are the solutions of

$$\frac{d}{d\xi} P\left[\xi, \eta_b(\xi)\right] = P_1\left[\xi, \eta_b(\xi)\right] + P_2\left[\xi, \eta_b(\xi)\right] \frac{d}{d\xi} \eta_b(\xi) = 0 .$$

(36)

It is assumed that $d\eta_b/d\xi$ at the stationary phase point is finite (were it in-finite, two branch points would have coalesced in the η integration, in which case (B-7) would no longer be valid). Equation (36) is equivalent to the condi-tion that the tangential derivative of $P(\xi, \eta)$ on the branch curve of $\varkappa_\ell$ be zero. Thus, the branch curve contributions come from the critical points (ξ_c, η_c) on the branch curves at which the tangential derivative of $P(\xi, \eta)$ vanishes. Performing the stationary phase integration, one finds that

$$\underline{I}_{B.C.} \sim \frac{\pi \sqrt{2}}{k_o} \sum_\ell \sum_{C.P.} \left\{ U\left[\pm(\eta_s - \eta_b)\right] \frac{\partial \hat{\underline{F}}}{\partial \sqrt{g_\ell}} \sqrt{\frac{\partial g_\ell}{\partial \eta}} \frac{e^{-jk_o P} e^{-j\frac{\pi}{4}(3 sgn \frac{\partial P}{\partial \eta} + sgn \frac{d^2 P}{d\xi^2})}}{|\partial P/\partial \eta|^{3/2} |d^2 P/d\xi^2|^{1/2}} \right\}_{(\xi_c, \eta_c)}$$

(37)

where the first sum is taken over all critical points, at which $P(\xi, \eta)$ is real, on that portion of the branch curve of $\varkappa_\ell$ on which $\varkappa_\ell$ is itself real. The second sum is taken over the various branch curves appearing in $\underline{F}(\xi, \eta)$ but not in $P(\xi, \eta)$.

2. Ray Interpretation of the Branch Curve Contribution

As pointed out in Section C, the branch curve of $\varkappa_\ell$ on which $\varkappa_\ell$ is real is the projection into the (ξ, η) plane of the rim bounding the ℓth branch of the dispersion surface. On the rim, the ℓth branch adjoins another real branch $\varkappa_p$ of the dispersion surface and the normal is parallel to the (ξ, η) plane -- see Fig. 4-a where A-A is a segment of the rim. With this description of the dispersion surface near the rim of the ℓth branch, it will be shown that the critical point condition (36) can be interpreted in terms of a lateral ray that leaves the source along $\underline{\nu}_n$ -- see Fig. 4-b -- is incident on the interface at $(x', y', 0)$, travels along the interface parallel to $\underline{\nu}_\ell$ and then leaves the interface from the point $(x'', y'', 0)$ along the direction of $\underline{\nu}_m$, arriving at the observation point (x, y, z). While lateral ray contributions can exist in both the $\underset{\sim}{\epsilon}_1$ and $\underset{\sim}{\epsilon}_2$ media, the dispersion surfaces may be such that these contributions are present in only one medium, or in neither.

Since the segment of the lateral ray on the interface corresponds to the ℓth scattered ray at the critical angle, power flow on this segment will be in the direction of $\underline{\nu}_\ell$. Hence, lateral ray contributions will exist only for $\underline{\nu}_\ell \cdot \underline{L}_\ell \geq 0$ and one can replace the unit step function $U\left[\pm(\eta_s - \eta_b)\right]$ appearing in (37) by $U(\underline{\nu}_\ell \cdot \underline{L}_\ell)$. Verification of this intuitive argument by analytical methods is involved and will not be considered.

Using the form of $P(\xi, \eta)$ appearing in the scattered field integrals (4), the critical point condition (36) becomes

$$0 = \left[(x + z\frac{\partial \varkappa_m}{\partial \xi} - z'\frac{\partial \varkappa_n}{\partial \xi}) + (y + z\frac{\partial \varkappa_m}{\partial \eta} - z'\frac{\partial \varkappa_n}{\partial \eta})\frac{d\eta_b}{d\xi} \right]_{\eta = \eta_b(\xi)} :$$

$$n = \vec{1}, \vec{2} \; ; \; m = \begin{Bmatrix} \vec{3}, \vec{4} & \text{for } z > 0 \\ \overleftarrow{1}, \overleftarrow{2} & \text{for } z < 0 \end{Bmatrix} . \tag{38}$$

In order to verify the ray interpretation of (38), recognize that since $\underline{\nu}_\ell$ is normal to A-A in Fig. 4-a, it is also normal to the branch curve $\eta = \eta_b(\xi)$, which is the projection of the rim A-A, and hence

53

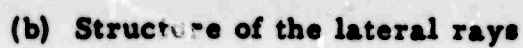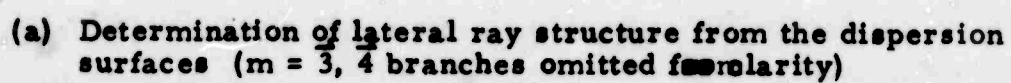(a) Determination of lateral ray structure from the dispersion
surfaces (m = 3, 4 branches omitted for clarity)

(b) Structure of the lateral rays

Fig. II-4

$$\underline{\nu}_\ell = \pm \left(\underline{x}_o \frac{d\eta_b}{d\xi} - \underline{y}_o \right) \Big/ \sqrt{\left(\frac{d\eta_b}{d\xi} \right)^2 + 1} \ . \tag{39}$$

If $\underline{L}_n = \underline{x}_o x' + \underline{y}_o y' - \underline{z}_o z'$, $\underline{L}_\ell = \underline{x}_o(x'' - x') + \underline{y}_o(y'' - y')$ and $\underline{L}_m = \underline{x}_o(x - x'') + \underline{y}_o(y - y'') + \underline{z}_o z$, it is easily verified with the help of (16) and (39) that (38) is equivalent to the condition $\underline{\nu}_n \times \underline{L}_n = \underline{\nu}_\ell \times \underline{L}_\ell = \underline{\nu}_m \times \underline{L}_m = 0$ for the same ξ_c and η_c with $\underline{\nu}_n \cdot \underline{L}_n$ and $\underline{\nu}_m \cdot \underline{L}_m$ positive.

Using the ray interpretation of (38), the various quantities appearing in (37) can be expressed in ray-optical terms -- see Appendix E. Finally, because the branch curve of $\varkappa_\ell$ is not the same as those of $\varkappa_m$ and $\varkappa_n$, this branch curve does not appear in A_n or $\underline{b}_m$ and hence

$$\frac{\partial \hat{\underline{F}}}{\partial \sqrt{g_\ell}} = \underline{b}_m \gamma_{\ell mn} A_n; \quad \gamma_{\ell mn} = \frac{\partial}{\partial \sqrt{g_\ell}} \hat{\Gamma}_{mn}(\xi, \eta, \sqrt{g_\ell}) \tag{40}$$

where $\hat{\Gamma}_{mn}(\xi, \eta, \sqrt{g_\ell}) = \Gamma_{mn}(\xi, \eta)$ in the vicinity of the branch curve of $\varkappa_\ell$. With the help of (40) and (E-1), (E-5), (E-7) and (E-10) of Appendix E, the lateral ray contribution to the scattered fields can be written as

$$(\underline{E}_\Gamma)_{B.C.} \sim$$

$$\frac{\pi\sqrt{2}}{k_o} \sum_{m,n} \sum_\ell \sum_{C.P.} \left| U(\underline{\nu}_\ell \cdot \underline{L}_\ell) \frac{\underline{b}_m \gamma_{\ell mn} A_n e^{-jk_o(N_n L_n + N_\ell L_\ell + N_m L_m)}}{\sqrt{L_\ell |Q_\ell| |(\underline{z}_o \times \underline{L}_\ell) \cdot \underline{D}_{\ell mn} \cdot (\underline{z}_o \times \underline{L}_\ell)|}} e^{-j\frac{\pi}{4}\delta_{\ell mn}} \right|_{(\xi_c, \eta_c)} . \tag{41}$$

The first sum is over all critical points (ξ_c, η_c) on those segments of the branch curve of $\varkappa_\ell$ on which $\varkappa_\ell$ is real. The ℓ summation is taken over all branch curves for which $\ell \neq m, n$ and that are not also branch curves of $\varkappa_m$ or $\varkappa_n$. The sums on m and n indicate summation over the possible incident and diffracted segments of the lateral rays.

The results given in (41) are not valid when the denominator goes to zero. This can happen if $|Q_\ell| \equiv 1/\sqrt{(\partial g_\ell/\partial \xi)^2 + (\partial g_\ell/\partial \eta)^2} = 0$, which corresponds to $|\xi_c|$, $|\eta_c| \to \infty$ along an open branch of $\eta = \eta_b(\xi)$. The denominator is also zero if $\underline{L}_\ell = 0$, which indicates that a stationary point of the m, n scattered rays lies on the branch curve of $\varkappa_\ell$ and occurs when the observation point lies on the surface bounding the region in which the lateral rays contribute to the field. Also, for some observation points it can happen that $(\underline{z}_o \times \underline{L}_\ell) \cdot \widetilde{D}_{\ell mn} \cdot (\underline{z}_o \times \underline{L}_\ell) = 0$ with $\underline{L}_\ell \neq 0$, which occurs when two critical points coalesce. The condition $Q_\ell = 0$ and $(\underline{z}_o \times \underline{L}_\ell) \cdot \widetilde{D}_{\ell mn} \cdot (\underline{z}_o \times \underline{L}_\ell) = 0$ for $\underline{L}_\ell \neq 0$ correspond to shadow boundaries and caustics in the lateral ray field, singularities that do not exist in the lateral ray fields excited by line sources[4] or by point sources in isotropic media.[26]

Since the lateral ray fields are of lower order in k_o than the scattered and direct ray fields, the latter will usually form the dominant contributions to the far fields of the source. However, in geometric optical shadow regions, the direct and scattered ray fields will be exponentially small (as will be all the terms in the asymptotic expansion of the stationary point contributions) so that the lateral ray fields, when present, form the dominant contribution.

Chapter III

GROUP VELOCITY AND POWER FLOW RELATIONS FOR SURFACE WAVES IN PLANE-STRATIFIED ANISOTROPIC MEDIA

A.   INTRODUCTION

In this chapter two aspects of the power flow associated with electromagnetic waves in plane-stratified, anisotropic, dispersive media and their application to surface wave propagation are considered.   The first aspect is that of the relation between the group velocity and the velocity of energy transport of surface waves; the second is the relation between a dyadic surface impedance and the power flow and stored energy in the structure it represents.

It is well known that monochromatic plane electromagnetic waves in a homogeneous, dispersive, anisotropic medium that is also lossless and linear, e.g., the ionosphere for small-signal propagation, carry power in the direction of the normal to the plane wave dispersion surface. Specifically, the velocity of energy transport of plane waves in such a medium is equal to the group velocity, that is, the gradient in the wave number space of the frequency.[15,23] As was seen in Chapter II, this relation between the group velocity and the velocity of energy transport finds an important application in the ray interpretation of the far fields radiated by sources in anisotropic media.

It is shown here that an analogous relation involving the group velocity holds for the case of surface waves in plane-stratified, dispersive, anisotropic media that are also lossless and linear, in that the group velocity of surface waves that can propagate in such a medium may be interpreted as the surface wave energy transport velocity. For such surface waves, the direction as well as the magnitude of the real part $\underline{s}$ of the complex Poynting vector is, in general, a function of z, the coordinate in the direction of stratification. (An example of this dependence is described in Chapter IV). Therefore, $\underline{s}$ divided by the energy density cannot be identically equal to the surface wave

group velocity, which is a vector independent of z. It will be shown, how-
ever, that the group velocity of the surface wave is identical to the velocity
of energy transport of the surface wave taken as a whole, i.e., the gradient
in the transverse wave number plane of the frequency is equal to the integral
over z of $\underline{s}$ divided by the corresponding integral over z of the stored energy
density. In a manner analogous to that for plane waves in anisotropic, homo-
geneous media, the relation between group velocity and energy transport
velocity for surface waves will prove useful in Chapter V where the ray in-
terpretation for the surface wave fields excited by a point source is formulated.

The proof of the relation between the group velocity and the energy
transport velocity is furnished for two configurations. In Section B, the case
considered is that of a plane-stratified medium filling all space, while
Section C contains the proof for the case of a plane-stratified medium filling
the half-space above a perfectly conducting plane at z = 0.

In Section D, the relation between the dyadic surface impedance at
z = d, which represents a plane-stratified, lossless, anisotropic medium fill-
ing the region $0 < z < d$ and bounded at z = 0 by a perfectly conducting plane,
and the power flow and stored energy in this region is considered. With the
help of the developments of Section B, it is shown that the power flow and
stored energy in the region $0 < z < d$ are directly related to the derivatives
of the surface impedance, with respect to transverse wave numbers and fre-
quency, and to the components of the r.f. magnetic field transverse to z at
z = d. The relation of power flow and energy to the surface reactance apply
for all frequencies and real transverse wave numbers, not just those asso-
ciated with surface waves. In particular, for surface waves propagating above
a dyadic impedance plane, the power flow and energy relations are shown to
be significant in calculating the energy transport velocity.

Section E is devoted to a discussion of the dyadic surface impedance
representation of a semi-infinite, plane-stratified, lossless, anisotropic
medium for ranges of frequency and transverse wave numbers for which the
fields in the medium are evanescent at infinity. Again the power flow and
stored energy relation involving the surface impedance are obtained. The

power division between the space inside and outside of a surface wave guiding structure is determined in terms of the dyadic surface impedances defined in Sections D and E.

Appendix F treats briefly the dyadic admittance representation of a medium above a perfectly conducting plane. At those values of frequency and transverse wave numbers where the impedance formalism breaks down, the admittance formalism may, in general, still be used. Power flow and stored energy relations in terms of the surface admittance are given.

The results derived in this chapter, for plane-stratified media that are uniform in the planes normal to the direction of stratification, are generalized in Appendix G to configurations that are periodic in the planes normal to the direction of stratification. For surface waves in periodic configurations, a group velocity-energy velocity relation similar to that described above holds for the averages (over the periodicity) of the Poynting vector and stored energy density. Also, it is shown that the average energy flow and average stored energy in periodic configurations represented by a dyadic surface impedance are simply related to the derivatives of the impedance with respect to transverse wave numbers and frequency.

B. STRATIFIED MEDIUM FILLING ALL SPACE

A lossless, anisotropic, dispersive, plane-stratified medium is assumed to fill all space. It is uniform in the x and y directions and its interaction with a monochromatic electromagnetic field can be described in terms of the constitutive parameters of the medium, the dielectric tensor $\underset{\sim}{\epsilon}$ and the permeability tensor $\underset{\sim}{\mu}$. Since the medium is lossless, $\underset{\sim}{\epsilon}$ and $\underset{\sim}{\mu}$ are Hermitian,[14,15] and because of the assumed uniformity in x and y, they are independent of these coordinates. The tensors $\underset{\sim}{\epsilon}$ and $\underset{\sim}{\mu}$ are analytic functions of the angular frequency ω and are assumed to be continuous functions of z except for a possibly denumerable number of finite jumps. The z dependence of $\underset{\sim}{\epsilon}$ and $\underset{\sim}{\mu}$ is further assumed to be such that the medium supports surface waves propagating transversely to z. Such surface waves are solutions of the source-free Maxwell equations and have the form

$$\left.\begin{array}{c} \underline{E}(\underline{r};\underline{k}_t,\omega) \\[2ex] \underline{H}(\underline{r};\underline{k}_t,\omega) \end{array}\right\} = \left\{\begin{array}{c} \underline{e}(z;\underline{k}_t,\omega) \\[2ex] \underline{h}(z;\underline{k}_t,\omega) \end{array}\right\} e^{-j\underline{k}_t\cdot\underline{\rho}} \qquad (1)$$

where $\underline{e}$ and $\underline{h}$ tend to zero as $|z|$ approaches infinity. As used throughout this chapter $\underline{\rho} = \underline{x}_o x + \underline{y}_o y$ is the position vector transverse to z and $\underline{k}_t = \underline{x}_o k_x + \underline{y}_o k_y$ is a real transverse wave vector. The vector amplitudes $\underline{e}$ and $\underline{h}$ are required to be such that the electric and magnetic energy densities, as well as $Re(\underline{e}\times\underline{h}^*)$, are integrable on the infinite interval $-\infty < z < \infty$. Because the dependence of $\underline{E}$ and $\underline{H}$ on x and y is $e^{-j\underline{k}_t\cdot\underline{\rho}}$, the electric and magnetic energy densities and $\underline{E}\times\underline{H}^*$ are independent of $\underline{\rho}$. Furthermore, since the field components transverse to z, $\underline{e}_t$ and $\underline{h}_t$ must be continuous in z across any jump in $\underset{\sim}{\epsilon}$ or $\underset{\sim}{\mu}$, they must be continuous functions of z. For simplicity, $\underline{e}$ and $\underline{h}$ are assumed to be Rms quantities.

In the absence of sources, Maxwell's equations in a medium described by $\underset{\sim}{\epsilon}$ and $\underset{\sim}{\mu}$ are

$$\left.\begin{array}{c} \nabla\times\underline{H} = j\omega\underset{\sim}{\epsilon}\cdot\underline{E} \\[3ex] \nabla\times\underline{E} = -j\omega\underset{\sim}{\mu}\cdot\underline{H} \end{array}\right\} \qquad (2)$$

where the harmonic time dependence $e^{j\omega t}$ has been suppressed. Substituting $\underline{E}$ and $\underline{H}$ from equation (1) into (2) results in six linear homogeneous equations in the six unknown field components, four ordinary differential equations in the variable z and two algebraic equations. For any particular medium that can support surface waves, these six equations will have solutions satisfying the cavity-type boundary conditions $\underline{e} = \underline{h} = 0$ at $|z| = \infty$, and possessing the integrability properties described above, only for restricted values of the parameters $\underline{k}_t$ and ω that some functional relation of the form

$$D_s(\underline{k}_t, \omega) = 0 \tag{3}$$

where in general D_s is a regular function of $\underline{k}_t$ and ω. Relation (3) is the surface wave dispersion relation and determines the possible surface waves that can propagate transversely to z in the particular plane-stratified medium.

Let $\underline{k}_t$ and ω be such as to satisfy the surface wave dispersion relation (3) and consider neighboring values $\underline{k}_t + d\underline{k}_t$ and $\omega + d\omega$, also satisfying (3). The fields of that surface wave propagating with wave vector $\underline{k}_t + d\underline{k}_t$ at the frequency $\omega + d\omega$ are given, to first order in differential quantities, by

$$\left.\begin{array}{l} \underline{E}(\underline{r}; \underline{k}_t + d\underline{k}_t, \omega + d\omega) = \underline{E}(\underline{r}; \underline{k}_t, \omega) + \delta \underline{E}(\underline{r}; \underline{k}_t, \omega) \\[2mm] \underline{H}(\underline{r}; \underline{k}_t + d\underline{k}_t, \omega + d\omega) = \underline{H}(\underline{r}; \underline{k}_t, \omega) + \delta \underline{H}(\underline{r}; \underline{k}_t, \omega) \end{array}\right\} \tag{4}$$

where the variation δ symbolizes the differential operation

$$\delta = d\underline{k}_t \cdot \nabla_{\underline{k}_t} + d\omega \frac{\partial}{\partial \omega} \quad , \tag{5}$$

with $\nabla_{\underline{k}_t} = \underline{x}_o \frac{\partial}{\partial k_x} + \underline{y}_o \frac{\partial}{\partial k_y}$, and the partial derivatives of $\underline{E}$ and $\underline{H}$ are evaluated at $(\underline{k}_t, \omega)$. Since $\underline{E}_t$ and $\underline{H}_t$ are continuous functions of z for both sets of values $(\underline{k}_t, \omega)$ and $(\underline{k}_t + d\underline{k}_t, \omega + d\omega)$, it is seen from (4) that the variations $\delta \underline{E}_t$ and $\delta \underline{H}_t$ must also be continuous functions of z. The differential equations that $\delta \underline{E}$ and $\delta \underline{H}$ satisfy can be found by applying the variation δ to

Maxwell's equations. Recalling (5) and because $\underset{\sim}{\epsilon}$ and $\underset{\sim}{\mu}$ do not depend on $\underline{k}_t$, the variation on Maxwell's equations results in

$$\nabla \times \delta \underline{H} = jd\omega \, \frac{\partial \omega \epsilon}{\partial \omega} \cdot \underline{E} + j\omega \underset{\sim}{\epsilon} \cdot \delta \underline{E} \left.\vphantom{\frac{\partial \omega \mu}{\partial \omega}}\right\}$$

$$\nabla \times \delta \underline{E} = jd\omega \, \frac{\partial \omega \mu}{\partial \omega} \cdot \underline{H} - j\omega \underset{\sim}{\mu} \cdot \delta \underline{H} \qquad (6)$$

Consider now the identity

$$\nabla \cdot (\underline{E}^* \times \delta \underline{H} + \delta \underline{E} \times \underline{H}^*) = \delta \underline{H} \cdot \nabla \times \underline{E}^* - \underline{E}^* \cdot \nabla \times \delta \underline{H}^* \cdot \nabla \times \delta \underline{E} - \delta \underline{E} \cdot \nabla \times \underline{H}^* \quad .$$

$$(7)$$

With the help of equations (2) and (6), the right-hand side of (7) can be re-written to give the relation

$$\nabla \cdot (\underline{E}^* \times \delta \underline{H} + \delta \underline{E} \times \underline{H}^*) = - jd\omega (\underline{E}^* \cdot \frac{\partial \omega \epsilon}{\partial \omega} \cdot \underline{E} + \underline{H}^* \cdot \frac{\partial \omega \mu}{\partial \omega} \cdot \underline{H}) \qquad (8)$$

when the assumption that ϵ and μ are Hermitian is used to write $\delta \underline{E} \cdot \underset{\sim}{\epsilon}^* \cdot \underline{E}^*$ as $\underline{E}^* \cdot \underset{\sim}{\epsilon} \cdot \delta \underline{E}$ and $\delta \underline{H} \cdot \underset{\sim}{\mu}^* \cdot \underline{H}^*$ as $\underline{H}^* \cdot \underset{\sim}{\mu} \cdot \delta \underline{H}$. The first term on the right-hand side of (8) is twice the time average electric energy density w_e while the second is twice the time average magnetic energy density w_h.[14,15,27] As pointed out, w_e and w_h are independent of $\underline{\rho}$. In terms of the total energy density $w = w_e + w_h$, equation (8) can then be written

$$\nabla \cdot (\underline{E}^* \times \delta \underline{H} + \delta \underline{E} \times \underline{H}^*) = -j2w\, d\omega \quad . \qquad (9)$$

The divergence term on the left-hand side of (9) is now evaluated by expanding $\delta \underline{E}$ and $\delta \underline{H}$ and subsequently applying the ∇ operator. With the help of (5) and (1), it is seen that

$$\delta \underline{E} = (\delta \underline{e} - jd\underline{k}_t \cdot \underline{\rho} \, \underline{e}) \, e^{-j\underline{k}_t \cdot \underline{\rho}} \left.\vphantom{\begin{array}{c}a\\b\end{array}}\right\}$$

$$\delta \underline{H} = (\delta \underline{h} - jd\underline{k}_t \cdot \underline{\rho} \, \underline{h}) \, e^{-j\underline{k}_t \cdot \underline{\rho}} \qquad (10)$$

The variations on the transverse vector amplitudes, $\delta \underline{e}_t$ and $\delta \underline{h}_t$, are continuous functions of z since $\delta \underline{E}_t$, $\delta \underline{H}_t$, $\underline{e}_t$ and $\underline{h}_t$ are, a fact that will prove useful later. Since $\underline{e}$ and $\underline{h}$ are independent of $\underline{\rho}$, using the above relations one has

$$\nabla \cdot (\underline{E}^* \times \delta \underline{H} + \delta \underline{E} \times \underline{H}^*)$$

$$= \nabla \cdot [\underline{e}^* \times \delta \underline{h} + \delta \underline{e} \times \underline{h}^* - j d\underline{k}_t \cdot \underline{\rho} (\underline{e}^* \times \underline{h} + \underline{e} \times \underline{h}^*)] \qquad (11)$$

$$= \frac{\partial}{\partial z} \underline{z}_o \cdot (\underline{e}^* \times \delta \underline{h} + \delta \underline{e} \times \underline{h}^*) - j2 d\underline{k}_t \cdot \underline{\rho} \frac{\partial}{\partial z} (\underline{z}_o \cdot \underline{s}) - j2 d\underline{k}_t \cdot \underline{s}$$

where $\underline{s}(z) = \mathrm{Re}(\underline{e} \times \underline{h}^*)$ is the real part of the complex Poynting vector $\underline{E} \times \underline{H}^* = \underline{e} \times \underline{h}^*$. It is easily seen that the term $\underline{z}_o \cdot \underline{s}$ is independent of z, ie., $\partial/\partial z(\underline{z}_o \cdot \underline{s}) = 0$, since in a source-free region filled with a lossless medium, the divergence of the real part of the Poynting vector is zero and, for the plane-stratified medium under discussion, $\underline{s}$ is independent of $\underline{\rho}$, so that $\frac{\partial}{\partial x} (\underline{x}_o \cdot \underline{s}) = \frac{\partial}{\partial y} (\underline{y}_o \cdot \underline{s}) = 0.$[#] Thus with the aid of (11), equation (9) becomes

$$j \frac{1}{2} \frac{\partial}{\partial z} \underline{z}_o \cdot (\underline{e}^* \times \delta \underline{h} + \delta \underline{e} \times \underline{h}^*) + d\underline{k}_t \cdot \underline{s} = w d\omega \quad . \qquad (12)$$

In the derivation of (12), the essential assumptions used are that the medium be lossless and that it be plane-stratified so that waves of the form given in (1) satisfy the source-free Maxwell equations. The assumption that $(\underline{k}_t, \omega)$ and $(\underline{k}_t + d\underline{k}_t, \omega + d\omega)$ satisfy the surface wave dispersion relation (3) serves to restrict the changes $d\underline{k}_t$ and $d\omega$ in $\underline{k}_t$ and ω to a surface in $\underline{k}_t - \omega$ space, so that $\delta \underline{e}_t$ and $\delta \underline{h}_t$ will be continuous functions of z for all $-\infty < z < \infty$ and tend to zero as $|z| \to \infty$.

Since the wave vector $\underline{k}_t + d\underline{k}_t$ and the frequency $\omega + d\omega$ satisfy the surface wave dispersion relation, to first order $d\omega = d\underline{k}_t \cdot \nabla_{\underline{k}_t} \omega(\underline{k}_t)$ where $\omega(\underline{k}_t)$ is the solution of the dispersion relation (3). Using this expression for $d\omega$, and after rearranging, equation (12) becomes

$$j \frac{1}{2} \frac{\partial}{\partial z} \underline{z}_o \cdot (\underline{e}^* \times \delta \underline{h} + \delta \underline{e} \times \underline{h}^*) = d\underline{k}_t \cdot (w \nabla_{\underline{k}_t} \omega - \underline{s}) . \qquad (13)$$

[#] Because $\underline{e}_t$ and $\underline{h}_t$ are continuous functions of z, $\underline{z}_o \cdot \underline{s}$ is a continuous function of z and therefore $\partial/\partial z(\underline{z}_o \cdot \underline{s})$ cannot have a delta function behavior at the jumps of ϵ or μ .

63

The term on the left of (13) does not vanish identically so that in general $\underline{s} \neq w \nabla_{\underline{k}_t} \omega$ and hence in the surface wave case $\nabla_{\underline{k}_t} \omega$ cannot be interpreted as a local velocity.

In order to eliminate the term on the left-hand side of (13), integrate this relation over z to obtain

$$j \frac{1}{2} \int_{-\infty}^{\infty} \frac{\partial}{\partial z} \underline{z}_o \cdot (\underline{e}^* \times \delta \underline{h} + \delta \underline{e} \times \underline{h}^*) dz = d\underline{k}_t \cdot (W \nabla_{\underline{k}_t} \omega - \underline{S}) \tag{14}$$

where

$$S = \int_{-\infty}^{\infty} \underline{s} \, dz \tag{15}$$

and

$$W = \int_{-\infty}^{\infty} w \, dz . \tag{16}$$

Because $s_z = \underline{z}_o \cdot \underline{s}$ is independent of z, as discussed above, and is zero at $|z| = \infty$, since $\underline{e}$ and $\underline{h}$ are zero there, s_z is zero for all values of z. Thus $\underline{s}$, and hence $\underline{S}$, are purely transverse vectors.

Recognizing that

$$\underline{z}_o \cdot (\underline{e}^* \times \delta \underline{h} + \delta \underline{e} \times \underline{h}^*) = \underline{z}_o \cdot (\underline{e}_t^* \times \delta \underline{h}_t + \delta \underline{e}_t \times \underline{h}_t^*) . \tag{17}$$

and using the fact that $\underline{e}_t$, $\underline{h}_t$, $\delta \underline{e}_t$ and $\delta \underline{h}_t$ are continuous functions of z, one has

$$\int_{-\infty}^{\infty} \frac{\partial}{\partial z} \underline{z}_o \cdot (\underline{e}^* \times \delta \underline{h} + \delta \underline{e} \times \underline{h}^*) dz = \underline{z}_o \cdot (\underline{e}_t^* \times \delta \underline{h}_t + \delta \underline{e}_t \times \underline{h}_t^*) \Big|_{-\infty}^{\infty} , \tag{18}$$

which vanishes as a consequence of the boundary conditions on $\underline{e}$ and $\underline{h}$ at $|z| = \infty$. Hence,

64

$$d\underline{k}_t \cdot (W \nabla_{\underline{k}_t} \omega - \underline{S}) = 0 \qquad (19)$$

and, since $\underline{S}$ is a purely transverse vector and $d\underline{k}_t$ is arbitrary, it follows that

$$\nabla_{\underline{k}_t} \omega = \underline{S} / W \quad . \qquad (20)$$

Although the real Poynting vector $\underline{s}$ can vary in magnitude and direction with z, the total real Poynting vector $\underline{S}$ is independent of z and represents the total surface wave power flow across a strip normal to $\underline{S}$, infinite in z and having unit width. The term W represents the total stored energy of the surface wave fields in an infinite cylinder, parallel to z, whose x-y cross section has unit area. Equation (20) thus states that the group velocity of the surface wave, $\nabla_{\underline{k}_t} \omega$, is equal to the velocity of energy transport $\underline{S}/W$ of the surface wave as a whole. This statement for the surface waves in plane-stratified media replaces the relation $\nabla_k \omega = \underline{s}/w$ for plane waves in homogeneous anisotropic media and will be used in Chapter V to interpret the surface wave contributions to the fields excited by the point source of Chapter I in terms of surface wave rays.

C. STRATIFIED MEDIUM ABOVE A PERFECTLY CONDUCTING PLANE

The plane-stratified medium described in the first section is now assumed to fill the half-space above a perfectly conducting plane at $z = 0$. Again, assume that the z dependence of ϵ and μ is such that surface waves of the form given in (1) can propagate transversely to the direction of stratification. The vector amplitudes $\underline{e}$ and $\underline{h}$ of these waves tend to zero as z approaches infinity and satisfy the boundary condition $\underline{e}_t = 0$ at $z = 0$. The electric and magnetic energy densities, as well as $\text{Re}(\underline{e} \times \underline{h}^*)$, are now assumed to be integrable on the semi-infinite interval $0 < z < \infty$. As discussed in the previous section, $\underline{e}_t$ and $\underline{h}_t$ must be continuous functions of z. Solutions of Maxwell's equations satisfying the above conditions occur only for values of $\underline{k}_t$ and ω that obey a surface wave dispersion relation, $D_s(\underline{k}_t, \omega) = 0$, valid for the semi-infinite medium.

As in the previous section, the fields at two neighboring sets of values, $(\underline{k}_t, \omega)$ and $(\underline{k}_t + d\underline{k}_t, \omega + d\omega)$, both of which satisfy the dispersion relation, are considered. Using equation (4), the fields $\underline{E}$ and $\underline{H}$ at $(\underline{k}_t + d\underline{k}_t, \omega + d\omega)$ are found, to first order, in terms of the fields and their derivatives, with respect to k_x, k_y and ω, evaluated at $(\underline{k}_t, \omega)$. Since the variations in the fields, $\delta\underline{E}$ and $\delta\underline{H}$, in this problem also satisfy (6), equation (13) holds in this case as well. Because the term on the left-hand side of (13) is, in general, not zero, $\nabla_{\underline{k}_t}\omega$ again cannot be interpreted as a local surface wave energy velocity. However, upon integration of (13) over the interval $0 < z < \infty$, the left-hand side vanishes and $\nabla_{\underline{k}_t}\omega$ can again be interpreted as the velocity of energy transport of the surface wave as a whole. To see this, one recognizes that since $\underline{e}_t = 0$ at $z = 0$, $\delta\underline{e}_t$ must also be zero there. Hence, using equation (17) and recalling that $\underline{e}$ and $\underline{h}$ are zero at $z = \infty$, it is seen that

$$\int_0^\infty \frac{\partial}{\partial z} \underline{z}_o \cdot (\underline{e}^* \times \delta\underline{h} + \delta\underline{e} \times \underline{h}^*)dz = \underline{z}_o \cdot (\underline{e}_t^* \times \delta\underline{h}_t + \delta\underline{h}_t + \delta\underline{e}_t \times \underline{h}_t^*)\Big|_0^\infty = 0 \ .$$

(21)

Defining

$$W = \int_0^\infty w\,dz \qquad\qquad (22)$$

and

$$S = \int\limits_0^\infty \underline{s}\, dz \qquad (23)$$

($\underline{S}$ being a purely transverse vector since $s_z = 0$) the integration of (13) over the interval $0 < z < \infty$ gives, in view of (21),

$$0 = d\underline{k}_t \cdot (W \nabla_{\underline{k}_t} \omega - \underline{S}) \quad . \qquad (24)$$

Again, because $d\underline{k}_t$ is arbitrary, it follows that

$$\nabla_{\underline{k}_t} \omega = \underline{S}/W \quad . \qquad (25)$$

That is to say, for surface waves about a perfectly conducting plane, the group velocity $\nabla_{\underline{k}_t} \omega$ is equal to the velocity of energy transport $\underline{S}/W$ of the surface wave as a whole.[*]

----

[*] If a second perfectly conducting plane at $z = d > 0$ is present, it is easily seen that (25) is still valid for the fields between the conducting planes if $\underline{S}$ and W are now taken as

$$\underline{S} = \int\limits_0^d \underline{s}\, dz \text{ and } W = \int\limits_0^d w\, dz \quad .$$

Thus for waves in a parallel plate wave guide filled with a plane-stratified, lossless, anisotropic medium, the group velocity is equal to the velocity of energy transport.

D.   SURFACE IMPEDANCE AND POWER FLOW RELATIONS

When formulating steady-state electromagnetic problems involving
fields of the form given in (1) in a lossless, plane-stratified anisotropic
medium above a perfectly conducting plane at $z = 0$, it is sometimes profitable
to represent the effect of the structure below a plane $z = d > 0$ on the fields
in the region $z > d$ by a surface impedance dyadic at $z = d$. The impedance
dyadic $\underset{\sim}{Z}$ may then be employed as an equivalent boundary condition at $z = d$
when solving for the fields in the region $z > d$. In this section the relation
between the derivatives of the impedance dyadic, with respect to the spatial
wave numbers k_x and k_y, and the power flowing in the region $0 < z < d$ will
be established and the significance of this relation for surface waves supported
by such an equivalent impedance plane will be pointed out. The relation be-
tween $\partial \underset{\sim}{Z} / \partial \omega$ and stored energy in the region $0 < z < d$ will also be established.

In order to define $\underset{\sim}{Z}$ and to find its relation to power flow and stored
energy in the region $0 < z < d$, consideration is first given to the auxiliary
problem of finding the fields in this region when $\underline{H}_t$ of the form given in (1)
is specified at $z = d$. Thus, one looks in the region $0 < z < d$ for the solution
of Maxwell's equations that satisfies the boundary conditions

$$\underline{E}_t = 0 \tag{26}$$

at $z = 0$ and

$$\underline{H}_t (\underline{r}, t) = \underline{h}_d \, e^{j(\omega t - \underline{k}_t \cdot \underline{\rho})} \tag{27}$$

at $z = d$. All values of $\underline{k}_t$ and ω, except those at which $\underset{\sim}{Z}$ is singular, are con-
sidered (for further discussion, see Appendix F). No restrictions are placed
on the fields in the region $z > d$. In fact, the medium filling the region above
the plane $z = d$ may be taken to be arbitrarily stratified, since, with $\underline{H}_t$ rigidly
prescribed at $z = d$, the medium does not affect the fields for $0 < z < d$. The
medium filling the region $0 < z < d$ is assumed to be lossless, uniform in x
and y and characterized by $\underset{\sim}{\epsilon}$ and $\underset{\sim}{\mu}$ which are analytic functions of ω.

Specification of the above boundary conditions is sufficient, in general, to uniquely determine the fields, and hence the power flow and stored energy, in the region $0 < z < d$. Solving this auxiliary problem for arbitrary polarizations of $\underline{h}_d$ then permits a unique determination of the dyadic surface impedance $\underset{\sim}{Z}$. Having determined $\underset{\sim}{Z}$ from the auxiliary problem, one can now solve for the fields above the impedance plane $z = d$ in terms of $\underset{\sim}{Z}$, the excitation in the region $z > d$, and the boundary conditions at $z = \infty$. The requirement that $\underline{H}_t$ be continuous across $z = d$ now permits one to uniquely determine the fields, and thus the power flow and stored energy, in the region $0 < z < d$ in terms of $(\underline{H}_t)_{z = d}^+$ and the given $\underset{\sim}{Z}$.

In practice, the auxiliary problem need be solved for only two linearly independent polarizations of $\underline{h}_d$, since the linearity of Maxwell's equations permits the solution for any other polarization of $\underline{h}_d$ to be expressed in terms of those for the two independent polarizations. Thus, at each of the values of $\underline{k}_t$ and ω to be considered, one solves for the fields in the region $0 < z < d$ when $\underline{h}_d$ takes on two linearly independent polarizations, e.g., $\underline{h}_d = \underline{x}_o$ and $\underline{h}_d = \underline{y}_o$. Having found the fields, which will be of the form given in (1), for both polarizations of $\underline{h}_d$, $\underset{\sim}{Z}$ may uniquely be defined by requiring that the relation

$$(\underline{E}_t)_{z = d} = \underset{\sim}{Z} \cdot (\underline{z}_o \times \underline{H}_t)_{z = d} \tag{28}$$

be satisfied for both sets of fields. This requirement is equivalent to specifying four inhomogeneous, linearly independent equations from which the four unknown elements of $\underset{\sim}{Z}$ can be found. If one now wishes to solve for fields of the form given in (1), in the region $z > d$, relation (28) may be used as a boundary condition at $z = d$, which will ensure that the transverse fields connect continuously to valid fields in the region $0 < z < d$. That is, if $\underline{e}$ and $\underline{h}$ in the region $z > d$ are such that (28) is satisfied, then, taking $\underline{h}_d$ as $(\underline{h}_t)_{z = d}^+$, the corresponding $\underline{e}$ in the region $0 < z < d$ will be such that $(\underline{e}_t)_{z = d}^- = (\underline{e}_t)_{z = d}^+$.

Having thus defined $\underset{\sim}{Z}$, the meaning of its derivatives with respect to k_x, k_y and ω can be determined. To this end, assume that the fields in the

region $0 < z < d$ are known and $\underline{h}_d$ of (27) has been selected such that the derivatives of the fields with respect to k_x, k_y and ω exist. Equation (12) can now be employed where $d\underline{k}_t$ and $d\omega$ in the variation δ are arbitrary and independent. Equation (12) is valid for the fields in the region $0 < z < d$ since the assumptions used in deriving it are also satisfied in the present case - see the text after (12). The restrictions placed on $d\underline{k}_t$ and $d\omega$ in the first section are not necessary in the present discussion since, as previously mentioned, solutions of Maxwell's equations for which $\underline{e}_t$ and $\underline{h}_t$ are continuous in z will exist in the region $0 < z < d$ for all $\underline{k}_t$ and ω (excepting the singular points of $\underset{\sim}{Z}$, as discussed in Appendix F, thus ensuring that $\delta\underline{e}_t$ and $\delta\underline{h}_t$ are continuous functions of z for all $d\underline{k}_t$ and $d\omega$. Since the fields are bounded as z approaches d and as z approaches 0, it is permissible to integrate (12) over the closed interval $0 \leq z \leq d$. Performing the integration and using (17) yields the relation

$$j \frac{1}{2} \underline{z}_o \cdot (\underline{e}_t^* \times \delta\underline{h}_t + \delta\underline{e}_t \times \underline{h}_t^*)_{z=d} = W_d \, d\omega - d\underline{k}_t \cdot \underline{S}_d \quad . \quad (29)$$

Here

$$W_d = \int_0^d w \, dz \quad\quad\quad (30)$$

and

$$\underline{S}_d = \int_0^d \underline{s} \, dz \quad . \quad\quad\quad (31)$$

Note that since $\frac{\partial}{\partial z} s_z = \nabla \cdot \underline{s} = 0$ and $(s_z)_{z=0} = 0$, $s_z = 0$ for all $0 < z < d$ and hence $\underline{S}_d$ is a transverse vector.

Since $\underline{E}$ and $\underline{H}$ have the form given in (1), the impedance relation (28) may be rewritten as

$$(\underline{e}_t)_{z=d} = \underset{\sim}{Z} \cdot (\underline{z}_o \times \underline{h}_t)_{z=d} \quad . \quad\quad\quad (32)$$

Applying the variation δ to the above equation gives

$$(\delta\underline{e}_t)_{z=d} = \underset{\sim}{Z} \cdot (\underline{z}_o \times \delta\underline{h}_t)_{z=d} + \delta\underset{\sim}{Z} \cdot (\underline{z}_o \times \underline{h}_t)_{z=d} \quad . \quad (33)$$

Using $(\underline{e}_t)_{z=d}$ from (32) and $(\delta\underline{e}_t)_{z=d}$ from (33), it can be verified that

$$\underline{z}_o \cdot (\underline{e}_t^* \times \delta\underline{h}_t + \delta\underline{e}_t \times \underline{h}_t^*)_{z=d} = -[(\underline{z}_o \times \underline{h}_t^*) \cdot \underset{\sim}{\delta Z} \cdot (\underline{z}_o \times \underline{h}_t)]_{z=d}$$

(34)

when the anti-Hermitain property* of $\underset{\sim}{Z}$ is used to write
$[(\underline{z}_o \times \underline{h}_t^*) \cdot \underset{\sim}{Z} \cdot (\underline{z}_o \times \delta\underline{h}_t)]_{z=d} = -[(\underline{z}_o \times \delta\underline{h}_t) \cdot \underset{\sim}{Z}^* \cdot (\underline{z}_o \times \underline{h}_t^*)]_{z=d}$. With relation (34), equation (29) becomes

$$-j\frac{1}{2}[(\underline{z}_o \times \underline{h}_t^*) \cdot \underset{\sim}{\delta Z} \cdot (\underline{z}_o \times \underline{h}_t)]_{z=d} = W_d\,d\omega - d\underline{k}_t \cdot \underline{S}_d \ . \qquad (35)$$

Since dk_x, dk_y and $d\omega$ are all independent, one finds that

$$j\frac{1}{2}[(\underline{z}_o \times \underline{h}_t^*) \cdot \frac{\partial \underset{\sim}{Z}}{\partial k_x} \cdot (\underline{z}_o \times \underline{h}_t)]_{z=d} = S_{dx}$$

$$j\frac{1}{2}[(\underline{z}_o \times \underline{h}_t^*) \cdot \frac{\partial \underset{\sim}{Z}}{\partial k_y} \cdot (\underline{z}_o \times \underline{h}_t)]_{z=d} = S_{dy}$$

(36)

and that

$$-j\frac{1}{2}[(\underline{z}_o \times \underline{h}_t^*) \cdot \frac{\partial \underset{\sim}{Z}}{\partial \omega} \cdot (\underline{z}_o \times \underline{h}_t)]_{z=d} = W_d \quad . \qquad (37)$$

It is thus seen that W_d and $\underline{S}_d$ can be found knowing only $\underset{\sim}{Z}$ and $(\underline{h}_t)_{z=d}$. As previously pointed out, if fields of the form given in (1) exist in the region $z > d$ and satisfy the impedance boundary condition at $z = d$, there will be unique fields in the region $0 < z < d$ that satisfy the continuity conditions $(\underline{h}_t)_{z=d^-} = (\underline{h}_t)_{z=d^+}$ and $(\underline{e}_t)_{z=d^-} = (\underline{e}_t)_{z=d^+}$. Because of the continuity of $\underline{h}_t$ at $z = d$, the power flow and stored energy associated with the

----

*

The impedance dyadic Z is anti-Hermitian, i.e., the matrix representation for Z has the property that the transpose conjugate $\underset{\sim}{Z}^+$ is equal to $-\underset{\sim}{Z}$. This property follows from the facts that $s_z = 0$ for all $z < d$ and that the fields are continuous as z approaches d from below so that $\mathrm{Re}(\underline{e}_t \times \underline{h}_t^*)_{z=d}$ must be zero. (28)

fields in the region $0 < z < d$ can be calculated from relations (36) and (37) using $(\underline{h}_t)_{z=d} = \lim_{z \downarrow d} \underline{h}_t$, i.e., the limit of $\underline{h}_t$ as z approaches d from above.

Since the relations (36) and (37) hold for arbitrary $\underline{k}_t$ and ω, they are valid, in particular, for values of $\underline{k}_t$ and ω that correspond to a surface wave. Thus relations (36) and (37), with appropriate values of $\underline{k}_t$ and ω, furnish an alternative way of calculating that portion of the surface wave power flowing in the slab and that portion of the stored energy of the surface wave which is in the slab

The relation between power flow and the derivatives of $\underset{\sim}{Z}$ with respect to k_x and k_y given in (36) does not appear to have been previously recognized. While the connection between stored energy and $\partial \underset{\sim}{Z} / \partial \omega$, to the best of our knowledge, has not been shown explicitly for the case of traveling waves, the connection between stored power and the impedance matrix of a lossless junction is well known. [29]

The consistency of relations (36) and (37) for surface waves with the results obtained in the second section will now be shown. Consider a surface wave propagating in a lossless plane-stratified medium above a surface impedance plane at $z = d$. The surface impedance $\underset{\sim}{Z}$ is assumed to be known and to represent the effect of a plane-stratified, lossless medium above a perfectly conducting plane at $z = 0$. The surface wave fields in the region $z > d$ are assumed to be of the form given in (1) with $\underline{k}_t$ and ω related through the appropriate surface wave dispersion relation. The surface wave fields satisfy (13), which, when integrated over the interval $d < z < \infty$, yields the relation

$$- j \frac{1}{2} \underline{z}_o \cdot (\underline{e}_t^* \times \delta\underline{h}_t + \delta\underline{e}_t \times \underline{h}_t^*)_{z=d} = d\underline{k}_t \cdot \left[\nabla_{\underline{k}_t} \omega \int_d^\infty w\,dz - \int_d^\infty \underline{s}\,dz \right] . \quad (38)$$

Since $\underline{e}_t$ and $\underline{h}_t$ satisfy the impedance condition (32), equation (34) holds. Using (34) and the fact that for the surface wave $d\omega = d\underline{k}_t \cdot \nabla_{\underline{k}_t} \omega$, the above equation can be written as

$$d\underline{k}_t \cdot \nabla_{\underline{k}_t} \omega \left\{ \int_d^\infty w\,dz - j\frac{1}{2}\left[(\underline{z}_o \times \underline{h}_t^*) \cdot \frac{\partial Z}{\partial \omega} \cdot (\underline{z}_o \times \underline{h}_t)\right]_{z=d} \right\}$$

$$= d\underline{k}_t \cdot \left\{ \int_d^\infty \underline{s}\,dz + \underline{x}_o\frac{1}{2}\left[(\underline{z}_o \times \underline{h}_t^*) \cdot \frac{\partial Z}{\partial k_x} \cdot (\underline{z}_o \times \underline{h}_t)\right]_{z=d} \right.$$

$$\left. + \underline{y}_o\frac{1}{2}\left[(\underline{z}_o \times \underline{h}_t^*) \cdot \frac{\partial Z}{\partial k_y} \cdot (\underline{z}_o \times \underline{h}_t)\right]_{z=d} \right\} \quad . \tag{39}$$

As discussed above, the terms containing $\partial Z/\partial k_x$ and $\partial Z/\partial k_y$ that appear in (39) are equal to the x and y components of the power flow $\underline{S}_d$ below the plane $z = d$. Furthermore, the term containing $\partial Z/\partial \omega$ is equal to the stored energy, per unit area in the x-y plane, below the plane $z = d$, namely, W_d. Thus (39) may be written

$$d\underline{k}_t \cdot \nabla_{\underline{k}_t} \omega \left\{ \int_d^\infty w\,dz + W_d \right\} = d\underline{k}_t \cdot \left\{ \int_d^\infty \underline{s}\,dz + \underline{S}_d \right\} \tag{40}$$

or, since $d\underline{k}_t$ is arbitrary,

$$\nabla_{\underline{k}_t} \omega \left\{ \int_d^\infty w\,dz + W_d \right\} = \int_d^\infty \underline{s}\,dz + \underline{S}_d \quad . \tag{41}$$

Finally, from the definition of W_d and $\underline{S}_d$ given in (30) and (31), equation (41) is seen to reduce to

$$\nabla_{\underline{k}_t} \omega \int_0^\infty w\,dz = \int_0^\infty \underline{s}\,dz \quad , \tag{42}$$

which is precisely the relation found to hold in the previous section for surface waves above a perfectly conducting plane at $z = 0$. Hence if a surface impedance boundary condition representing a plane-stratified medium above a perfectly conducting plane is used when solving for surface waves, the resultant group velocity $\nabla_{\underline{k}_t} \omega$ is equal to the energy transport velocity of the entire surface wave, not to just that portion of the surface wave above the impedance plane.

E. SURFACE IMPEDANCE FOR THE CASE OF EVANESCENT WAVES

In the derivation of the power flow and energy relations for a surface impedance representing a plane-stratified medium above a perfectly conducting plane, the presence of the conducting plane served to ensure that $s_z = 0$ and that the stored energy, per unit area in the x-y plane, and power flow are finite in the region $0 < z < d$ for all possible polarizations of $(\underline{h}_t)_{z = d}$ and all real values of $\underline{k}_t$ and ω. Since the fields of evanescent waves in a semi-infinite plane-stratified medium also possess these two properties, one would expect power flow and energy relations similar to (36) and (37) to exist in this case for the surface impedance representing the semi-infinite medium.

Let a semi-infinite, plane-stratified, lossless, dispersive, aniso-tropic medium fill the region above the plane $z = d$. By analogy to the case of the medium above a perfectly conducting plane, consideration is first given to the auxiliary problem of finding those fields in the region $z > d$ which satisfy the boundary condition

$$(\underline{H}_t)_{z = d} = \underline{h}_d \; e^{j(\omega t - \underline{k}_t \cdot \underline{\rho})} \tag{43}$$

at $z = d$ and the boundary conditions

$$\lim_{z \to \infty} (\underline{E}, \underline{H}) = 0 \quad . \tag{44}$$

In addition, it is required that $\int_d^\infty \underline{s} \, d z$ and $\int_d^\infty w \, d z$ exist. The term "evane-scent", as used in the rest of this section, will refer to fields satisfying (44) and the foregoing integral requirements. Evanescent fields will also have the property that $s_z = 0$. The auxiliary problem is to be solved for all polari-aations of $\underline{h}_d$ so that the surface impedance may be defined.

In general, only for limited regions in $\underline{k}_t - \omega$ space will the auxiliary problem have unique, non-trivial, evanescent solutions that satisfy (43) for all $\underline{h}_d$ and thus permit definition of the surface impedance $\underset{\sim}{Z}_s$. Other values of $\underline{k}_t$ and ω will not be considered for one of two reasons. First, in media having an appropriate z dependence, non-unique, cavity-type, evanescent solutions satisfying (43) with $\underline{h}_d = 0$ may exist for points lying on surfaces in

$\underline{k}_t$ - ω space. In such cases, $\underset{\sim}{Z}_s$ will have singularities on these surfaces. (Discussion of such points and the derivation of a surface admittance formalism that is, in general, regular at such points, are analogous to those given in Appendix F for a medium of firite thickness above a perfectly conducting plane.) Second, in some regions of $\underline{k}_t$ - ω space, fields satisfying (43) will not be of the evanescent type for most or all polarizations of $\underline{h}_d$.[#] Thus, unless alternate boundary conditions are specified at $z = \infty$, such as the radiation condition, the fields, and hence $\underset{\sim}{Z}_s$, cannot be uniquely defined. Even if boundary conditions are impose at $z = \infty$ and if $\underset{\sim}{Z}_s$ is defined in this case (it is no longer anti-Hermitian), the associated fields do not possess the integration properties necessary to derive simple power flow and stored energy relations.

Hence only those regions in $\underline{k}_t$ - ω space in which the auxiliary problem has unique, non-trivial solutions satisfying (43) and (44) for all $\underline{h}_d \neq 0$ will be considered here. The regions where the auxiliary problem can be solved, the nature of which depends on the particular medium under discussion, are assumed to exist and to form open sets, i.e., not merely surfaces, so that k_x, k_y, and ω will be continuous, independent variables within these regions.

Thus restricting $\underline{k}_t$ and ω to those regions where unique, non-trivial solutions of the auxiliary problem are assumed to exist for all polarizations of $\underline{h}_d$, the surface impedance dyadic $\underset{\sim}{Z}_s$ can be defined for the semi-infinite region. Since the linearity of Maxwell's equations permits the solutions for all $\underline{h}_d$ to be expressed as a superposition of the solutions for two linearly independent polarizations of $\underline{h}_d$, one need consider only two such polarizations, e.g., $\underline{h}_d = \underline{x}_o$ and $\underline{h}_d = \underline{y}_o$. From the solutions of the auxiliary problem, which will be of the form given in (1), for these two polarizations, $\underset{\sim}{Z}_s$ can be found uniquely from the requirement that the relation

----

[#] An example of a region where no evanescent waves exist is formed by the points in and on the cone $\omega^2 = \dfrac{1}{\epsilon_o \mu_o} (k_x^2 + k_y^2)$ when the medium being studied is free space. Outside this cone unique, non-trivial solutions of the auxiliary problem exist for all $\underline{h}_d$.

$$\left(\underline{e}_t\right)_{z=d} = \underset{\sim s}{Z} \cdot \left(-\underline{z}_o \times \underline{h}_t\right)_{z=d} \qquad (45)$$

be satisfied by the fields of both solutions.*

By analogy to the discussion given in the previous section, $\underset{\sim s}{Z}$ may be used as a boundary condition at $z=d$ when solving for the fields below this plane. Also, requiring $\underline{h}_t$ to be continuous at $z=d$ uniquely determines the fields above this plane when the fields below are known.

Assuming $\underset{\sim s}{Z}$ and the fields in the region $z > d$ to be known, equation (12) is employed in finding the power flow and energy relations in this region. Equation (12) is valid for the fields in the region $z > d$ since the assumptions used in deriving it are satisfied in the present case - see the text after (12). The differential quantities $d\underline{k}_t$ and $d\omega$ in the variation δ are arbitrary and independent since k_x, k_y and ω are independent variables. Integrating (12) from $z = d$ to $z = \infty$ gives

$$-j\frac{1}{2}\underline{z}_o \cdot \left(\underline{e}_t^* \times \delta\underline{h}_t + \delta\underline{e}_t \times \underline{h}_t^*\right)_{z=d} = W_s d\omega - d\underline{k}_t \cdot \underline{S}_s \qquad (46)$$

where

$$W_s = \int_d^\infty w\, dz \qquad (47)$$

and the purely transverse vector $\underline{S}_s$ is

$$\underline{S}_s = \int_d^\infty \underline{s}\, dz \quad . \qquad (48)$$

In a manner similar to that of the previous section, the term on the left-hand side of (46) can be written in terms of $\delta\underset{\sim s}{Z}$ if the anti-Hermitian property of $\underset{\sim s}{Z}$ is taken into account. That $\underset{\sim s}{Z}$ is anti-Hermitian follows from the fact

---
*
In the above relation, $-\underline{z}_o$ is used instead of $\underline{z}_o$, as was used in (28) and (32) for the medium above a perfectly conducting plane, because $-\underline{z}_o$ is the outward unit normal for the configuration being considered. The convention of using the outward unit normal in defining the impedance is based on the desire to have the impedance matrix be positive-definite when loss is present in the structure.

that $s_z = 0$ for evanescent fields in a lossless, plane-stratified medium.
In terms of $\delta Z_{\sim s}$, (46) becomes

$$-j\frac{1}{2}\left[(-\underline{z}_o \times \underline{h}_t^*) \cdot \delta Z_{\sim s} \cdot (-\underline{z}_o \times \underline{h}_t)\right]_{z=d} = W_s \, d\omega - d\underline{k}_t \cdot \underline{S}_s \; . \qquad (49)$$

Since dk_x, dk_y and $d\omega$ are all independent, the above relation can hold only
if

$$\left[\underline{x}_o \frac{j}{2}(-\underline{z}_o \times \underline{h}_t^*) \cdot \frac{\partial Z_{\sim s}}{\partial k_x} \cdot (-\underline{z}_o \times \underline{h}_t) \right.$$

$$\left. + \underline{y}_o \frac{j}{2}(-\underline{z}_o \times \underline{h}_t^*) \cdot \frac{\partial Z_{\sim s}}{\partial k_y} \cdot (-\underline{z}_o \times \underline{h}_t)\right]_{z=d} = \underline{S}_s \qquad (50)$$

and

$$-j\frac{1}{2}\left[(-\underline{z}_o \times \underline{h}_t^*) \cdot \frac{\partial Z_{\sim s}}{\partial \omega} \cdot (-\underline{z}_o \times \underline{h}_t)\right]_{z=d} = W_s \; . \qquad (51)$$

The foregoing relations should be compared to (36) and (37). Note
that if $\underline{z}_o$ instead of $-\underline{z}_o$ had been used in (45), the above relations would
contain an additional minus sign.

The concept of a surface impedance to describe the effect of the medium
above the plane $z = d$ on the fields below this plane can be employed to derive
the dispersion relation for surface waves. The physical configuration to be
considered here consists of a plane-stratified, lossless, anisotropic medium
above the plane $z = d > 0$ and a second plane-stratified, lossless, anisotropic
medium between a perfectly conducting plane at $z = 0$ and the plane $z = d$. It
will be assumed that the values of $\underline{k}_t$ and ω of interest are such that the
medium above the plane $z = d$ is representable in terms of an anti-Hermitian
surface impedance $Z_{\sim s}$ that satisfies (45). This restriction on $\underline{k}_t$ and ω is
equivalent to the requirement that the fields in the region $z > d$ be of the sur-
face wave type for all $(\underline{h}_t)_{z=d}$. (In special cases, surface waves may exist
when the fields in the region $z > d$ are of the surface wave type for only one

polarization of $(\underline{h}_t)_{z=d}$. Such cases are not included in the present discussion.) The structure below the plane $z = d$ is assumed to be represented by the surface impedance $\underset{\sim}{Z}$ that satisfies (32).

Since $\underline{e}_t$ and $\underline{h}_t$ for the surface waves are continuous functions of z, these quantities must be the same in both (32) and (45). Thus subtracting these two equations gives

$$(\underset{\sim}{Z} + \underset{\sim}{Z}_s) \cdot (\underline{z}_o \times \underline{h}_t)_{z=d} = 0 \ , \tag{52}$$

which is a homogeneous set of two linear equations in the two unknown elements of $(\underline{z}_o \times \underline{h}_t)_{z=d}$. For non-trivial solutions of (52) to exist one requires that $\det(\underset{\sim}{Z} + \underset{\sim}{Z}_s) = 0$, which gives the surface wave dispersion relation $D_s(\underline{k}_t, \omega) = 0$. At those values of $\underline{k}_t$ and ω which satisfy the surface wave dispersion relation, $(\underline{z}_o \times \underline{h}_t)_{z=d}$ can be found. If the partial derivatives of $\underset{\sim}{Z}$ and $\underset{\sim}{Z}_s$ with respect to k_x, k_y and ω are calculated, the power flow and stored energy can now be found in each region by using (36), (37), (50) and (51).

Thus it is seen that the knowledge of $\underset{\sim}{Z}$ and $\underset{\sim}{Z}_s$ for the lossless plane-stratified structures previously described is sufficient to find the surface wave dispersion relation and the division of power flow and stored energy between the two regions. Also, this procedure can be applied when the structure below the plane $z = d$ is a semi-infinite medium whose regions in $\underline{k}_t - \omega$ space, where the reactive surface impedance may be defined, intersect the corresponding regions for the medium above the plane $z = d$.

Chapter IV

SURFACE WAVES ON A UNIAXIAL PLASMA SLAB; THEIR
GROUP VELOCITY AND POWER FLOW

A. INTRODUCTION

The group velocity of a surface wave propagating in a plane-stratified, anisotropic, dispersive medium that is also linear and lossless was shown in Chapter III to be equal to the velocity of energy transport of the surface wave as a whole. This velocity is defined as the integral of the real part of the Poynting vector over the coordinate in the direction of stratification divided by the integral of the stored energy density over this coordinate. In this chapter the above relation is verified by direct calculation for the case of surface waves supported by a uniaxial, cold-electron plasma slab. The plasma slab is assumed to be of infinite extent and to be located in free space. A static magnetic field of infinite strength and parallel to the interfaces between the plasma and free space generates the anisotropy.

The characteristics of trapped surface waves propagating on anisotropic plasma slabs have been discussed in the literature for various specific directions of propagation relative to the static magnetic field. Wait[30] has considered the surface waves propagating on a thin plasma slab with an arbitrary static magnetic field. Requiring the plasma slab to be thin reduces the effect of the static magnetic field to that which would be produced by the component normal to the slab alone. Meltz and Shore[31] discuss the excitation of surface waves on a slab of arbitrary thickness when the static magnetic field is perpendicular to the slab and of infinite strength. In both of these cases, the anisotropy is such that the slab configurations have rotational symmetry about the coordinate normal to the slab and hence the characteristics of the surface waves will be independent of the direction of propagation. Furthermore, as in isotropic slab configurations, the velocity of energy transport of surface waves on these slab configurations will be parallel to the transverse wave vector.

When the static magnetic field is parallel to the air-plasma inter-
faces, the effect of the resultant anisotropy is more striking since then the
characteristics of the surface waves on the slab depend on their directions
of propagation with respect to the static magnetic field. Also, the velocity
of energy transport will not be parallel, in general, to the transverse wave
vector. Examples found in the literature, of surface waves on slab con-
figurations with axis of anisotropy parallel to the interfaces, do not illus-
trate these anisotropic effects as they are restricted either to propagation
along[31, 32, 33] or normal[34] to the static magnetic field. In either case,
the velocity of energy transport is parallel to the transverse wave vector.
In this paper, however, the surface wave fields are considered for arbitrary
directions of propagation with respect to the static magnetic field of infinite
strength. It will be shown that for this configuration, the velocity of energy
transport of each surface wave is not parallel, in general, to the transverse
wave vector, and that the direction, as well as the magnitude, of the real
part of the complex Poynting vector varies with the coordinate normal to the
slab. Thus the slab configuration provides a non-trivial example of the
equality of the surface wave's group velocity and its energy transport velo-
city. The excitation of the surface waves is not considered here.

In Section B the fields and dispersion relation of the E-type surface
waves, which have no component of R.F. magnetic field along the static
magnetic field, are found. A graphical procedure for solving the dispersion
relation and the properties of the dispersion curves are discussed in Section
C. Section D is devoted to an analytical verification of the equality of group
velocity and energy transport velocity for the surface waves. In Appendix H,
it is proved that the uniaxial slab configuration can support only the E-type
surface waves described in this chapter.

B. FIELDS AND DISPERSION RELATION

In this section, the fields and dispersion relation for surface waves on a uniaxial electron plasma slab are found. The plasma within the slab is homogeneous and the superimposed D. C. magnetic field, which is assumed to be of infinite strength, is parallel to the y axis (see Fig. 1). In the linear or small signal approximation, the interaction of the uniaxial plasma with a monochromatic electromagnetic field may be described by a relative dielectric tensor $\underset{\sim}{\epsilon}'$. Neglecting collision loss, when the D.C. magnetic field is in the y direction, $\underset{\sim}{\epsilon}'$ takes the form[31, 32]

$$[\underset{\sim}{\epsilon}'] = \begin{bmatrix} 1 & 0 & 0 \\ 0 & 1-X & 0 \\ 0 & 0 & 1 \end{bmatrix} \tag{1}$$

where $X = (\omega_p/\omega)^2$ and ω_p is the electron plasma frequency. Thus in the plasma slab $\underset{\sim}{\epsilon} = \epsilon_o \underset{\sim}{\epsilon}'$ while in the air regions $\underset{\sim}{\epsilon} = \epsilon_o \underset{\sim}{1}$, where $\underset{\sim}{1}$ is the unit dyadic. The permeability tensor $\underset{\sim}{u}$ is given everywhere by $\underset{\sim}{u} = u_o \underset{\sim}{1}$.

The surface wave fields, which decay exponentially in the air regions, have transverse dependence $e^{-j(k_x x + k_y y)}$, k_x and k_y being real transverse wave numbers. These fields will be constructed from those plane wave solutions appropriate to the plasma region and those appropriate to the free space regions. The plane wave solutions appropriate to the plasma slab are those waves of the form

$$\left. \begin{matrix} \underline{E}(\underline{r}, \underline{k}) \\ \\ \underline{H}(\underline{r}, \underline{k}) \end{matrix} \right\} = \left\{ \begin{matrix} \underline{e}'(\underline{k}) \\ \\ \underline{h}'(\underline{k}) \end{matrix} \right\} e^{-j\underline{k} \cdot \underline{r}} \tag{2}$$

which can propagate in an infinite homogeneous plasma described by the relative dielectric tensor $\underset{\sim}{\epsilon}'$ given in (1). Similarly, the plane wave solutions appropriate to the free space are those having the form given in (2) which can exist when the plasma slab is absent.
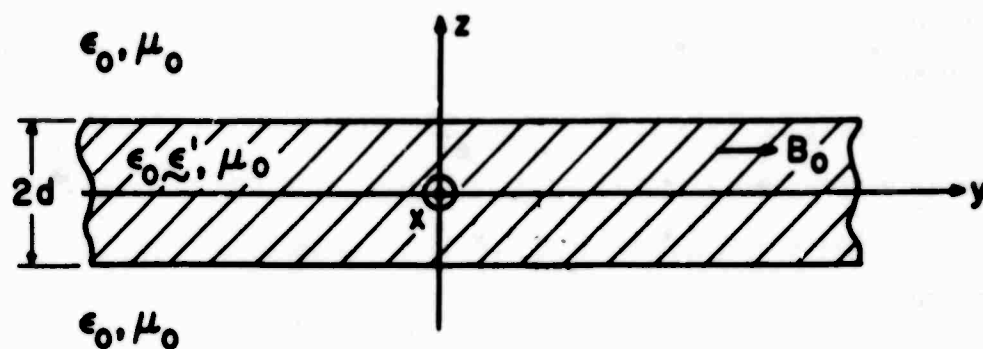
Fig. IV-1   Anisotropic plasma slab configuration

The plasma plane waves are found by substituting $\underline{E}$ and $\underline{H}$ from (2) into Maxwell's equations. The resultant equations are, when the time dependence $e^{j\omega t}$ is suppressed,

$$\underline{k} \times \underline{e}' = \omega \mu_o \underline{h}'$$

$$\underline{k} \times \underline{h}' = -\omega \epsilon_o \underset{\sim}{\epsilon}' \cdot \underline{e}'$$

(3)

Multiplying the first equation by $\underline{k} \times$ and substituting the second gives $\underline{k} \times (\underline{k} \times \underline{e}') = -k_o^2 \underset{\sim}{\epsilon}' \cdot \underline{e}'$, with $k_o^2 = \omega^2 \epsilon_o \mu_o$. Expanding the triple cross-product, this equation may be written in dyadic form as

$$(k_o^2 \underset{\sim}{\epsilon}' + \underline{k}\underline{k} - k^2 \underset{\sim}{1}) \cdot \underline{e}' = 0 \quad ,$$

(4)

which is equivalent to three homogeneous equations in three unknowns. For there to be non-trivial solutions of (4), the determinant of the matrix representation of the dyadic operator $(k_o^2 \underset{\sim}{\epsilon}' + \underline{k}\underline{k} - k^2 \underset{\sim}{1})$ must vanish. Letting $\underline{k} = \underline{k}_t + \underline{z}_o \kappa$, with $\underline{k}_t = \underline{x}_o k_x + \underline{y}_o k_y$, the vanishing of the determinant results in the plane wave dispersion relation $D_p(\underline{k}, \omega) = 0$ for an infinitely extended, homogeneous, uniaxial plasma. This plane wave dispersion relation may be solved for κ. Four solutions result, which are

$$\kappa = \left\{ \begin{array}{c} \pm \sqrt{k_o^2 - \underline{k}_t^2} \\[3mm] \pm \sqrt{(1-X)(k_o^2 - k_y^2) - k_x^2} \end{array} \right\} \qquad (5)$$

The sign choice before each root refers to waves carrying power or decaying in the positive or negative z direction. Substituting each of the four solutions given in (5) into (4), the corresponding field vector $\underline{e}'$ can be found. Finally, the pertinent $\underline{h}'$ can be calculated from (3).

The above method may be repeated to find the plane wave fields $\underline{e}'_a$ and $\underline{h}'_a$ for free space. Since $\underline{k}_t$ must be the same for the entire surface wave if the transverse fields are to be continuous everywhere across the planes $z = \pm d$, it follows that the free space wave vector $\underline{k}_a = \underline{k}_t + \underline{z}_o \kappa_a$. Substituting the form of $\underline{E}$ and $\underline{H}$ given in (2) into Maxwell's equations for free space gives

$$\left. \begin{array}{c} \underline{k}_a \times \underline{e}'_a = \omega\mu_o \underline{h}'_a \\[3mm] \underline{k}_a \times \underline{h}'_a = -\omega\epsilon_o \underline{e}'_a \end{array} \right\} \qquad (6)$$

From (6), the homogeneous equations that determine $\underline{e}'_a$ are found, in dyadic form to be

$$\left[(k_o^2 - \underline{k}_a^2)\underset{\sim}{1} + \underline{k}_a \underline{k}_a \right] \cdot \underline{e}'_a = 0 \quad . \qquad (7)$$

From the requirement that the determinant of the matrix representation of $[(k_o^2 - \underline{k}_a^2)\underset{\sim}{1} + \underline{k}_a \underline{k}_a]$ vanish for non-trivial solutions of $\underline{e}'_a$ to exist, one can solve for κ_a as

$$\kappa_a = \pm \sqrt{k_o^2 - \underline{k}_t^2} \qquad (8)$$

When these values of κ_a are used, (7) reduces to $\underline{k}_a \cdot \underline{e}'_a = 0$, i.e., the plane wave electric field is orthogonal to the wave vector $\underline{k}_a$, a condition that does not uniquely determine $\underline{e}'_a$. Commonly chosen solutions for $\underline{e}'_a$

are those corresponding to TM and TE modes with respect to the z direction. Other possible choices for $\underline{e}'_a$, which will prove more useful in this analysis, are those of the so-called E-type and H-type modes, which are appropriate linear combinations of the TM and TE modes. The E-type modes with respect to y are characterized by the vanishing of the y component of the magnetic field, while the H-type modes are characterized by the vanishing of the y component of the electric field.

In each region, the surface wave fields will be a combination of the plane wave solutions appropriate to that region, the relative amplitudes of which can be found from the radiation condition and the continuity conditions at z = ± d. Since the free space outside the slab is homogeneous, the surface waves are characterized by an exponential decay of their fields away from the slab. Such decay requires that $\varkappa_a$ be imaginary and that for Region 1 the sign choice in (8) be taken to give $\varkappa_a = -j|\varkappa_a|$, so that the fields will decay in the positive z direction. For the plane waves in Region 3, the sign must be taken so as to give $\varkappa_a = j|\varkappa_a|$, which will result in fields that decay in the negative z direction.

It will be shown later that a surface wave, whose fields in the plasma slab are a combination of those plane wave fields corresponding to $\varkappa = \pm \sqrt{(1-X)(k_o^2 - k_y^2) - k_x^2}$, exists only for X > 1. In Appendix H it is shown that H-type surface wave modes, characterized by the vanishing of the y component of the electric field, cannot propagate on the uniaxial plasma slab. The plane wave fields in the plasma region corresponding to $\varkappa = \pm \sqrt{(1-X)(k_o^2 - k_y^2) - k_x^2}$ are E-type modes and have the form

$$\left. \begin{aligned} \underline{e}' &= A\left[\underline{x}_o k_x k_y - \underline{y}_o(k_o^2 - k_y^2) + \underline{z}_o k_y \varkappa \right] \\[2mm] \underline{h}' &= A\omega\epsilon_o\left[\underline{x}_o \varkappa - \underline{z}_o k_x \right] \end{aligned} \right\} \tag{9}$$

with A an arbitrary constant.

As mentioned earlier, the only requirement on $\underline{e}'_a$ is that $\underline{k}_a \cdot \underline{e}'_a = 0$. Hence, we may arbitrarily select the transverse part of $\underline{e}'_a$ and then use the requirement $\underline{k}_a \cdot \underline{e}'_a = 0$ to find the corresponding z component of $\underline{e}'_a$. A particularly useful form of the transverse part of $\underline{e}'_a$ is obtained by choosing it to be identical with the transverse part of $\underline{e}'$ as given in (9). This choice will be seen to simplify the application of the continuity requirement on the transverse fields at $z = \pm d$. Following this procedure one finds

$$\underline{e}'_a = B\left[\underline{x}_o k_x k_y - \underline{y}_o(k_o^2 - k_y^2) + \underline{z}_o k_y \varkappa_a\right]$$

$$\underline{h}'_a = B\omega\epsilon_o\left[\underline{x}_o \varkappa_a - \underline{z}_o k_x\right] \tag{10}$$

with B an arbitrary constant. It is seen that the transverse part of $\underline{h}'_a$ has the same vector direction as the transverse part of $\underline{h}'$. It will thus be possible to satisfy the continuity conditions at $z = \pm d$ using only the plane waves exhibited in (9) and (10).

Since the wave number $\varkappa_a$ must be imaginary, let

$$\alpha = \sqrt{k_t^2 - k_o^2} \tag{11}$$

so that $\varkappa_a = \pm j\alpha$ where α is real and positive. Then in Region 1, $\varkappa_a = -j\alpha$, for decay in the positive z direction, and if $\underline{\rho} = \underline{x}_o x + \underline{y}_o y$, the fields are

$$\underline{E} = B_1\left[\underline{x}_o k_x k_y - \underline{y}_o(k_o^2 - k_y^2) - \underline{z}_o jk_y\alpha\right]e^{-\alpha z}\, e^{-j\underline{k}_t \cdot \underline{\rho}}$$

$$\underline{H} = B_1 \omega\epsilon_o\left[-\underline{x}_o j\alpha - \underline{z}_o k_x\right] e^{-\alpha z}\, e^{-j\underline{k}_t \cdot \underline{\rho}} \tag{12}$$

while in Region 3, $\varkappa_a = j\alpha$, and the corresponding fields are

$$\underline{E} = B_3 \left[\underline{x}_o k_x k_y - \underline{y}_o (k_o^2 - k_y^2) + \underline{z}_o jk_y \, \alpha \right] e^{\alpha z} \, e^{-j\underline{k}_t \cdot \underline{\rho}}$$

$$\underline{H} = B_3 \, \omega \epsilon_o \left[\underline{x}_o j\alpha - \underline{z}_o k_x \right] e^{\alpha z} \, e^{-j\underline{k}_t \cdot \underline{\rho}}$$

(13)

The constants B_1 and B_3 have yet to be determined.

For simplicity in what follows, define β as

$$\beta = \sqrt{(1 - X)(k_o^2 - k_y^2) - k_x^2}$$

(14)

so that in (5) $\kappa = \pm \beta$. It will be shown that for a surface wave to propagate on the slab β must be real. The fields in Region 2 will be the sum of the fields of the two plane waves having the vector form displayed in (9) and traveling in opposite directions along z. The most general form of such a sum is

$$\underline{E} = \left\{ \left[\underline{x}_o k_x k_y - \underline{y}_o (k_o^2 - k_y^2) \right] (A_1 e^{-j\beta z} + A_2 e^{j\beta z}) \right.$$

$$\left. + \underline{z}_o k_y \beta (A_1 e^{-j\beta z} - A_2 e^{j\beta z}) \right\} e^{-j\underline{k}_t \cdot \underline{\rho}}$$

(15-a)

and

$$\underline{H} = \omega \epsilon_o \left\{ \underline{x}_o \beta (A_1 e^{-j\beta z} - A_2 e^{j\beta z}) \right.$$

$$\left. - \underline{z}_o k_x (A_1 e^{-j\beta z} + A_2 e^{j\beta z}) \right\} e^{-j\underline{k}_t \cdot \underline{\rho}}$$

(15-b)

with A_1 and A_2 to be determined from the boundary conditions at $z = \pm d$.

Requiring $\underline{E}_t$ and $\underline{H}_t$ to be continuous at $z = \pm d$ results in four homogeneous equations in four unknowns from which the relative amplitudes as well as the surface wave dispersion relation can be found. The continuity conditions at $z = d$ given the equations

$$B_1 e^{-\alpha d} = A_1 e^{-j\beta d} + A_2 e^{j\beta d}$$

$$-j\alpha \ B_1 e^{-\alpha d} = \beta \ (A_1 e^{-j\beta d} - A_2 e^{j\beta d})$$

(16-a)

while those at $z = -d$ result in

$$B_3 e^{-\alpha d} = A_1 e^{j\beta d} + A_2 e^{-j\beta d}$$

$$j\alpha \ B_3 e^{-\alpha d} = \beta (A_1 e^{j\beta d} - A_2 e^{-j\beta d})$$

(16-b)

Elimination of B_1 from the first two equations and B_3 from the second two gives the set

$$0 = A_1 e^{-j\beta d} (1 + \frac{\beta}{j\alpha}) + A_2 e^{j\beta d} (1 - \frac{\beta}{j\alpha})$$

$$0 = A_1 e^{j\beta d} (1 - \frac{\beta}{j\alpha}) + A_2 e^{-j\beta d} (1 + \frac{\beta}{j\alpha})$$

(17)

which has a non-trivial solution for A_1 and A_2 only if the determinant of the coefficients is zero. The vanishing of the determinant yields the surface wave dispersion relation

$$e^{j4\beta d} - \left(\frac{j\alpha + \beta}{j\alpha - \beta} \right)^2 = 0 .$$

(18)

If expressions (11) and (14) for α and β in terms of k_x, k_y and $k_o = \omega \sqrt{\epsilon_o u_o}$ are substituted into (18), the dispersion relation is seen to be of the form $D_s(\underline{k}_t, \omega) = 0$.

C.   PROPERTIES OF THE DISPERSION RELATION

As given in (14), β is either real or imaginary for all real k_x and k_y. First, it is verified that no solutions of (18) exist for which β is imaginary. If β is imaginary, i.e., $\beta = \pm j|\beta|$, then (18) becomes

$$e^{\mp 4|\beta|d} = \left(\frac{\alpha \pm |\beta|}{\alpha \mp |\beta|} \right)^2 \qquad (19)$$

The left-hand side is less (greater) than unity while the right-hand side is greater (less) than unity. This contradiction verifies the assertion. When β is real, however, both terms in (18) have magnitude unity so that a solution is possible. In order to find the range of frequencies for which (18) has solutions, based on the restriction that β be real, plot for all $X > 0$ those regions in the $k_x - k_y$ plane where β is real and the region where α is real (see Fig. 2). From Fig. 2 it is seen that the regions where β is real and the region where α is real overlap only when $X > 1$. Hence the possibility that surface waves can propagate exists only for $X > 1$. In passing, observe that (18) remains invariant under the substitution of $-\beta$ for β . Thus it is sufficient to consider only positive values of β. Since the slab configuration has mirror symmetry in the plane $z = 0$, the surface wave fields will correspond to either an open-circuit or a short-circuit bisection of the slab (even and odd solutions in z). The dispersion relation given in (18) can be split into two independent dispersion relations, one giving the open-circuit bisection solutions and the other the short-circuit bisection solutions. These are

$$e^{j2\beta d} = \pm \frac{j\alpha + \beta}{j\alpha - \beta} \qquad (20)$$

where the plus and minus signs correspond to short-circuit and open-circuit bisections, respectively. Using the plus sign for the short-circuit bisection case, the dispersion relation may be put in the form

$$\alpha = -\beta \cot \beta d \qquad , \qquad (21)$$

whereas if the minus sign is used, the dispersion relation for the open-circuit

bisection case can bewritten

$$\alpha = \beta \tan \beta d \qquad (22)$$

with α and β as given in (11) and (14).

A graphical method for solving equations (21) and (22) is described below. In order to show that equations (21) and (22) are satisfied for real values of k_x, k_y and $\omega < \omega_p$, i.e., $X > 1$, the plots of (21) and (22) in the β-α plane are considered. Since α and β have been taken to be positive, only the first quadrant is of interest. Adding α^2 to β^2 gives $\alpha^2 + \beta^2 = X(k_y^2 - k_o^2)$ when (11) and (14) are used. Because $k_y^2 > k_o^2$ for surface waves, as can be seen from Fig. 2, the plot of this relation in the β-α plane is a circle whose radius is $\sqrt{X(k_y^2 - k_o^2)}$. The intersection of this circle with the plot of (21) or (22) gives α and β from which k_x can be found using

$$k_x = \pm \sqrt{\frac{1}{X}\left[(X-1)\alpha^2 - \beta^2\right]} . \qquad (23)$$

But k_x must be real so that in the first quadrant only those intersections for which $\alpha \geq \dfrac{1}{\sqrt{X-1}} \beta$ give values of α and β which correspond to an actual surface wave. Since α and β depend only on k_y^2 and k_x^2 and not merely on k_y or k_x, constant ω surface wave dispersion curves will have mirror symmetry about the k_x and k_y axes in the k_x-k_y plane. Thus, knowing the relation between k_x and k_y for k_x, $k_y \geq 0$ is sufficient to determine the entire dispersion curve.

Figure 3 has been sketched to show the method outlines above for finding that k_x which satisfies (21) when k_y and k_o are given. Each branch of $-\beta \cot \beta d$ depicted in Fig. 3 corresponds to a particular short-circuit bisection surface wave mode. Since there are an infinite number of such branches, there will be an infinite number of short-circuit bisection surface wave modes when $X(k_y^2 - k_o^2) \to \infty$. For a finite value of $X(k_y^2 - k_o^2)$ only a finite number of surface wave modes can propagate. For values of α and β in the shaded region of Fig. 3, k_x, as found from
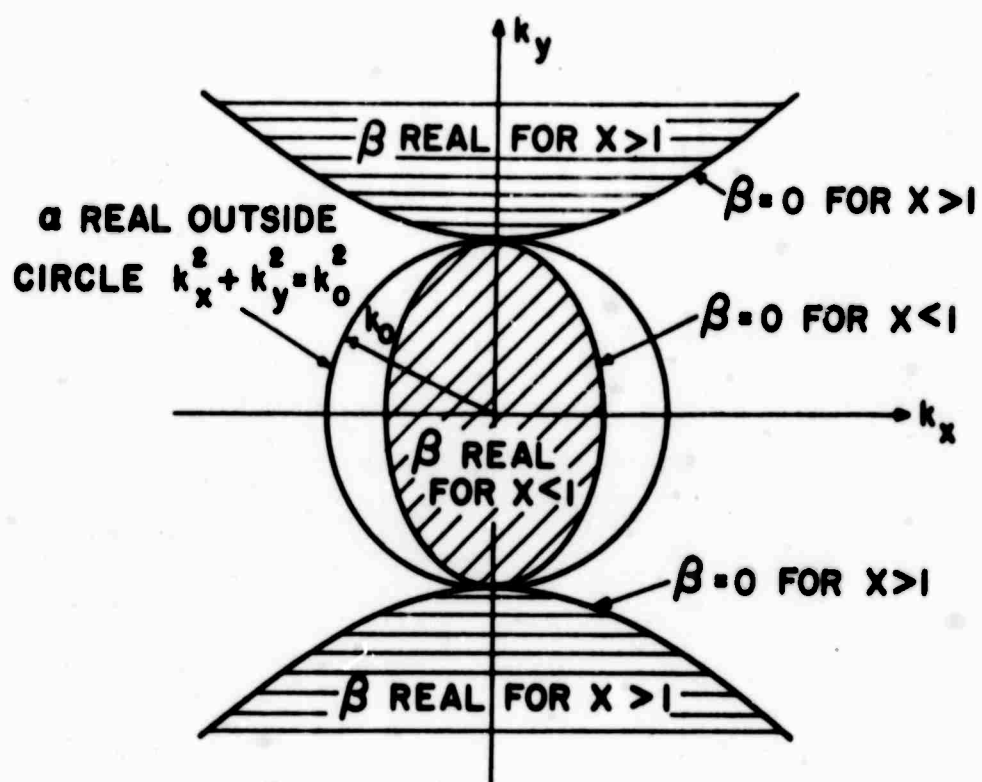
Fig. IV-2   Regions of real β and α in the k_x-k_y plane

$k_x = \pm \sqrt{\frac{1}{X} [(X-1) \alpha^2 - \beta^2]}$, is imaginary. Thus it is seen that for fixed k_o each mode has a minimum value of $k_y^2 > k_o^2$ at which $k_x = 0$ and below which no real solutions for k_x exist. The minimum value of k_y^2 for which a particular surface wave mode can exist is found from the condition that the circle $\alpha^2 + \beta^2 = X(k_y^2 - k_o^2)$, the line $\alpha = \frac{1}{\sqrt{X-1}} \beta$ and that branch of $\alpha = -\beta \cot \beta d$ corresponding to the mode in question all intersect at a common point. As k_y^2 increases from its minimum value, k_y and the corresponding solutions for k_x for each branch of $-\beta \cot \beta d$ trace out the surface wave dispersion curves in the $k_x - k_y$ plane of the short-circuit bisection modes.

In a similar fashion, Fig. 4 depicts the method for finding that k_x which satisfies (22) when k_y and k_o are given. From this figure and Fig. 3, it is seen that the lowest surface wave mode on the slab, i.e., the one with the smallest value of β , is that open-circuit bisection mode corresponding to the branch of $\beta \tan \beta d$ starting at $\beta = 0$. As in the case of the short-circuit bisection modes, k_x corresponding to values of β and α in the shaded region of Fig. 4 is imaginary. Thus for each of the higher open-circuit bisection modes there will be a minimum value of $k_y^2 > k_o^2$ at which $k_x = 0$ and below which no real solution for k_x exists. For the lowest open-circuit bisection mode $[\frac{d}{d\beta}(\beta \tan \beta d)]_{\beta = 0} = 0$ so that a part of the branch of $\beta \tan \beta d$ starting at $\beta = 0$ lies in the shaded region of Fig. 4. Hence there will also be a minimum value of $k_y^2 > k_o^2$ for the lowest surface wave mode below which no real solution for k_x exists. As in the short-circuit bisection case, when k_y^2 increases from its minimum value for a particular mode and for a fixed k_o, k_y and the corresponding value of k_x trace out the dispersion curve of that open-circuit bisection mode.

In what follows, the basic properties of the surface wave dispersion curves will be derived. For any one mode, these properties lead to the form of the dispersion curves shown in Fig. 5, which has been drawn for two different frequencies $\omega_2 > \omega_1$. In order to find the shape of the dispersion curves of any one mode and for fixed ω, consider the corresponding branch of $-\beta \cot \beta d$ in Fig. 3 or of $\beta \tan \beta d$ in Fig. 4. As pointed out previously, the
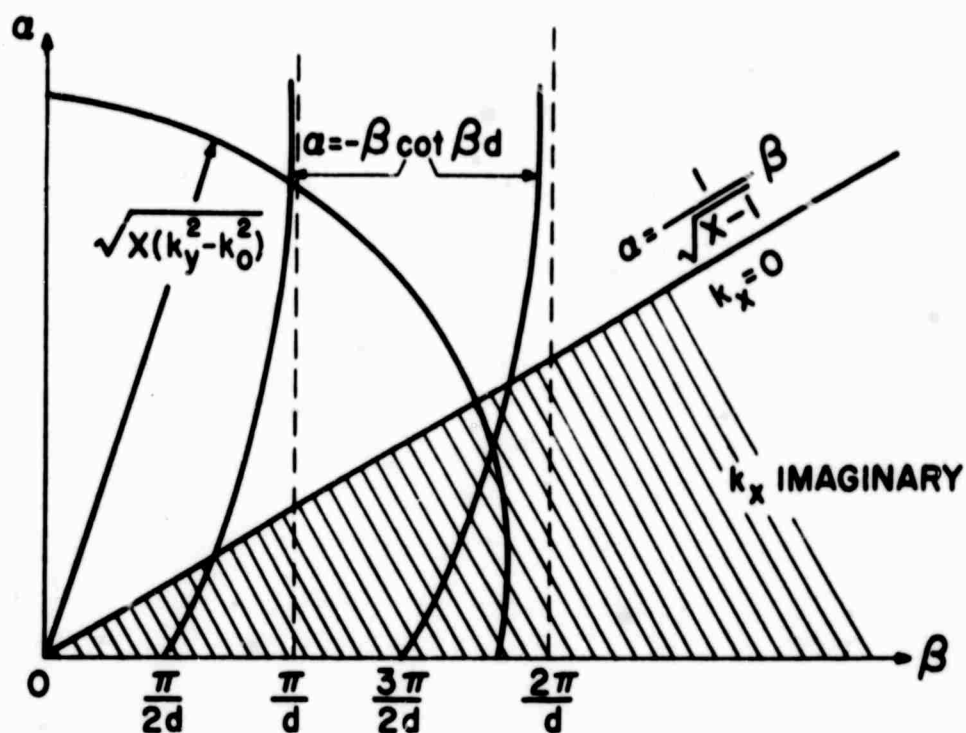
Fig. IV-3   Construction for finding solutions of the surface wave
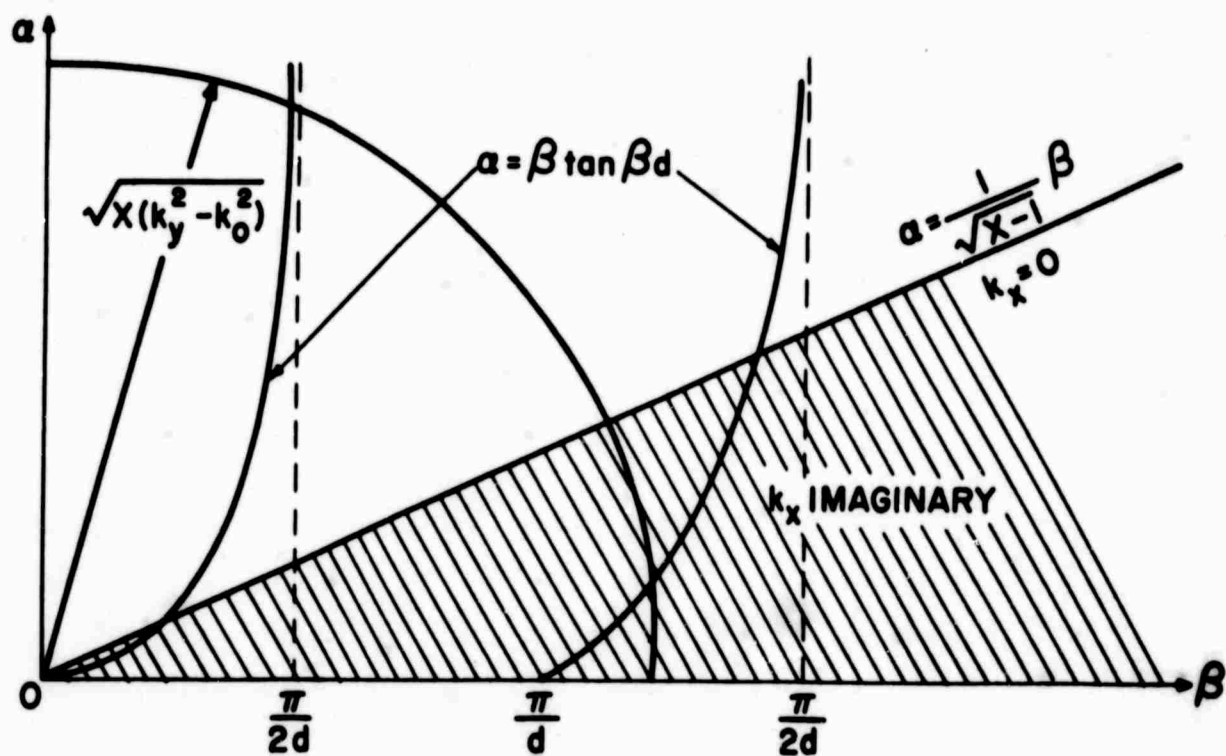dispersion relation for the short-circuit bisection case

Fig. IV-4   Construction for finding solutions of the surface wave
dispersion relation for the open-circuit bisection case

dispersion curves are symmetric about the k_x and k_y axes so that one need find only that portion of the curves in the first quadrant of Fig. 5. Also, as was previously discussed, in the first quadrant of Fig. 5, k_y takes on its minimum value, which is greater than k_o at $k_x = 0$, i.e., where the dispersion curve crosses the k_y axis. It will first be shown that in the first quadrant, k_x is a single-valued, monotonically increasing function of k_y. These two facts indicate that the inverse function, $k_y = k_y(k_x)$, is single-valued and monotonically increasing in the first quadrant as is depicted in Fig. 5. Other fundamental properties of that portion of the dispersion curve in the first quadrant of Fig. 5 that will be established are: 1) $dk_y/dk_x = 0$ at $k_x = 0$; 2) asymptotically as $k_y \to \infty$, $k_y \sim k_x / \sqrt{X-1}$ and the dispersion curve everywhere lies above the asymptote $k_y = k_x / \sqrt{X-1}$; 3) the value of k_y at $k_x = 0$, as well as the slope of the asymptote, increase with ω. One question that has not yet been answered analytically is whether the surface wave dispersion curves have inflection points.

To see that in the first quadrant of Fig. 5, k_x is a single-valued function of k_y, observe that for $\beta > 0$, $\alpha > 0$ each branch of $-\beta \cot \theta d$ in Fig. 3 and each branch of $\beta \tan \theta d$ in Fig. 4 intersects the circle $\alpha^2 + \beta^2 = X(k_y^2 - k_o^2)$ only once. Thus for a given ω_p and for each value of k_y and ω there will be only one set of values (β, α) for each mode and hence from (23) only one value of $k_x > 0$ for each mode. Therefore, in the first quadrant of Fig. 5, k_x is a single-valued function of k_y. That k_x is a monotonically increasing function of k_y can be inferred from the sign of dk_x/dk_y. Since k_x and k_y satisfy the surface wave dispersion relation $D_s(k, \omega) = 0$, dk_x/dk_y for fixed ω is given by $dk_x/dk_y = - \dfrac{\partial D_s}{\partial k_y} \Big/ \dfrac{\partial D_s}{\partial k_x}$. Using D_s as given in the left-hand side of (18), with α and β defined in (11) and (14), it is found that

$$\frac{dk_x}{dk_y} = \frac{k_y}{k_x} \frac{\alpha d(X-1) + k_x^2 / (k_y^2 - k_o^2)}{\alpha d + 1} \quad . \tag{24}$$

From (24) it is seen that in the first quadrant of Fig. 5, $dk_x/dk_y > 0$ and hence, $k_x(k_y)$ is a monotonically increasing function. Furthermore, (24)
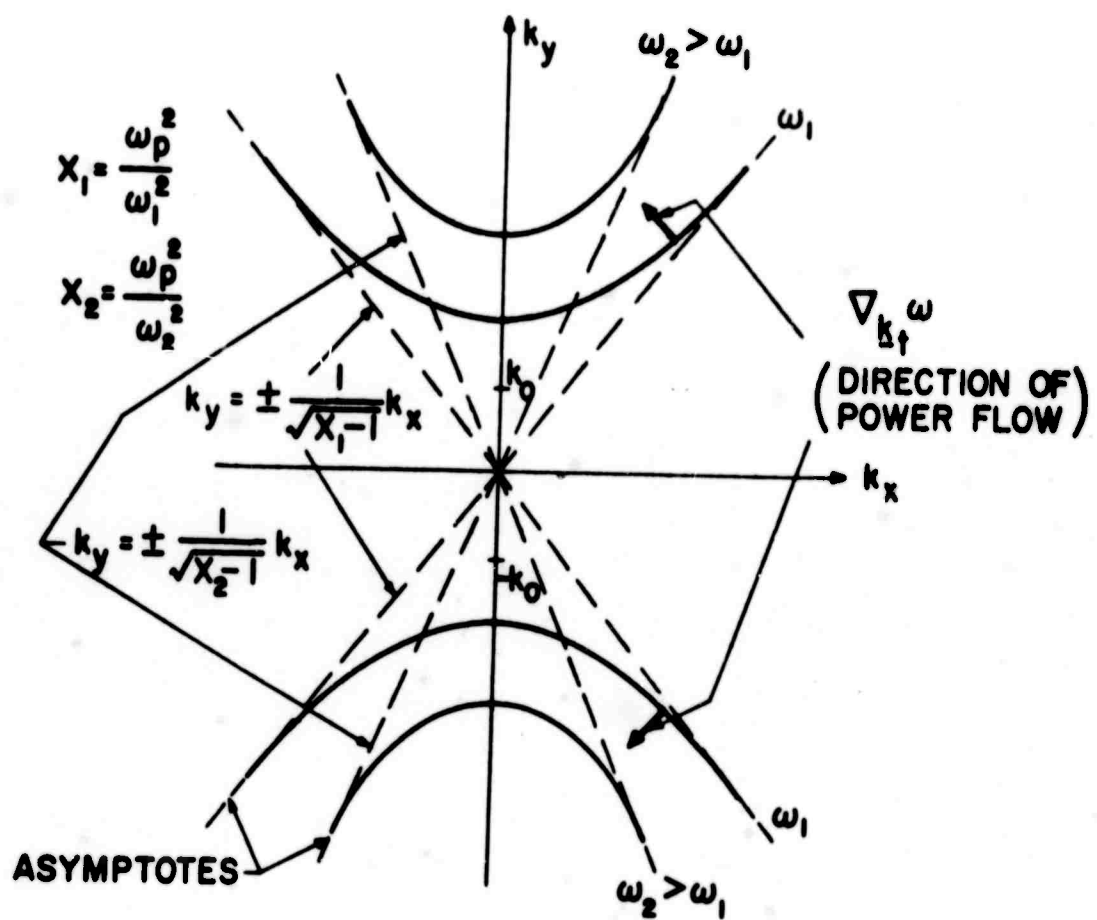
Fig. IV-5   Dispersion curves for a typical surface wave mode with ω as a parameter

shows that $dk_y/dk_x = 0$ at $k_x = 0$ as is depicted in Fig. 5.

As $k_y \to \infty$, the value of β at the intersection of the circle $\alpha^2 + \beta^2 = X(k_y^2 - k_o^2)$ and any one branch of $-\beta \cot \beta d$ in Fig. 3 or any one branch of $\beta \tan \beta d$ in Fig. 4 approaches a constant. Thus, since k_o has been assumed constant, $\alpha^2 \sim X k_y^2$ as $k_y \to \infty$ and hence, from (23), k_x in the first quadrant of Fig. 5 is asymptotically given by $k_x \sim k_y \sqrt{X-1}$ or conversely $k_y \sim k_x/\sqrt{X-1}$. That the dispersion curve lies above the asymptote line $k_y = k_x/\sqrt{X-1}$, as shown in the first quadrant of Fig. 5, can be deduced from the definition of β given in (12). Since β is real for the surface waves and $X > 1$, $(X-1) k_y^2 - k_x^2 = \beta^2 + k_o^2(X-1) > 0$ and therefore in the first quadrant $k_y > k_x/\sqrt{X-1}$, which proves that the dispersion curve lies above the asymptote line. When ω increases but remains below ω_p, X decreases to unity and hence the slope of the asymptote, $1/\sqrt{X-1}$, increases as is depicted in Fig. 5. Furthermore, as ω increases the slope of the line $\alpha = \beta/\sqrt{X-1}$ in Fig. 3 and Fig. 4 increases. Hence the values of β and α at $k_x = 0$ as determined from the intersection of the line $\alpha = \beta/\sqrt{X-1}$ with any branch of $-\beta \cot \beta d$ in Fig. 3 or of $\beta \tan \beta d$ in Fig. 4, must increase. Because k_o increases with ω and X decreases, the quantity $\frac{1}{X}(\alpha^2 + \beta^2) + k_o^2 = k_y^2$ must increase and thus the magnitude of k_y at $k_x = 0$ increases with ω. The above-described variation with ω of k_y at $k_x = 0$ is depicted in Fig. 5.

Thus the fundamental properties previously stated for the surface wave dispersion curves of any one mode are seen to hold. These properties indicate that the dispersion curves will have the form depicted in Fig. 5, with the possible exception of inflection points, for two different frequencies. From Fig. 3 and Fig. 4 it can also be seen that surface waves exist for all ω in the range $0 < \omega < \omega_p$. Lastly, since in the first quadrant of Fig. 5, $dk_y/dk_x \geq 0$, which follows from (24), and since the dispersion curve for $\omega = \omega_2$ lies above that for $\omega = \omega_1 < \omega_2$, the x component of $\nabla_{\underline{k}_t} \omega$ must everywhere be negative. That the dispersion curve for $\omega = \omega_2$ lies above that for $\omega = \omega_1 < \omega_2$ follows from the fact that at $k_x = 0$ the $\omega = \omega_1$ curve lies above the $\omega = \omega_2$ curve and the two curves never cross since

$\nabla_{\underline{k}_t} \omega$, which is given in (42), is never infinite. The observation that $\underline{x}_o \cdot \nabla_{\underline{k}_t} \omega > 0$ is confirmed by the analytic expression for $\nabla_{\underline{k}_t} \omega$ given in (42) and indicates that the surface waves are of the backward wave type with respect to the x direction.

D. GROUP VELOCITY AND ENERGY TRANSPORT VELOCITY

Having established the basic properties of the dispersion relation of the surface waves on a uniaxial plasma slab, the equality of group velocity and energy transport velocity for these surface waves will be verified by direct calculation. As derived in Chapter III, this equality states that

$$\nabla_{\underline{k}_t} \omega = \int_{-\infty}^{\infty} \underline{s}\, dz \Big/ \int_{-\infty}^{\infty} w\, dz \tag{25}$$

where $\underline{s}$ represents the real part of the complex Poynting vector $\underline{E} \times \underline{H}^*$ and w the time average stored energy density. To this end, the relative field amplitudes are first calculated. Since one of the coefficients A_1, A_2, B_1 and B_3 is arbitrary, for simplicity let

$$A_1 = -A_o(\beta - j\alpha)\, e^{j\beta d} \tag{26}$$

where A_o is arbitrary. Then from (17) it is found that

$$A_2 = -A_o(\beta + j\alpha)\, e^{-j\beta d} \tag{27}$$

while from (16-a)

$$B_1 = -2\beta A_o\, e^{\alpha d} \quad . \tag{28}$$

Using the dispersion relation in the form given in (18), which is valid for both open-circuit and short-circuit bisection modes, it follows that

$$B_3 = -2\beta A_o \frac{\beta + j\alpha}{\beta - j\alpha}\, e^{-j2\beta d}\, e^{\alpha d} \quad . \tag{29}$$

With these expressions in equations (12), (13) and (15) for the fields in the three regions, $\underline{s}$ in Region 1 is found to be

$$\underline{s} = 4|A_o|^2 \beta^2 \omega \epsilon_o\, e^{-2\alpha(z-d)} [\underline{x}_o k_x(k_o^2 - k_y^2) + \underline{y}_o k_y(\alpha^2 + k_x^2)] \tag{30}$$

while in Region 3 it is

$$\underline{s} = 4|A_o|^2 \beta^2 \omega \epsilon_o e^{2\alpha(z+d)} [\underline{x}_o k_x (k_o^2 - k_y^2) + \underline{y}_o k_y(\alpha^2 + k_x^2)] \qquad (31)$$

and finally in Region 2 it is

$$\underline{s} = |A_o|^2 \omega \epsilon_o(\alpha^2 + \beta^2) \left\{ 2[\underline{x}_o k_x(k_o^2 - k_y^2) + \underline{y}_o k_y(\beta^2 + k_x^2)] + \right.$$

$$\left. + \left[\frac{\beta + j\alpha}{\beta - j\alpha} e^{j2\beta(z-d)} + \frac{\beta - j\alpha}{\beta + j\alpha} e^{-j2\beta(z-d)} \right] \cdot \left[\underline{x}_o k_x(k_o^2 - k_y^2) + \underline{y}_o k_y(k_y^2 - \beta^2) \right] \right\} \ .$$

$$(32)$$

The quantity $\underline{S} = \displaystyle\int_{-\infty}^{\infty} \underline{s}\, dz$ is now calculated to be

$$\underline{S} = 4|A_o|^2 \omega \epsilon_o(\alpha^2 + \beta^2) \left\{ -\underline{x}_o k_x(k_y^2 - k_o^2) \left[\frac{1}{\alpha} + d \right] \right.$$

$$\left. + \underline{y}_o k_y \left[\frac{1}{\alpha} k_x^2 + d(X-1)(k_y^2 - k_o^2) \right] \right\} \ . \qquad (33)$$

In order to determine the stored energy, observe that in the plasma slab

$$\left[\frac{\partial \omega \epsilon}{\partial \omega} \right] = \epsilon_o \left[\frac{\partial \omega \epsilon'}{\partial \omega} \right] = \epsilon_o \begin{bmatrix} 1 & 0 & 0 \\ 0 & 1+X & 0 \\ 0 & 0 & 1 \end{bmatrix} \ . \qquad (34)$$

Thus in Region 2, the time averaged stored energy density, which is given by[14], [15]

$$w = \frac{1}{2} \left[\underline{E}^* \cdot \frac{\partial \omega \epsilon}{\partial \omega} \cdot \underline{E} + u_o |\underline{H}|^2 \right] \ , \qquad (35)$$

is found to be

$$w = \frac{1}{2} |A_o|^2 \epsilon_o(\alpha^2 + \beta^2) \left\{ 4(k_y^2 - k_o^2)(X k_y^2 - k_o^2) - \right.$$

$$\left. - \left[\frac{\beta + j\alpha}{\beta - j\alpha} e^{j2\beta(z-d)} + \frac{\beta - j\alpha}{\beta + j\alpha} e^{-j2\beta(z-d)} \right] \cdot \left[(\beta^2 - k_x^2)(k_o^2 + k_y^2) - (1+X)(k_y^2 - k_o^2) \right] \right\} \ .$$

$$(36)$$

Outside the slab, the time averaged stored energy density has the form

$$w = \frac{1}{2}\left[\epsilon_o\,|\underline{E}|^2 + u_o\,|\underline{H}|^2\right]\tag{37}$$

so that in Region 1

$$w = 2|A_o|^2\,\epsilon_o\,\beta^2\left[(k_o^2 + k_y^2)(k_x^2 + \alpha^2) + (k_y^2 - k_o^2)^2\right]e^{-2\alpha(z-d)}\tag{38}$$

while in Region 3

$$w = 2|A_o|^2\,\epsilon_o\,\beta^2\left[(k_o^2 + k_y^2)(k_x^2 + \alpha^2) + (k_y^2 - k_o^2)^2\right]e^{2\alpha(z+d)}\ .\tag{39}$$

Calculating $W = \displaystyle\int_{-\infty}^{\infty} w\,dz$, it is found that

$$W = 4|A_o|^2\,\epsilon_o(\alpha^2 + \beta^2)\left\{d(k_y^2 - k_o^2)(Xk_y^2 - k_o^2) + \frac{1}{\alpha}\left[k_x^2 k_y^2 + (k_y^2 - k_o^2)^2\right]\right\}\ .\tag{40}$$

In deriving the above power and energy formulas, extensive use has been made of the dispersion relation given in (18) and the formulas (11) and (14) for α and β. Using the above expressions for $\underline{S}$ and W, the energy transport velocity is seen to be

$$\frac{\underline{S}}{W} = \omega\,\frac{-\underline{x}_o k_x(k_y^2 - k_o^2)(\frac{1}{\alpha} + d) + \underline{y}_o k_y\left[\frac{1}{\alpha}k_x^2 + d(X-1)(k_y^2 - k_o^2)\right]}{d(k_y^2 - k_o^2)(Xk_y^2 - k_o^2) + \frac{1}{\alpha}\left[k_x^2 k_y^2 + (k_y^2 - k_o^2)^2\right]}\ .\tag{41}$$

In order to compute the group velocity $\nabla_{\underline{k}_t}\omega$, the formula $\nabla_{\underline{k}_t}\omega = -\nabla_{\underline{k}_t}D_s\,/\,\dfrac{\partial D_s}{\partial\omega}$ from implicit function theory will be used where the function $D_s(\underline{k}_t,\omega)$ is the left-hand side of (18). It is found that

$$\nabla_{\underline{k}_t} \omega = \omega \; \frac{-\underline{x}_o k_x (\frac{1}{\alpha} + d) + \underline{y}_o k_y \left[d(X-1) + \frac{k_x^2 X}{\alpha(\alpha^2 + \beta^2)} \right]}{d(X k_y^2 - k_o^2) + \frac{1}{\alpha}(k_y^2 - k_o^2) + \frac{k_x^2 k_y^2}{\alpha(k_y^2 - k_o^2)}} \; . \qquad (42)$$

If both the numerator and denominator of the above expression are multiplied by $(k_y^2 - k_o^2)$ and it is recognized that $X(k_y^2 - k_o^2) = \alpha^2 + \beta^2$, $\nabla_{\underline{k}_t} \omega$ will be seen to be identical with $\underline{S}/W$, as predicted in Chapter III.

The example worked out above also illustrated that fact that, in general, the direction of $\underline{s}$ as well as its magnitude can vary with z. This can be seen from equation (32) for $\underline{s}$ in Region 2 if it is recognized that the vectors $[\underline{x}_o k_x (k_o^2 - k_y^2) + \underline{y}_o k_y (\beta^2 + k_x^2)]$ and $[\underline{x}_o k_x (k_o^2 - k_y^2) + \underline{y}_o k_y (k_x^2 - \beta^2)]$ are parallel only for $k_x = 0$. Since the coefficient of the first vector is independent of z while the coefficient of the second vector depends on z, the direction of the vector sum, which gives $\underline{s}$, will depend on z for all surface waves for which $k_x \neq 0$.

Chapter V

EVALUATION AND INTERPRETATION OF THE SURFACE WAVE
CONTRIBUTIONS TO THE FAR FIELDS

A. INTRODUCTION

In this chapter, the surface wave contributions to the far fields radiated by a point source in the presence of a planar interface between two anisotropic, lossless media are evaluated. The surface wave fields are found from the asymptotic evaluation of the rigorous Fourier integral expressions for the fields given in Chapter I. Using the group velocity-energy flow relation derived in Chapter III for surface waves in plane-stratified, anisotropic, lossless media, the surface wave contributions to the point source fields are interpreted as arising from surface wave rays. These rays are the two-dimensional trajectories of total energy flow of the surface wave propagating along the interface. The surface wave fields are then cast into a ray-optical form containing such physically significant quantities as ray length and ray-refractive index. The asymptotic evaluation of the surface wave contributions and their ray-optical interpretation are given in Section B.

As an illustration of the effects of anisotropy on the surface waves radiated by a point source, a particular problem is considered in Section C. The configuration studied consists of a homogeneous, gyrotropic, cold electron plasma above a perfectly conducting plane. The gryrotropic anisotropy is assumed to be produced by a static magnetic field parallel to the conductor. The source is taken as a small slot in the conductor in which the electric field is specified. Strong angular dependence is found for both the surface wave dispersion curve and the surface wave radiation pattern, which are evaluated numerically for a particular choice of plasma parameters. The direct ray radiation pattern is also evaluated. Note that since the source is on the interface, all stationary point contributions will correspond to rays proceeding from the source to the observation point. The presence of the conductor will only influence the ray field amplitudes but not the ray structure.

B. SURFACE WAVE CONTRIBUTIONS TO THE FAR FIELDS

The surface wave contributions to the far fields radiated by the point source of Chapter I arise from the residues at certain poles, called surface wave poles, in the η integration for the scattered field integrals (II-4). The integration over ξ of the residues by the method of stationary phase yields the surface wave contributions. The surface wave poles are those points on the real η axis at which the common denominator $d(\xi, \eta)$, as defined in (I-47), of the scattering coefficients vanishes and the Fourier transform of the total scattered field $\underline{E}_\Gamma$, as found by substituting (II-4) into (II-3) and interchanging the order of summation and integration, is singular. Note that $d(\xi, \eta)$ will vanish at branch points of the $\varkappa$'s at which $\varkappa$ is complex or imaginary. While the integrands of the individual integrals in (II-4) will be singular at such points, no net contribution to $\underline{E}_\Gamma$ will come from these points unless the Fourier transform of $\underline{E}_\Gamma$ is itself singular.

In view of the above comments, the surface wave pole locus is defined as the locus of points in the real (ξ, η) plane at which $d(\xi, \eta) = 0$ and the Fourier transform of $\underline{E}_\Gamma$ is singular.[*] In order to interpret the surface wave pole contributions in terms of surface waves, it is first necessary to argue that the surface wave pole locus is the surface wave dispersion curve in the sense defined in Chapter III, for the planar interface configuration. In other words, it is necessary to show that for (ξ, η) on the surface wave pole locus, a solution of the source-free Maxwell equations exists having transverse dependence $e^{-jk_o(\xi x + \eta y)}$ and such that the transverse electric and magnetic fields are continuous across the interface and the fields decay

----

[*] The presence of particular subscripts in the definition (I-47) for $d(\xi, \eta)$ implies that only particular branches of the multivalued functions $\varkappa(\xi, \eta)$ for each media be used in evaluating $d(\xi, \eta)$. However, in performing the steepest descent integration of (II-4) over η, the complex η plane must be viewed as a sixteen-sheeted Riemann surface with $d(\xi, \eta)$ defined on all sheets. Thus, while $d(\xi, \eta)$ is defined along the original integration path, which lies on one of the Riemann sheets, such that at its real axis zeros $\text{Re}(-j\varkappa_m z) < 0$, $d(\xi, \eta)$ may have real axis zeros on other sheets at which $\text{Re}(-j\varkappa_m z) > 0$. Such zeros correspond to improper surface waves that grow exponentially away from the interface and are not intercepted during the deformation of the integration path for $|y| >> |z|, |z'|$, as was assumed in Appendix B.

away from the interface. The fact that $d(\xi, \eta) = 0$ on the surface wave pole locus implies that a non-trivial solution of (I-42) for the b_m's and c_m's exists when $a_{\vec{1}} = a_{\vec{2}} = 0$. Thus, for ξ and η on the surface wave pole locus, there exist solutions of the source-free Maxwell equations having transverse dependence $e^{-jk_o(\xi x + \eta y)}$ and such that the transverse electric and magnetic fields are continuous across the interface.

That the fields decay away from the interface can be shown from the continuity condition

$$\sum_{\vec{3},\vec{4}} c_m \, \Psi_t(\varkappa_m) = \sum_{\overleftarrow{1}\,\overleftarrow{2}} b_m \, \Psi_t(\varkappa_m), \qquad (1)$$

i.e., from (I-42) for $a_{\vec{1}} = a_{\vec{2}} = 0$. Forming the inner product, with respect to Γ_z, of each side of (1) with itself and using the orthogonality condition (I-28) gives

$$\sum_{\vec{3},\vec{4}} |c_m|^2 \, M_m \, \delta_{\varkappa_m, \varkappa_m^*} = \sum_{\overleftarrow{1},\overleftarrow{2}} |b_m|^2 \, M_m \, \delta_{\varkappa_m, \varkappa_m^*}. \quad (2)$$

Since $\delta_{\varkappa_m, \varkappa_m^*} = 0$ unless $\varkappa_m$ is real, the sums in (2) reduce to the sums over the upgoing propagating modes of the $\underset{\sim}{\epsilon}_2$ medium and the downgoing propagating modes of the $\underset{\sim}{\epsilon}_1$ media. But for $\varkappa_m$ real by direct expansion of M_m of (I-30), it can be shown that $M_m = 2\,\mathrm{Re}[\underline{z}_o \cdot (\underline{\mathscr{L}}_{tm} \times \underline{\mu}_{tm}^*)]$. Thus, for $\varkappa_{\vec{3}}$ or $\varkappa_{\vec{4}}$ real, $M_{\vec{3}}$ or $M_{\vec{4}}$ is positive while for $\varkappa_{\overleftarrow{1}}$ or $\varkappa_{\overleftarrow{2}}$ real, $M_{\overleftarrow{1}}$ or $M_{\overleftarrow{2}}$ is negative. Because $|c_m|^2$, $|b_m|^2 \geq 0$, the left-hand side of (2) is greater than or equal to zero while the right-hand side is less than or equal to zero. Hence, the equality in (2) holds only when both sides are zero, which implies that those c_m's and b_m's corresponding to real $\varkappa_m$'s must be zero on the surface wave pole locus.

Thus, when a solution of the homogeneous equations (1) exists, the only non-zero c_m's and b_m's are those corresponding to complex or imaginary $\varkappa_m$. Since the c_m's and b_m's corresponding to real $\varkappa_m$'s are zero on the surface wave pole locus, those Γ_{mn}'s having the same values of m will be finite on the surface wave pole locus so that no residue term will appear in

the η integration of the integrands in (II-4) at which κ_m is real. In other words, the surface waves will contain only those modes of the $\varepsilon_{\sim 1}$ and $\varepsilon_{\sim 2}$ media that decay away from the interface - see previous footnote. This completes the proof that the surface wave pole locus, as defined above, is the surface wave dispersion curve of the planar interface configuration.

In the foregoing discussion it was shown that on those portions of the surface wave pole locus at which a particular scattered wave number κ_m is real, the Γ_{mn}'s having the same m must be finite. However the discussion did not lead to the conclusion that if an incident wave number κ_n were real on a portion of the surface wave pole locus, the Γ_{mn}'s having the same n must be finite there. Thus, if two wave numbers of the $\varepsilon_{\sim 1}$ media are real and two are complex or imaginary, and hence the conjugate of each other, the upgoing propagating plane wave excited by the source may excite a surface wave whose fields in the $\varepsilon_{\sim 1}$ media are entirely those of the one evanascent downgoing plane wave.

1. Integration of the Residue Contributions Over ξ

Writing the scattering coefficients of (I-46) and (I-50) as

$$\Gamma_{mn}(\xi, \eta) = \gamma_{mn}(\xi, \eta) / d(\xi, \eta) \qquad (3)$$

and recalling the form of $\underline{F}(\xi, \eta)$ when the generic integral (II-5) represents the scattered field integrals (II-4), $\underline{f}(\xi, \eta)$ defined in (B-8) of Appendix B is seen to be $\underline{f}(\xi, \eta) = \underline{b}_m \gamma_{mn} A_n$. Furthermore, $P(\xi, \eta)$ for the integrals of (II-4) is $P(\xi, \eta) = \xi x + \eta y + \kappa_m z - \kappa_n z'$. Using these forms for $\underline{f}(\xi, \eta)$ and $P(\xi, \eta)$ in (B-9) gives the surface wave pole contributions to the η integration in (II-4). Finally, writing the surface wave contribution $(\underline{I}_{mn})_{S.W.}$ to $\underline{I}_{mn}$ of (II-4) as the integral over ξ of the residues, and substituting this expression into (II-3) gives the surface wave contribution to $\underline{E}_\Gamma$. Since the pole location $\eta_p(\xi)$ in the η integration is the same for all m and n, and since the γ_{mn}'s corresponding to a real κ_m are zero anyway, the summation over the poles may be taken outside the summation over m and n. Thus, the surface wave contribution to $\underline{E}_\Gamma$ is

$$(\underline{E}_T)_{S.W.} = -2\pi j \, \text{sgn} \, y \sum_{p=-\infty}^{\infty} \int \sum_{m,n} \left\{ \frac{\underline{b}_m \gamma_{mn} A_n}{d_2(\xi,\eta)} e^{-jk_o(\varkappa_m z - \varkappa_n z')} \right\} e^{-jk_o[\xi x + \eta_p(\xi)y]} \frac{d\xi}{\eta_p(\xi)},$$

(4)

where the order of summation over m and n and integration over ξ have also been interchanged. In (4), $n = \vec{1}, \vec{2}$ and $m = \vec{3}, \vec{4}$ for $z > 0$, while for $z < 0$, $m = \overleftarrow{1}, \overleftarrow{2}$.

The integration over ξ indicated in (4) is now to be carried out asymptotically by the method of stationary phase. In performing this evaluation, it will be assumed that $\sqrt{x^2 + y^2}$ is much greater than $|z|$ or $|z'|$ – see Section 3 of Appendix B. Mathematically, the importance of this assumption is that the large parameter in the asymptotic evaluation can be taken as $\sqrt{x^2 + y^2}$. When $\sqrt{x^2 + y^2}$ is used as the large parameter in (4), the term $e^{-jk_o(\varkappa_m z - \varkappa_n z')}$ for fixed z and z' will be slowly varying compared to $e^{-jk_o[\xi x + \eta_p(\xi)y]}$ and may thus be considered as an amplitude function. Thus, for $\sqrt{x^2 + y^2} >> |z|, |z'|$ the stationary points of (4) will be the same for all m and n and will be the solutions of

$$x + y \frac{d}{d\xi} \eta_p(\xi) = 0 \quad . \tag{5}$$

The ray-optical significance of the assumption $\sqrt{x^2 + y^2} << |z|, |z'|$ is that for observation points satisfying it, the fields associated with the pole contributions may be viewed as arising from propagating modal surface waves. If the foregoing assumption is not made, the stationary points are those of $\xi x + \eta_p y + \varkappa_m z - \varkappa_n z'$. In this case the stationary points are, in general, different for each m and n and are complex. Furthermore, the ray interpretation would be in terms of complex rays, as discussed by Keller and Karl[35] for the pole contributions in isotropic media. Finally, since the ray paths would be different, in general, for each m and n, the modal character of the pole contributions would be lost.

If ξ_p is a real solution of (5) and $\eta_p = \eta_p(\xi_p)$ is the corresponding value of η on the surface wave dispersion curve, then performing the stationary phase evaluation[22] of (4) under the assumption $\sqrt{x^2 + y^2} >> |z|$, $|z'|$ gives to $0(1/\sqrt{x^2 + y^2})$

$$(\underline{E}_\Gamma)_{S.W.} \sim$$

$$-j\frac{(2\pi)^{3/2}}{\sqrt{k_o}} \operatorname{sgn} y \sum_p \left\{ \frac{e^{-j(\xi x + \eta y)} \; e^{-j\frac{\pi}{4}\operatorname{sgn}(y\frac{d^2\eta_p}{d\xi^2})}}{d_2(\xi,\eta)\sqrt{|y d^2\eta_p/d\xi^2|}} \sum_{m,n} \underline{b}_m \gamma_{mn} A_n e^{-jk_o(\varkappa_m z - \varkappa_n z')} \right\}_{(\xi_p,\eta_p)}.$$

$$(6)$$

In (6), the summation over p is taken over all points (ξ_p, η_p) satisfying (5) on those portions of the surface wave dispersion curve for which the y component of the real part of the total surface wave Poynting vector has the same sign as the observation coordinate y - see text before (B-8) in Appendix B. Expression (6) for $(\underline{E}_\Gamma)_{S.W.}$ is not valid for ξ_p near the branch points of the possibly multivalued function $\eta = \eta_p(\xi)$, in which case two poles are close together in the η integration and $d^2\eta_p/d\xi^2 \to \infty$. It will be seen in the next section that this occurs when $|y| << |x|$. However, this singularity in (6) is introduced by the choice of the (x, y) coordinates and will not be present when (6) is re-expressed in ray-optical terms. The actual singularities of the surface wave contribution to the far fields are considered in the next section.

2.   Ray-Optical Interpretation of the Surface Wave Contribution

In order to cast the surface wave contribution to $\underline{E}_\Gamma$ into ray-optical form, first consider the ray interpretation of the stationary phase condition (5). As demonstrated in Chapter III, a modal surface wave propagating with transverse wave numbers ξ and η will carry energy in the direction of the normal to the dispersion curve at the point (ξ, η). Let the unit normal to the dispersion curve having the same sense as the energy flow of the corresponding modal surface wave be $\underline{\nu}_s$. The normal $\underline{\nu}_s$ can be written as

$$\underline{\nu}_s = \pm (\underline{x}_o \frac{d\eta_p}{d\xi} - \underline{y}_o) \Big/ \sqrt{\left(\frac{d\eta_p}{d\xi}\right)^2 + 1} \quad , \qquad (7)$$

where the minus (plus) sign applies for modal surface waves carrying energy in the plus (minus) y direction. Using (7), it is easily verified that the stationary phase condition (5) is equivalent to $\underline{\nu}_s \times \underline{\rho} = 0$ where $\underline{\rho} = \underline{x}_o x + \underline{y}_o y$ is the transverse displacement of the observation point from the source. In addition, the radiation condition, as applied in the residue evaluation given in Section 3 of Appendix B, implies that $\underline{\nu}_s \cdot \underline{\rho} > 0$. Thus, surface wave contributions to $\underline{E}_\Gamma$ come from those points on the surface wave dispersion curve at which $\underline{\nu}_s$ is parallel to and has the same sense as the transverse displacement $\underline{\rho}$.

In other words, while the source radiates a continuum of modal surface waves corresponding to all points on the surface wave dispersion curve, only those carrying energy in the direction of the transverse displacement $\underline{\rho}$ will contribute to the fields at the observation point. This interpretation is independent of z and z' so long as $\sqrt{x^2 + y^2} >> |z|$, $|z'|$. That the ray interpretation is independent of z and z' is to be expected since the surface wave energy flow is the integral over z of the local Poynting vector. Effectively, the radiated surface wave fields may be viewed as arising from two-dimensional surface wave rays that are trajectories of energy flow. In this view, the z and z' dependence of the surface wave fields merely describe the local field strength and excitation.

With the above ray interpretation of the stationary phase condition (5), the various quantities appearing in (6) can be cast into ray-optical form. To this end, the curvature C_s of the surface wave dispersion curve is written as

$$C_s = \frac{d^2}{d\xi^2} \eta_p(\xi) \cos^3 \phi \quad , \qquad (8)$$

where $\cos \phi = \underline{\nu}_s \cdot \underline{y}_o$. At (ξ_p, η_p), $y = \rho \cos \phi$ with $\rho = |\underline{\rho}|$ so that from (8)

$$y \frac{d^2 \eta_p}{d\xi^2} = \rho \, C_s / \cos^2 \phi \qquad (9)$$

and hence

$$\text{sgn}\left(y \frac{d^2 \eta_p}{d\xi^2}\right) = \text{sgn} \, C_s \quad . \qquad (10)$$

Note that C_s is positive if the center of curvature is on the same side of the dispersion curve $\underline{\nu}_s$ and is negative otherwise.

Since the dispersion curve is the solution of $d(\xi, \eta) = 0$, the gradient in the (ξ, η) plane of $d(\xi, \eta)$, evaluated at points on the dispersion curve, is parallel to $\underline{\nu}_s$. Thus, on the dispersion curve

$$\underline{\nu}_s = (\underline{x}_o d_1 + \underline{y}_o d_2) / Q_s \quad , \qquad (11)$$

where $Q_s = \pm \sqrt{(d_1)^2 + (d_2)^2}$, the sign being chosen so that expression (11) for $\underline{\nu}_s$ has the correct sense. From (11) and the definition of $\cos \phi$, it is seen that on the surface wave dispersion curve,

$$d_2(\xi, \eta) = Q_s \cos \phi \quad . \qquad (12)$$

Defining the surface wave ray-refractive index N_s as

$$N_s \equiv \underline{\nu}_s \cdot \underline{k}_t \qquad (13)$$

where $\underline{k}_t = \underline{x}_o \xi_p + \underline{y}_o \eta_p$, the phase term $\xi_p x + \eta_p y$ in (6) is equal to $N_s \rho$. Finally, recognizing that $\text{sgn} \, y = \text{sgn}(\cos \phi)$ and using (9) and (12),

$$\left[\frac{\text{sgn} \, y}{d_2(\xi, \eta)\sqrt{|y \, d^2 \eta_p / \xi^2|}} \right]_{(\xi_p, \eta_p)} = \left[\frac{1}{Q_s \sqrt{\rho |C_s|}} \right]_{(\xi_p, \eta_p)} . \qquad (14)$$

With the help of (13) and (14), the surface wave contribution (6) to $\underline{E}_\Gamma$ can be rewritten in the from

$$(\underline{E}_\Gamma) \quad \sim$$
$$\text{S. W.}$$

$$-j\frac{(2\pi)^{3/2}}{\sqrt{k_o}} \sum_p \left\{ \frac{e^{-jk_o N_s \rho} \, e^{-j\frac{\pi}{4} \operatorname{sgn} C_s}}{Q_s \sqrt{\rho |C_s|}} \sum_{m,n} \underline{b}_m \gamma_{mn} A_n e^{-jk_o(\varkappa_m z - \varkappa_n z')} \right\}_{(\xi_p, \eta_p)} ,$$

$$(15)$$

where $n = \vec{1}, \vec{2}$ and $m = \vec{3}, \vec{4}$ for $z > 0$, while for $z < 0$, $m = \overleftarrow{1}, \overleftarrow{2}$. In (15), the summation over m is required by the fact that the fields of the surface waves that can propagate on the interface are, in general a superposition of the evanescent or inhomogeneous plane wave fields of the $\underset{\sim}{\epsilon}_1$ and $\underset{\sim}{\epsilon}_2$ media. The summation over n indicates that the surface waves are excited, in general, by both modal fields incident on the interface. Finally, the summation over the points (ξ_p, η_p) indicates that a surface wave contribution to $\underline{E}_\Gamma$ arises from each point on the surface wave dispersion curve, which may have several branches, at which $\underline{\nu}_s$ is parallel to and has the same sense as $\underline{\rho}$.

The stationary phase condition (5) implies quadratic phase change when the observation point moves parallel to the z = 0 plane and perpendicular to $\underline{k}_t$. Thus, for $\rho >> |z|, |z'|$ the surface wave fields may be viewed as arising from surface wave rays whose fields are locally those of modal surfaces waves. This view is supported by the $1/\sqrt{\rho}$ dependence of the fields in (15), which implies conservation of modal surface wave energy in a tube of surface wave rays, i.e., in a wedge region of infinite extent along z. As in the case of the ordinary rays of geometrical optics, the above ray interpretation of the surface wave fields should prove useful in evaluating the surface wave contribution in problems not amenable to rigorous analysis.

For $\rho >> |z|, |z|$, the direct and scattered ray fields found in

Charter II vary as $1/\rho$. Thus, for observation and source points near the interface the surface wave fields will form the dominant contribution to the field.

Expression (15) for the surface wave contribution is not valid for (ξ_p, η_p) near an inflection point of the surface wave dispersion curve. At such points, the curvature $C_s \approx 0$ and the corresponding observation points lie near a shadow boundary of the surface wave fields. Also, for observation points such that (ξ_p, η_p) is near a cusp or crossing of the dispersion curve with itself, (15) may no longer be valid since $C_s Q_s \approx 0$. For (ξ_p, η_p) approaching a branch curve of $\varkappa_m$ at which $\varkappa_m$ is real, (15) is no longer valid. This is because $d(\xi, \eta)$ explicitly depends on the $\varkappa_m$'s of (15) and for (ξ_p, η_p) approaching a branch curve of $\varkappa_m$ at which it is real, $d_1(\xi, \eta)$ and $d_2(\xi, \eta)$ in Q_s will approach infinity. However, the nature of the singularity in the surface wave fields given in (15) cannot be predicted in such a case since C_s may approach zero. Similarly, (15) may not be valid for (ξ_p, η_p) approaching a branch curve of $\varkappa_n$ at which it is real since $d_1(\xi, \eta)$ and $d_2(\xi, \eta)$ will approach infinity. In this case, however, $A_n(\xi, \eta)$ also approaches infinity -- see (I-54) and footnote on page 32 of Chapter II - so that the nature of the singularity cannot be predicted. Also, as $|\xi_p|$, $|\eta_p| \to \infty$ along an open branch of the surface wave dispersion curve, C_s will approach zero. But since Q_s may approach infinity in this case, the nature of the singularity in (15) cannot be predicted. For those cases where the nature of the singularity of (15) cannot be predicted, in general, the behavior of the first-order asymptotic expression for the surface wave fields can be determined an any specific problem.

Unlike surface waves excited by a line source or by a point source in isotropic media, the possible variation of the quantities in (15), when either the $\underset{\sim}{\varepsilon}_1$ or $\underset{\sim}{\varepsilon}_2$ media is anisotropic, indicate that the point source surface wave fields may have a marked angular dependence aside from any asymmetry due to excitation. This dependence can include singularities such as shadow boundaries. In the next section a specific configuration is considered in which the surface wave radiation pattern exhibits such an angular dependence.

C. Surface Waves in a Gyrotropic Plasma Above a Perfect Conductor

As an illustration of the foregoing results for the surface wave contributions to the far fields radiated by a point source, these results will be applied to a specific configuration. This configuration consists of a gyrotropic, homogeneous, cold, electron plasma filling the half-space above a perfectly conducting plane. The static magnetic field that causes the plasma to be gyrotropic is assumed to be parallel to the conducting plane. Excitation of the R. F. fields is by an electric field impressed in a small slot cut in the conducting plane.

This configuration has been chosen because it is known to support surface waves. Furthermore, the analysis of the configuration for the surface wave and direct ray fields is relatively simple for appropriate ranges of plasma and cyclotron frequencies. For these ranges of cyclotron and plasma frequencies, no lateral rays will be present. Note that since the source is on the plasma-conductor interface, all rays associated with the stationary point contributions will proceed directly from the source to the observation point.

In studying propagation transverse to the static magnetic field in this configuration, Ishimaru[36] and Seshadri[37] found that a surface wave with no phase variation along the static magnetic field $\underline{B}_o$ can propagate in the direction $\underline{z}_o \times \underline{B}_o$ but not in the direction $-\underline{z}_o \times \underline{B}_o$. Adachi and Mushiake[38] represent the fields radiated by a phased line source along the static magnetic field in terms of a Fourier integral and plot the phase velocity curve of the surface waves $(1/\sqrt{\xi^2 + \eta^2}$ as a function of the angle $\tan^{-1}(\xi/\eta))$ for two different sets of values of the ratios of plasma and cyclotron frequency to wave frequency. They do not however evaluate the Fourier integral to obtain the surface wave fields.

Because of the mechanism of excitation chosen in this example, the double Fourier integral expression for the radiated fields is most conveniently expressed in a form that is somewhat different than that derived in Chapter I. In Section 1 below, the form of the integral representation in

terms of the transform variables ξ and η is derived. Comparing this form with that of the integrals in (II-4), the results of Chapter II and Section A of this chapter are used to find the various contributions to the fields radiated by the slot. In Section 2 below, results of numerical evaluation of the surface wave and direct ray radiation patterns are presented for a particular set of values of the ratios of plasma and cyclotron frequency to wave frequency.

1. Ray-Optical Expressions for the Radiated Fields

As depicted in Fig. 1, the z axis is chosen normal to the conducting plane, the y axis is taken in the same direction as the static magnetic field and the origin of the (x, y, z) coordinate system is located at the center of the slot. For simplicity, the impressed electric field in the slot is taken to be $\underline{E}_o = E_o \underline{x}_o$ with time dependence $e^{j\omega t}$. The total fields radiated by the slot must satisfy the boundary condition

$$\underline{E}_t(x, y, 0) = \begin{cases} \underline{E}_o & \text{for } (x, y) \text{ in the slot} \\ \\ 0 & \text{for } (x, y) \text{ out of the slot} \end{cases} \tag{16}$$

and the radiation condition at infinity. If the slot is small compared to wave length, the boundary condition (16) can be replaced by the approximate boundary condition

$$\underline{E}_t(x, y, 0) = A_o \underline{E}_o \delta(x) \delta(y) \quad , \tag{17}$$

where A_o is the area of the slot.

As in Chapter I, the radiated fields may be represented as a double Fourier integral transformation of the form given in (I-2). Furthermore, from Chapter I it is seen that the transforms of the fields, $\underline{\varepsilon}(\xi, \eta; z)$ and $\underline{H}(\xi, \eta; z)$, will be superpositions of the modal fields $\underline{\varepsilon}_m(\xi, \eta) e^{-jk_o x_m z}$ and $\underline{H}_m(\xi, \eta) e^{-jk_o x_m z}$ of the plasma medium. Because of the radiation condition at $z \to \infty$, only the upgoing $m = \vec{3}, \vec{4}$ modes of the plasma medium are used in the superposition. Thus
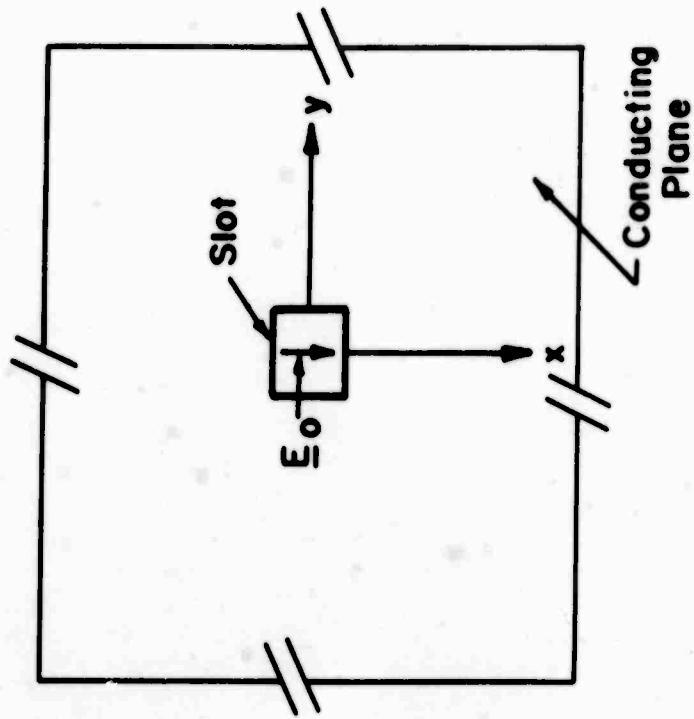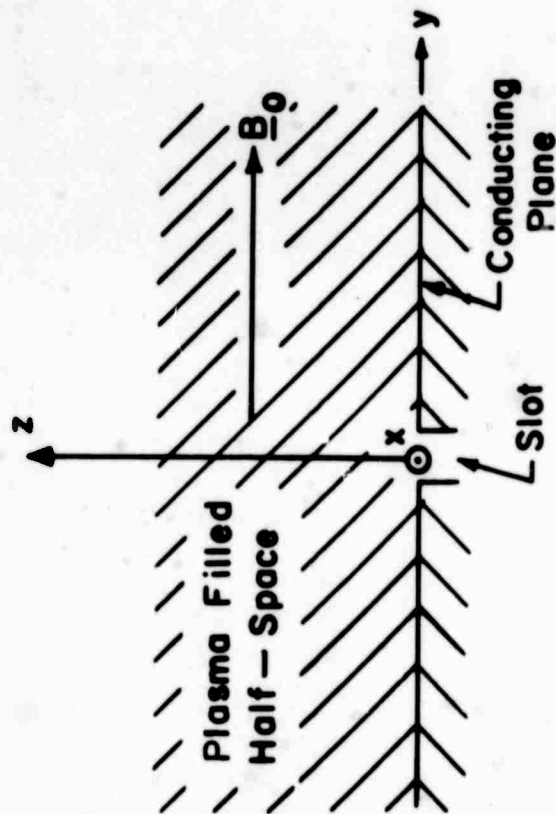
(a) Side View

(b) Top View

Fig. V-1 Grounded gyrotropic plasma configuration

$$\left.\begin{array}{c}\underline{E}(\underline{r})\\ \underline{H}(\underline{r})\end{array}\right\} = \sum_{\vec{3},\vec{4}} \iint_{-\infty}^{\infty} A_m(\xi,\eta) \left\{\begin{array}{c}\underline{\mathscr{E}}_m(\xi,\eta)\\ \underline{\mu}_m(\xi,\eta)\end{array}\right\} e^{-jk_o(\xi x + \eta y + \varkappa_m z)} d\xi\, d\eta \quad ,$$

(18)

where the A_m's are to be determined from the boundary condition (17) at $z = 0$.

Using the Fourier representation for $\delta(x)\,\delta(y)$ in (17) and using (18) for $\underline{E}_t(x, y, 0)$, the boundary condition (17) becomes

$$\sum_{\vec{3},\vec{4}} \iint_{-\infty}^{\infty} A_m(\xi,\eta)\, \underline{\mathscr{E}}_{tm}(\xi,\eta)\, e^{-jk_o(\xi x + \eta y)} d\xi\, d\eta$$

$$= A_o\, \underline{E}_o\, (\frac{k_o}{2\pi})^2 \iint_{-\infty}^{\infty} e^{-jk_o(\xi x + \eta y)} d\xi\, d\eta \quad .$$

(19)

Because of the orthogonality of the exponentials on the infinite interval, (19) implies that

$$\sum_{\vec{3},\vec{4}} A_m(\xi,\eta)\, \underline{\mathscr{E}}_{tm}(\xi,\eta) = A_o\, \underline{E}_o\, (\frac{k_o}{2\pi})^2 \quad .$$

(20)

Crossing both sides of (20) with $\underline{\mathscr{E}}_{t\vec{4}}$ and then $\underline{\mathscr{E}}_{t\vec{3}}$ and dotting with $\underline{z}_o$ gives

$$A_{\vec{3}} = -A_o\, (\frac{k_o}{2\pi})^2\, \underline{z}_o \cdot (\underline{\mathscr{E}}_{t\vec{4}} \times \underline{E}_o)/ \underline{z}_o \cdot (\underline{\mathscr{E}}_{t\vec{3}} \times \underline{\mathscr{E}}_{t\vec{4}})$$

$$\left.\begin{array}{c}\\ \\ A_{\vec{4}} = A_o\, (\frac{k_o}{2\pi})^2\, \underline{z}_o \cdot (\underline{\mathscr{E}}_{t\vec{3}} \times \underline{E}_o)/ \underline{z}_o \cdot (\underline{\mathscr{E}}_{t\vec{3}} \times \underline{\mathscr{E}}_{t\vec{4}})\end{array}\right\}$$

(21)

Since the A_m's of (21) have branch singularities of both $\varkappa_{\vec{3}}$ and $\varkappa_{\vec{4}}$ and can have pole singularities, the integrals in (18) are of the form given in (II-4) with z' set to zero, i.e, for the source at the interface, and $A_m = \sum_n \Gamma_{mn} A_n$. This similarity permits the use of the results of Chapter II and Section A of this chapter in determining the ray-optical fields radiated by the slot.

For $z' = 0$, the roots L_{m1} and L_{m2} of (II-24) are zero and hence $L_m > L_{m1}, L_{m2}$ so that δ_{mn} in (II-26) is given by (II-27). Thus, writing $L_m = L \equiv \sqrt{x^2 + y^2 + z^2}$, since L_m is the same for all rays, and writing δ_{mn} as δ_m, the stationary point or direct ray contributions to (18) are given by (II-26) with $L_n = 0$ and $\sum_n \Gamma_{mn} A_n = A_m$, i.e.,

$$(\underline{E})_{S.P.} \sim \frac{2\pi}{k_o} \sum_{\vec{3},\vec{4}} \sum_{S.P.} \left\{ \frac{\underline{b}_m A_m |\cos\theta_m|}{L\sqrt{|G_m|}} e^{-jk_o L N_m} e^{-j\frac{\pi}{4}\delta_m} \right\}_{(\xi_s, \eta_s)}$$

(22)

In (22), the stationary point summation is over all points on the mth branch of the dispersion surface of the plasma medium at which $\underline{\nu}_m$ is in the direction of the displacement from the slot to the observation point.

Since $A_{\vec{3}}$ and $A_{\vec{4}}$ of (21) have the same denominator, they can be written as

$$A_m(\xi, \eta) = a_m(\xi, \eta) / d(\xi, \eta) , \qquad (23)$$

where the poles of A_m are given by the zeros of (ξ, η). Thus, from (15) for $z' = 0$ and $\sum_n \gamma_{mn} A_n = a_m$, the surface wave contribution to $\underline{E}$ of (18) is

$$(\underline{E})_{S.W.} \sim -j\frac{(2\pi)^{3/2}}{\sqrt{k_o}} \sum_p \left\{ \frac{e^{-jk_o N_s \rho} e^{-j\frac{\pi}{4}\text{sgn}\, C_s}}{Q_s\sqrt{\rho|C_s|}} \sum_{\vec{3},\vec{4}} \underline{b}_m a_m e^{-jk_o \kappa_m z} \right\}_{(\xi_p, \eta_p)}$$

(24)

Expressions similar to (22) and (24) hold for $(\underline{H})_{S.P.}$ and $(\underline{H})_{S.W.}$ with $\underline{b}_m$ replaced by $\underline{\mu}_m$. For the choice of plasma parameters made in the next section, (18) will have no lateral ray contribution. However, for other choices of the plasma parameters, lateral ray contributions can exist and would be given by (II-41) with $z' = 0$, i.e., with the incident segment $\underline{L}_n$ of the ray set equal to zero, and $\sum_n \gamma_{\ell mn} A_n = a_{\ell m}$ with $a_{\ell m}$ defined from A_m

in analogy to (II-40).

In order to evaluate the ray-optical fields radiated by the slot, it is necessary to know the functional form of the various quantities appearing in (22) and (24). The modal quantitites $\varkappa_m$, $\underline{\mathscr{E}}_m$ and $\underline{\mathscr{H}}_m$ are most easily calculated if it is recognized that the modal or polarization vectors $\underline{\mathscr{E}}_m$ and $\underline{\mathscr{H}}_m$ are those of a wave propagating as $e^{-jk_o \underline{k}_m \cdot \underline{r}}$, where $\underline{k}_m = \underline{x}_o \xi + \underline{y}_o \eta + \underline{z}_o \varkappa_m$, in the plasma. Substituting this form into Maxwell's equations gives

$$\left. \begin{array}{c} k_o \underline{k}_m \times \underline{\mathscr{E}}_m = \omega u_o \underline{\mathscr{H}}_m \\[2em] k_o \underline{k}_m \times \underline{\mathscr{H}}_m = -\omega \epsilon_o \underset{\sim}{\epsilon} \, \underline{\mathscr{E}}_m \end{array} \right\} \tag{25}$$

In (25), $\underset{\sim}{\epsilon}$ is the relative dielectric tensor of the cold, electron plasma. Crossing the first equation of (25) by $\underline{k}_m$ and substituting the second into the result, one obtains

$$\left[\underset{\sim}{\epsilon} + \underline{k}_m \underline{k}_m - k_m^2 \underset{\sim}{1} \right] \cdot \underline{\mathscr{E}}_m = 0 \quad . \tag{26}$$

For (26) to have a non-trivial solution $\underline{\mathscr{E}}_m$, the determinant of the dyadic $[\underset{\sim}{\epsilon} + \underline{k}_m \underline{k}_m - k_m^2 \underset{\sim}{1}]$ must be zero. This condition gives the plane wave dispersion equation (I-24) from which $\varkappa_{n\lambda}$ can be found. The solution of (26) for $\underline{\mathscr{E}}_m$ is then found by substituting $\varkappa_m$ into (26). The magnetic field polarization vector $\underline{\mathscr{H}}_m$ is then given by the first equation in (25).

In the small signal approximation, a cold, electron plasma with static magnetic field in the y direction can be represented by the relative dielectric tensor

$$\underset{\sim}{\epsilon} = \begin{bmatrix} \epsilon_1 & 0 & \epsilon_3 \\ 0 & \epsilon_2 & 0 \\ -\epsilon_3 & 0 & \epsilon_1 \end{bmatrix} \quad , \tag{27}$$

where

$$\epsilon_1 = 1 + \frac{X}{Y^2 - 1}$$

$$\epsilon_2 = 1 - X \qquad\qquad (28)$$

$$\epsilon_3 = j\frac{XY}{Y^2 - 1}$$

In (28), $X = (w_p/w)^2$ is the square of the ratio of the plasma frequency to wave frequency and $Y = w_c/w$ is the ratio of cyclotron frequency to wave frequency. Note that $w_p^2 = N q^2/\epsilon_o m$ where N is the electron density, q the magnitude of the electron charge and m the electron mass. Also, $w_c = q B_o/m$ where the strength B_o of the static magnetic field is positive if the field is in the plus y direction and minus otherwise.

Substituting $\underset{\sim}{\epsilon}$ from (27) into (26) and setting the determinant of the dyadic equal to zero, one finds that the plane wave dispersion relation reduces to a bi-quadratic whose solution is

$$\varkappa_m = \left\{ \epsilon_2 + \frac{\epsilon_1 - \epsilon_2}{2\epsilon_1} - \frac{\epsilon_1 + \epsilon_2}{2\epsilon_1}\eta^2 - \xi^2 \right.$$

$$\left. \pm \frac{\epsilon_1 - \epsilon_2}{2\epsilon_1}\sqrt{\eta^4 - 2\eta^2\frac{\epsilon_1 + \epsilon_2 - 2\epsilon_1\epsilon_2}{\epsilon_1 - \epsilon_2} + 1} \right\}^{1/2} \qquad (29)$$

In deriving (29), use was made of the relation $\epsilon_3^2 = -(\epsilon_1 - 1)(\epsilon_1 - \epsilon_2)$, which is easily verified from (28). For η real, the argument of the inner root is taken as 0 or $\pi/2$. The plus sign is used for $\varkappa_{\vec{3}}$ and the minus sign for $\varkappa_{\vec{4}}$. The argument of the outer root is taken such that $\varkappa_{\vec{3}}$ and $\varkappa_{\vec{4}}$ correspond to upgoing waves.

Knowing $\varkappa_m$, the electric field polarization vector is found from (26) to be

$$\underline{\mathcal{b}}_m = \underline{x}_o \eta \left[\varkappa_m \epsilon_3 - \xi(\epsilon_1 - \xi^2 - \eta^2 - \varkappa^2_m) \right]$$

$$+ \underline{y}_o \left[\epsilon^2_3 + (\epsilon_1 - \eta^2)(\epsilon_1 - \xi^2 - \eta^2 - \varkappa^2_m) \right]$$

$$+ \underline{z}_o \eta \left[-\xi \epsilon_3 - \varkappa_m(\epsilon_1 - \xi^2 - \eta^2 - \varkappa^2_m) \right] \quad . \tag{30}$$

Using (30) in the first equation of (25),

$$\underline{\mu}_m = \sqrt{\frac{\epsilon_o}{\mu_o}} \left\{ \underline{x}_o \left[-\varkappa_m \epsilon^2_3 - \xi \eta^2 \epsilon_3 - \varkappa_m \epsilon_1(\epsilon_1 - \xi^2 - \eta^2 - \varkappa^2_m) \right] \right.$$

$$+ \underline{y}_o \epsilon_3 \eta (\xi^2 - \varkappa^2_m)$$

$$+ \left. \underline{z}_o \left[\xi \epsilon^2_3 - \varkappa_m \eta^2 \epsilon_3 + \xi \epsilon_1(\epsilon_1 - \xi^2 - \eta^2 - \varkappa^2_m) \right] \right\} \quad . \tag{31}$$

Because $\underline{E}_o = \underline{x}_o E_o$, $\underline{z}_o \cdot (\underline{\mathcal{b}}_{tm} \times \underline{E}_o) = -E_o \mathcal{b}_{ym}$, and expanding $\underline{z}_o \cdot (\underline{\mathcal{b}}_{t3} \times \underline{\mathcal{b}}_{t4})$ with the help of (30), the a_m's and $d(\xi, \eta)$ of (23) can be written as

$$a_{\vec{3}}(\xi, \eta) = A_o E_o \mathcal{b}_{y\vec{4}} \left(\frac{k_o}{2\pi}\right)^2 / \epsilon_3 \eta (\varkappa_{\vec{3}} - \varkappa_{\vec{4}})$$

$$\left. \right\} \tag{32}$$

$$a_{\vec{4}}(\xi, \pi) = A_o E_o \mathcal{b}_{y\vec{3}} \left(\frac{k_o}{2\pi}\right)^2 / \epsilon_3 \eta (\varkappa_{\vec{4}} - \varkappa_{\vec{3}})$$

and

$$d(\xi, \eta) = \epsilon^2_3 + \xi (\varkappa_{\vec{3}} + \varkappa_{\vec{4}}) \epsilon_3 + (\epsilon_1 - \eta^2)(\epsilon_1 - \xi^2 - \eta^2 + \varkappa_{\vec{3}} \varkappa_{\vec{4}}) \quad . \tag{33}$$

From (32) and (33) it is seen that (18) is invariant under the interchange of $\vec{3}$ and $\vec{4}$. Thus, as argued in Section 2 of Appendix B, branch points of $\varkappa_{\vec{3}}$ and $\varkappa_{\vec{4}}$ due to the inner root in (29) at which they are complex or imaginary, and hence equal, will not be branch points of (18). Since the singularity $\varkappa_{\vec{3}} = \varkappa_{\vec{4}}$ in (32) is of the branch type, i.e., $\varkappa_{\vec{3}} - \varkappa_{\vec{4}}$ approaches zero as

$\sqrt{\eta - \eta_b}$, this singularity will not appear in the fields. In the next section, it will be argued that the apparent singularity $\eta = 0$ in (32) is not a singularity of (18) and hence, the only pole singularities in (18) are due to zeros of $d(\xi, \eta)$.

Knowing $\kappa_m(\xi, \eta)$, the quantities $\cos \theta_m$, G_m and N_m in (22) can be found using (II-16), (II-17) and (II-18). Also, δ_m in (22) can be found from (II-14), where $P_{uu} = z \dfrac{\partial^2}{\partial u^2} \kappa_m$ and $P_{vv} = z \dfrac{\partial^2}{\partial v^2} \kappa_m$, and the stationary points (ξ_s, η_s) from (II-15) with $z' = 0$. From the solution of the pole locus condition $d(\xi, \eta) = 0$, the surface wave dispersion curve $\eta = \eta_p(\xi)$ can be found. The solution $\eta = \eta_p(\xi)$ can then be used to calculate C_s, Q_s and N_s in (24) from equations (7), (8), and (13) and the definition of Q_s given after (11). The point (ξ_p, η_p) can be found from (5) using the solution $\eta = \eta_p(\xi)$.

2. Surface Wave and Direct Ray Radiation Patterns

For the sample calculation of the radiation patterns given here, the plasma parameters were taken as $\omega_p/\omega = 5.0$ and $|\omega_c/\omega| = 1.5$. This choice was made as being representative of the range of X and Y for which surface waves exist and only one direct ray, at most, reaches each observation point in the plasma. If the parameters had been chosen such that two or more direct rays could reach an observation point, a beat pattern would exist in the fields. This beat pattern would result from the fact that the wave vectors of the several rays would not be the same. In this case, the direct ray radiation pattern would not be independent of L.

For the above choice of parameters $\epsilon_1 = 21$, $\epsilon_2 = -24$ and from (29) and the text following, it can be shown that $\kappa_{\frac{1}{4}}$ is complex or imaginary for all real ξ and η. Moreover, from (29), the dispersion surface is seen to be a surface of revolution about the η axis. The plane curve whose rotation about the η axis generates the dispersion surface is given in Fig. 2. This curve has open branches extending to infinity along the asymptotes indicated in Fig. 2.

Because the plane wave dispersion surface is one of revolution, its normal $\underline{\nu}$ at any point will lie in the plane containing η axis and the point in question, i.e., in the plane of the generating curve. The sense of the normal shown in Fig. 2 was taken in accordance with the fact that for lossless media, the wave vector $\underline{k}$ and the real part $\underline{s}$ of the complex Poynting vector of the associated plane wave make an angle less than or equal to 90°. From the sense of $\underline{\nu}$ in Fig. 2, it is seen that $\kappa_{\overline{3}}$ will be negative for values of ξ and η for which it is real.

As a point on the generating curve of Fig. 2 moves to infinity, the angle between $\underline{\nu}$ at the point and the η axis will increase monotonically to some maximum value. The maximum value of the angle between $\underline{\nu}$ and the η axis, which for the plasma parameters used here is 43.1°, is the complement of the angle between the asymptotes of Fig. 2 and the η axis. Thus, since the dispersion surface is one of revolution about the η axis, all its normals lie within the two sheets of a cone whose axis is the η axis and whose half-angle is 43.1°. Because the direct rays excited in the plasma by the slot are in the direction of $\underline{\nu}$, they all lie within that region above the (x, y) plane that is inside the two sheets of a cone whose axis is the y axis and whose half-angle is 43.1°. Moreover, since the generating curve of Fig. 2 has no inflection points, which can be demonstrated analytically, and the dispersion surface is one of revolution, $G_m \to 0$ only for $\eta \to \infty$ and only one direct ray reaches each observation point in the illuminated region. No propagating direct rays reach observation points outside the illuminated region described above.

At the branch points of the inner root of (29), $\kappa_{\overline{3}}$ is imaginary for the plasma parameters used here. Thus, the branch curve of $\kappa_{\overline{3}}$ at which it is real is that corresponding to the outer root, and hence is the locus of points at which $\kappa_{\overline{3}} = 0$. Because of this, the branch curve of $\kappa_{\overline{3}}$ at which it is real will coincide with the generating curve of Fig. 2 when this curve lies in the (ξ, η) plane.

The surface wave dispersion curve, which is given in Fig. 3, was found numerically for $B_o > 0$ from the condition $d(\xi, \eta) = 0$ with $d(\xi, \eta)$ as given in (33). Because η appears only in even powers in (29) and (33), the surface wave dispersion curve is symmetric about the ξ axis. For $B_o > 0$, the dispersion curve crosses the ξ axis at $\xi = -\sqrt{\epsilon_1}$, as can easily be shown from (29) and (33). The surface wave dispersion curve terminates on the branch curve $\kappa_{\overline{3}} = 0$ where it is tangent to the branch curve, as is indicated in Fig. 3.*

In addition to being zero on the surface wave dispersion curve of Fig. 3, $d(\xi, \eta)$ vanishes on the locus of points $\eta = \pm \sqrt{\epsilon_1 + |\epsilon_3|}$, $\xi > 0$. This locus of points, except for the two points where it is crossed by the dispersion curve of Fig. 3, is not part of the pole locus of (18). That these points are not part of the pole locus follows from the fact that the form given in (30) for $\underline{b}_{\overline{3}}$ vanishes at these points. Thus, $\underline{e}_{\overline{3}}$, $\underline{\mu}_{\overline{3}}$, $a_{\overline{4}}$ and $d(\xi, \eta)$ all vanish as $\underline{b}_{\overline{3}}$, and hence the integrand of (18) is regular at these points. Similarly, the locus of points $\eta = 0$, which from (32) appears to be a pole locus, is not a locus of poles of (18), except for the single point where the surface wave dispersion curve crosses the ξ axis. For $\eta = 0$, $\underline{b}_{\overline{3}}$ given in (30) is zero and, as in the above discussion, the integrand of (18) is regular.

For $\omega_p/\omega = 10$ and $|\omega_c/\omega| = 3$, i.e., at an ω half that used in computing the curves of Fig. 3, the value of $\sqrt{\xi^2 + \eta^2}$ calculated by Adachi and Mushiake[38] on the surface wave dispersion curve is less than that for the dispersion curve of Fig. 3 along any radius in the (ξ, η) plane that intersects both curves. That the value of $\sqrt{\xi^2 + \eta^2}$ on the dispersion curve increases with ω along any radius implies that the radial component of $\nabla_{\underline{k}_t} \omega$ points away from the origin, where $\underline{k}_t$ is the unnormalized transverse wave vector $k_o(\underline{x}_o \xi + \underline{y}_o \eta)$. Since the normal $\underline{\nu}_s$ to the dispersion curve is to be taken in the direction of energy flow of the corresponding surface wave, which itself is in the direction of $\nabla_{\underline{k}_t} \omega$, $\underline{\nu}_s$ must have a positive radial

----
*

By straightforward calculation, it can be shown that $d\eta_p/d\xi = -d_1/d_2$, where d_2 and d_2 are the derivatives of $d(\xi, \eta)$, is equal to $d\eta_b/d\xi$ at the termination of the surface wave dispersion curve.
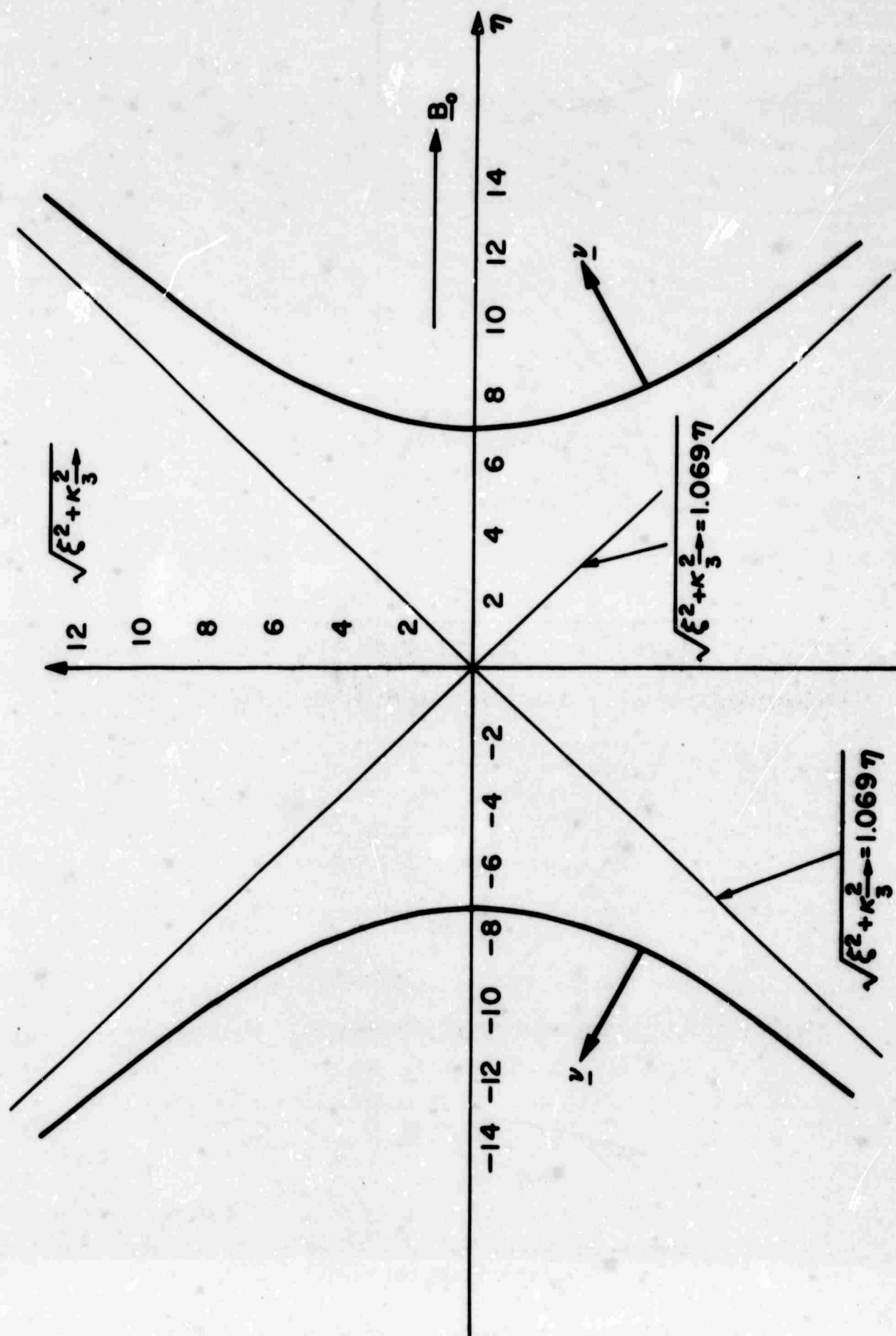
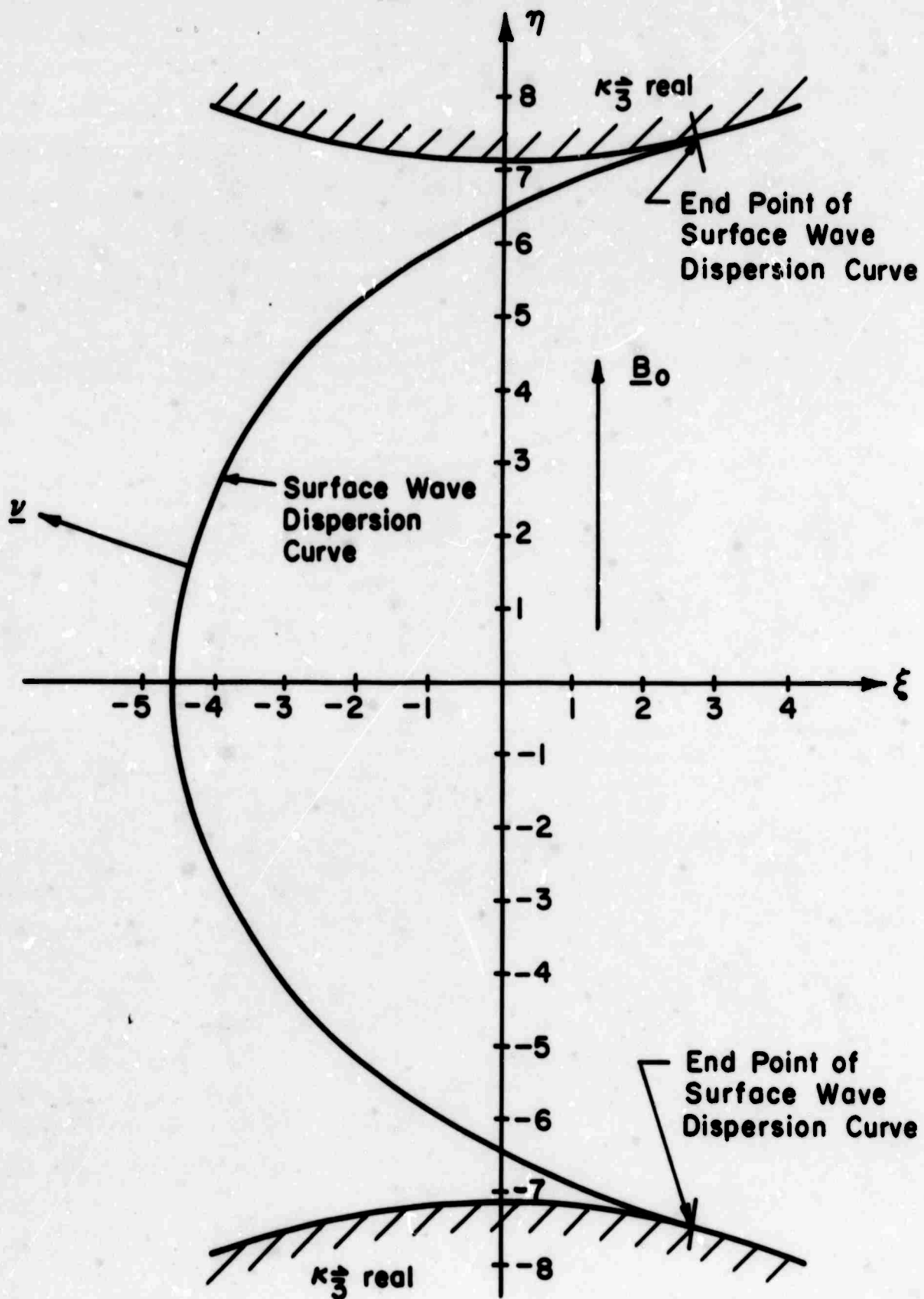Fig. V-2 Generating curve for plasma dispersion surface $-\eta_-/\eta = 5.0$; $|\eta_+/\eta_-| = 1.5$

Fig. V-3 Surface wave dispersion curve for plasma-conductor interface —
$w_p/w = 5.0$, $|w_c/w| = 1.5$

component. The sense indicated in Fig. 3 for $\underline{\nu}_s$ is seen to be in agreement with the above requirement. While the foregoing assignment of the sense of $\underline{\nu}_s$ was not checked analytically for all points on the dispersion curve because of the complexity of the functions involved, it has been verified analytically at the points where the dispersion curve crosses the ξ and η axes.

From the approximation $d\eta_p/d\xi \approx \Delta\eta_p/\Delta\xi$ and the calculated values of $\eta_p(\xi)$, $d\eta_p/d\xi$ for $\eta_p > 0$ was found to be a monotonically decreasing function of ξ. Since $d\eta_p/d\xi$ is a monotonically decreasing function of ξ for $\eta_p > 0$, and because of the symmetry of the dispersion curve about the ξ axis, as a point on the dispersion curve moves away from the ξ axis, the angle between the normal $\underline{\nu}_s$ at the point and the $-\xi$ axis increases monotonically up to a maximum. The maximum occurs at the end point of the dispersion curve and for the curve of Fig. 3 was found to be 75.1°. Thus, the propagating surface waves excited by the slot illuminate only those points within a wedge-shaped region centered about the -x axis whose half-angle is 75.1°. Furthermore, within this wedge, only one surface wave ray reaches each observation point, and hence the sum over p in (24) reduces to a single term.

The real part $\underline{S}$ of the total Poynting vector of the surface wave propagating on the plasma-conductor interface is, in accordance with Chapter III, given by

$$\underline{S} = \int_o^\infty Re\left[(\underline{E})_{S.W.} \times (\underline{H})^*_{S.W.}\right] dz \quad . \tag{34}$$

Substituting the expressions for the surface wave fields given in (24) into (34), and recalling that only one surface wave ray, at most, reaches each observation point, one find that

$$\underline{S} = \frac{(2\pi)^3}{k_o} \frac{1}{\rho Q_s^2 |C_s|} \int_o^\infty \sum_{m,n} Re\left\{a_m a_n^* \underline{\delta}_m \times \underline{H}_n^* e^{-jk_o(x_m - x_n^*)z}\right\} dz \tag{35}$$

$$(m, n = \vec{3}, \vec{4})$$

evaluated at (ξ_p, η_p). A polar plot of the surface wave radiation pattern $g_s(\Psi)$, i.e., $|\underline{S}| \rho$ normalized to its maximum value versus the angle $\Psi = \tan^{-1}(-y/x)$, is given in Fig. 4 for $\omega_p/\omega = 5.0$ and $|\omega_c/\omega| = 1.5$. This plot is the surface wave radiation pattern of the plasma-conductor interface for slot excitation with $\underline{E}_o = \underline{x}_o E_o$.

As can readily be verified analytically, the radiation pattern of Fig. 4 is symmetric about $\Psi = 0$. Had the field in the slot been taken as $\underline{E}_o = \underline{y}_o E_o$, $(E_z)_{S.W.}$ and $(H_y)_{S.W.}$ would have odd symmetry about $\Psi = 0$ and hence the surface wave radiation pattern would have a null at $\Psi = 0$, although it would still by symmetric about $\Psi = 0$. For $\underline{E}_o$ in some other direction, the radiation pattern is not symmetric about $\Psi = 0$. As discussed previously, the propagating surface wave contributions to the far fields exist only for $|\Psi| \leq 75.1^{\circ}$.

For the direct rays, the real part $\underline{s}$ of the local Poynting vector is

$$\underline{s} = \text{Re}\left[(\underline{E})_{S.P.} \times (\underline{H}^*)_{S.P.}\right] . \tag{36}$$

Since only one direct ray, at most, reaches each point in the plasma, the sums in expression (22) reduce to a single term having $m = \vec{3}$. Thus,

$$\underline{s} = \left(\frac{2\pi}{k_o}\right)^2 \frac{|A_{\vec{3}}|^2 \cos^2\theta_{\vec{3}}}{L^2 |G_{\vec{3}}|} \text{Re}(\underline{\mathscr{E}}_{\vec{3}} \times \underline{\mathscr{H}}_{\vec{3}}^*) \tag{37}$$

evaluated at (ξ_s, η_s). In Fig. 5, the direct ray radiation pattern g_d, which is defined as $|\underline{s}| L^2$ normalized to the maximum value of $|\underline{S}| \rho$ for the surface waves, is plotted for observation directions in the (y, z) plane.

The angle ϕ in the polar plot of Fig. 5 is defined as $\tan^{-1}(z/y)$. Note that in the (y, z) plane, $\sin^2\phi = \cos^2\theta_{\vec{3}}$ so that from (37), g_d vanishes at $\phi = 0, 180^{\circ}$, as indicated in Fig. 4. Also, g_d is symmetric about $\phi = 90^{\circ}$ since the dispersion surface is about $\eta = 0$ and $\underline{s}$ is an even function of η_s. As discussed previously, the propagating direct rays illuminate only that region between the conductor and the two sheets of the cone whose axis is the y axis and whose half-angle is 43.1°. Thus g_d can be non-zero only for

observation directions making an angle less than or equal to 43.1° with the y axis, as is shown in Fig. 5. For Φ approaching 43.1° from below and approaching 136.9° from above, g_d is singular since for these directions, the direct ray contribution comes from points $|k_{\underline{3}}| \to \infty$ on the open branches of the dispersion surface where the Gaussian curvature $G_{\underline{3}} \to 0$. This singularity has been shown to result from the use of the approximate boundary condition (17). For an actual slot of finite extent, g_d will have a maximum near $\Phi = 43.1^{\circ}$, 136.9° but will remain finite. [39]

Since the plasma medium is rotationally symmetric about the y axis, the pattern function of the terms $|\text{Re}(\underline{\varrho}_{\underline{3}} \times \underline{\mu}_{\underline{3}}^{*})| / |G_{\underline{3}}|$ will also be rotationally symmetric about the y axis. Thus, variations in the pattern of g_d in planes containing the y axis are produced only by the variation of $|A_{\underline{3}}|^2 \cos^2 \theta_{\underline{3}}$. Note that since $d(\zeta, \eta)$, in the definition of $A_{\underline{3}}$ is not a symmetric function of ζ, the radiation patterns in the planes $x = \alpha z$ and $x = -\alpha z$ will not be the same. Defining $\Phi = \tan^{-1}(\sqrt{x^2 + z^2} / y)$, in any plane containing the y axis, g_d will be symmetric about $\Phi = 90^{\circ}$ since $A_{\underline{3}}$ is a symmetric function of η. Furthermore, in any plane containing the y axis, g_d will exhibit a singularity at $\Phi = 43.1^{\circ}$, 136.9° and will be zero for $43.1 < \Phi < 136.9^{\circ}$, as was discussed for the direct ray radiation pattern in the (y, z) plane. In the (x, y) plane $g_d = 0$ since for $z = 0, \cos \theta_{\underline{3}} = 0$. In Fig. 6 and Fig. 7, g_d has been plotted as a polar function of Φ for the planes $x = z$ and $x = -z$, respectively.

$$|S| \rho = .038 (K_0 A_0 E_0)^2 g_s$$
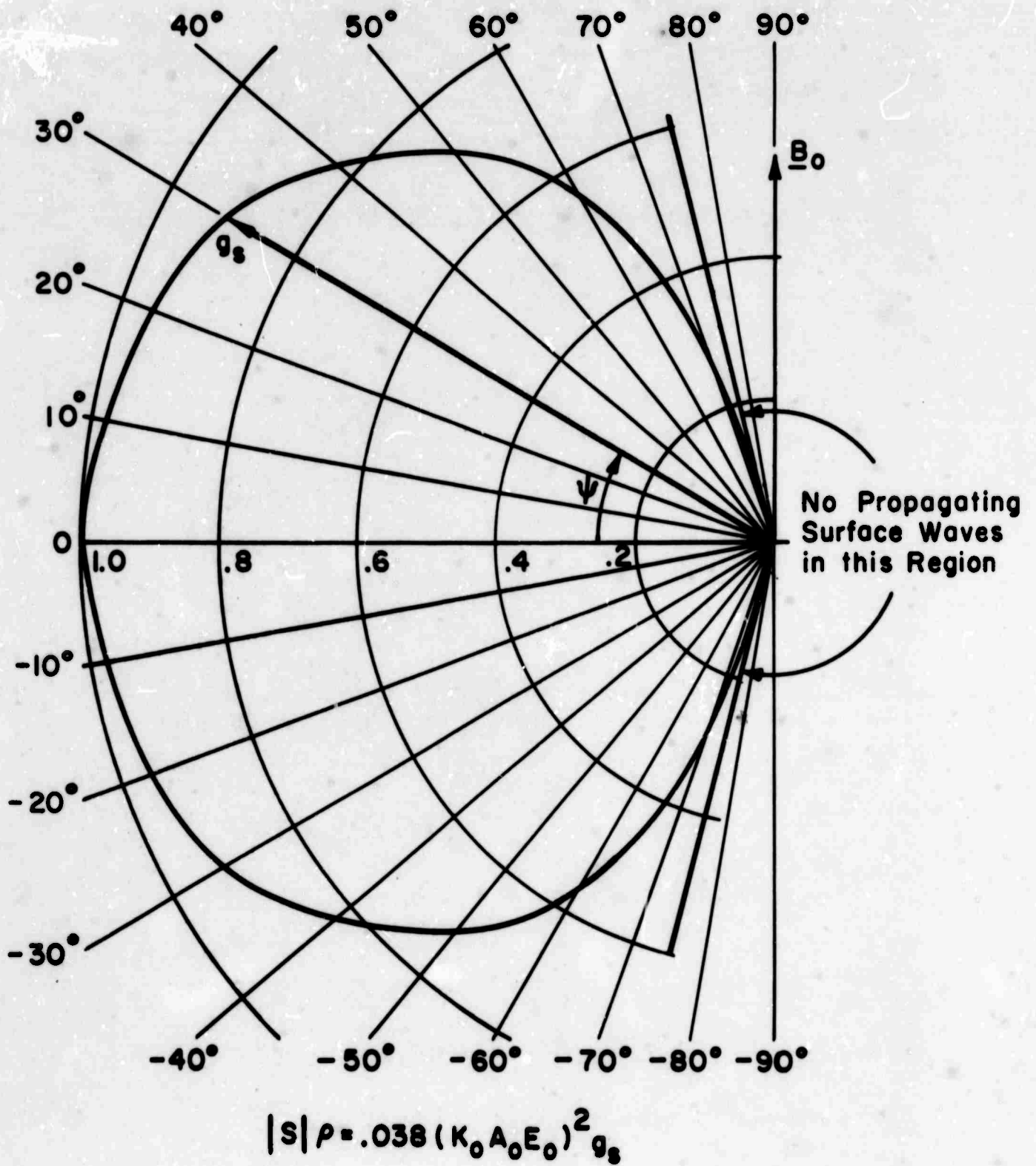
Fig. V-4 Surface wave radiation pattern for plasma-conductor interface --
$\omega_p/\omega = 5.0$, $|\omega_c/\omega| = 1.5$
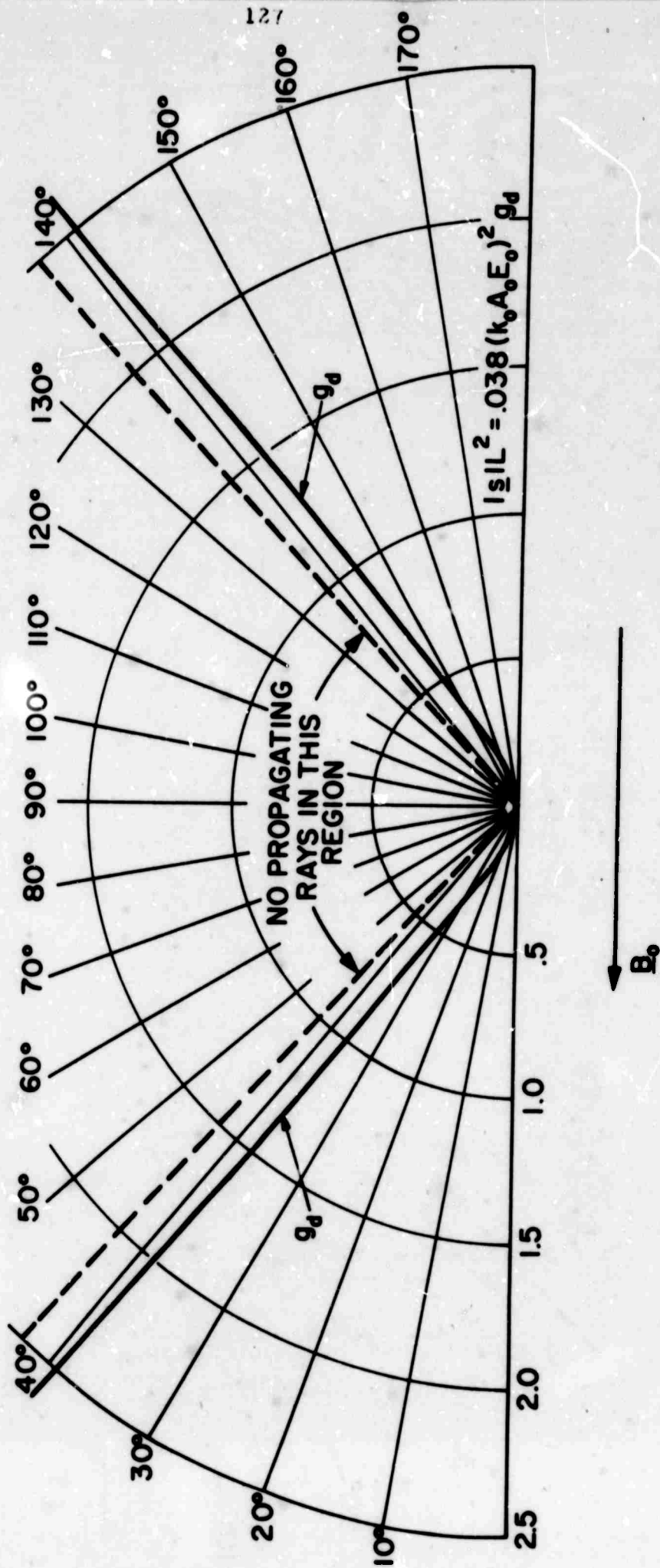
Fig. V-5   Direct ray radiation pattern in the (y, z) plane-$x_p/w = 5.0$, $|x_c/w| = 1.5$
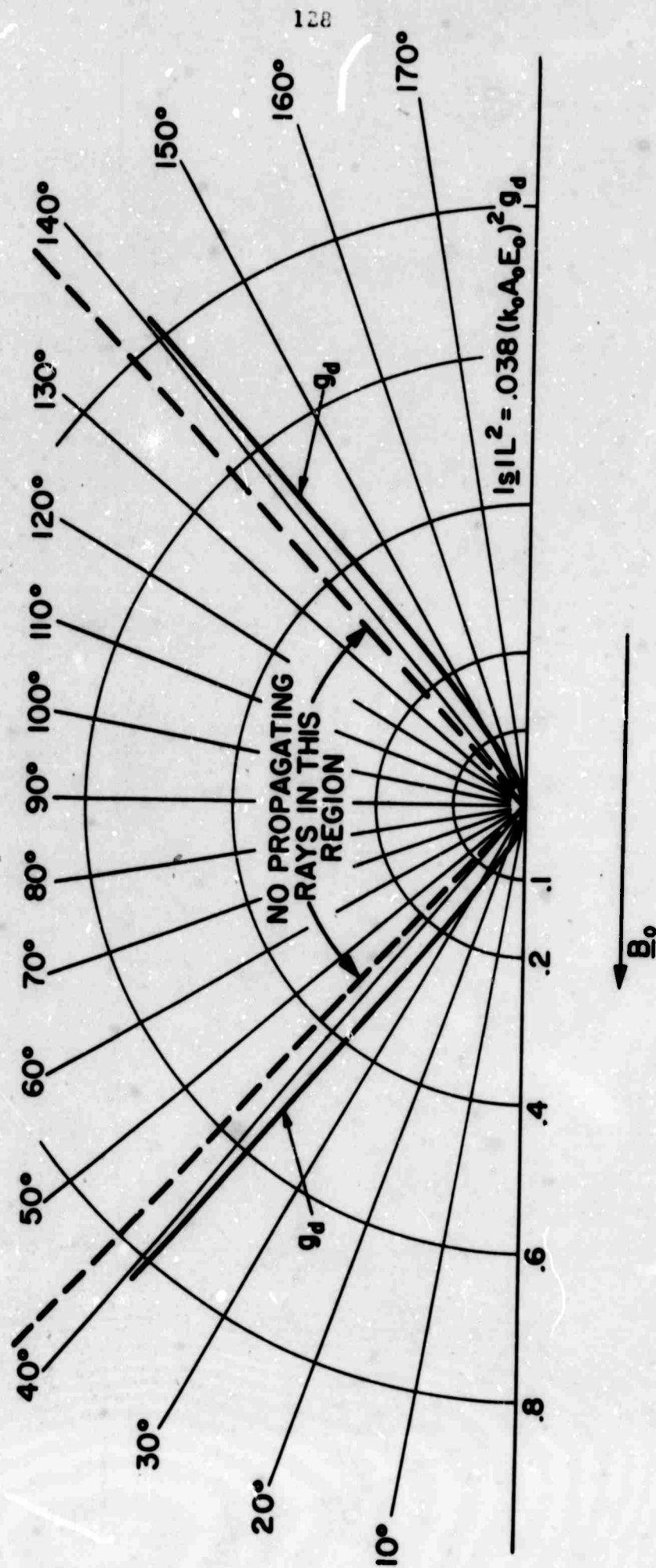
Fig. V-7 Direct ray radiation pattern in the plane $x=z -\omega_p/\omega = 5.0, |u_c/v| = .5$

129

$|\underline{S}|L^2 = .038 \, (k_o A_o E_o)^2 g_d$

NO PROPAGATING RAYS IN THIS REGION

g_d

B_o

Fig. V-7   Direct ray radiation pattern in the plane $x = -z$ --- $\tau_p/\omega = 5.0$, $|\omega_c/\omega| = 1.5$

130

SUMMARY

In Chapter I, the form of the double Fourier integral representation for the fields radiated by a point source in the presence of a planar interface between two arbitrary, lossless, homogeneous, anisotropic media was found. The stationary point and branch curve contributions to the asymptotic evaluation of the Fourier integral representation were considered in Chapter II. The stationary point contributions were interpreted in terms of direct, transmitted and reflected rays, which are the trajec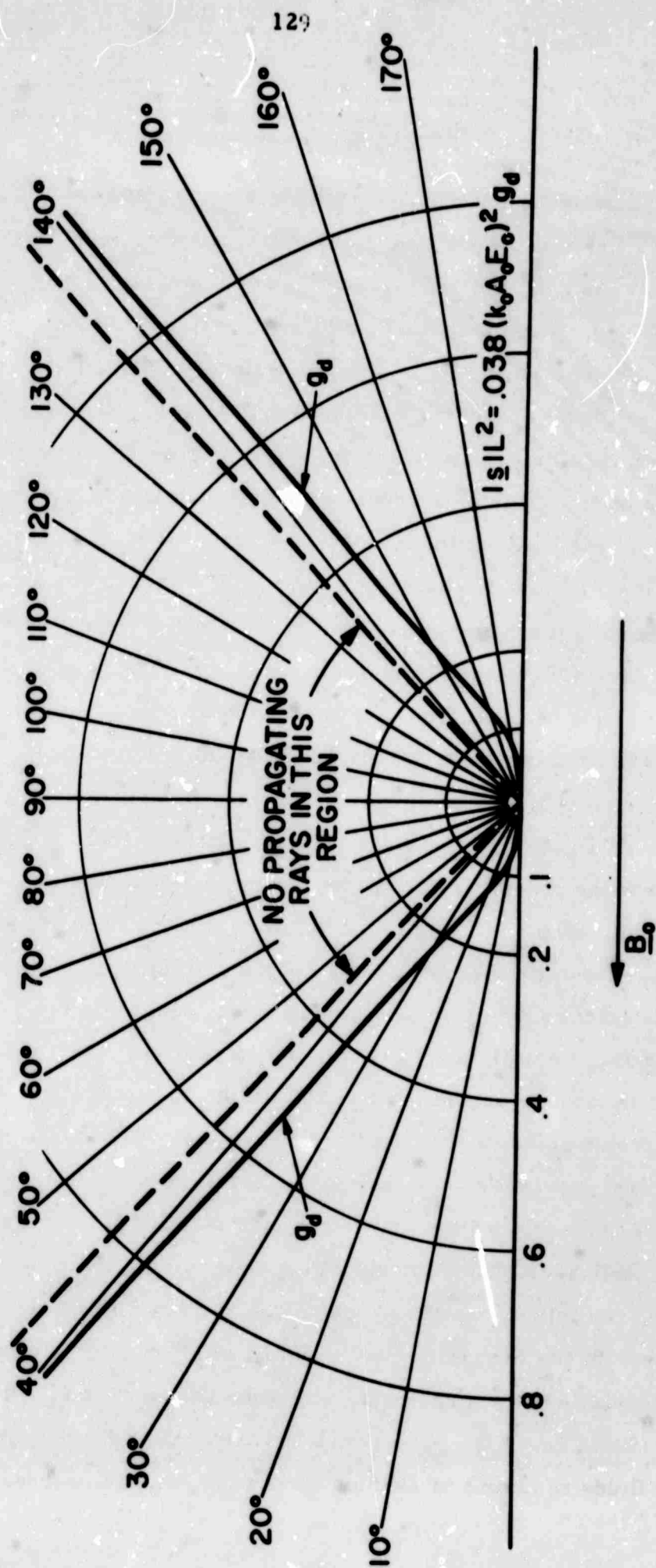tories of energy flow in lossless media, and the associated fields were cast into ray-optical form. The ray-optical form of the fields discloses the local nature of ray propagation. This local nature suggests ways of extending the ray-optical results to geometries not amenable to rigorous analysis. One such extension was considered in Chapter II, where the fields reflected from and transmitted through a curved interface between two anisotropic media were calculated.

In Chapter II, the branch curve contributions were interpreted in terms of lateral rays and the fields cast into ray-optical form. The lateral ray is the trajectory of energy flow of a ray having three segments, one of which lies in the interface. While the branch curve contributions are of lower order than the stationary point contributions, in geometric-optical shadow regions where the stationary point contributions are exponentially small in all orders, the lateral ray fields will form the dominant contribution to the far fields. Unlike the lateral rays excited by a line source or point-source lateral rays in isotropic media, the point-source lateral ray fields in an isotropic media can have strong directional dependence other than that introduced by the source. This dependence can include caustics and shadow boundaries.

The ray interpretation of the stationary point and branch curve contributions to the far fields was based on the fact that plane waves in lossless media carry energy in the direction of the normal to the plane wave dispersion surface. In order to interpret the real pole contributions to the far fields in terms of surface wave rays, it was necessary to derive

a relation between surface wave group velocity and energy velocity analogous to that for plane waves. Such a relation was derived in Chapter III for surface waves in arbitrarily plane-stratified, lossless, anisotropic media. It was found that the surface wave group velocity was equal to the ratio of the integral, over the coordinate of stratification, of the real part of the complex Poynting vector to the corresponding integral of the energy density. Thus, the real part of the integrated Poynting vector of a surface wave is in the direction of the normal to the surface wave dispersion curve. The necessity for integrating the local Poynting vector over the coordinate of stratification results from the fact that its direction, as well as magnitude, can vary with this coordinate.

The relations between the energy flow and stored energy in a plane-stratified structure and the derivatives, with respect to the transverse wave numbers and frequency, of the dyadic surface impedance representing the structure were also determined in Chapter III. The significance of these relations for surface waves on a dyadic surface impedance plane was discussed.

As an example of the effect of anisotropic media on surface wave propagation, the surface waves on a uniaxial plasma slab were found in Chapter IV. The effect of the anisotropy is clearly seen in the surface wave dispersion curve, which has an infinite number of open branches, i.e., the branches do not encircle the origin. Furthermore, these surface waves illustrate the fact that the direction of the Poynting vector can vary with the coordinate of stratification.

In Chapter V, the real pole contributions to the far fields of a point source in the presence of a planar interface between two anisotropic, lossless media were evaluated. Using the relation between the group velocity and the energy velocity of surface waves derived in Chapter III, the real pole contributions were interpreted in terms of surface wave rays. These rays are the two-dimensional trajectories of energy flow in lossless media. In the far field, the surface wave contribution at all points along a line perpendicular to the interface comes from

the same surface wave ray. In effect, surface wave ray propagation is a two-dimensional phenomenon, the variation in the third dimension merely describing the local strength of the surface wave fields. For source and observation points near the interface the surface wave contribution varies as the inverse square root of the distance between these points while the direct and scattered ray fields vary as the inverse of this distance. Thus, for source and observation points near the interface, the surface wave rays give the dominant contribution to the far fields.

Unlike the surface wave fields excited by a line source or a point source in isotropic media, the surface waves in anisotropic media due to a point source may have a directional dependence other than that introduced by the source. This directional dependence can include such features as shadow boundaries. As an illustration of the directional dependence of the surface wave fields, a specific configuration was considered in Chapter V. This configuration consisted of a gyrotropic plasma above a perfectly conducting plane. The gyrotropic anisotropy was assumed to be produced by a static magnetic field parallel to the conductor and excitation of the R. F. fields was by an impressed electric field in a slot cut in the conductor. In this configuration, the surface wave fields are confined to a wedge region centered about the direction perpendicular to the static magnetic field and lying entirely on one side of the static magnetic field.

Appendix A

EXCITATION COEFFICIENTS OF PROPAGATING
PLANE WAVES

For the case of point source excitation and real $\varkappa_n$, it is possible to find a particularly convenient form for the excitation coefficient A_n given in (I-54). Substituting the form (I-36) for $\hat{\mathfrak{z}}_o(\underline{k}_t)$ into (I-54) gives, for $\varkappa_n$ real,

$$A_n = -e_n \left(\frac{k_o}{2\pi}\right)^2 \left\{ \Psi_t^+(\varkappa_n) \cdot \begin{bmatrix} \underline{J}_{ot} \\ \underline{M}_{ot} \end{bmatrix} - \Psi_t^+(\varkappa_n) \cdot W_{tz} W_z \begin{bmatrix} \underline{J}_{oz} \\ \underline{M}_{oz} \end{bmatrix} \right\} \Big/ M_n . \qquad \text{(A-1)}$$

For lossless media, $\underline{\varepsilon}$ is Hermitian so that ε_{tz} in (I-6) is equal to $\underline{\varepsilon}_{zt}^*$, and hence from (I-11), (I-12) and (I-13) it is seen that

$$W_{tz} W_z = \begin{bmatrix} \dfrac{1}{\varepsilon_{zz}} \underline{\varepsilon}_{tz} & -\dfrac{k_o}{\omega\mu_o} \underline{z}_o \times \underline{k}_t \\ \\ \dfrac{k_o}{\omega\varepsilon_o \varepsilon_{zz}} \underline{z}_o \times \underline{k}_t & 0 \end{bmatrix} = W_{zt}^+ . \qquad \text{(A-2)}$$

Using (A-2), the product $\Psi_t^+(\varkappa_n) \cdot W_{tz} W_z$ in (A-1) can be written as

$$\Psi_t^+(\varkappa_n) \cdot W_{tz} W_z = \left[W_{zt} \cdot \Psi_t(\varkappa_n) \right]^+ . \qquad \text{(A-3)}$$

But $\Psi_t(\varkappa_n)$ represents the transverse electric and magnetic field polarization vectors of the plane wave propagating as $\exp\left[-jk_o(\xi x + \eta y + \varkappa_n z)\right]$. The z components $\Psi_z(\varkappa_n)$ of the polarization vectors of this plane wave are given in terms of the transverse components by (I-52). Thus, with the help of (A-3) and (I-52), it is seen that the bracketed term in (A-1) can be written as

$$\Psi_t^+(x_n) \cdot \begin{bmatrix} \underline{J}_{ot} \\ \underline{M}_{ot} \end{bmatrix} + \Psi_z^+(x_n) \begin{bmatrix} J_{oz} \\ M_{oz} \end{bmatrix} = \underline{\mathcal{C}}_n^* \cdot \underline{J}_o + \underline{\mathcal{H}}_n^* \cdot \underline{M}_o \qquad (A-4)$$

where $\underline{\mathcal{C}}_n$ and $\underline{\mathcal{H}}_n$ are the polarization vectors of the plane wave fields.

Consider now the normalizing constant M_n in (A-1), which is defined in (I-30). By direct expansion it is possible to show that for real x_n

$$M_n = 2 \, \text{Re} \left[(\underline{\mathcal{C}}_{nt} \times \underline{\mathcal{H}}_{nt}^*) \cdot \underline{z}_o \right] = 2 \, s_{nz} \qquad (A-5)$$

where s_{nz} is the z component of the real part $\underline{s}_n$ of the modal complex Poynting vector $\underline{\mathcal{C}}_n \times \underline{\mathcal{H}}_n^*$. Recognizing that e_n, as defined in (I-41), has the same sign as s_{nz}, it is seen that

$$M_n/e_n = 2 \, | \cos \theta_n | | \, \text{Re} \, (\underline{\mathcal{C}}_n \times \underline{\mathcal{H}}_n^*) | \qquad (A-6)$$

where θ_n is the angle between the positive z axis and $\underline{s}_n$. Finally, substituting (A-4) for the bracketed term in (A-1) and using (A-6), one obtains

$$A_n = \left(\frac{k_o}{2\pi} \right)^2 (\underline{\mathcal{C}}_n^* \cdot \underline{J}_o + \underline{\mathcal{H}}_n^* \cdot \underline{M}_o)/2 | \cos \theta_n | | \text{Re} \, (\underline{\mathcal{C}}_n \times \underline{\mathcal{H}}_n^*) | \qquad (A-7)$$

which directly exhibits the dependence of the dependence of the excitation coefficient A_n on the strength of the point source and the polarization vectors $\underline{\mathcal{C}}_n$ and $\underline{\mathcal{H}}_n$ of a propagating plane wave.

135

Appendix B

STEEPEST DESCENT EVALUATION OF THE
INTEGRAL OVER η

In order to asymptotically evaluate double integrals of the form given in (II-5) by the method outlined in Section B of Chapter II, it is essential to first evaluate

$$\int_{-\infty}^{\infty} \underline{F}(\xi,\eta) e^{-jk_0 P(\xi,\eta)} d\eta \qquad (B-1)$$

by the method of steepest descent. In performing the integration indicated in (B-1), ξ is assumed to be real and is held constant. Also, $\varkappa_m$ and $\varkappa_n$ are assumed to be continuous functions for ξ and η real so that $P(\xi,\eta)$ will be continuous.

Because the various wave numbers $\varkappa$ appearing in the factors of (II-2) and (II-4) are the roots of quartics, the complex η plane will consist of four Riemann sheets in the case of the direct field integrals (II-2) while for the scattered field integrals (II-4) it will consist of sixteen sheets (as argued in Section 2, the $\varkappa$'s are the only multivalued functions appearing in the integrands of (II-2) and (II-4)). The various Riemann sheets are connected at the branch points of the $\varkappa$'s and along the associated branch cuts. With these comments in mind, the path of integration for (B-1) is the real η axis on an appropriate Riemann sheet with suitable indentations into the complex η plane about the branch point and pole singularities of the integrand.

Since the Fourier integral representation for the fields was originally defined with the summation signs of (I-55), (I-56) and (I-57) inside the integration signs, the branch cuts are the same for all direct field integrals and for all scattered field integrals. In order to satisfy the radiation condition, the branch cuts originating at each real axis branch point of the $\varkappa$'s at which the wave number is real are taken such that on the indented portions of about the branch points of the integrations paths for the various

scattered and direct field integrals $-j\varkappa_n (z - z')$ in (II-2) and $-j\varkappa_m z$ or $j\varkappa_n z'$ in (II-4) has a negative real part. Finally, the branch cuts may not cross the real η axis since otherwise the continuity assumption made above would be violated. While the foregoing restrictions on the branch cuts are relevant to the steepest descent evaluation of (B-1), the ray-optical expressions for the far fields are formulated in such a way that the branch cuts need not be considered.

The asymptotic evaluation of (B-1) has been considered by many authors and only a brief discussion of the features of the evaluation pertinent to the present analysis is given here[11,22,40]. In particular, when $\underline{F}(\xi,\eta)$ and $P(\xi,\eta)$ are those of the integrands of (II-2) and (II-4), (B-1) represents the direct or scattered portions of the fields radiated by a phased line source along the x direction[4]. Appropriate to the present analysis, only the contributions to (B-1) arising from real, isolated saddle points, branch points and poles will be considered. In the phased line source problem, the contributions from these points correspond to direct and scattered rays, lateral rays and surface waves, respectively. In applying the steepest descent technique to the evaluation of (B-1), the original path of integration in the complex η plane is deformed into the steepest descent path, taking due account of any intercepted singularities.

1) Real, Isolated Saddle Point Contributions

The saddle points in the η integration (for fixed ξ) are the solutions of

$$P_2(\xi, \eta) \equiv \frac{\partial}{\partial \eta} P(\xi, \eta) = 0. \tag{B-2}$$

The real saddle points are the real solutions of (B-2) and the first-order contribution to (B-1) from these points is

$$\left(\int d\eta \right)_{\substack{\text{saddle} \\ \text{point}}} \sim \sqrt{\frac{2\pi}{k_o}} \sum_s \left\{ \frac{\underline{F}(\xi,\eta_s)}{\sqrt{|P_{22}(\xi,\eta_s)|}} e^{-jk_o P(\xi,\eta_s)} e^{-j\frac{\pi}{4} \operatorname{sgn} P_{22}(\xi,\eta_s)} \right\} \tag{B-3}$$

where the sum is taken over all real saddle points η_s. In (B-3),

$P_{22}(\xi,\eta) \equiv \dfrac{\partial^2}{\partial\eta^2} P(\xi,\eta)$ and the function $\operatorname{sgn} X = -1$ for $X < 0$, while for

$X > 0$, $\operatorname{sgn} X = 1$ and for $X = 0$, $\operatorname{sgn} X = 0$. Expression (B-3) is valid when the saddle points are isolated from each other and from the branch points and poles of the integrand of (B-1).

2) Real, Isolated Branch Point Contributions

When the integrand of (B-1) represents that of (II-2) or (II-4), the branch points in $\underline{F}(\xi,\eta)$ and $P(\xi,\eta)$, considered as functions of η, are those that occur in the solution of (I-24) for the single-valued functions $\varkappa_n(\xi,\eta)$. This is seen from the fact that the eigen or transverse polarization vectors of (I-23) can be written as polynomials in ξ, η and $\varkappa_n$ (any other normalizing factor in the mode vectors will cancel out among the factors in (II-2) and (II-4)). Hence, the z component of the polarization vectors given in (I-52) is a polynomial in ξ, η and $\varkappa_n$. Furthermore, the scattering coefficients of (I-46) and (I-52) and the excitation coefficient A_n of (I-54) are ratios of such polynomials and thus have only the branch points of the $\varkappa$'s.

Those branch points of the $\varkappa$'s at which the wave number complex or imaginary need not be considered since they are not branch points of the total Fourier field transforms as given in (I-55), (I-56) and (I-57). This is seen from the fact that at a branch point, two solutions of (I-24) for the $\varkappa$'s of the ε_1 medium are equal or two solutions of (I-24) for the $\varkappa$'s of the $\underset{\sim}{\varepsilon}_2$ medium are equal. If the two $\varkappa$'s that are equal at the branch point are complex or imaginary, they both correspond to upgoing or to downgoing waves, i.e., at the branch point $\varkappa_1^{\rightarrow} = \varkappa_2^{\rightarrow}$ or $\varkappa_1^{\leftarrow} = \varkappa_2^{\leftarrow}$ or $\varkappa_3^{\rightarrow} = \varkappa_4^{\rightarrow}$ or $\varkappa_3^{\leftarrow} = \varkappa_4^{\leftarrow}$. Thus, such a branch point connects two Riemann sheets on which $\varkappa$ is an upgoing or downgoing wave number. But (I-55), (I-56) and (I-57) are invariant under the interchange of $\overset{\rightarrow}{1}$ and $\overset{\rightarrow}{2}$, the interchange of $\overset{\leftarrow}{1}$ and $\overset{\leftarrow}{2}$, the interchange of $\overset{\rightarrow}{3}$ and $\overset{\rightarrow}{4}$ and the interchange of $\overset{\leftarrow}{3}$ and $\overset{\leftarrow}{4}$. Hence, the branch points at which the $\varkappa$'s are complex or imaginary do not appear in the total fourier field transforms. Any contribution to one of the integrals defined in (II-2) or (II-4) arising from

branch points of one of the κ's at which κ is complex or imaginary will be canceled by a similar contribution to another of the integrals[7]. If $P(\xi, \eta)$ is complex at some branch point, the contribution from this branch point will be exponentially small so that only the branch points of the κ's on the real axis and at which $P(\xi, \eta)$ is real need be considered. Such branch points will be called real. Note, branch points at which $\text{Re}[-jP(\xi, \eta)]$ is positive cannot be intercepted in the deformation of the original integration path since they lie in hill regions.

The real branch points of κ_m and κ_n appearing in $P(\xi, \eta)$ are not intercepted in deforming the original integration path into the steepest descent path since the radiation condition requires that the original integration path be indented about them in such a way that $-j\kappa_n(z-z')$ in (II-2) and $-j\kappa_m z$ or $j\kappa_n z'$ in (II-4) have negative real parts. Furthermore $d\kappa/d\eta \rightarrow \infty$ at a branch point of κ so that $-jP(\xi, \eta)$ will have a negative real part on the indented portion of the integration path about the branch points of κ_m and κ_n even if the real part of $-j\eta y$ is positive there. Because of this, the indented portions of the original integration path will lie in the valley regions to start with, and hence the real branch points of $P(\xi, \eta)$ will not be intercepted. When the integrand of (B-1) represents that of the direct field integrals (II-2), no branch point contributions will arise since $\underline{F}(\xi, \eta)$ contains only the branch points of that κ_n appearing in $P(\xi, \eta)$. However, Γ_{mn} in the scattered field integrals (II-4) depdends on all the κ's so that these integrals may have branch point contributions.

For those real branch points intercepted in the deformation of the original integration path, the branch cut may be chosen to lie along the steepest descent path through the branch point. With this choice of the branch cut, the principal contribution to the branch cut integral will come from the vicinity of the real branch point. In the vicinity of an isolated first-order, real branch point $\eta = \eta_b$ of $\underline{F}(\xi, \eta)$, the dependence of $\underline{F}(\xi, \eta)$ on η can be exhibited as $F(\xi, \eta) = \overline{\underline{F}}(\xi, \eta, \sqrt{\eta - \eta_b})$ where $\partial \overline{\underline{F}}/\partial \eta$ is regular at the branch point. Assuming $\underline{F}(\xi, \eta)$ itself to be bounded at branch points that are not also branch points of $P(\xi, \eta)$, to first order in

the vicinity of η_b

$$\underline{F}(\xi,\eta) \approx \underline{F}(\xi,\eta_b) + \frac{\partial \underline{F}}{\partial \eta}(\eta-\eta_b) + \frac{\partial \underline{F}}{\partial \sqrt{\eta-\eta_b}}\sqrt{\eta-\eta_b} \qquad (B-4)$$

with only the last term contributing to the branch cut integral. In the definition of $\underline{F}$ and in (B-4), $\sqrt{\eta-\eta_b}$ is assumed positive for $\eta-\eta_b$ positive real and the branch cut for this root is taken along the cut originally used in defining $\underline{F}(\xi,\eta)$.

Assuming that the branch point η_b is not a branch point of $P(\xi,\eta)$ and that no saddle points are near the branch point, $P(\xi,\eta)$ may be approximated to first order in the vicinity of η_b as

$$P(\xi,\eta) \approx P(\xi,\eta_b) + P_2(\xi,\eta_b)(\eta-\eta_b) \qquad (B-5)$$

with $P_2(\xi,\eta_b) \neq 0$. Because the principal contribution to a branch cut integral comes from the vicinity of the real branch point, the approximate expressions (B-4) and (B-5) for $\underline{F}(\xi,\eta)$ and $P(\xi,\eta)$ may be used in the integration.

If $P_2(\xi,\eta_b)$ is positive (negative), using (B-5) in (B-1) it is seen that the valley region in the vicinity of η_b lies below (above) the real η axis. Thus, using the approximations described in the previous paragraphs, the branch cut integral becomes

$$2\frac{\partial \underline{F}}{\partial \sqrt{\eta-\eta_b}}e^{-jk_oP}\int_{\eta_b}^{\eta_b-j\infty \, \mathrm{sgn}\, P_2}\sqrt{\eta-\eta_b}\,e^{-jk_oP_2(\eta-\eta_b)}d\eta \qquad (B-6)$$

where $\dfrac{\partial \underline{F}}{\partial \sqrt{\eta-\eta_b}}$, $P(\xi,\eta)$ and $P_2(\xi,\eta)$ are evaluated at $\eta=\eta_b$. The path of integration in (B-6) is along the right-hand side of the branch cut of $\sqrt{\eta-\eta_b}$, which is taken here as lying along $\mathrm{Re}\,\eta=\eta_b$. The integral in (B-6) can easily be evaluated using the substitution $s = jk_o(\eta-\eta_b)P_2(\xi,\eta_b)$ where s is positive real. With this substitution and recalling the

definition of $\sqrt{\eta - \eta_b}$ in the previous paragraph,

$$\sqrt{\eta - \eta_b} = \sqrt{s/k_o |P_2|} \, \exp\left(-j\frac{\pi}{4}\, \text{sgn}\, P_2\right).$$

Performing the integration indicated in (B-6) and summing over the various real branch points of $\underline{F}(\xi,\eta)$ that are not also branch points of $P(\xi,\eta)$, the real branch point contributions to (B-1) are given to $O(1/k_o^{3/2})$ by

$$\left(\int d\eta\right)_{\substack{\text{branch}\\ \text{point}}} \sim \frac{\sqrt{\pi}}{k_o^{3/2}} \sum_b \left\{ U\left[\pm(\eta_s - \eta_b)\right] \frac{\partial \overline{F}}{\partial\sqrt{\eta - \eta_b}} \frac{e^{-jk_o P}}{|P_2|^{3/2}} e^{-j\frac{3\pi}{4}\,\text{sgn}\,P_2} \right\}_{\eta = \eta_b}.$$

$$(B-7)$$

Expression (B-7) is valid when the branch points are isolated from each other and from the saddle points. The Heaviside unit step function $U\left[\pm(\eta_s - \eta_b)\right]$ is included in (B-7) to indicate that a particular branch point will be intercepted during the deformation of the integration path only for certain values of η_s (the value of η_s depends on ξ and on the coordinates of the observation point). The choice of the plus or minus sign can be determined in any particular problem. Strictly speaking, the single step function is not sufficient to describe when a particular branch point is intercepted if (B-1) has several real saddle points. However, for convenience the single step function of (B-7) is retained here but is replaced in Section E of Chapter II by a ray-optical expression that is valid no matter how many saddle points occur in (B-1).

3) Surface Wave Pole Contributions

Net pole contributions to the total radiated fields can occur only in the scattered fields. These pole contributions are associated with those zeros of the common denominator $d(\xi,\eta)$ of the scattering coefficients at which the Fourier transform of the total scattered field $\underline{E}_\Gamma$ is singular. To within the factor $e^{-jk_o(\xi x + \eta y)}$, the Fourier transform of $\underline{E}_\Gamma$ is the integrand found by substituting (II-4) into (II-3) and interchanging the order of summation and integration. The integrands of the individual integrals in

(II-2) and (II-4) can also have pole singularities in the η plane at those branch points of the κ's at which ι is complex or imaginary. However, any contribution from such branch points to one of the integrals (II-2) or (II-4) -- except when this point is also a pole of the transform of $\underline{E}_\Gamma$ -- will be canceled by a similar contribution to another integral. Thus, only contributions from those poles of the integrands of the integrals of (II-4) that are poles of the transform of $\underline{E}_\Gamma$ need be found.

The poles giving a net contribution to $\underline{E}_\Gamma$ that are of interest here are those poles, called surface wave poles, lying on the real η axis on that Riemann sheet on which the original integration path is defined since only these poles give rise to surface waves propagating along the interface.[#] In order to satisfy the radiation condition for $|y| \to \infty$, the surface wave poles intercepted during the deformation of the integration path must be such that the y component of the total modal surface wave power, i.e., $\int_{-\infty}^{\infty} \underline{Y}_0 \cdot \underline{s}\,dz$ where $\underline{s}$ is the real part of the complex Poynting vector associated with the modal surface wave fields for (ξ, η) appropriate to the pole, has the same sign as y. The above requirement is satisfied if the original integration path is deformed above (below) those surface wave poles contributing for y positive (negative). That these indentations are correct is seen from the fact that for y positive (negative), the integration in (B-1) could be carried out by deforming the integration path into the lower (upper) half of the η plane. With the foregoing indentations about the surface wave poles, it is seen that the integration about the poles contributing for y positive (negative) is to be taken in the clockwise (counter-clockwise) sense about the poles.

For reasons that will be discussed at appropriate points in this analysis, the surface wave contribution will be considered only for observation points such that $\sqrt{x^2 + y^2} >> |z|$, $|z'|$. Since the choice of the

---

[#] In limited regions of space poles corresponding to other wave types, e.g., leaky waves[41,42], may be intercepted. Such pole contributions are not considered here.

(x, y) coordinates is arbitrary, under the above restriction the (x, y) coordinates can always be chosen such that $|y| >> |z|$, $|z'|$, which insures that all surface wave poles appropriate to the sign of y are intercepted during the deformation of the integration path. To see that all appropriate surface wave poles will be intercepted for $|y| >> |z|$, $|z'|$, recognize that for this case the saddle points will coaless with certain branch points of κ_m and κ_n appearing in $P(\xi, \eta)$. Thus, if the branch curves associated with these branch points are taken along the steepest descent paths through the branch points, the steepest descent path for y positive (negative) is the same as obtained by deforming the original integration path in the lower (upper) half-plane, in which case all appropriate surface wave poles are intercepted.

Writing $\underline{F}(\xi, \eta)$ as

$$\underline{F}(\xi, \eta) = \underline{f}(\xi, \eta) / d(\xi, \eta) \tag{B-8}$$

where the poles of $\underline{F}(\xi, \eta)$ are given by the zeros of $d(\xi, \eta)$, for $|y| >> |z|$, $|z'|$ so that all appropriate surface wave poles are intercepted for $y \gtrless 0$, the surface wave pole contributions to (B-1) are

$$\left(\int d\eta \right)_{pole} = -2\pi j \; sgny \sum_{p} \left\{ \frac{\underline{f}(\xi, \eta)}{d_2(\xi, \eta)} e^{-jk_o P(\xi, \eta)} \right\}_{\eta = \eta_p} \tag{B-9}$$

where the sum is taken over the contributing surface wave poles and $d_2(\xi, \eta) = \frac{\partial}{\partial \eta} d(\xi, \eta)$. If $|y|$ is not taken sufficiently large, some or all of the surface wave poles will not be intercepted in the deformation of the original integration path. This reflects the fact that in such a case, exponentially small errors in the saddle point evaluation (due to the finite radius of convergence for the series expansion of $\underline{F}(\xi, \eta)$ about the saddle point) are larger than the pole contribution.

Appendix C

SCATTERED RAY TANGENCIES TO A CAUSTIC
AND EXPRESSIONS FOR δ

In Section 1 of this appendix expression (II-14) for δ is established and is then used to derive (II-20), which applies when $P(\xi, \eta)$ is the phase function found in the direct ray integrals (II-2). The properties of the roots L_{m1} and L_{m2} of (II-24) are considered in Section 2. First, the conditions under which the roots are real are found. For those conditions under which the roots are certain to be real, the number of positive roots is determined, i.e., the number of scattered ray tangencies to an actual caustic. These results are presented in Table C-1, which also contains the value of δ_{mn} along the scattered ray. In Section 3 it is shown that the change in δ_{mn} along a scattered ray, as a point of tangency to a caustic is crossed, can be found from the ray direction, the normal to the caustic and the shape of the mth branch of the dispersion surface.

1) Verification of (II-14) and (II-20)

In establishing (II-14), recognize from (II-13) that

$$\delta = (\text{sgn } P_{22}) \left[1 + \text{sgn} (P_{11} P_{22} - P_{12}^2) \right] . \qquad (C-1)$$

The second derivatives of the phase $P(\xi, \eta)$ in the generic integral (II-5) contain only z, z' and the second derivatives of $\varkappa_m$ and $\varkappa_n$. Since $\varkappa_m$ and $\varkappa_n$ are point functions, P_{11}, P_{22} and P_{12} are the elements of a symmetric second-rank tensor. Thus if the (u, v) coordinate system, rotated from the (ξ, η) system by an angle ϕ, is such that at the stationary point in question $P_{uv} = 0$, where the u and v subscripts indicate partial differentiation, then

$$P_{11} P_{22} - P_{12}^2 = P_{uu} P_{vv} \qquad (C-2-a)$$

and

$$P_{22} = \sin^2 \varphi \, P_{uu} + \cos^2 \varphi \, P_{vv} . \qquad (C-2-b)$$

Therefore, if both P_{uu} and P_{vv} are positive (negative), then $P_{11}P_{22} - P_{12}^2 > 0$ and $P_{22} > 0$ ($P_{22} < 0$) so that from (C-1) one finds that $\delta = 2$ ($\delta = -2$). If P_{uu} and P_{vv} are of opposite sign, $P_{11}P_{22} - P_{12}^2 < 0$ and from (C-1), $\delta = 0$. These cases can be summarized in the form

$$\delta = \operatorname{sgn} P_{uu} + \operatorname{sgn} P_{vv}, \qquad (C-3)$$

as was to be shown.

In order to show that for the direct rays

$$\delta = \operatorname{sgn} K_{n1} + \operatorname{sgn} K_{n2} , \qquad (C-4)$$

as stated in (II-20), where K_{n1} and K_{n2} are the principal curvatures of the nth branch of the dispersion surface, recall that in the (u, v) coordinate system $P_{uu} = (z - z') \dfrac{\partial^2 \varkappa_n}{\partial u^2}$, $P_{vv} = (z - z') \dfrac{\partial^2 \varkappa_n}{\partial v^2}$ and

$0 = P_{uv} = (z - z') \dfrac{\partial^2 \varkappa_n}{\partial u \partial v}$. The Gaussian curvature of the nth branch of the dispersion surface is the product of the principal curvatures and can be written as[25]

$$G_n = K_{n1} \, K_{n2} = \left(-\frac{\partial^2 \varkappa_n}{\partial u^2} \, \frac{\partial^2 \varkappa_n}{\partial v^2} \right) \nu_{nz}^4 \qquad (C-5)$$

while twice the mean curvature is the sum of the principal curvatures and can be written[25]

$$2H_n = K_{n1} + K_{n2} = \left\{ \left[1 + \left(\frac{\partial \varkappa_n}{\partial v} \right)^2 \right] \frac{\partial^2 \varkappa_n}{\partial u^2} + \left[1 + \left(\frac{\partial \varkappa_n}{\partial u} \right)^2 \right] \frac{\partial^2 \varkappa_n}{\partial v^2} \right\} \nu_{nz}^3 . \qquad (C-6)$$

Here, $\nu_{nz} = \underline{z}_o \cdot \underline{\nu}_n$ and the principal curvatures are positive or negative as the corresponding centers of curvature lie on the same or opposite side of the surface as the normal $\underline{\nu}_n$. Since the sense of $\underline{\nu}_n$ is taken to be the same as that of the power flow of the corresponding plane wave,

$(z - z')$ and ν_{nz} have the same sign. Thus P_{uu} and P_{vv} are both positive (negative) when K_{m1} and K_{n2} are both positive (negative). Also P_{uu} and P_{vv} are of opposite sign if K_{n1} and K_{n2} are, thus verifying (C-4) and (II-20).

2) The Nature of the Roots L_{m1} and L_{m2}

In studying the roots L_{m1} and L_{m2} of (II-24) for the rays scattered from a planar interface, those combinations of signs of the principal curvatures of the mth and n^{th} branches of the dispersion surfaces for which the roots are real and those combinations for which the roots can be complex are first found. Since the Hessian $P_{11} P_{22} - P_{12}^2$ is an invariant, it can be evaluated in the (σ, τ) coordinate system defined by the requirement that $\dfrac{\partial^2 \varkappa_m}{\partial \sigma \, \partial \tau} = 0$ at the stationary point in question. With this choice of the (σ, τ) system

$$P_{11} P_{22} - P_{12}^2 = L_m^2 \nu_{mz}^2 \frac{\partial^2 \varkappa_m}{\partial \sigma^2} \frac{\partial^2 \varkappa_m}{\partial \tau^2} + L_m \nu_{mz} |z'| \left[\frac{\partial^2 \varkappa_m}{\partial \sigma^2} \frac{\partial^2 \varkappa_n}{\partial \tau^2} + \frac{\partial^2 \varkappa_m}{\partial \tau^2} \frac{\partial^2 \varkappa_n}{\partial \sigma^2} \right]$$

$$+ |z'|^2 \left[\frac{\partial^2 \varkappa_n}{\partial \sigma^2} \frac{\partial^2 \varkappa_n}{\partial \tau^2} - \left(\frac{\partial^2 \varkappa_n}{\partial \sigma \, \partial \tau} \right)^2 \right] . \quad \text{(C-7)}$$

Consider now the (s, t) coordinate system defined by the requirement that $\dfrac{\partial^2 \varkappa_n}{\partial s \, \partial t} = 0$ at the stationary point. If φ is the angle between the s and σ and if $\alpha = \cos \varphi$, then

$$\frac{\partial^2 \varkappa_n}{\partial \sigma^2} = \alpha^2 \frac{\partial^2 \varkappa_n}{\partial s^2} + (1 - \alpha^2) \frac{\partial^2 \varkappa_n}{\partial t^2}$$

$$\left. \begin{array}{c} \\ \\ \\ \\ \end{array} \right\} \quad \text{(C-8)}$$

$$\frac{\partial^2 \varkappa_n}{\partial \tau^t} = (1 - \alpha^2) \frac{\partial^2 \varkappa_n}{\partial s^2} + \alpha^2 \frac{\partial^2 \varkappa_n}{\partial t^2}$$

and

$$\frac{\partial^2 \varkappa_n}{\partial \sigma^2} \frac{\partial^2 \varkappa_n}{\partial \tau^2} - \frac{\partial^2 \varkappa_n}{\partial \sigma \partial \tau}^2 = \frac{\partial^2 \varkappa_n}{\partial s^2} \frac{\partial^2 \varkappa_n}{\partial t^2} . \quad \text{(C-9)}$$

With (C-8) and (C-9), (C-7) can be rewritten

$$P_{11}P_{22} - P_{12}^2 = L_m^2 \nu_{mz}^2 \frac{\partial^2 \varkappa_m}{\partial \sigma^2} \frac{\partial^2 \varkappa_m}{\partial \tau^2} + |z'|^2 \frac{\partial^2 \varkappa_n}{\partial s^2} \frac{\partial^2 \varkappa_n}{\partial t^2} \qquad (C-10)$$

$$+ L_m |z'| \left\{ \nu_{mz} \frac{\partial^2 \varkappa_m}{\partial \sigma^2} \left[(1-\alpha^2) \frac{\partial^2 \varkappa_n}{\partial t^2} + \alpha^2 \frac{\partial^2 \varkappa_n}{\partial t^2} \right] + \nu_{mz} \frac{\partial^2 \varkappa_m}{\partial \tau^2} \left[\alpha^2 \frac{\partial^2 \varkappa_n}{\partial s^2} + (1-\alpha^2) \frac{\partial^2 \varkappa_n}{\partial t^2} \right] \right\},$$

which will have real roots L_{m1} and L_{m2} if its discriminant is positive. The hybrid notation in (C-10) is used since the signs of the second derivatives of $\varkappa_m$ and $\varkappa_n$ can easily be related to the signs of the corresponding principal curvatures only when the mixed second partial derivatives are zero. Defining $q_m = \dfrac{\partial^2 \varkappa_m}{\partial \sigma^2} \bigg/ \dfrac{\partial^2 \varkappa_m}{\partial \tau^2}$ and $q_n = \dfrac{\partial^2 \varkappa_n}{\partial s^2} \bigg/ \dfrac{\partial^2 \varkappa_n}{\partial t^2}$, the discriminant of (C-10) will be positive if

$$Q \equiv \alpha^4 (q_m - 1)^2 (q_n - 1)^2 - 2\alpha^2 (q_m - 1)(q_n - 1)(q_m q_n + 1) + (q_m q_n - 1)^2 \quad (C-11)$$

is positive.

At any particular stationary point, q_m, q_n and α are known so that Q is known. However, for the present study it is more convenient to consider Q as a quadratic in α^2 with q_m and q_n as parameters and to investigate the sign of Q in the interval $0 \leq \alpha^2 \leq 1$ corresponding to real angles φ. At $\alpha^2 = 0$

$$Q = (q_m q_n - 1)^2 \geq 0 \qquad (C-12)$$

while at $\alpha^2 = 1$

$$Q = (q_m - q_n)^2 \geq 0. \qquad (C-13)$$

As a function of α^2, Q has a minimum value of

$$Q_{min} = -4 q_m q_n \qquad (C-14)$$

occurring at

$$\alpha^2 = \frac{q_m q_n + 1}{(q_m - 1)(q_n - 1)} \ . \tag{C-15}$$

From (C-5), when represented in the (σ, τ) coordinate system for which $\dfrac{\partial^2 \kappa_m}{\partial \sigma \partial \tau} = 0$, it is seen that G_m and q_m are of the same sign. Similarly, G_n and q_n are of the same sign. Thus, using these relations and (C-14) and (C-15) and the fact that $Q \geq 0$ at $\alpha^2 = 0, 1$, the sign of Q in the interval $0 \leq \alpha^2 \leq 1$ can be determined for the three separate cases that must be considered.

Case I: G_m and G_n positive

In this case q_m and q_n are both positive and from (C-15) the minimum value of Q occurs outside the interval $0 \leq \alpha^2 \leq 1$. Since $Q \geq 0$ at $\alpha^2 = 0, 1$ the value of Q in the interval $0 \leq \alpha^2 \leq 1$ is always greater than or equal to zero and hence only for real values of L_m will $P_{11}P_{22} - P_{12}^2 = 0$.

Case II: G_m and G_n of opposite sign

In this case q_m and q_n are of opposite sign so that the minimum value of Q, as given in (-14), and hence Q for all α^2, is greater than or equal to zero. Again, $P_{11}P_{22} - P_{12}^2 = 0$ only for real values of L_m.

Case III: G_m and G_n negative

In this case q_m and q_n are both negative and the minimum value of Q, which is now negative, occurs within the interval $0 \leq \alpha^2 \leq 1$. Thus, for this combination of signs of the Gaussian curvatures, and for values of φ such that $\cos^2\varphi$ lies between the roots of (C-11), the values of L_m for which $P_{11}P_{22} - P_{12}^2 = 0$ will be complex and consequently (II-24) will have complex roots L_{m1} and L_{m2}. For real φ and when $\cos^2\varphi$ is not between the roots of (C-11), Q is the positive and $P_{11}P_{22} - P_{12}^2$ will vanish for real values of L_m.

In summary, only for that combination of signs of the principal curvatures of the mth and n^{th} branches of the dispersion surfaces indicated in the last case of Table C-1 can the roots L_{m1} and L_{m2} be complex.

For those combinations of signs of the Gaussian curvatures for

which (II-24) is certain to have real roots L_{m1} and L_{m2}, the number of positive roots, i.e., the number of times a ray scattered from a planar interface is tangent to an actual caustic, can now be determined. The results are summarized in Table C-1. From this table it is seen that a simple inspection of the dispersion surfaces for the signs of the principal curvatures is sufficient to determine, in all but one case, the number of times a scattered ray is tangent to a caustic. For the case when K_{n1} and K_{n2} are of opposite sign and K_{m1} and K_{m2} are also of opposite sign, it is not longer possible to predict the nature of L_{m1} and L_{m2} from a simple inspection of the mth and n^{th} branches of the dispersion surfaces since the nature of the roots depends not only on the shape of the two branches of the dispersion surfaces but also on their orientation, as was shown above.

To derive the number of tangencies of the scattered ray to an actual caustic, as given in Table C-1, it is necessary to consider the signs of the coefficients in (C-10) for the various cases appearing in Table C-1. To facilitate these considerations, observe from (C-5) and (C-6), when represented in the (σ, τ) coordinate system for which $\dfrac{\partial^2 \kappa_m}{\partial \sigma \partial \tau} = 0$, that $\nu_{mz} \dfrac{\partial^2 \kappa_m}{\partial \sigma^2}$ and $\nu_{mz} \dfrac{\partial^2 \kappa_m}{\partial \tau^2}$ will both be positive (negative) if K_{m1} and K_{m2} are both positive (negative) and will be of opposite sign if K_{m1} and K_{m2} are. Similarly, since for the scattered rays $\nu_{nz} > 0$, $\dfrac{\partial^2 \kappa_n}{\partial s^2}$ and $\dfrac{\partial^2 \kappa_n}{\partial t^2}$ will both be positive (negative) if K_{n1} and K_{n2} are both positive (negative) and will be of opposite sign if K_{m1} and K_{m2} are.

<u>Case I:</u>　K_{m1}, K_{m2}, K_{n1}, K_{n2} positive

For $|\alpha| \leq 1$, i.e., for real angles φ, all the coefficients in (C-10) are positive so that (C-10) will have no positive roots.

<u>Case II:</u>　K_{m1}, K_{m2}, K_{n1}, K_{n2} negative

Again, for $|\alpha| \leq 1$ the coefficients in (C-10) are positive and hence (C-10) will have no positive roots.

Table C-1

The Number of Tangencies to an Actual Caustic of a Point
Source Ray Scattered by a Planar Interface and the Value
of δ_{mn} Along the Scattered Portion of the Ray

Signs of K_{m1} and K_{m2}	Signs of K_{n1} and K_{n2}	Number of Tangencies to Caustic	Value of δ_{mn} (L_{m2} assumed to be greater than L_m)
both positive	both positive	0	2
both negative	both negative	0	-2
both positive (negative)	both negative (positive)	2	$2 \mathrm{sgn} K_{n1}, \quad 0 \leq L_m < L_{m1}$ $0, \quad L_{m1} < L_m < L_{m2}$ $2 \mathrm{sgn} K_{m1}, \quad L_m > L_{m2}$
both positive or negative	one positive and one negative	1	$0, \quad 0 \leq L_m < L_{m2}$ $2 \mathrm{sgn} K_{m1}, \quad L_m > L_{m2}$
one positive and one negative	both positive or negative	1	$2 \mathrm{sgn} K_{n1}, \quad 0 \leq L_m < L_{m2}$ $0, \quad L_m > L_{m2}$
one positive and one negative	one positive and one negative	solve (C-10) for roots	Use (II-14)

Case III: K_{m1}, K_{m2} positive (negative) and K_{n1}, K_{n2} negative (positive)

The coefficient of L_m^2 in (C-10) and the constant term are positive but the coefficient of L_m is negative so that both roots of (C-10) are positive.

Case IV: K_{m1} and K_{m2} of the same sign and K_{n1} and K_{n2} of opposite sign

In this case the coefficient of L_m^2 in (C-10) is positive while the constant term is negative and hence there will be one positive and one negative root of (C-10) independent of the sign of the coefficient of L_m.

Case V: K_{m1} and K_{m2} of opposite sign and K_{n1} and K_{n2} of the same sign

Now the coefficient of L_m^2 is negative while the constant term in (C-10) is positive and hence (C-10) will have one positive and one negative root.

The value of δ_{mn} along the rays scattered from a planar interface is displayed in Table C-1 for all but the last combination of signs of the principal curvatures of the mth and n^{th} branches of the dispersion surfaces under the assumption that the roots of (C-10) are ordered such that $L_{m1} < L_{m2}$. The evaluation of δ_{mn} is based on the following properties: a) it can change value only at the tangencies to a caustic; b) it can take on only the values ± 2 or 0; c) for $L_m \to \infty$, $\delta_{mn} = \text{sgn}K_{m1} + \text{sgn}K_{m2}$; for $L_m = 0$, $\delta_{mn} = \text{sgn}K_{n1} + \text{sgn}K_{n2}$. These properties have been discussed in Section C of Chapter II and are easily seen to lead to Table C-1.

When K_{m1} and K_{m2}, as well as K_{n1} and K_{n2} are of opposite sign, $\delta_{mn} = 0$ if the scattered ray is never tangent to an actual caustic surface, i.e., when L_{m1} and L_{m2} are negative real or complex. If the scattered ray is tangent to a caustic, it will have two points of tangency and $\delta_{mn} = 0$ between the interface and the first point of tangency as well as beyond the second point of tangency. Between the two points of tangency, δ_{mn} is either +2 or -2 and is most easily determined from (II-14).

3) Determination of the Change in δ_{mn} When the Normal to the
    Caustic Is Known

It will now be shown that the change in δ_{mn}, as the ray tangency to a caustic is crossed, is $2\text{sgn}C_m$ where C_m is the curvature at the point $\underline{k}_m$ of the curved formed by the intersection of the mth branch of the

dispersion surface and the plane parallel to $\underline{v}_m$ and to the normal $\underline{n}$ to the caustic surface at the point of tangency. The point $\underline{k}_m$ in $\underline{k}$ space is determined by the wave numbers $(\xi, \eta, \varkappa_m)$ of the scattered ray. The virtue of this formulation for the change in δ_{mn} is that it depends only on the caustic surface and the dispersion surface of the scattered ray and is valid irrespective of how the caustic is produced, e.g., this formulation holds for the rays scattered at a curved interface, as is discussed in Section D of Chapter II.

At the point of tangency of the scattered ray to the caustic either P_{uu} or P_{vv} is zero. For definiteness, assume that $P_{vv} = 0$ at the tangency point in question. The change in $\operatorname{sgn} P_{vv}$ across the tangency point, as one proceeds in the direction of $\underline{v}_m$ along the ray, is simply equal to $2\operatorname{sgn}(v_{mz} \dfrac{dP_{vv}}{dz})$ evaluated at the tangency point.[#] Thus the change $\Delta\delta_{mn}$ in the value of δ_{mn} across the tangency point is

$\Delta\delta_{mn} = 2\operatorname{sgn}\left[v_{mz} \dfrac{d}{dz} P_{vv}(z_1)\right]$ where z_1 is the value of z at the tangency point. Since the (ξ, η) coordinate system is arbitrary, let it be such that the (u, v) coordinate system coincides with it for $z = z_1$. Note that the (u, v) coordinate system will vary along the ray if the coordinate systems in which the mixed second-partial derivatives of $\varkappa_m$ and $\varkappa_n$ vanish are different. Using the fact that P_{vv} is eigenvalue of the symmetric matrix whose elements are P_{11}, P_{22} and P_{12}, it is easily

established that $\dfrac{d}{dz} P_{vv}(z_1) = \dfrac{\partial^2 \varkappa_m}{\partial \eta^2}$ so that

$$\Delta\delta_{mn} = 2\operatorname{sgn}\left(v_{mz} \frac{\partial^2 \varkappa_m}{\partial \eta^2}\right). \tag{C-16}$$

The curvature $C_{\xi m}$ of the plane curve formed by the intersection of the the mth branch of the dispersion surface with the constant ξ plane

---

[#] It is assumed that $dP_{vv}/dz \neq 0$ since otherwise the tangency point would be a focus.

passing through the point $\underline{k}_m$ can be put into the form

$$C_{\xi m} = \frac{\partial^2 \varkappa_m}{\partial \eta^2} \, \nu_{mz}^3 / (\nu_{my}^2 + \nu_{mz}^2)^{3/2} \tag{C-17}$$

when the sense of the normal to the plane curve is assumed to be that of the projection of $\underline{\nu}_m$ into the constant ξ plane and the usual definition of the sign of the curvature holds. Thus, from (C-16) and (C-17) it is seen that

$$\Delta \delta_{mn} = 2 \, \text{sgn} \, C_{\xi m} \, . \tag{C-18}$$

In order to show that $\text{sgn} \, C_{\xi m} = \text{sgn} C_m$, with C_m as previously defined, it is first shown that the normal $\underline{n}$ to the caustic at the tangency point has no component along $\underline{x}_o$. The stationary point condition $P_1 = P_2 = 0$ and the caustic condition $P_{11} P_{22} - P_{12}^2 = 0$ may be viewed as giving points on the caustic surface in parametric form, where the wave numbers ξ and η are the parameters. Using this parametric representation of the caustic, it is possible to show that the normal $\underline{n}$ is in the direction

$$\underline{x}_o \left(P_{22} \frac{\partial z}{\partial \xi} - P_{12} \frac{\partial z}{\partial \eta} \right) + \underline{y}_o \left(P_{11} \frac{\partial z}{\partial \eta} - P_{12} \frac{\partial z}{\partial \xi} \right)$$

$$+ \underline{z}_o \left[P_{11} \frac{\partial \varkappa_m}{\partial \eta} \frac{\partial z}{\partial \eta} + P_{22} \frac{\partial \varkappa_m}{\partial \xi} \frac{\partial z}{\partial \xi} - P_{12} \left(\frac{\partial \varkappa_m}{\partial \xi} \frac{\partial z}{\partial \eta} + \frac{\partial \varkappa_m}{\partial \eta} \frac{\partial z}{\partial \xi} \right) \right] \tag{C-19}$$

with $z(\xi, \eta)$ as found from the caustic conditions $P_{11} P_{22} - P_{12}^2 = 0$. At $z = z_1$, the (ξ, η) and (u, v) coordinates coincide so that $P_{22} = P_{vv} = 0$ and $P_{12} = P_{uv} = 0$ and from (C-19) it is seen that the $\underline{x}_o$ component of $\underline{n}$ is zero. Thus, $\underline{n}$ is parallel to the constant ξ plane passing through the point $\underline{k}_m$, and hence a line parallel to $\underline{n}$ and passing through the point $\underline{k}_m$ lies in this plane. This line also lies in the plane normal to $\underline{\nu}_m \times \underline{n}$ and passing through $\underline{k}_m$ and is therefore the intersection of the constant ξ plane and the plane normal to $\underline{\nu}_m \times \underline{n}$. Furthermore, since $\underline{n}$ is perpendicular to $\underline{\nu}_m$ ($\underline{n}$ is normal to the caustic and $\underline{\nu}_m$ is tangent to it), the line of intersection of the two planes is tangent to the mth branch

of the dispersion surface. Because of this $C_{\xi m} = \cos \Psi \, C_m$ where Ψ is the angle between $\underline{\nu}_m$ and its projection into the constant ξ plane. Since $\Psi < 90^\circ$, $\operatorname{sgn} C_{\xi m} = \operatorname{sgn} C_m$ and hence (C-18) can be written

$$\wedge \delta_{mn} = 2 \operatorname{sgn} C_m \qquad \text{(C-20)}$$

While (C-20) is difficult to apply in general, it is quite easily used when the principal curvatures of the mth branch of the dispersion surfaces have the same sign. In this case, the sign of C_m is simply that of the principal curvatures, e.g., in isotropic media C_m is negative.

Appendix D

DIVERGENCE COEFFICIENT FOR POINT-SOURCE RAYS
SCATTERED AT A CURVED INTERFACE

In this appendix the flux tube divergence factor for rays scattered from a gently curved interface between two lossless, anisotropic media is derived. The method used here requires a knowledge of the point of intersection of the scattered rays with a constant z plane in terms of the incident ray wave numbers. The divergence factor is then expressed in terms of the Jacobian of this transformation. It has been verified that the result derived here reduces properly: a) when the interface is planar; b) when the media are isotropic;[43,44] c) for the transmitted rays when the two media are identical.

The steps used in calculating the divergence factor are first outlined and then the complete algebraic steps necessary for this calculation are given. For convenience and clarity, quantities related to the incident rays and quantities related to the scattered rays are indicated by the superscripts i and s, respectively, rather than the subscripts n and m used elsewhere.

1) Outline of Procedure

Step 1: Assume that a ray from the source is incident on the interface $z = f(x, y)$ at the point $[x^o, y^o, f(x^o, y^o)]$ -- see Fig. D-1. This ray is defined by its wave numbers $[\xi^i, \eta^i, \varkappa^i, (\xi^i, \eta^i)]$ where $\varkappa^i(\xi^i, \eta^i)$ is one of the real solutions of the dispersion relation (I-24). Since the ray travels in the direction of the normal $\underline{\nu}^i$ to the dispersion surface, the x and y coordinates of the point of incidence are given by the solution of

$$x^o + \left[f(x^o, y^o) - z' \right] \varkappa_1^i (\xi^i, \eta^i) = y^o + \left[f(x^o, y^o) - z' \right] \varkappa_2^i (\xi^i, \eta^i) = 0 \quad (D-1)$$

where the 1 and 2 subscripts refer to the partial derivatives of $\varkappa^i(\xi, \eta)$.

Step 2: Knowing the normal $\underline{n}_o$ to the interface at the point of incidence, the scattered ray wave numbers can be found from Snell's
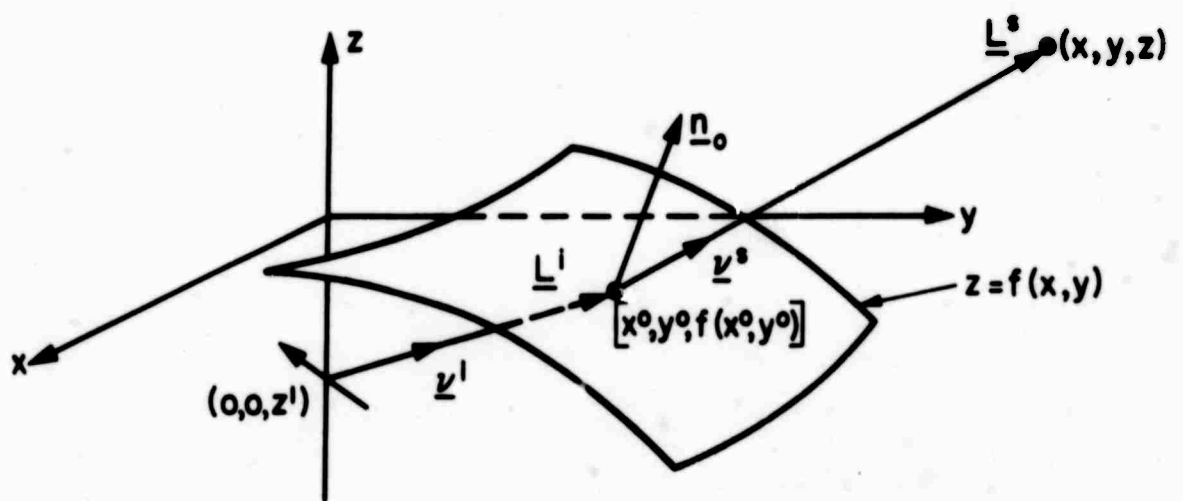
Fig. D-1   Ray scattering by a curved interface

law $\underline{n}_o \times (\underline{k}^s - \underline{k}^i) = 0$. If the scattered ray wave numbers are $[\xi^s, \eta^s, \varkappa^s(\xi^s, \eta^s)]$ then Snell's law can be expanded to

$$\xi^s - \xi^i = \left[\varkappa^s(\xi^s, \eta^s) - \varkappa^i(\xi^i, \eta^i) \right] \frac{n_{ox}}{n_{oz}}$$

$$\eta^s - \eta^i = \left[\varkappa^s(\xi^s, \eta^s) - \varkappa^i(\xi^i, \eta^i) \right] \frac{n_{oy}}{n_{oz}}$$

(D-2)

which can be solved for ξ^s and η^s as functions of ξ^i and η^i.

Step 3: The normal $\underline{v}^s$ to the $\varkappa^s$ branch of the dispersion surface at the point $[\xi^s, \eta^s, \varkappa^s(\xi^s, \eta^s)]$ is from (II-16)

$$\underline{v}^s = \pm \left[\underline{x}_o \varkappa_1^s(\xi^s, \eta^s) + \underline{y}_o \varkappa_2^s(\xi^s, \eta^s) - \underline{z}_o \right] \Big/ \sqrt{\left[\varkappa_1^s(\xi^s, \eta^s) \right]^2 + \left[\varkappa_2^s(\xi^s, \eta^s) \right]^2 + 1}$$

(D-3)

with the partial derivatives $\varkappa_1^s(\xi^s, \eta^s)$ and $\varkappa_2^s(\xi^s, \eta^s)$ evaluated at (ξ^s, η^s). Since the vector $\underline{L}^s = \underline{x}_o(x - x^o) + \underline{y}_o(y - y^o) + \underline{z}_o[z - f(x^o, y^o)]$ from the point of incidence to an observation point along the scattered ray must be parallel to $\underline{v}^s$, the coordinates of the observation point must satisfy

$$(x - x^o) + \left[z - f(x^o, y^o) \right] \varkappa_1^s(\xi^s, \eta^s) = (y - y^o) + \left[z - f(x^o, y^o) \right] \varkappa_2^s(\xi^s, \eta^s) = 0 .$$

(D-4)

Step 4: For fixed z, (D-4) may be solved for x and y, which are seen to ultimately be functions of ξ^i and η^i. Considering the pencil of incident rays whose ξ^i and η^i wave numbers lie in some elemental region having area $d\xi^i \, d\eta^i$, the corresponding scattered rays will pass through a small region in the constant z plane whose area is

$d\xi^i \, d\eta^i \, J(x, y; \xi^i, \eta^i)$ where $J(x, y; \xi^i, \eta^i) = \left| \dfrac{\partial x}{\partial \xi^i} \dfrac{\partial y}{\partial \eta^i} - \dfrac{\partial x}{\partial \eta^i} \dfrac{\partial y}{\partial \xi^i} \right|$ is the

Jacobian of the transformation. Note that the Jacobian is a function of z and hence of the distance $L^s = |\underline{L}^s|$ along the scattered ray pencil. The ray divergence factor is defined in (II-30) where $da(L_m)$ is the

normal corss-sectional area of the scattered ray flux tube. Alternatively,

$D^{si}(L^s) = \sqrt{da_z(L^s) / da_z(0)}$ where $da_z(L^s)$ is the cross-sectional area of

the ray tube in a constant z plane. Thus $D^{si}(L^s)$ will be the square root

of the ratio of $J(x, y; \xi^i, \eta^i)$ at L^s to $J(x, y; \xi^i, \eta^i)$ at $L^s = 0$. Since the

ray structure is independent of the choice of the (x, y, z) coordinate system,

so is the value of $D^{si}(L^s)$.

2) Details of the Calculation

The details of the calculation for the partial derivatives $\partial x/\partial \xi^i$,

$\partial x/\partial \eta^i$, $\partial y/\partial \xi^i$ and $\partial y/\partial \eta^i$ appearing in the Jacobian will now be consid-

ered. Because of the length of the expressions involved, only $\partial x/\partial \xi^i$ is

calculated. The remaining derivatives are listed in (D-15),(D-16) and

(D-17).

Solving (D-4) for x gives

$$x = x^o - \left[z - f(x^o, y^o) \right] x_1^s(\xi^s, \eta^s) \tag{D-5}$$

from which one obtains for constant z

$$\frac{\partial x}{\partial \xi^i} = \frac{\partial x^o}{\partial \xi^i} + \left[f_x o \frac{\partial x^o}{\partial \xi^i} + f_y o \frac{\partial y^o}{\partial \xi^i} \right] x_1^s(\xi^s, \eta^s) - \left[z - f(x^o, y^o) \right] \frac{\partial}{\partial \xi^i} x_1^s(\xi^s, \eta^s) \tag{D-6}$$

where

$$\frac{\partial}{\partial \xi^i} x_1^s(\xi^s, \eta^s) = x_{11}^s(\xi^s, \eta^s) \frac{\partial \xi^s}{\partial \xi^i} + x_{12}^s(\xi^s, \eta^s) \frac{\partial \eta^s}{\partial \xi^i} \tag{D-7}$$

and $f_x o = \partial f/\partial x$ evaluated at (x^o, y^o) and similarly for $f_y o$. Taking the

partial derivatives of the equations (D-2) with respect to ξ^i yields

$$\frac{\partial \xi^s}{\partial \xi^i} - 1 = \left[\varkappa_1^s(\xi^s,\eta^s)\frac{\partial \xi^s}{\partial \xi^i} + \varkappa_2^s(\xi^s,\eta^s)\frac{\partial \eta^s}{\partial \xi^i} - \varkappa_1^i(\xi^i,\eta^i)\right]\frac{n_{ox}}{n_{oz}}$$

$$+ \left[\varkappa^s(\xi^s,\eta^s) - \varkappa^i(\xi^i,\eta^i)\right]\frac{\partial}{\partial \xi^i}\left(\frac{n_{ox}}{n_{oz}}\right)$$

$$\left. \begin{array}{l} \\ \\ \\ \end{array} \right\} \qquad \text{(D-8)}$$

$$\frac{\partial \eta^s}{\partial \xi^i} = \left[\varkappa_1^s(\xi^s,\eta^s)\frac{\partial \xi^s}{\partial \xi^i} + \varkappa_2^s(\xi^s,\eta^s)\frac{\partial \eta^s}{\partial \xi^i} - \varkappa_1^i(\xi^i,\eta^i)\right]\frac{n_{oy}}{n_{oz}}$$

$$+ \left[\varkappa^s(\xi^s,\eta^s) - \varkappa^i(\xi^i,\eta^i)\right]\frac{\partial}{\partial \xi^i}\left(\frac{n_{oy}}{n_{oz}}\right)$$

and this set of equations may be solved for $\partial \xi^s/\partial \xi^i$ and $\partial \eta^s/\partial \xi^i$. Since $\underline{n}_o$ is given by

$$\underline{n}_o = (-\underline{x}_o f_x{}^o - \underline{y}_o f_y{}^o + \underline{z}_o)/\sqrt{(f_x{}^o)^2 + (f_y{}^o)^2 + 1} \qquad \text{(D-9)}$$

it is found that

$$\frac{\partial}{\partial \xi^i}\left(\frac{n_{ox}}{n_{oz}}\right) = -\left(f_{x^o x^o}\frac{\partial x^o}{\partial \xi^i} + f_{x^o y^o}\frac{\partial y^o}{\partial \xi^i}\right)$$

$$\left. \begin{array}{l} \\ \\ \end{array} \right\} \qquad \text{(D-10)}$$

$$\frac{\partial}{\partial \xi^i}\left(\frac{n_{oy}}{n_{oz}}\right) = -\left(f_{x^o y^o}\frac{\partial x^o}{\partial \xi^i} + f_{y^o y^o}\frac{\partial y^o}{\partial \xi^i}\right)$$

Finally, $\partial x^o/\partial \xi^i$ and $\partial y^o/\partial \xi^i$ can be found from (D-1) and are the solutions of the set of equations

$$\frac{\partial x^o}{\partial \xi^i} = -\left[f(x^o,y^o) - z'\right]\varkappa_{11}^i(\xi^i,\eta^i) - \left(f_{x^o}\frac{\partial x^o}{\partial \xi^i} + f_{y^o}\frac{\partial y^o}{\partial \xi^i}\right)\varkappa_1^i(\xi^i,\eta^i)$$

$$\left. \begin{array}{l} \\ \\ \end{array} \right\} \qquad \text{)D-11)}$$

$$\frac{\partial y^o}{\partial \xi^i} = -\left[f(x^o,y^o) - z'\right]\varkappa_{12}^i(\xi^i,\eta^i) - \left(f_{x^o}\frac{\partial x^o}{\partial \xi^i} + f_{y^o}\frac{\partial y^o}{\partial \xi^i}\right)\varkappa_2^i(\xi^i,\eta^i)$$

The solutions of (D-11) for $\partial x^o/\partial\xi^i$ and $\partial y^o/\partial\xi^i$ can now be substituted into (D-10) and these expressions substituted into (D-8). The solutions of (D-8) for $\partial\xi^s/\partial\xi^i$ and $\partial\eta^i/\partial\xi^i$ can be used to find $\dfrac{\partial}{\partial\xi^i}\varkappa_1^s(\xi^s,\eta^s)$ in

(D-6), which together with $\partial x^o/\partial\xi^i$ and $\partial y^o/\partial\xi^i$ from (D-11) gives $\partial x/\partial\xi^i$.

Instead of going through the above procedure in an arbitrary (x,y,z) coordinate system, the calculations are simplified if a particular (x,y,z) system is used. Choosing the (x,y,z) system such that at the point of incidence, the interface is tangent to the $z = 0$ plane, i.e., $f(x^o,y^o) = 0$ and $f_xo = f_yo = 0$, then $\underline{n}_o = \underline{z}_o$. In this case (D-11) becomes

$$\left.\begin{aligned}\frac{\partial x^o}{\partial\xi^i} &= z'\varkappa_{11}^i(\xi^i,\eta^i)\\[2mm]\frac{\partial y^o}{\partial\xi^i} &= z'\varkappa_{12}^i(\xi^i,\eta^i)\end{aligned}\right\}.\qquad\text{(D-12)}$$

Since $n_{ox} = n_{oy} = 0$, (D-2) gives $\xi^s = \xi^i$ and $\eta^s = \eta^i$ so that with the help of (D-10) the solutions of (D-8) are

$$\left.\begin{aligned}\frac{\partial\xi^s}{\partial\xi^i} &= 1 - z'(\varkappa^s - \varkappa^i)(f_xo_xo\,\varkappa_{11}^i + f_xo_yo\,\varkappa_{12}^i)\\[2mm]\frac{\partial\eta^s}{\partial\xi^i} &= -z'(\varkappa^s - \varkappa^i)(f_xo_yo\,\varkappa_{11}^i + f_yo_yo\,\varkappa_{12}^i)\end{aligned}\right\}\qquad\text{(D-13)}$$

where $\varkappa^s$, $\varkappa^i$, $\varkappa_{11}^i$ and $\varkappa_{12}^i$ are evaluated at (ξ^i,η^i). Using (D-13) in (D-7) and with the help of (D-12), (D-6) becomes

$$\frac{\partial x}{\partial\xi^i} = (z'\varkappa_{11}^i - z\varkappa_{11}^s) + zz'(\varkappa^s-\varkappa^i)\Big[\varkappa_{11}^s(f_xo_xo\,\varkappa_{11}^i+f_xo_yo\,\varkappa_{12}^i)+\varkappa_{12}^s(f_xo_yo\,\varkappa_{11}^i+f_yo_yo\,\varkappa_{12}^i)\Big].$$
$$\text{(D-14)}$$

In a similar manner the other derivatives appearing in the Jacobian can be evaluated and can be shown to be

$$\frac{\partial x}{\partial \eta^i} = (z'\varkappa_{12}^i - z\varkappa_{12}^s) + zz'(\varkappa^s - \varkappa^i)\left[\varkappa_{11}^s(f_{oo\,xx}\varkappa_{12}^i + f_{oo\,xy}\varkappa_{22}^i) + \varkappa_{12}^s(f_{oo\,xy}\varkappa_{12}^i + f_{oo\,yy}\varkappa_{22}^i)\right] ,$$

$$(D-15)$$

$$\frac{\partial y}{\partial \xi^i} = (z'\varkappa_{12}^i - z\varkappa_{12}^s) + zz'(\varkappa^s - \varkappa^i)\left[\varkappa_{12}^s(f_{oo\,xx}\varkappa_{11}^i + f_{oo\,xy}\varkappa_{12}^i) + \varkappa_{22}^s(f_{oo\,xy}\varkappa_{11}^i + f_{oo\,yy}\varkappa_{12}^i)\right]$$

$$(D-16)$$

and

$$\frac{\partial y}{\partial \eta^i} = (z'\varkappa_{22}^i - z\varkappa_{22}^s) + zz'(\varkappa^s - \varkappa^i)\left[\varkappa_{12}^s(f_{oo\,xx}\varkappa_{12}^i + f_{oo\,xy}\varkappa_{22}^i) + \varkappa_{22}^s(f_{oo\,xy}\varkappa_{12}^i + f_{oo\,yy}\varkappa_{22}^i)\right] .$$

$$(D-17)$$

With the above expressions for the partial derivatives, the Jacobian can be written as

$$J(x,y;\xi^i,\eta^i) = \left| \left[(z'\varkappa_{11}^i - z\varkappa_{11}^s)(z'\varkappa_{22}^i - z\varkappa_{22}^s) - (z'\varkappa_{12}^i - z\varkappa_{12}^s)^2\right] \right.$$

$$+ zz'^2(\varkappa^s - \varkappa^i)\left[\varkappa_{11}^i\varkappa_{22}^i - (\varkappa_{12}^i)^2\right]\left[\varkappa_{11}^s f_{oo\,xx} + 2\varkappa_{12}^s f_{oo\,xy} + \varkappa_{22}^s f_{oo\,yy}\right] \qquad (D-18)$$

$$- z^2 z'(\varkappa^s - \varkappa^i)\left[\varkappa_{11}^s\varkappa_{22}^s - (\varkappa_{12}^s)^2\right]\left[\varkappa_{11}^i f_{oo\,xx} + 2\varkappa_{12}^i f_{oo\,xy} + \varkappa_{22}^i f_{oo\,xy}\right]$$

$$\left. + z^2 z'^2(\varkappa^s - \varkappa^i)^2\left[\varkappa_{11}^i\varkappa_{22}^i - (\varkappa_{12}^i)^2\right]\left[\varkappa_{11}^s\varkappa_{22}^s - (\varkappa_{12}^s)^2\right]\left[f_{oo\,xx}f_{oo\,yy} - (f_{oo\,xy})^2\right] \right|$$

with $\varkappa^s$, $\varkappa^i$ and their derivatives evaluated at (ξ^i, η^i). Symbolizing the Jacobian in (D-18) as $J(z)$ to indicate its z dependence, the divergence coefficient D^{si} for the point-source rays scattered at a curved interface is

$$D^{si} = \sqrt{J(z) / J(0)} .$$

$$(D-19)$$

The Jacobian (D-18) could be rephrased in terms of the ray-optical quantities: a) the principal curvatures of the $\varkappa^s$, $\varkappa^i$ and $f(x,y)$ surfaces; b) the angles between the directions that define the orientation of these surfaces; c) the normal distances $z = \underline{n}_o \cdot \underline{L}^s$ and $z' = \underline{n}_o \cdot \underline{L}^i$; d) the normal wave numbers $\varkappa^s = \underline{n}_o \cdot \underline{k}^s$ and $\varkappa^i = \underline{n}_o \cdot \underline{k}^i$. However, such a representation for $J(z)$ is probably not the most

convenient form for calculating it and therefore is not given here. Note that the first term in (D-18) is the Hessian for the rays scattered by a planar interface, the other terms being corrections due to the curvature of the interface. From (D-18) it is seen that the divergence factor is quadratic in z, indicating that the rays scattered from a curved interface may be at most twice tangent to a caustic.

Appendix E

RAY-OPTICAL REPRESENTATION FOR THE LATERAL RAY FIELDS

The ray-optical interpretation of the critical point condition given
in Section E-2 of Chapter II permits the re-expression of the various quan-
tities appearing in (II-37) in ray-optical terms that are invariant under a
rotation of the (x, y) plane. At the critical point, the phase function $P(\xi, \eta)$
of the integrands of (II-4) can be written as

$$P(\xi_c, \eta_c) = \left[\xi_c x' + \eta_c y' - \varkappa_n z'\right] + \left[\xi_c(x''-x') + \eta_c(y''-y')\right] + \left[\xi_c(x-x'') + \eta_c(y-y'') + \varkappa_m z\right]$$

$$= N_n L_n + N_\ell L_\ell + N_m L_m \qquad (E-1)$$

where N_n, N_ℓ and N_m are the ray-refractive indices given in (II-17) of the
various branches of the dispersion surfaces at the critical point and
$L_n = |\underline{L}_n|$, $L_\ell = |\underline{L}_\ell|$ and $L_m = |\underline{L}_m|$.

It will now be shown that the quantities $P_2^2(d^2P/d\xi^2)$, $|\partial g_\ell/\partial \eta|/|P_2|$
$\text{sgn}(d^2P/d\xi^2)$ and $\exp\left[-j(\frac{3\pi}{4}\text{sgn } P_2 - \arg\sqrt{\partial g/\partial \eta})\right]$ appearing in (II-37) can
also be expressed in ray-optical terms. From the condition $\underline{\nu}_m \times \underline{L}_m = \underline{\nu}_n \times \underline{L}_n = 0$ and the form of $P(\xi, \eta)$, it is easily shown that

$$L_{\ell x} \equiv x'' - x' = P_1(\xi_c, \eta_c); \quad L_{\ell y} \equiv y'' - y' = P_2(\xi_c, \eta_c) . \qquad (E-2)$$

Expanding $d^2P\left[\xi, \eta_b/(\xi)\right]/d\xi^2$ and using (E-2) one finds

$$P_2\frac{d^2P}{d\xi^2} = L_{\ell y}^2 P_{11} - 2L_{\ell x}L_{\ell y}P_{12} + L_{\ell x}^2 P_{22} + L_{\ell y}^3\frac{d^2\eta_b}{d\xi^2} \qquad (E-3)$$

at the critical point. Since $\underline{\nu}_\ell$ is normal to the curve $g_\ell(\xi, \eta) = 0$, it can be
written as $\underline{\nu}_\ell = Q_\ell(\underline{x}_o g_{\ell 1} + \underline{y}_o g_{\ell 2})$ where $Q_\ell = \pm 1/\sqrt{g_1^2 + g_2^2}$, the sign being
chosen such that this expression for $\underline{\nu}_\ell$ has the proper sense. Also,
$g_\ell\left[\xi, \eta_b(\xi)\right] \equiv 0$ so that all its derivatives with respect to ξ are zero.
Using the above form for $\underline{\nu}_\ell$ and the first two derivatives of $g_\ell\left[\xi, \eta_b(\xi)\right]$,

it can be shown that

$$\frac{d^2\eta_b}{d\xi^2} = \frac{Q_\ell}{\nu^3_{\ell y}} (g_{\ell 11}\nu^2_{\ell y} - 2 g_{\ell 12}\nu_{\ell x}\nu_{\ell y} + g_{\ell 22}\nu^2_{\ell x}) . \qquad (E-4)$$

Finally, at the critical point, $\underline{\nu}_\ell = \underline{L}_\ell / L_\ell$ so that substituting (E-4) into (E-3) gives

$$\left(P_2 \frac{d^2 P}{d\xi^2}\right)_{(\xi_c, \eta_c)} = (\underline{z}_o \times \underline{L}_\ell) \cdot \underset{\sim}{D}_{\ell mn} \cdot (\underline{z}_o \times \underline{L}_\ell) \qquad (E-5)$$

where $\underset{\sim}{D}_{\ell mn}$ is the symmetric dyadic having elements $(P_{ij} + L_\ell Q_\ell g_{\ell ij})$ with i, j = 1, 2. Hence $P^2_2 (d^2 P/d\xi^2)$ at the critical point is independent of the choice of the (x, y) coordinate system. Since $P^2_2 > 0$, at the critical point

$$sgn(d^2 P/d\xi^2) = sgn\left[P^2_2 (d^2 P/d\xi^2)\right] = sgn\left[(\underline{z}_o \times \underline{L}_\ell) \cdot \underset{\sim}{D}_{\ell mn} \cdot (\underline{z}_o \times \underline{L}_\ell)\right]$$

$$(E-6)$$

and is also independent of the (x, y) coordinates. Furthermore, using (E-2) and the foregoing expressions for $\underline{\nu}_\ell$, at the critical point

$$\frac{|\partial g_\ell /\partial \eta|}{|P_2|} \equiv \left|\frac{g_{\ell 2}}{P_2}\right| = \frac{1}{L_\ell |Q_\ell|} \quad , \qquad (E-7)$$

which is independent of the (x, y) coordinates.

The remaining quantity to be considered is $\exp\left[-j(\frac{3\pi}{4} sgn P_2 - arg\sqrt{\partial g_\ell /\partial \eta})\right]$. As was argued in Section E-2 of Chapter II, $sgn L_{\ell y} = sgn \nu_{\ell y}$ so that from (E-4), $sgn P_2(\xi_c, \eta_c) = sgn \nu_{\ell y}$. Also, in Section E-1 of Chapter II, $arg\sqrt{\partial g_\ell(\xi, \eta_b)/\partial \eta}$ was defined to be $arg\sqrt{g_\ell [\xi, \eta_b + \Delta]}$ where Δ is a small positive quantity -- see text after (II-35). Thus, at the critical point

$$\frac{3\pi}{4} \operatorname{sgn} P_2 - \arg\sqrt{\partial g_\ell / \partial \eta} = \frac{3\pi}{4} \operatorname{sgn} \nu_{\ell y} - \arg\sqrt{g_\ell(\zeta_c, \eta_c + \Delta)} . \qquad \text{(E-8)}$$

Using (E-8), the invariance of $\exp\left[-j(\frac{3\pi}{4} \operatorname{sgn} P_2 - \arg\sqrt{\partial g_\ell / \partial \eta})\right]$ will be shown by considering the sign of $\nu_{\ell y}$ and the shape, near the critical point, of the trace of the $\varkappa_\ell$ and $\varkappa_P$ branches of the dispersion surface in a constant $\zeta = \zeta_c$ plane passing through the critical point. The four possible combinations of the sign of $\nu_{\ell y}$ and shape of the foregoing curves are depicted in Table E-1. The arrows in Table E-1 indicate the direction of the projection into the constant $\zeta = \zeta_c$ plane of $\underline{\nu}$ corresponding to a wave carrying energy in the plus z direction. The sign of $\nu_{\ell y}$ at the critical point is as specified for each case. Recall that near the branch curve, $\varkappa_\ell \approx g_\ell^o \pm \sqrt{g_\ell}$ -- see text before (II-33) -- where $\arg\sqrt{g_\ell}$ is assumed to be taken such that the plus sign applies if $\varkappa_\ell$ corresponds to an upgoing wave and the minus sign applies otherwise. The value of g_ℓ^o at the critical point is indicated in Table E-1. Furthermore, the values given in Table E-1 for $\arg\sqrt{g_\ell(\zeta_c, \eta_c + \Delta)}$ satisfy the above assumption on $\arg\sqrt{g_\ell}$ for $\eta \mapsto \eta_c + \Delta$. Using (E-8), it is easily verified for each case in Table E-1 that at the critical point

$$\exp\left[-j(\frac{3\pi}{4} \operatorname{sgn} P_2 - \arg\sqrt{\partial g_\ell / \partial \eta})\right] = \exp\left[j\frac{\pi}{4}(2 - \operatorname{sgn} C_\ell)\right] \qquad \text{(E-9)}$$
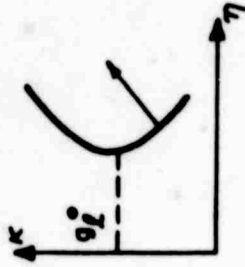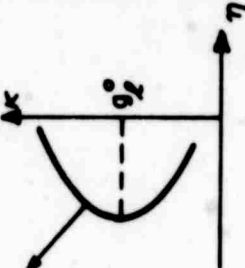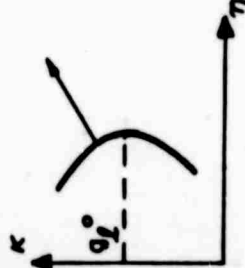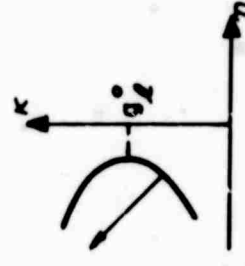
where C_ℓ is the curvature of the curves in Table E-1. But $\operatorname{sgn} C_\ell$ is independent of the angle between $\underline{\nu}_\ell$ and the constant $\zeta = \zeta_c$ plane passing through the critical point. Thus $\operatorname{sgn} C_\ell$, and hence the left-hand side of (E-9), will be independent of the (x, y) coordinate system. For convenience, let

$$\delta_{\ell mn} = \operatorname{sgn}\left[(\underline{z}_o \times \underline{L}_\ell) \cdot \underline{D}_{\ell mn} \cdot (\underline{z}_o \times \underline{L}_\ell)\right] - (2 - \operatorname{sgn} C_\ell) . \qquad \text{(E-10)}$$

The terms of the sum indicated in (II-37) have thus been shown to be independent of the choice of the (x, y) coordinate system and to be expressible in ray-optical form .

Table E-1

The Shape of the Dispersion Curves and the Sign of $\nu_{\ell y}$ in the Constant $\zeta = \zeta_c$ Plane Passing Through the Critical Point

Appendix F

A SURFACE ADMITTANCE REPRESENTATION FOR
PLANE-STRATIFIED CONFIGURATIONS

In order to define that $\underset{\sim}{Z}$ which represents a plane-stratified, loss-less, dispersive, anisotropic medium above a perfectly conducting plane, the auxiliary problem, with boundary conditions (III-26) and (III-27), was first considered. For most values of the parameters $\underline{k}_t$ and ω, the auxiliary problem will have unique non-trivial solutions of the form given in (III-1) for all $\underline{h}_d \neq 0$. At the remaining values of $\underline{k}_t$ and ω, which lie on surfaces in $\underline{k}_t - \omega$ space, non-unique cavity-type solutions will exist for $\underline{h}_d = 0$ and no solutions satisfying the boundary condition (III-27) will exist for all $\underline{h}_d \neq 0$. The non-unique solutions exist when the plane $z = d$ corresponds to a magnetic field null and would give infinite values for some or all of the components of the impedance dyadic $\underset{\sim}{Z}$. For this reason such values of $\underline{k}_t$ and ω are excluded from the consideration of $\underset{\sim}{Z}$. Although the surface impedance formalism breaks down at these values of $\underline{k}_t$ and ω, a surface admittance formalism will in general remain valid.

The surface admittance $\underset{\sim}{Y}$ is the inverse of $\underset{\sim}{Z}$, when both $\underset{\sim}{Z}$ and its inverse exist, and is regular at those values of $\underline{k}_t$ and ω for which $\underset{\sim}{Z}$ cannot be defined. In studying the properties of $\underset{\sim}{Y}$, one would consider the fields in the region $0 < z < d$ with $\underline{E}_t$, rather than $\underline{H}_t$, specified at $z = d$. Thus to find the admittance, one requires that $\underset{\sim}{Y}$ be such as to satisfy the relation

$$(\underline{z}_o \times \underline{h}_t)_{z=d} = \underset{\sim}{Y} \cdot (\underline{e}_t)_{z=d} \qquad (F-1)$$

for two field solutions in the region $0 < z < d$. The two field solutions to be used are those satisfying the boundary condition

$$(\underline{E}_t)_{z=d} = \underline{e}_d \, e^{j(\omega t - \underline{k}_t \cdot \underline{\rho})} \qquad (F-2)$$

at $z = d$ with $\underline{e}_d$ taking on two linearly independent forms. If (F-1) is satisfied

for these two field solutions, because of linearity, it will be satisfied by the solutions for all possible $\underline{e}_d$. Those values of $\underline{k}_t$ and ω for which non-trivial solutions exist when $\underline{e}_d = 0$ are excluded from consideration. The impedance formalism may, however, be used, in general, at such values.

The energy and power relations containing $\underset{\sim}{Y}$ can be derived from reasoning similar to that used for $\underset{\sim}{Z}$. They are

$$j\frac{1}{2}\left[\underline{e}_t^* \cdot \frac{\partial \underset{\sim}{Y}}{\partial k_x} \cdot \underline{e}_t\right]_{z=d} = S_{dx}$$

$$j\frac{1}{2}\left[\underline{e}_t^* \cdot \frac{\partial \underset{\sim}{Y}}{\partial k_y} \cdot \underline{e}_t\right]_{z=d} = S_{dy}$$

(F-3)

and

$$-j\frac{1}{2}\left[\underline{e}_t^* \cdot \frac{\partial \underset{\sim}{Y}}{\partial \omega} \cdot \underline{e}_t\right]_{z=d} = W_d .$$

(F-4)

Appendix G

GROUP VELOCITY AND POWER FLOW RELATIONS FOR
SURFACE WAVES IN PERIODIC CONFIGURATIONS

In this appendix the power flow and energy relations derived in
Chapter III for plane-stratified media are generalized   lossless struc-
tures that are stratified in one direction and periodic in planes transverse
to the direction of stratification. The fundamental translation vectors
describing the periodicity of the structure in the planes perpendicular to
the direction of stratification are assumed to be the same for all planes.
In their most general form, the structures treated here consist of a
periodic array of identical perfectly conducting scatterers imbedded in a
periodic, lossless, dispersive, anisotropic medium which may be bounded
by a perfect conductor of periodic shape. Moreover, the fundamental
translation vectors need not be orthogonal.

It is first shown for surface waves propagating in such structures
that the group velocity is equal to the velocity of energy transport -- see
Section 1. For the periodic structures considered here, the velocity of
energy transport is the ratio of the integral over the coordinate of strati-
fication of the period average of the real part of the complex Poynting
vector to the integral of the period average of the stored energy density.
A proof of this relation for surface waves propagating on a periodic,
anisotropically conducting surface has previously been given by
Gans[45]. Also, Kay[46] has shown that the group velocity is in the
direction of energy flow for the specific case of surface waves in
air above a finned conducting surface. However, the problem con-
sidered by Kay is highly restricted in that no power flows between
the fins to within the approximations used in the derivation.

The relations between power flow and stored energy in a periodic
structure and the dyadic surface impedance representing the structure,
when such a representation is possible, are derived in Section 2. These
relations are similar to (III-36) and (III-37). It is possible to represent a

periodic structure by a dyadic surface impedance when the media above the structure is uniform in the planes parallel to the planes of stratification of the structure and when the transverse wave numbers and frequency are such that at the plane on which the surface impedance is defined, the fields can be approximated by the fundamental space harmonic.

1) Group Velocity and Energy Velocity

The most general form of the configurations covered by this analysis consists of a periodic array of identical perfectly conducting scatterers imbedded in a periodic, anisotropic, lossless, dispersive medium which may or may not be bounded from below by a perfectly conducting surface having periodic shape. The periodicity in ρ, i.e., in the planes of constant z, is assumed to be described by the fundamental translation vectors $\underline{a}$ and $\underline{b}$. These vectors, which need not be orthogonal, have the property that, when viewed from any point $\underline{\rho} + \underline{z}_0 z$ the configuration looks the same as when viewed from the points $\underline{\rho} + n\underline{a} + m\underline{b} + \underline{z}_0 z$ where n and m are integers. The vectors $\underline{a}$ and $\underline{b}$ describe a unit cell which is a cylinder parallel to the z axis, and extending from $z = -\infty$ to $z = \infty$, and whose cross-section in any constant z plane is a parallelogram having sides formed by $\underline{a}$ and $\underline{b}$ -- see Fig. G-1. If the configuration is periodic in one direction only, the other translation vector may be taken arbitrarily. The case of a configuration uniform in $\underline{\rho}$ is also covered here when both $\underline{a}$ and $\underline{b}$ are taken arbitrarily.

While the discussion given in this section applies to configurations with a periodic array of scatterers and a periodic medium, it is also valid when no scatterers are present and when the medium is uniform in $\underline{\rho}$. The discussion is also valid when the medium, in any of the above cases, is bounded from below by a perfectly conducting surface whose shape may be a periodic function of $\underline{\rho}$. The medium is assumed to be described by the Hermitian tensors $\underline{\varepsilon}$ and $\underline{\mu}$ which, when the medium is periodic, are periodic functions of $\underline{\rho}$. They are further assumed to be continuous functions of position except for finite jumps on a set of zero volume and are allowed to be functions of ω. The only restriction on the z dependence of
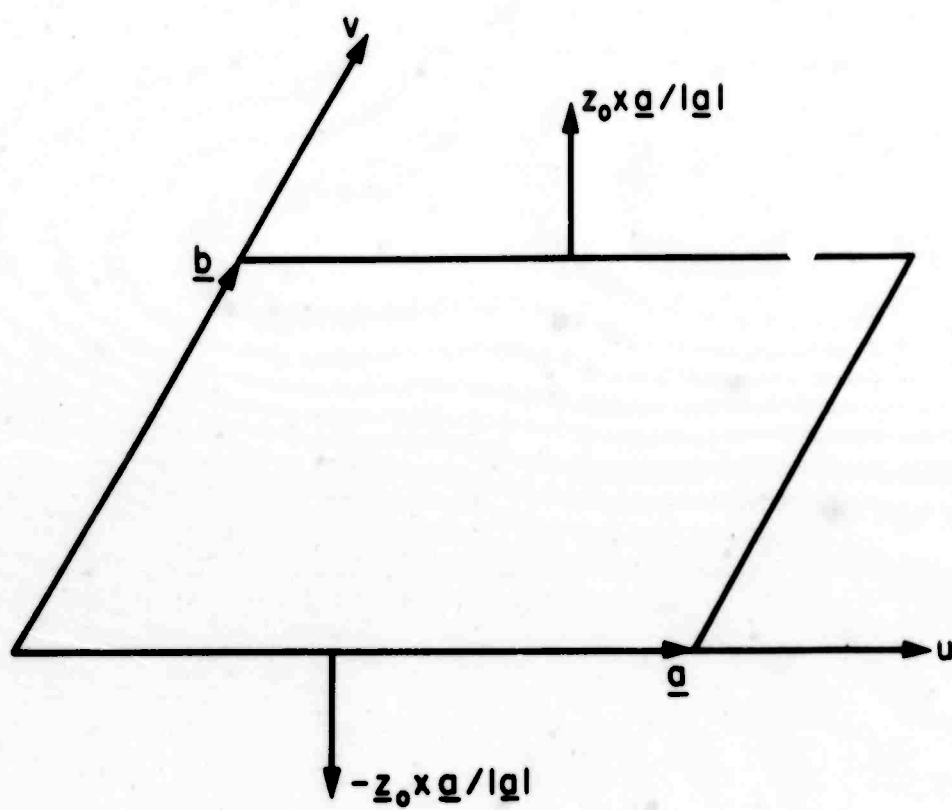
Fig. G-1   Cross-section of a unit cell

the configuration is that it be such that surface waves, of the form
described in the following paragraph, be solutions of Maxwell's equations.

The surface wave solutions that are assumed to exist have the
form

$$
\left.\begin{array}{c} \underline{E}\,(\underline{r}\;;\;\underline{k}_t,\,\omega) \\[2em] \underline{H}\,(\underline{r}\;;\;\underline{k}_t,\,\omega) \end{array}\right\} = \left\{\begin{array}{c} \underline{e}\,(\underline{\rho},z\;;\;\underline{k}_t,\,\omega) \\[2em] \underline{h}\,(\underline{\rho},z\;;\;\underline{k}_t,\,\omega) \end{array}\right\} e^{-j\underline{k}_t\,\cdot\,\underline{\rho}}\,, \tag{G-1}
$$

where $\underline{k}_t = \underline{x}_o\,k_x + \underline{y}_o\,k_y$ is a real wave vector and $\underline{e}$ and $\underline{h}$ are periodic
functions of $\underline{\rho}$ whose periodicity is described by the fundamental transla-
tion vectors $\underline{a}$ and $\underline{b}$. This form of the fields is consistent with Floquet's
theorem for waves in periodic configurations. The $\underline{r}$ dependence of $\underline{E}$
and $\underline{H}$ is further assumed to be such that they approach zero as $|z| \to \infty$
and $\underline{E} \times \underline{H}^*$, as well as the electric and magnetic energy densities, are
integrable over a unit cell. Note that the entire foregoing description of
the fields applies when the configuration includes a perfectly conducting
bounding surface if the fields below the surface, which are unrelated to
those above, are taken as zero. Also, if the configuration is uniform in
some direction, $\underline{e}$ and $\underline{h}$ are independent of the coordinate along that
direction.

In addition to the above-described requirements on the spatial depen-
dence of $\underline{E}$ and $\underline{H}$, their tangential components must satisfy appropriate
boundary conditions on the surface of the perfectly conducting scatterers
and on the bounding surface, when either of these are present, and on the
discontinuity surfaces of $\underset{\sim}{\epsilon}$ and $\underset{\sim}{\mu}$ At the surface of the scatterers and on
the bounding surface $\underline{n} \times \underline{E} = 0$, and hence $\underline{n} \times \underline{e} = 0$, where $\underline{n}$ is the
normal to the surface. The vectors $\underline{n} \times \underline{E}$ and $\underline{n} \times \underline{H}$, and hence $\underline{n} \times \underline{e}$
and $\underline{n} \times \underline{h}$, must be continuous across those surfaces at which $\underset{\sim}{\epsilon}$ and $\underset{\sim}{\mu}$
are discontinuous, $\underline{n}$ being the normal to these surfaces.

As in the case of a medium uniform in $\underline{\rho}$, Maxwell's equations have
solutions of the form described above only for those values of the

parameters $\underline{k}_t$ and ω satisfying some relation $D_s(\underline{k}_t, \omega) = 0$, which is called the surface wave dispersion relation. Let $(\underline{k}_t, \omega)$ be one set of values satisfying the dispersion relation and $(\underline{k}_t + d\underline{k}_t, \omega + d\omega)$ be a neighboring set of values also satisfying the dispersion relation. Then, to first order, the fields associated with the latter set of values are given by

$$\underline{E}(\underline{r} ; \underline{k}_t + d\underline{k}_t, \omega + d\omega) = \underline{E}(\underline{r} ; \underline{k}_t, \omega) + \delta\underline{H}(\underline{r} ; \underline{k}_t, \omega)$$
$$\underline{H}(\underline{r} ; \underline{k}_t + d\underline{k}_t, \omega + d\omega) = \underline{H}(\underline{r} ; \underline{k}_t, \omega) + \delta\underline{E}(\underline{r} ; \underline{k}_t, \omega)$$

$$, \quad (G-2)$$

where the variation δ symbolizes the differential operation $\delta = d\underline{k}_t \cdot \nabla_{kt} + d\omega \frac{\partial}{\partial\omega}$. Since $\underline{E} \times \underline{H}^*$, for both sets of values of wave vector and frequency, is integrable over a unit cell, $\underline{E}^* \times \delta\underline{H}$ and $\delta\underline{E} \times \underline{H}^*$ are also integrable over a unit cell. Similarly, because of the boundary conditions $\underline{E}$ and $\underline{H}$ are required to satisfy, it is seen that $\underline{n} \times \delta\underline{E}$ is zero on the surface of the scatterers and on the bounding surface, when these are present. Furthermore, $\underline{n} \times \delta\underline{E}$ and $\underline{n} \times \delta\underline{H}$ must be continuous functions across the discontinuity surfaces of $\underset{\sim}{\epsilon}$ and $\underset{\sim}{\mu}$. Finally $\delta\underline{E}$ and $\delta\underline{H}$ satisfy the differential equations (III-6).

Consider now the quantity $\nabla \cdot (\underline{E}^* \times \delta\underline{H} + \delta\underline{E} \times \underline{H}^*)$. In Chapter III, by expanding the divergence of the cross-products and using (III-2), (III-6) and the Hermitian properties of $\underset{\sim}{\epsilon}$ and $\underset{\sim}{\mu}$, this quantity was shown to be equal to $-j\omega d\omega$ at points within a lossless medium, where $w = \frac{1}{2}\underline{E}^* \cdot \frac{\partial\omega\underset{\sim}{\epsilon}}{\partial\omega} \cdot \underline{E} + \frac{1}{2}\underline{H}^* \cdot \frac{\partial\omega\underset{\sim}{\mu}}{\partial\omega} \cdot \underline{H}$ is the energy density. At points within and on the scatterers and the bounding surface, $\underline{E}^* \times \delta\underline{H} + \delta\underline{E} + \underline{H}^*$ and the stored energy density w are both zero. Hence, for all points, the relation

$$\nabla \cdot (\underline{E}^* \times \delta\underline{H} + \delta\underline{E} \times \underline{H}^*) = -j2wd\omega \qquad (G-3)$$

holds. From the form of $\underline{E}$ and $\underline{H}$ in (G-1), w is seen to be a periodic function of $\underline{\rho}$.

Alternatively, using the form of $\underline{E}$ and $\underline{H}$ in (G-1), $\delta\underline{E}$ and $\delta\underline{H}$ may first be expanded as

$$\left.\begin{array}{l} \delta\underline{E} = (\delta\underline{e} - j\,d\underline{k}_t \cdot \underline{\rho}\,\underline{e})\,e^{-j\underline{k}_t \cdot \underline{\rho}} \\[12pt] \delta\underline{H} = (\delta\underline{h} - j\,d\underline{k}_t \cdot \underline{\rho}\,\underline{h})\,e^{-j\underline{k}_t \cdot \underline{\rho}} \end{array}\right\} \,, \qquad (G-4)$$

where $\delta\underline{e}$ and $\delta\underline{h}$ are periodic in $\underline{\rho}$. From the above equations, it is recognized that $\delta\underline{e}$ must satisfy the boundary condition $\underline{n} \times \delta\underline{e} = 0$ on the scatterers and on the bounding surface. Also, $\underline{n} \times \delta\underline{e}$ and $\underline{n} \times \delta\underline{h}$ must be continuous across the discontinuity surfaces of $\underline{\epsilon}$ and $\underline{\mu}$. With the above forms for $\delta\underline{E}$ and $\delta\underline{H}$, (G-3) becomes

$$-j2wd\omega = \nabla \cdot [\,\underline{e}^* \times \delta\underline{h} + \delta\underline{e} \times \underline{h}^* - 2jd\underline{k}_t \cdot \underline{\rho}\,\underline{s}\,] \qquad (G-5)$$

or, since in a lossless medium the divergence of the real part $\underline{s}$ of the complex Poynting vector is zero,

$$-j2wd\omega = -j2d\underline{k}_t \cdot \underline{s} + \nabla \cdot (\underline{e}^* \times \delta\underline{h} + \delta\underline{e} \times \underline{h}^*) \,. \qquad (G-6)$$

Note that $\underline{s}$ is a periodic function of $\underline{\rho}$.

Solving the surface wave dispersion relation for $\omega = \omega(\underline{k}_t)$, to first order $d\omega = d\underline{k}_t \cdot \nabla_{\underline{k}_t}\omega$ and (G-6) may be written

$$d\underline{k}_t \cdot (w\,\nabla_{\underline{k}_t}\omega - \underline{s}) = j\frac{1}{2}\nabla \cdot (\underline{e}^* \times \delta\underline{h} + \delta\underline{e} \times \underline{h}^*) \,. \qquad (G-7)$$

In general, $\nabla \cdot (\underline{e}^* \times \delta\underline{h} + \delta\underline{e} \times \underline{h}^*) \neq 0$ so that the group velocity $\nabla_{\underline{k}_t}\omega$ is unequal to the local energy velocity $\underline{s}/w$. It is for this reason that (G-7) is integrated over the volume of a unit cell, since then the right-hand side of the resultant equation, as argued below, is zero.

The volume integral of the right-hand side of (G-7) over the unit cell is converted into a surface integral over the surface of the cell using the divergence theorem. The contribution to the surface integral from the end faces of the unit cell at $z = -\infty$ and $z = \infty$ is zero since $\underline{e}$, $\underline{h}$, $\delta\underline{e}$ and $\delta\underline{h}$ are zero there. Next, consider the contribution from the two side walls parallel to the vector $\underline{a}$. On one of these side walls, the

unit normal vector is $\underline{n} = \underline{z}_o \times \underline{a}/|\underline{a}|$ while on the other it is $\underline{n} = -\underline{z}_o \times \underline{a}/|\underline{a}|$ -- see Fig. G-1. Because of the periodicity of $\underline{e}$, $\underline{h}$, $\delta\underline{e}$ and $\delta\underline{h}$, the value of $\underline{e}^* \times \delta\underline{h} + \delta\underline{e} \times \underline{h}^*$ at a point $\underline{\rho} + \underline{z}_o z$ on one side wall is equal to its value at the corresponding point $\underline{\rho} + \underline{b} + \underline{z}_o z$ on the opposite side wall. Thus, for each contribution to the surface integral of $\underline{n} \cdot (\underline{e}^* \times \delta\underline{h} + \delta\underline{e} \times \underline{h}^*)$ from one of the side walls, there will be a contribution of equal magnitude but opposite sign from the other, and hence the sum of the surface integrals over these two side walls is zero. Similarly, the sum of the surface integrals over the two side walls parallel to $\underline{b}$ is also zero. Therefore, the integral of (G-7) over a unit cell reduces to

$$d\underline{k}_t \cdot \nabla_{\underline{k}_t} \omega \int_{-\infty}^{\infty} dz \iint_p w \, da = d\underline{k}_t \cdot \int_{-\infty}^{\infty} dz \iint_p \underline{s} \, da \qquad (G-8)$$

where $\iint_p da$ stands for integration over a constant z cross-section of the unit cell.

In order to properly interpret the above equation, some properties of the integral of $\underline{s}$ must be established. It will first be shown that for any value of z, $\iint_p s_z \, da = 0$. To see this, consider the surface integral of $\underline{s} \cdot \underline{n}$ over the surface enclosing that portion of a unit cell lying below some constant z plane. Since the medium is lossless, $\nabla \cdot \underline{s} = 0$ and hence, using the divergence theorem, the surface integral is zero. The integral of $\underline{s} \cdot \underline{n}$ on the end face at $z = -\infty$ is zero because $\underline{s}$ is zero there. Using the same arguments given previously for the surface integral of $\underline{n} \cdot (\underline{e}^* \times \delta\underline{h} + \delta\underline{e} \times \underline{h}^*)$, the integral over the side walls can be shown to be zero. Thus, the surface integral on the top face of the region, where $\underline{n} = \underline{z}_o$, must be zero. Since the value of z on the top face was arbitrary, $\iint_p s_z \, da = 0$ for all z. The significance of this result is that the triple integration of $\underline{s}$ indicated on the right-hand side of (G-8) results in a purely transverse vector. Because of this and the fact the k_x and k_y can vary independently, (G-8) implies that

$$\nabla_{\underline{k}_t} \omega \int_{-\infty}^{\infty} dz \iint_p w\, da = \int_{-\infty}^{\infty} dz \iint_p \underline{s}\, da . \qquad (G-9)$$

The triple integral of w in the foregoing equation is seen to be the electromagnetic energy in the unit cell. The meaning of the integral of $\underline{s}$ is shown below to represent the average power flow in the surface wave times the cross-sectional area of the unit cell. In demonstrating this, the (u,v) coordinate system, in the (x,y) plane, is introduced. The u coordinate is taken in the direction of the translation vector $\underline{a}$ and v is taken in the direction of $\underline{b}$ -- see Fig. G-1. This coordinate system has the property that for a given value of u, the quantities w and $\underline{s}$ are periodic functions of v with period $b = |\underline{b}|$, while for a given value of v, they are periodic functions of u with period $a = |\underline{a}|$.

Let $\underline{u}_o = \underline{a}/a$ be the unit vector along u and $\underline{v}_o = \underline{b}/b$ be the unit vector along v. Also, let $\underline{u}_1$ and $\underline{v}_1$ be a reciprocal set of vectors to $\underline{u}_o$ and $\underline{v}_o$ having the properties that $\underline{u}_1 \cdot \underline{v}_o = \underline{v}_1 \cdot \underline{u}_o = 0$ and $\underline{u}_1 \cdot \underline{u}_o = \underline{v}_1 \cdot \underline{v}_o = 1$. In the (u,v,z) coordinate system, $\underline{s} = \underline{u}_o s_u + \underline{v}_o s_v + \underline{z}_o s_z$, where $s_u = \underline{s} \cdot \underline{u}_1$, $s_v = \underline{s} \cdot \underline{v}_1$ and $s_z = \underline{s} \cdot \underline{z}_o$. The area element da can be expressed in terms of du and dv as $da = \dfrac{A}{ab} du\, dv$, where $A = ab\, |\underline{u}_o \times \underline{v}_o|$ is the area of any constant z cross-section of a unit cell. Recalling that $\iint_p s_z\, da = 0$ for all z and defining the triple integral of $\underline{s}$ appearing on the right-hand side of (G-9) as $A\underline{\overline{S}}$, for reasons that will become apparent later, it is seen that

$$\underline{\overline{S}} = \frac{1}{ab} \int_0^a du \int_0^b dv \int_{-\infty}^{\infty} (\underline{u}_o s_u + \underline{v}_o s_v)\, dz . \qquad (G-10)$$

Note that since $\underline{s}$, and hence $\int_{-\infty}^{\infty} \underline{s}\, dz$, are periodic functions of v, their integral over a period in v is independent of where the start of the period is taken. Similarly, $\underline{s}$, and hence $\int_0^b dv \int_{-\infty}^{\infty} \underline{s}\, dz$, are periodic functions of u so that their integral over a period in u can be started from any point. For convenience, the periods have been taken as starting at $u = 0$ and $v = 0$

in (G-10).

As an aid to the interpretation of (G-10), it will be proven that $\int_0^b dv \int_{-\infty}^\infty s_u \, dz$ is independent of u. Consider a region formed from that portion of a unit cell lying between the plane u = 0 in the (u, v, z) coordinate system and the plane u = α < a -- see Fig. G-2. In this region $\nabla \cdot \underline{s} = 0$ so that the integral of $\underline{s} \cdot \underline{n}$ over the surface of the region is zero. The integrals over the end faces at $|z| = \infty$ are zero and the integrals over the side walls at v = 0 and v = b cancel because of the periodic dependence of $\underline{s}$ on v. On the side wall u = α, the normal is given by $\underline{n} = \underline{u}_1 / |\underline{u}_1|$, while on the side wall at u = 0, $\underline{n} = -\underline{u}_1 / |\underline{u}_1|$. Thus, the surface integral over the infinite cylinder, whose cross-section is shown in Fig. G-2, reduces to

$$\frac{1}{|\underline{u}_1|} \int_0^b dv \int_{-\infty}^\infty (s_u)_{u=\alpha} \, dz - \frac{1}{|\underline{u}_1|} \int_0^b dz \int_{-\infty}^\infty (s_u)_{u=0} \, dz = 0 \quad . \quad (G-11)$$

But α is arbitrary so that $\int_0^b dv \int_{-\infty}^\infty s_u \, dz$ is independent of u. A similar argument can be used to prove that $\int_0^a du \int_{-\infty}^\infty s_v \, dz$ is independent of v. Using these two facts, $\underline{S}$ given in (G-10) is seen to be

$$\underline{S} = \frac{\underline{u}_0}{b} \int_0^b dv \int_{-\infty}^\infty s_u \, dz + \frac{\underline{v}_0}{a} \int_0^a du \int_{-\infty}^\infty s_v \, dz \quad . \quad (G-12)$$

It will now be shown that $\underline{S}$ as given in (G-12) can be interpreted as the average power in the surface wave. Consider the planar surface lying between the two lines u = α_1, v = β_1 and u = α_2, v = β_2, which are parallel to the z axis. In order to calculate the total power P passing through the above planar surface, construct an infinite cylinder of triangular cross-section between this plane and the two intersecting planes u = α_2 and v = β_1 -- see Fig. G-3. The total power P is the surface integral of $\underline{s} \cdot \underline{\nu}$, where $\underline{\nu}$ is the unit normal indicated in Fig. G-3. Again, the fact that $\nabla \cdot \underline{s} = 0$ requires that P be equal to the power entering the triangular cylinder through
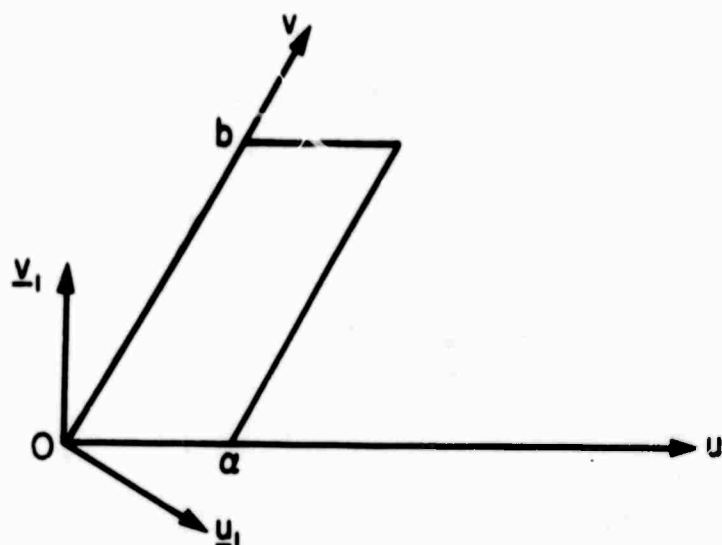
Fig. G-2   Cross-section of cylinder used in proving that $\int\limits_{0}^{b} dv \int\limits_{-\infty}^{\infty} s_u \, dz$ is independent of u
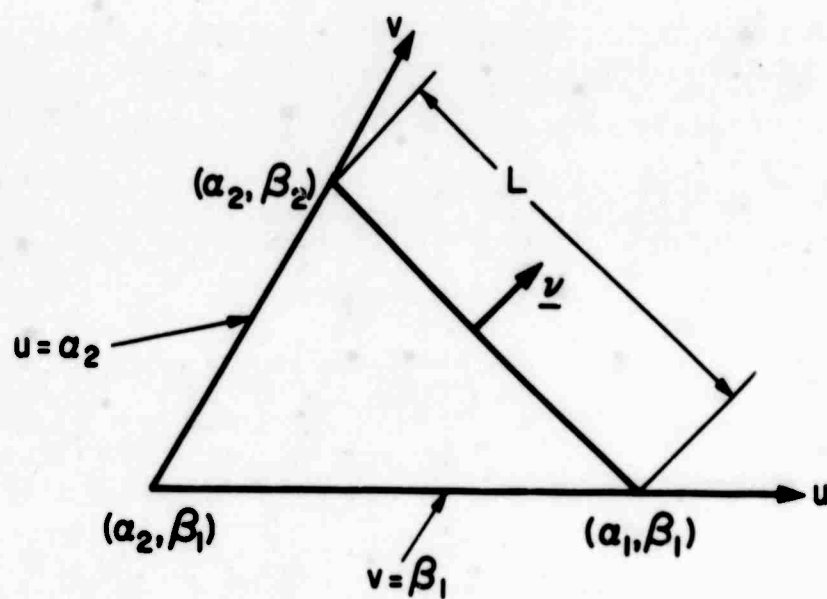

Fig. G-3   Cross-section of the triangular cylinder

$u = \alpha_2$ and $v = \beta_1$ sides of the cylinder.

The unit normal on the $u = \alpha_2$ side of the cylinder is $\underline{u}_1/|\underline{u}_1|$ and that on the $v = \beta_1$ side is $\underline{v}_1/|\underline{v}_1|$ so that

$$P = \frac{1}{|\underline{u}_1|} \int_{\beta_1}^{\beta_2} dv \int_{-\infty}^{\infty} (s_u)_{u=\alpha_2} dz + \frac{1}{|\underline{v}_1|} \int_{\alpha_2}^{\alpha_1} du \int_{-\infty}^{\infty} (s_v)_{v=\beta_1} dz \qquad (G\text{-}13)$$

where $s_u = \underline{s} \cdot \underline{u}_1$ and $s_v = \underline{s} \cdot \underline{v}_1$. In general, $\beta_2 - \beta_1$ will not correspond to an integral number of periods along v and hence the first integral in (G-13) cannot be exactly replaced by

$$\frac{\beta_2 - \beta_1}{b} \int_0^b dv \int_{-\infty}^{\infty} s_u dz ,$$

which, as previously proved, is independent of α_2. However, the absolute error introduced by making this replacement is always less than or equal to some fixed number which is independent of $\beta_1 - \beta_2$, i.e., it is independent of the length L in Fig. 3. The error is due to the deviation of the actual power associated with the leftover fraction of a period from that same fraction of the power associated with a complete period. Since the absolute error l as a fixed upper limit, the relative error decreases as L increases. In the same way, the relative error involved in replacing the second integral of (G-13) by

$$\frac{\alpha_1 - \alpha_2}{a} \int_0^a du \int_{-\infty}^{\infty} s_v dz ,$$

which is independet of β_1, can be made arbitrarily small by selecting L large enough. To within the above-described approximations, P can be written

$$P = \frac{\beta_2 - \beta_1}{|\underline{u}_1| b} \int_0^b dv \int_{-\infty}^{\infty} s_u dz + \frac{\alpha_1 - \alpha_2}{|\underline{v}_1| a} \int_0^a du \int_{-\infty}^{\infty} s_v dz . \qquad (G\text{-}14)$$

In order to find $\beta_2 - \beta_1$ and $\alpha_1 - \alpha_2$ in terms of L and $\underline{v}$, the law of sines, which can be written as

$$\frac{\underline{z}_0 \cdot (\underline{u}_0 \times \underline{v}_0)}{L} = \frac{\underline{z}_0 \cdot [\underline{u}_0 \times (\underline{z}_0 \times \underline{v})]}{\beta_2 - \beta_1} = \frac{\underline{z}_0 \cdot [\underline{v}_0 \times (\underline{z}_0 \times \underline{v})]}{\alpha_1 - \alpha_2} , \quad \text{(G-15)}$$

is used. From (G-15) it is found that

$$\frac{\beta_2 - \beta_1}{|\underline{u}_1|} = L\underline{v} \cdot \underline{u}_0 \quad ; \quad \frac{\alpha_1 - \alpha_2}{|\underline{v}_1|} = L\underline{v} \cdot \underline{v}_0 \quad . \quad \text{(G-16)}$$

With the help of (G-12) and (G-16), P as given in (G-14) can be written as

$$P = L\underline{v} \cdot \underline{\overline{S}} \quad . \quad \text{(G-17)}$$

Equation (G-17) serves as the basis for interpreting $\underline{\overline{S}}$ as the average power flow for the surface wave as a whole, in the sense that the power passing through any plane surface infinite in z and lying between two lines parallel to the z axis is given approximately by the normal component of $\underline{\overline{S}}$ times the width of the surface. Further, the relative error in the approximation decreases as the width increases.

Defining $\overline{W}$ by the equation

$$\overline{W} = \frac{1}{A} \int_{-\infty}^{\infty} dz \iint_P w \, dz \quad , \quad \text{(G-18)}$$

$\overline{W}$ is seen to represent the average energy in cylinders infinite in z, parallel to the z axis and having normal cross-sections of unit area. Finally, recalling the definition of $\underline{\overline{S}}$ -- see text before (G-10) -- (G-9) can be written as

$$\nabla_{\underline{k}_t} \omega = \underline{\overline{S}} / \overline{W} \quad . \quad \text{(G-19)}$$

Thus the energy velocity $\underline{\overline{S}} / \overline{W}$ of surface waves in periodic configurations is equal to the group velocity.

2) Surface Impedance Representing a Periodic Configuration

In many configurations of the type described in the previous section, the entire region above some plane $z = 1$ is filled with a medium which is uniform in $\underline{\rho}$ rather than periodic. In such cases, it is sometimes possible to represent the effect of the structure below a plane $z = d > 1$ on the propagation of fields having the form (G-1) in the region $z > d$ by a dyadic surface impedance defined at $z = d$. This impedance representation is possible in those ranges of values of $\underline{k}_t$ and ω for which the higher space harmonics that go to make up $\underline{e}$ and $\underline{h}$ in (G-1) will have decayed sufficiently so that $\underline{e}$ and $\underline{h}$ can be approximated at $z = d$ by the zero-order space-harmonic fields, which are independent of $\underline{\rho}$. Note that in this discussion $\underline{k}_t$ and ω are independent variables, i.e., they are not required to satisfy a surface wave dispersion relation.

As in the case of a plane-stratified medium above a perfectly conducting plane, which was discussed in Section D of Chapter III, two linearly independent solutions of the form given in (G-1) in the region $z \leq d$ are needed to uniquely define the dyadic surface impedance $\underset{\sim}{Z}$ through the relation

$$(\underline{e}_t)_{z=d} = \underset{\sim}{Z} \cdot (\underline{z}_o \times \underline{h}_t)_{z=d} \quad . \tag{G-20}$$

In writing (G-20), is assumed to be sufficiently large so that $\underline{e}_t$ and $\underline{h}_t$ are indeed independent of $\underline{\rho}$. Moreover, it is assumed that none of the linearly independent solutions in the region $z \leq d$ has a magnetic field null of the fundamental space harmonic at $z = d$, since otherwise $\underset{\sim}{Z}$ could not be uniquely defined. However, when such a null exists at $z = d$, it is in general possible to formulate a dyadic surface admittance representation for the structure in a manner similar to that given in Appendix F for the case of plane-stratified configurations. Relation (G-20) can now be used as a boundary condition at $z = d$ when solving for the fields in the region $z > d$ and ensures that the transverse fields for $z > d$ will connect continuously to valid solutions in the region $z \leq d$ -- see Section D of Chapter III.

When the structure below the plane $z = d$ is such that $\underset{\sim}{Z}$ is anti-Hermitian, it will be shown that the power flow and stored energy below the plane $z = d$ can be computed from relations analogous to those of (III-36) and (III-?7). The dyadic surface impedance will be anti-Hermitian, if, as will be assumed, the region in which the waves exist is bounded from below by a perfectly conducting, possibly periodic, surface. Note that the presence of the bounding conductor is sufficient to ensure that $\underset{\sim}{Z}$ is anti-Hermitian but is not a necessary condition. The presence of the bounding conductor ensures that the average power in the z direction is zero, i.e., that $\iint\limits_{p} s_z \, da = 0$, as can be seen from the proof given in the previous section. At $z = d$, $\underline{e}_t$ and $\underline{h}_t$ are independent of $\underline{\rho}$ so that s_z is independent of $\underline{\rho}$ and must therefore be identically zero. This last fact implies that $\underset{\sim}{Z}$ will be anti-Hermitian.

As in the previous section, the fields at neighboring sets of values $(\underline{k}_t, \omega)$ and $(\underline{k}_t + d\underline{k}_t, \omega + d\omega)$, where $d\underline{k}_t$ and $d\omega$ are now independent, are considered. Requiring the derivatives of $\underline{E}$ and $\underline{H}$ with respect to k_x, k_y and ω to exist, the fields at $(\underline{k}_t + d\underline{k}, \omega + d\omega)$ are again given to first order by (G-2). Expansion of the quantity $\nabla \cdot (\underline{E}^* \times \delta \underline{H} + \delta \underline{E} \times \underline{H}^*)$ leads, as before to (G-6), which may be written as

$$w d\omega - d\underline{k}_t \cdot \underline{S} = j \frac{1}{2} \nabla \cdot (\underline{e}^* \times \delta \underline{h} + \delta \underline{e} \times \underline{h}^*) . \qquad (G-21)$$

Equation (G-21) is now integrated over the volume of the region composed of that portion of a unit cell lying below the plane $z = d$. Taking the fields below the perfectly conducting surface, which are unrelated to those above, to be zero, the z integration may be taken from $z = -\infty$ to $z = d$. The volume integral of the right-hand side of (G-21) is converted to a surface integral using the divergence theorem. As previously argued, the net contribution from the integrals over the side walls is zero because of the periodic nature of $\underline{e}$, $\underline{h}$, $\delta \underline{e}$ and $\delta \underline{h}$. Since the fields are zero at $z = -\infty$, the contribution from the end face at $z = -\infty$ is zero, and hence the integration over the

entire surface reduces to the integral over the end face at $z = d$ of the quantity $\underline{z}_o \cdot (\underline{e}^* x\ \delta\ \underline{h} + \delta\ \underline{e}\ x\ \underline{h}^*)_{z=d}$. But, by assumption, this quantity is independent of $\underline{\rho}$ for $z = d$, and hence its integral is equal to the product of the area A of the end face and the quantity $\underline{z}_o \cdot (\underline{e}^* x\ \delta\ \underline{h} + \delta\ \underline{e}\ x\ \underline{h}^*)_{z=d}$.

If the operation δ is applied to (G-20) and the resultant equation for $(\delta\ \underline{e}_t)_{z=d}$ is used together with (G-20) itself and with (III-17) and the anti-Hermitian property of $\underset{\sim}{Z}$, it is seen that

$$\underline{z}_o \cdot (\underline{e}^* x\ \delta \underline{h} + \delta\ \underline{e}\ x\ \underline{h}^*)_{z=d} = -\left[(\underline{z}_o x \underline{h}_t^*) \cdot \delta \underset{\sim}{Z} \cdot (\underline{z}_o x \underline{h}_t)\right]_{z=d} \quad \text{(G-22)}$$

Thus the integration of (G-21) over the region described above leads to the relation

$$-j\frac{1}{2}\left[(\underline{z}_o x \underline{h}_t^*) \cdot \delta \underset{\sim}{Z} \cdot (\underline{z}_o x \underline{h}_t)\right]_{z=d} = \overline{W}_d\ d\omega - d\underline{k}_t \cdot \overline{\underline{S}}_d \quad , \quad \text{(G-23)}$$

where

$$\overline{W}_d = \frac{1}{A} \int\limits_{-\infty}^{d} dz \iint\limits_{p} w\, da \quad \text{(G-24)}$$

and the transverse vector $\overline{\underline{S}}_d$ is given by

$$\overline{\underline{S}}_d = \frac{1}{A} \int\limits_{-\infty}^{d} dz \iint\limits_{p} \underline{S}\, da \quad . \quad \text{(G-25)}$$

Because dk_x, dk_y and $d\omega$ are independent variations, (G-23) implies that

$$j\frac{1}{2}\left[(\underline{z}_o x \underline{h}_t^*) \cdot \frac{\partial}{\partial k_x} \underset{\sim}{Z} \cdot (\underline{z}_o x\ \underline{h}_t)\right]_{z=d} = \overline{S}_{dx}$$

$$\left.\vphantom{\int}\right\} \quad \text{(G-26)}$$

$$j\frac{1}{2}\left[(\underline{z}_o x \underline{h}_t^*) \cdot \frac{\partial}{\partial k_y} \underset{\sim}{Z} \cdot (\underline{z}_o x \underline{h}_t)\right]_{z=d} = \overline{S}_{dy}$$

and that

$$-j\frac{1}{2}\left[(\underline{z}_o \times \underline{h}_t^*) \cdot \frac{\partial}{\partial \omega}\ \underset{\sim}{Z} \cdot (\underline{z}_o \times \underline{h}_t)\right]_{z=d} = \overline{W}_d \ . \qquad (G-27)$$

From the definition of $\overline{W}_d$, the term on the left-hand side of (G-27) is seen to represent the average electromagnetic energy stored in cylinders parallel to the z axis, extending from $z = -\infty$ to $z = d$ and having cross-sections of unit area. The interpretation of $\overline{\underline{S}}_d$, and hence the terms on the left-hand side of (G-26), as the average power flow below the plane $z = d$ is similar to that given in the previous section for surface waves in periodic configurations. That is, the power passing through any plane surface extending from $z = -\infty$ to $z = d$, and lying between two lines parallel to the z axis, is approximately given by the normal component of $\overline{\underline{S}}_d$ times the width of the surface, where the relative error in the approximation decreases as the width increases. Proof of the validity of this interpretation of $\overline{\underline{S}}_d$ follows exactly that given in the previous section for $\overline{\underline{S}}$, with the end face at $z = \infty$ replaced by the end face at $z = d$. The replacement of the end face at $z = \infty$ by that at $z = d$ is possible since the only property of the end face at $z = \infty$ that was used in the discussion of $\overline{\underline{S}}$ was that $s_z = 0$ there; in the present problem $s_z = 0$ at $z = d$.

Thus, for structures that are periodic in two dimensions and that can be represented at some plane $z = d$ by an anti-Hermitian dyadic surface impedance $\underset{\sim}{Z}$, the average power flow $\overline{\underline{S}}_d$ and average stored energy $\overline{W}_d$ in the structure can be found knowing only $\underset{\sim}{Z}$ and $(\underline{h}_t)_{z=d}$.

Appendix H

ON THE POSSIBLE EXISTENCE OF H-TYPE SURFACE WAVES
ON A UNIAXIAL PLASMA SLAB

The purpose of this appendix is to investigate the possible con-
tribution to a surface wave field from the plane wave fields in the plasma
that are associated with the solutions $\varkappa = \pm \sqrt{k_o^2 - \underline{k}_t^2}$ of the plasma wave
dispersion relation. The vector character of these plasma waves is that
of H-type modes and has the form

$$
\left.
\begin{aligned}
\underline{e}' &= C[\underline{x}_o \varkappa - \underline{z}_o k_x] \\
\underline{h}' &= \frac{C}{\omega\mu_o} [-\underline{x}_o k_y k_x + \underline{y}_o(k_o^2 - k_y^2) - \underline{z}_o \varkappa k_y]
\end{aligned}
\right\}
\tag{H-1}
$$

with C an arbitrary constant. The vector character of those plane waves
in the air regions that have the H-type mode form, and will thus allow a
simple application of the continuity conditions at $z = \pm d$, is

$$
\left.
\begin{aligned}
\underline{e}_a' &= D[\underline{x}_o \varkappa_a - \underline{z}_o k_x] \\
\underline{h}_a' &= \frac{D}{\omega\mu_o} [-\underline{x}_o k_y k_x + \underline{y}_o(k_o^2 - k_y^2) - \underline{z}_o \varkappa_a k_y]
\end{aligned}
\right\}
\tag{H-2}
$$

with $\varkappa_a = \pm j\alpha$ and α as defined in Eq. (IV-11). Note that $\varkappa = \pm j\alpha$ also.

In Region 1, $\varkappa_a$ must be taken as $-j\alpha$ to ensure that $\underline{E}$ and $\underline{H}$ are
zero at $z = \infty$. Similarly, in Region 3, $\varkappa_a$ must be taken as $j\alpha$. Denot-
ing the amplitudes in Regions 1 and 3 as D_1 and D_3, respectively, and
letting C_1 and C_2 be the amplitudes of the plasma plane waves corre-
sponding to $\varkappa = -j\alpha$ and $\varkappa = j\alpha$, respectively, the continuity conditions
at $z = d$ result in the equations

$$
\left.
\begin{aligned}
-D_1 e^{-\alpha d} &= -C_1 e^{-\alpha d} + C_2 e^{\alpha d} \\
D_1 e^{-\alpha d} &= C_1 e^{-\alpha d} + C_2 e^{\alpha d}
\end{aligned}
\right\}
\tag{H-3}
$$

when the fields in Region 2 are assumed to be the sum of the two H-type
plane waves. The continuity conditions at $z = -d$ can be written as

$$D_3 e^{-\alpha d} = -C_1 e^{\alpha d} + C_2 e^{-\alpha d} \left.\vphantom{\begin{matrix}a\\b\end{matrix}}\right\}$$

$$D_3 e^{-\alpha d} = C_1 e^{\alpha d} + C_2 e^{-\alpha d} \left.\vphantom{\begin{matrix}a\\b\end{matrix}}\right\} \qquad (H-4)$$

These equations have only the trivial solutions $C_1 = C_2 = D_1 = D_3 = 0$ and hence no surface wave can exist whose fields in the plasma are a sum of the two H-type plasma plane waves, which propagate as $\kappa = \pm j\alpha$.

The physical reason why no surface wave exists that contains the above-mentioned plane waves is that the waves of this polarization do not "see" the plasma, since the infinite D.C. magnetic field along y prevents the electrons from moving in response to an R.F. electric field that, as in this case, is purely transverse to y. In effect, for waves of this polarization, no slab on which to have surface waves is present.

BIBLIOGRAPHY

1. R. Mittra and G. L. Duff, "A Systematic Study of the Radiation Patterns of a Dipole in a Magnetoplasma Based on a Classification of the Associated Dispersion Surfaces", Radio Science 69D (1965), pp. 681-692.

2. M. J. Lighthill, "Studies on Magneto-Hydrodynamic Waves and Other Anisotropic Wave Motions", Phil. Trans. Royal Soc. London 252 (1960), Sec. A, pp. 397-430.

3. S. R. Seshadri and A. Hessel, "Radiation From a Source Near a Plane Interface Between an Isotropic and a Gyrotropic Dielectric", Canadian Jnl. of Phy. 42 (1964), pp. 2153-2172.

4. L. B. Felsen and S. Rosenbaum, "Ray optics for Radiation Problems in Anisotropic Regions With Boundaries, Part I: Line Source Excitation", to be published in the Aug. 1967 issue of Radio Science.

5. S. Rosenbaum, "Radiation and Diffraction in Anisotropic Media", Ph. D. thesis, Electrophysics Dept., Polytechnic Inst. of Brooklyn (1966).

6. B. Rulf and L. B. Felsen, "Diffraction by Objects in Anisotropic Media", Proceedings of the Symposium on Quasi-Optics, M. R. I. Symposia Series Vol. XIV, Poly Press, New York (1964), pp. 107-147.

7. E. Arbel, "Radiation From a Point Source in an Anisotropic Medium", Microwave Research Inst., Polytechnic Inst. of Brooklyn, Rpt. PIB MRI-861-60 (1960).

8. J. R. Wait, "The Electromagnetic Fields of a Dipole in the Presence of a Thin Plasma Sheet", Appl. Sci. Res. B8 (1960), pp. 397-417.

9. J. B. Keller, "Geometrical Theory of Diffraction", in Calculus of Variations and its Applications, McGraw-Hill Book Co., New York (1958).

10. J. B. Keller, "Geometrical Theory of Diffraction", Jnl. Opt. Soc. of America 52 (1962), pp. 116-130.

11. L. M. Brekhovshikh, Waves in Layered Media, Academic Press, New York (1960).

12. L. B. Felsen, "On the Use of Refractive Index Diagrams for Source-Excited Anisotropic Regions", Radio Science 69D (1965), pp. 155-169.

13. A. D. Bresler, G. H. Joshi and N. Marcuvitz, "Orthogonality Properties for Modes in Active and Passive Uniform Waveguides", Jnl. Appl. Phys. 29 (1958), pp. 794-799.

14. L. D. Landau and E. M. Lifshitz, <u>Electrodynamics of Continuous Media</u>, Pergamon Press, New York (1960), pp. 253-256, 314, 331.

15. T. H. Stix, <u>The Theory of Plasma Waves</u>, McGraw-Hill Book Co., New York (1962), pp. 45-51.

16. G. Hadley, <u>Linear Algebra</u>, Addison-Wesley Publishing Co., Massachusetts (1961), pp. 249-250.

17. N. Chako, "Développement asymptotique d'intégrales doubles que l'on recontre dans la théorie de la diffraction", Comptes Rendus des Séances <u>247</u>(1958), pp. 436-438.

18. N. Chako, "Application de la methode de la phase stationnaire dans le théorie de la diffraction des images optiques", Comptes Rendus des Séances <u>247</u> (1958), pp. 580-582.

19. N. Chako, "Calcul d'intégrales doubles pour de grandes valeurs d'un paramétre", Comptes Rendus des Séances <u>247</u> (1958), pp. 637-639.

20. B. Nagel, "The Saddle Point Method for Multiple Integrals, With an Application to the Evaluation of Radial Coulomb Matrix Elements for Large Multipole Orders", Arkiv för Fysik <u>27</u> (1964), pp. 181-192.

21. D. S. Jones and M. Kline, "Asymptotic Expansion of Multiple Integrals and the Method of Stationary Phase", Jnl. of Math. and Phy. <u>37</u> (1958-59), pp. 1-28.

22. H. Jeffreys, <u>Asymptotic Approximations</u>, Oxford University Press, London (1962).

23. W. P. Allis, S. J. Buchsbaum and A. Bers, <u>Waves in Anisotropic Plasmas</u>, John Wiley and Sons, New York (1962), pp. 103-106.

24. T. H. Stix, p. 32.

25. A. R. Forsyth, <u>Lectures on the Differential Geometry of Curves and Surfaces</u>, Cambridge University Press, London (1920), p. 61.

26. L. M. Brekhovshikh, pp. 245-287.

27. A. Tonning, "A Contribution to the General Theory of Linear Networks", Norwegian Defense Research Establishment, Rpt. 28 (1959), pp. 13-23.

28. A. D. Bresler, "The Far Fields Excited by a Point Source in a Passive Dissipationless Anisotropic Uniform Waveguide", Microwave Research Inst., Polytechnic Inst. of Brooklyn, Rpt. R-683-58 (1958), p. 12.

29. C. G. Montgomery, R. H. Dicke and E. M. Purcell, <u>Principles of Microwave Circuits</u>, McGraw-Hill Book Co., New York (1948), pp. 151-153.

30. J. R. Wait, "Propagation of Electromagnetic Waves Along a Thin Plasma Sheet", Canadian Jnl. of Phy. <u>38</u> (1960), pp. 1586-1594.

31. G. Meltz and R. A. Shore, "Leaky Waves Supported by Uniaxial Plasma Layers", IEEE Trans. <u>AP-13</u> (1965), pp. 94-105.

32. F. M. Labianca, "The Electromagnetic Fields of Certain Uniaxially Anisotropic Dielectric Slabs", Microwave Research Inst., Polytechnic Inst. of Brooklyn, Rpt. PIB MRI-1150-63 (1963).

33. H. Hodara and G. I. Cohn, "Wave Propagation in Magneto-Plasma Slabs", IRE Trans. <u>AP-10</u> (1962), pp. 452-459.

34. S. R. Seshadri and W. F. Pickard, "Surface Waves on an Anisotropic Plasma Sheath", IEEE Trans. <u>MTT-12</u> (1964), pp. 529-541.

35. J. B. Keller and F. C. Karal, "Surface Wave Excitation and Propagation", Jnl. Appl. Phys. <u>31</u> (1960), pp. 1039-1046.

36. A. Ishimaru, "The Effect of a Unidirectional Surface Wave Along a Perfectly Conducting Plane on the Radiation From a Plasma Sheath", in <u>Electromagnetic Aspects of Hypersonic Flight</u>, Spartan Books, Baltimore, Md. (1964), pp. 147-168.

37. S. R. Seshadri, "Excitation of Surface Waves on a Perfectly Conducting Screen Covered With Anisotropic Plasma", IRE Trans. <u>MTT-10</u> (1962), pp. 573-578.

38. S. Adachi and Y. Mushiake, "Surface Waves Along a Perfectly Conducting Plane Covered With Semi-Infinite Magneto-Plasma", Radio Science <u>69D</u> (1965), pp. 171-175.

39. E. Arbel and L. B. Felsen, "Theory of Radiation From Sources in Anisotropic Media, Part II", in <u>Electromagnetic Theory and Antennas, Part I</u>, Pergamon Press, New York (1963), pp. 421-459.

40. L. B. Felsen and N. Marcuvitz, "Modal Analysis and Synthesis of Electromagnetic Fields", Microwave Research Inst., Polytechnic Inst. of Brooklyn, Rpt. R-776-59 (1959).

41. S. Barone and A. Hessel, "Leaky Wave Contributions to the Fields of a Line Source Above a Dielectric Slab - Part II", Microwave Research Inst., Polytechnic Inst. of Brooklyn, Rpt. R-698-58 (1958).

42. T. Tamir and A. A. Oliner, "Guided Complex Waves - Part 1, Fields at an Interface", Proc. IEE 110 (1963), pp. 310-324.

43. J. B. Keller and H. B. Keller, "Determination of Reflected and Transmitted Fields by Geometrical Optics", Jnl. of the Optical Soc. of America 40 (1950), pp. 48-52.

44. H. J. Riblet and C. B. Barker, "A General Divergence Formula", Jnl. Appl. Phys. 19 (1948), pp. 63-70.

45. M. J. Gans, "Surface Waves on Anisotropic Surfaces", Electronics Research Laboratory, University of California, Rpt. 65-26 (1965).

46. A. F. Kay, "Excitation Efficiency of Surface Waves Over Corrugated Metal and Doubly Corrugated Metal and in Dielectric Slabs on a Ground Plane", Technical Research Group, Rpt. No. 5 (1956).

DOCUMENT CONTROL DATA - R & D

(Security classification of title, body of abstract and indexing annotation must be entered when the overall report is classified)

1 ORIGINATING ACTIVITY *(Corporate author)*	2a. REPORT SECURITY CLASSIFICATION
POLYTECHNIC INSTITUTE OF BROOKLYN ELECTROPHYSICS DEPT., GRADUATE CENTER ROUTE 110, FARMINGDALE, N.Y. 11735	Unclassified
	2b. GROUP

3. REPORT TITLE

AN APPROACH TO RAY OPTICS IN ANISOTROPIC MEDIA

4. DESCRIPTIVE NOTES *(Type of report and inclusive dates)*

Scientific   Interim

5. AUTHOR(S) *(First name, middle initial, last name)*

H. L. Bertoni and A. Hessel

6. REPORT DATE	7a. TOTAL NO. OF PAGES	7b. NO. OF REFS
June 1967	200	46
8a. CONTRACT OR GRANT NO. NONR 839(38)	9a. ORIGINATOR'S REPORT NUMBER(S)	
b. PROJECT NO.	PIBMRI-1366-67	
ARPA Order No. 529		
c. Program Code No. 5730	9b. OTHER REPORT NO(S) *(Any other numbers that may be assigned this report)*	
d.		

10. DISTRIBUTION STATEMENT

Distribution of this document is unlimited.

11. SUPPLEMENTARY NOTES	12. SPONSORING MILITARY ACTIVITY
	Department of the Navy, Code 427 Advanced Research Projects Agency Washington, D. C. 20360

13. ABSTRACT

A description of the far fields radiated by an electromagnetic point source in the presence of bounded, lossless, anisotropic media is formulated in terms of ray optics. The ray-optical description is a generalization of classical geometrical optics and has previously been used to describe the fields radiated in isotropic media and those radiated by line sources in anisotropic media. In formulating the ray-optical description, the fields radiated by a point source in the presence of a planar interface between two homogeneous, lossless media of arbitrary anisotropy are first presented in terms of a double Fourier integral. This rigorous integral representation is then evaluated asymptotically to find the first-order stationary point, branch curve and surface wave pole contributions.

Using the equality of group velocity and velocity of energy transport for plane waves in anisotropic media, the stationary point contributions are interpreted in terms of direct and scattered (transmitted and reflected) rays and the associated fields are cast into ray-optical form. Locally, the direct and scattered ray fields are those of plane waves carrying energy in the ray direction and are scattered at the interface according to Snell's law. The ray-optical forms of these ray fields exhibit their dependence on properties local to the ray path, thus permitting the extension of the ray-optical results to problems not amenable to rigorous analysis. Such an extension is considered for the case of scattering at a gently curved interface between two homogeneous anisotropic media. The branch curve contributions are interpreted in terms of lateral rays whose fields also are locally those of plane waves carrying energy in the ray direction.

DD FORM 1473
1 NOV 65

14. KEY WORDS	LINK A		LINK B		LINK C	
	ROLE	WT	ROLE	WT	ROLE	WT
Ray-optics Anisotropic media Surface waves Anisotropic interface						